# THEORETICAL AND EXPERIMENTAL ANALYSIS FOR OPTIMIZING THE PERFORMANCE OF A SLPP

by

C Icannis Papaicannou

A thesis submitted to the

Faculty of Graduate Studies and Research

in partial fulfillment of the requirements for the degree of

Master of Engineering

Department of Mechanical Engineering

McGill University

Montreal, Canada

August, 1985

#### ABSTRACT

Solar liquid piston pumps (SLPPs) could help relieve the energy problem of many developing countries of the Third World, where solar energy is abundant. The major advantage of the SLPP is its simplicity of design and low level of maintenance required.

Previous theoretical work on the computer model was extended to predict the scale effects on the performance. Based on these results two models implementing different condenser designs were constructed and tested experimentally. It was found that in general the experimental results were in qualitative agreement with the theoretical ones.

The technical aspects of integrating the SLPP with a solar collector and implementing thermosyphon forces for the circulation of the hot water, were analysed. The operation of such a system was found to be feasible.

## RESUME

Les pompes solaires à piston liquide (SLPPs) pourraient réduire les problèmes énergétiques de plusieurs pays en voie de développement du Tiers Monde, dans lesquels l'énergie solaire se retrouve en abondance. Les plus grands avantages de cette technique sont la simplicité de sa conception et l'entretien limité qu'elle nécessite.

Les travaux précédents effectués sur le modèle numérique ont été développé pour pouvoir prédire la gamme de résultats possibles dans son application. A partir de ces résultats, deux prototypes ont été construits à partir de différent plans du condenseur et ont été testés expérimentalement. Les résultats de ces expériences ses sont généralement avérés similaires aux prédictions théoriques.

Nous avons étudié les aspects techniques de la combinaison de la SLPP avec un récepteur solaire qui utilise des forces thermosyphon pour la circulation de l'eau chaude. Le fonctionnement d'un tel système s'est révélé fonctionnel.

#### ACKNOWLEDGEMENTS

I would like to express my appreciation and my thankful feelings to my research adviser, Prof. C. L. Murphy for his careful guidance, patience, his constructive suggestions and remarks and for giving me the opportunity to work on this subject. It also appreciate greatly the work of Mr. Abeeku Brew-Hammond, on which part of this work has been based.

I would also like to thank the laboratory supervisor Mr. Jack Kelly and his staff, Charlie, Ed and John, for their assistance and suggestions before and during the experimental tests. Also, Mr. Charles Altman and Mr. Gregg Carruthers, who helped collect the experimental data and build the pressure-volume measuring device.

Finally, I would like to thank all my friends who helped me through different stages of this work, especially Mr. George Papagiannis whose expertise on computers was most valuable.

Last but not least, I wish to express my deep gratitude to my parents Constantinos and Fotini Papaioannou, for their support and encouragement throughout this whole period.

# TABLE OF CONTENTS

ABSTRACTii
RESUMEiii
ACKNOWLEDGEMENTSiv
TABLE OF CONTENTS
LIST OF FIGURESix
LIST OF TABLESxiv
NOMENCLATURExvi
CHAPTER 1: INTRODUCTION
1.1. HISTORICAL DEVELOPMENT OF SOLAR PUMPS
1.2. OPERATION OF THE SOLAR LIQUID PISTON PUMP6
1.3. REVIEW OF RESEARCH ON SOLAR LIQUID PISTON PUMPS
1.4. OBJECTIVES9
CHAPTER 2: THEORETICAL MODEL
2.1. BASIC MODEL
2.2. PHYSICS OF THE THEORETICAL MODEL11
2.2.1. THERMODYNAMIC CYCLE11
2.2.2. HEAT TRANSFER
2.2.3. ANALYSIS OF THE FLOW
Flow analysis of the three liquid columns15
a. Main cylinder16
b. Outlet pipe

' <b>.</b>	vi
c. Inlet pipe	18
2.2.4. GEOMETRICAL PARAMETERS	20
a. Liquid contact areas	20
b. Vapour volume	20
2.2.5. HEATER, CONDENSER AND LIQUID FREON TEMPERATURES	21
2.2.6. MASS AND ENERGY CONSERVATION	22
2.2.7. PERFORMANCE CRITERIA	23
2.3. THE COMPUTER PROGRAM	25
CHAPTER 3: THEORETICAL PREDICTIONS	28
3.1. RESULTS ON THE 10 cm MODEL	30
3.1.1. HOT WATER INLET TEMPERATURE	30
3.1.2. HOT WATER MASS FLOWRATE	31
3.1.3. COOLING WATER TEMPERATURE	31
3.1.4. SURFACE AREA OF THE LOWER PART OF THE HEATER	32
3.1.5. DISTANCE OF THE HEATER FROM THE TOP	33
3.1.6. DISTANCE OF THE CONDENSER FROM THE TOP	34
3.1.7. THICKNESS OF THE HEATER	35
3.2. SCALING	38
CHAPTER 4: EXPERIMENTAL MODELS	42
4.1. LABORATORY FACILITIES	43
4.2. 14 cm DIAMETER SLPP	
4.2.1. RESULTS	47
4.3. 12.7 cm DIAMETER SLPP	53
4.0.1	

P.

c .	vii
CHAPTER 5: discussion of the results	57
5.1. HOT WATER MASS FLOWRATE	58
5.2. HOT WATER INLET TEMPERATURE	60
5.3. HEATER POSITION	61
5.4. CONDENSER POSITION	63
5.5. CONDENSER TEMPERATURE	66
5.6. EVAPORATOR DIMENSIONS	67
5.7. COOLING WATER MASS FLOWRATE	68
5.8. REVERSING THE FLOWS	69
5.9. ALTERNATIVE COOLING WATER SUPPLY	71
CHAPTER 6: MATCHING SOLAR COLLECTOR WITH SLPP	74
6.1. THERMOSYPHON HEAD	75
6.2. FRICTION HEAD	78
6.2.1. PIPE CIRCUIT	
6.2.2. EVAPORATOR COIL	81
6.2.3. SOLAR COLLECTOR	82
6.3. SIZE OF SOLAR COLLECTOR	84
6.4. EXPERIMENTAL TESTS	86
CHAPTER 7: CONCLUSIONS AND RECOMMENDATIONS	
7.1. CONCLUSIONS	88
7.2. RECOMMENDATIONS FOR FUTURE WORK	89
REFERENCES	90
FIGURES	94

APPENDIX 1: TABLES....

				•					viii
1.1. T	EORETI C	AL RESU	JLTS	• • • • • •			<u> </u>		160
1.2. E	KPEŘIMÉN	TAL RES	SULTS	• • • • • • •		• • • • • •	••••	· • • • •	170
APPEND:	x 2: CO	MPUTER	PROGRAM	LISTIN	3		• • • • •		183

٩ -

ř

, 50

LIST	OF FIGURES	*
1.1.	Solar powered pumping systems	. 95
1.2.	Schematic of a SLPP	. 9,6
2.1.	Theoretical p-v diagram for the SLPP	, 97
2.2.	Theoretical and experimental p-h	•
	diagrams for the SLPP	. 98
3.1.	Flowrate vs Total head (var. T)	. 99
3.2.	Efficiency vs Total head (var. T )	100
3.3.	Flowrate vs Total head (var. m)	101
à <b>.4</b> .	Efficiency vs Total head (var. h)	102
3.5.	Flowrate vs Total head (var. T)	103
3.6.	Efficiency vs Total Head (var. T)	104
3.7.	Flowrate vs Total head (var. A )	105
3.8.	Efficiency vs Total head (var. A )	106
3.9.	Flowrate vs Total head (var. L)	107
3.10.	Efficiency vs Total head (var. L )	108
3.11.	Amplitude vs Total head (var. L)	109
3.12.	Frequency vs Total head (var. L )	110

	•	, х
3.13.	Flowrate vs Total head (var. L )	111
3.14.	Efficiency vs Total head (var. L )	112
3.15.	Amplitude vs L (var. total head)	113
3.16.	Flowrate vs Total head (var. L )	114
3.17.	Efficiency vs Total head (var. L )	115
3.18.	Frequency vs L (var. total head)	116
3.19.	Flowrate and Efficiency vs Total	
	head (var. L )	.117
3.20.	Efficiency vs Power output (var. T )	118
3.21.	Flowrate vs Total head	
	(var. Scale factor)	119
3.22.	Efficiency vs Total head	
	(var. Scale factor)	.120
3.23.	Amplitude vs Scale factor	
	(var. total head)	.12]
3,24.	Frequency vs Scale factor	
	(var, total head),	.122
3.25.	Flowrate vs Total head	
•	(var. T - scaled model)	.123

	•
	<b>xi</b>
3.26.	Efficiency vs Total head
	(var. T -scaled model)
3.27.	Flowrate vs Total head
	(var. m -scaled model)125
3.28.	Efficiency vs Total head
	(var. m -scaled model)
3.29.	Flowrate vs Total head
	(var. T -scaled model)127
3.30.	Efficiency vs Total head
*	(var. T -scaled model)128
3.31.	Flowrate vs Total head
	(var. A -scaled model)
3.32.	Efficiency vs Total head
	(var. A -scaled model)
3.33.	Flowrate vs Total head
•	(var. L and L -scaled model)
3.34.	Efficiency vs Total head
	(var. L and L -scaled model)
3.35,	Flowrate vs Total head
	(var. L -scaled model)

		Kii
3.36.	Efficiency vs Total head	
	(var. L -scaled model),	.134
4.1.	Schematic of laboratory test facilities	.13!
4.2.	•	
	pressure-volume diagrams	.13
4.3.	Typical pressure-volume diagram	.13
4.4.	Assembly drawing to scale	
	of 14 cm SLPP	.138
1.5.	Flowrate vs Total head	
	(var. m -14 cm SLPP)	.139
1.6.	Flowrate vs Total head	
	(var. m -14 cm SLPP)	.14(
1.7.	Flowrate vs Total head	
•	(var. T -14 cm SLPP)	.143
1.8.	Flowrate vs Total head .	
	(var. L -14 cm SLPP)	142
1.9.	Flowrate vs Total head	
	(var. L -14 cm SLPP)	143
.10.	Flowrate vs Total head	
	(var. in- and outlet conf14 cm SLPP)	144
.11.	Flowrate vs Discharge head	
	(alt. cooling water supply)	145

{

	4.12.	Efficiency vs Power output	
		(var. T -14 cm SLPP)	.146
	4.13.	Assembly drawing to scale	
		of 12.7 cm SLPP	.147
,	4.14.	Flowrate vs Total head	
•	,	(var. m and m -12.7 cm SLPP)	.148
	4.15.	Flowrate vs Total head	
٦,		(var. m and m -12.7 cm SLPP)	.149
	4.16.	Flowrate vs Total head	ı
		(var. m and m -12.7 cm SLPP)	.150
_	4.17,.	Flowrate vs'Total head (var. T -12.7 cm SLPP)	.151
	4.18.	Flowrate vs Total head	ر
<u>•</u> .	~	(var. m -12.7 cm SLPP)	.152
	6.1.	Schematic of the SLPP-collector installation	.153
	6.2.	Thermosyphon head	.154
	6.3.	Friction losses in pipe circuit (non-D)	.155
	6.4.	Friction losses in coil	.156
	6.5.	Friction losses in solar collectors	.157
	6.6.	Collector efficiency curve	.158
	6.7.	Thermal syphon test heat exchanger	.159

LIST OF TABLES (.	APPENDIX	1)
-------------------	----------	----

1.	Variation	of	T
2.	Variation	of	ћ
3.	Variation	of	T
4.	Variation	of	A
5.	Variation	of	L
6.	Variation	of	L
7.	Variation	of	L164
8.	Variation	of	scale factor165
9.	Variation	of	T (scaled model)166
10.	Variation	of	m (scaled model)166
11.	Variation	of	T (scaled model)167
12.	Variation	of	A (scaled model)
13.	Variation	of	L and L (scaled model)
14.	Variation	of	L (scaled model)169
15.	Variation	of	m (14 cm model)171
16.	Variation	of	m (14 cm model)173

r	•	
, , , , , , , , , , , , , , , , , , ,	•	,
•	·	
	3	, <b>xv</b>
17. Variation of T (1	14 cm model)	175
18. Variation of L (14	d cm model)	176
19. Variation of L (1	14 cm model)	177
20. Switching the inlet	s and outlets of the	evaporator
and the condens	ser (14 cm model)	179
21. Alternative cooling	g water supply	p.
(14 cm model)		180
22. Variation of m and	1 h (12.7 cm model).	181
23. Variation of T (1	L2.7 cm model)	182

1

,

\*

4

## NOMENCLATURE

```
Α
     -area
     -constant
d, D -diameter
     -factor
f
F
     -force
     -gravity acceleration
g
     -incident radiant energy
G
     -enthalpy
     -height
h
     -heat transfer coefficient
h '
     -latent heat of vapourization
h
     -head
Н
     -constant
K
1, L -length
m, M -mass
p
     -pressure
     -power
p
q, Q -heat transfer rate
Q -discharge
     -Reynolds number
     -specific gravity
S
```

-time

t, T -temperature

```
u, V -velocity
```

Y -distance of freon liquid-vapour interface from top of heat exchanger

W -work

n -efficiency

p -density

τ -period of oscillation

∀ -volume

# Subscripts

a	-atmosphere
b	-body
С	-collector
С	-condenser
cc	-condenser coil
cl	-condenser/liquid
ct ,	-top of condenser coil
cv-1	-condensation from vapour to liquid
cyl	-cylinder
eff	-effective
el-v	-evaporation from liquid to vapour
ຄນລກ	-avanoration

```
-external
ext
f
          -freon
fric
          -friction
h
          -evaporator
hb
          -bottom of evaporator
hi
          -evaporator inlet
          -evaporator/liquid
hl
         -top of evaporator
ht
          -evaporator/vapour
hv
i
          -inlet
ind
          -indicated
L
         -freon liquid
         -liquid to condenser
lc
m
         -average
out
         -outlet
ov 、
         -overall
         -pressure
р
         -resultant
R
         -shear
T
         -temperature
T
         -thermosyphon
T
         -tilt
         -thickness
th
         -total
tot
```

-useful

u

хiх

-vapour

-vapour recondensation in the liquid

-water

Superscripts

n -new value

o -old value

#### CHAPTER 1: INTRODUCTION

Many underdeveloped and developing countries are plagued by drought, especially in Africa, where due to lack of water large portions of the land are left barren. The energy problem of these countries could be helped with the exploitation of solar energy, which is usually an abundant resource in these arid and semi-arid areas. Solar pumps could play an important role in providing water distribution systems for irrigation (1)\* and convenient storage for humans and livestock (2).

Conventional pumping technology which implements electric motors or fuel engines to drive mechanical pumps is currently more practical and efficient than solar pumping technology, which is still immature and expensive (3). However, due to the unavailability and unreliability of electricity and fuel resources in the above mentioned areas, independent solar pumping units, especially if they are of a simple design requiring a low level of maintenance, seem to be an ideal solution for irrigation systems in these isolated areas.

<sup>\*</sup> Numbers in parentheses indicate references.

#### 1.1. HISTORICAL DEVELOPMENT OF SOLAR PUMPS

Figure 1.1 illustrates the various options for solar powered pumping systems. In this figure, solar liquid piston pumps (SLPPs) fall in the category of "special design and pump".

A machine to pump water using solar energy was described for the first time by Solomon de Caux, a French engineer, in 1655 (4). However, the first experiments were carried out only in the late 19th century, by Guntner of Austria, Mouchot and Pifre of France, Ericson in the U.S.A. and Adams in India. Most of these early experiments incorporated tracking solar concentrators and Rankine engines which used steam as the working fluid. In addition, Ericson built seven open cycle hot-air engines (4).

An experiment carried out in 1885 by Charles Tellier at Auteuil, France, is the earliest known ancestor of Solar Liquid Pumps. The working fluid was ammonia, which was heated in solar collectors. The ammonia vapour thus produced provided the pumping action by displacing water inside an iron sphere. The ammonia was separated from the water with a flexible rubber membrane (4).

During the 1960's and the 1970's a variety of solar pump designs was made. T. Finestein's and E. Farber's Solar Stirling Engine, M. Borde's Solar MHD, C.D. West's Fluidyne,

D.P. Rao's SLPP, A. de Beer's and Pelegano's "Camel" Rocking
Beam Solar Pump, Minto's Solar Wheel and R. Bernard's Minimum
Maintenance Solar Pump. Also Thermo-electric and Photovoltaic
pumps and organic fluids for Rankine Cycle engines were
developed about the same time (3 to 9).

By 1981, emphasis was given to the implementation of photovoltaic cells, with at least 60 small pumps incorporating PV cells being installed around the world. Most of them were installed by the French company Pompes Guirard and Solar Electric International of the U.S. Although PV cells were too expensive to compete with solar thermal engines for irrigation systems, continuous production processes for producing the silicon wafers could bring their cost down significantly. However incorporating electric motors and mechanical pumps are relatively sophisticated systems to be maintained in isolated rural areas.

In contrast to PV pumps, solar thermal pumps are not yet produced on a completely commercial basis (3). However, the French company Sofretes has installed a significant number of field units, and there are also several others, like Ormat Turbines Ltd. (Israel), Dornier Systems (W. Germany), Hindustan Brown Boveri (India), Grinakers Ltd. (South Africa), Solar Pump Corporation, Barber Nichols and Sunpower Systems Inc. (U.S.A.). The degree of development of the available solar pumps however is not sufficient for competition with

conventional energy conversion systems. In any case they suffer the same disadvantages as the PV pumps in that they require a high level of technology and therefore they are difficult to maintain in isolated rural areas.

efficiencies due mainly to the low temperatures at which the solar energy is collected. The ideal Carnot efficiency for a hot temperature of 80°C and a cold temperature of 20°C is 17 %. A reasonably efficient thermal engine should achiève 20 % of the Carnot efficiency to give an overall thermal efficiency of about 3.5 %. The maximum theoretical efficiency obtainable from direct conversion of solar radiation to electricity with a PV device is about 21 %. Present efficiencies of the more economical silicon wafers are around 11 % to give an overall system efficiency of 4.5 % (3).

A wide range of efficiencies is claimed for thermal pumps depending on how specialized the design is, but mostly depending on the collector used and hence the temperature of the hot fluid available for heating. Bell's fluidyne, for instance, has an efficiency of 0.18 % whereas West and Pandey claim an efficiency of 7 % for theirs developed at the Metal Box Company in India (5). The overall system efficiency of the 5 kW solar pump installed by Sofretes in Niger (incorporating a flat plate solar collector) is 1.25 % while the efficiency of its Rankine engine/pump subsystem is about

2 % (3). System efficiencies of about 3 % are claimed for many organic Rankine cycle prototypes by other manufacturers. These efficiencies however, have not yet been confirmed by independent testing, with the exception of the Batelle pump, which was tested at Sandia Laboratories in the U.S. and the test's performed by Sir William Halcrow and partners in the U.K.

There are not many options for using the electrical output from PV pumping systems. Most designs use off-the-shelf commercially available electric motors and pumps. Research activity is limited almost entirely to the photovoltaic panel conversion components. Solar pumping thermal systems are more complex since all the components need to be designed to match the thermal input delivered to the system from the solar panels, or storage reservoirs if utilised. In addition, the output shaft torque and speed should be matched to a suitable pump to fulfill the required pumping conditions of head and mass flow of water. If no provision is made for storing the thermal energy from the solar panels, then the system must be designed to operate efficiently under daily and seasonal variations of the thermal input. Considering these requirements the design of solar thermal pumps is a fertile area for research.

## 1.2. OPERATION OF THE SOLAR LIQUID PISTON PUMP

In the SLPP, the up and down oscillations of a liquid column which is contained at the sealed upper part of a cylinder (figure 1.2) are converted into pumping action by two one way check valves at the inlet and outlet pipes located near the bottom of the cylinder.

These oscillations are generated by cyclic vaporization and condensation of the working fluid at the top of the cylinder. Trichlorotrifluoroethane (CCl<sub>2</sub>FCClF<sub>2</sub>), commonly known by the Dupont tradename of Freon 113 was used as the working fluid. It was chosen because its boiling point of 47°C at atmospheric pressure is suitable for use with flat plate solar collectors. A flexible polyethylene seal separates the Freon 113 from the water being pumped.

The liquid. Freon 113 is vapourized when it comes in contact with the evaporator and is condensed at the condenser. Although in the SLPP the working fluid goes through compression, evaporation, expansion and condensation as in a typical Rankine engine, it differs because all these processes take place within the same working volume instead of taking place in separate compartments. The disadvantage of this arrangement is that in some intervals of the time period of the cycle evaporation and condensation overlap. However, this disadvantage is offset by the simplicity of the SLPP.

The SLPP features the most simple design for a solar thermal pump, combining the thermal engine and the pump into one unit. The two mechanical pumps and the turbine reciprocating expander which are required for a solar organic Rankine cycle system are replaced by the oscillating column. The only mechanical moving parts required are two one way check valves.

The oscillatory motion of the liquid column is self-starting and remains stable provided that the hot and cold water flows through the evaporator and the condenser respectively, are sufficient to keep the corresponding temperatures above and below critical values. The critical temperatures depend on the suction and delivery pressure heads which also have critical maximum limits for sustained operation of the SLPP.

# 1.3. REVIEW OF RESEARCH ON SOLAR LIQUID PISTON PUMPS

In the department of Mechanical Engineering at McGill University, research on SLPPs started in 1976, when the oscillations of a liquid column inside a straight glass tube were theoretically and experimentally studied (10). Then some experiments were carried out with a fluidyne heat engine and a flash boiling liquid piston pump was developed (11, 12, 13). Eventually a circular model was designed and successfully

operated (14, 15).

Some modifications were done on this model concerning better sealing and a limited optimization of the relative positions of the evaporator and the condenser (16, 17). The performance characteristics of this modified 10 cm circular SLPP were studied experimentally, varying the inlet and outlet pipe lengths and obtaining pressure-volume diagrams (18). Then, a rectangular model was constructed (19) in an attempt to reduce the pressure drop across the evaporator. This model did not work very well initially, because of the poor mixing of the hot water in the evaporator. At this time it became apparent—that a computer simulation model would be needed in order to optimize the SLPP. A semi-empirical model was developed based on the results from the 10 cm circular model (20, 21).

Independent research has been carried out in India on the Hindustan Brown Boveri Mark 1 solar pump. Its basic operation is similar to the McGill SLPP except that vaporization takes place continuously in the solar collector and it is the condensation process that occurs intermittently (7, 8). As a consequence of the spatial separation of the condensation and evaporation processes, it is possible that the Mark 1 could achieve higher efficiencies than the McGill SLPP. Its system layout however, is far more complex than that of the McGill SLPP. It is possible that this, combined with

the use of flammable m-pentane as the working fluid, will counterbalance the lower efficiencies associated with the McGill SLPP.

#### 1.4. OBJECTIVES

The work in this thesis was focused on the following objectives:

- i) obtain theoretical predictions for the performance of the 10 cm circular model and of geometrically scaled models
- ii) construct and test experimentally a geometrically scaled model
- iii) study the technical aspects of matching the SLPP with a solar collector.

In order to achieve the first objective and to interpret the theoretical predictions, the work was based on the computer simulation program and the theoretical framework developed earlier by A. B. Hammond (20). For this reason and for conciseness, chapter 2 is a review of the theoretical modelling of the SLPP. Then chapters 3 and 4 deal with the theoretical and the experimental results respectively, while in chapter 5 the results from the two previous chapters are compared and discussed. Finally, chapter 6 discusses the matching of a solar collector with the SLPP.

## 2.1. BASIC MODEL

In this chapter, the physics of the theoretical model will be discussed leading to the description of the computer modelling of the SLPP.

The basic operation of the SLPP is analysed with reference to the p - V diagram, figure 2.1. At point 1 there is a maximum volume -minimum height of the liquid column- and a minimum pressure. At this point the inlet valve opens. The liquid starts moving upwards, reducing the volume of the vapour along the assumed line of constant pressure and temperature, 1-2. The liquid is below the heater level and net heat is rejected to the condenser by means of condensation. Water is taken in, increasing the momentum in the main cylinder and inlet pipe. At point 2 the liquid contacts the heater. Due to inertia effects, the volume continues to decrease and the vapour is compressed along an assumed constant quality line 2-3. During this time, evaporation of the liquid begins, which increases the pressure and inhibits the upward motion of the liquid until this motion is stopped (point 3). At this minimum volume and maximum

pressure, the inlet valve closes and the outlet valve opens. The pressure and the temperature are assumed to remain constant along the line 3-4 while vaporization is dominant. The volume is increased and water is forced out, increasing the momentum in the main cylinder and the outlet pipe. At point 4, saturated conditions for the vapour are assumed to be achieved. The liquid is no longer in contact with the heater and vaporization stops. However, the volume continues to decrease along the assumed 100 % quality line 4-1, due to inertia effects. At the same time, the pressure of the vapour is decreased due to condensation, until the downward motion is arrested.

### 2.2. PHYSICS OF THE THEORETICAL MODEL

## 2.2.1. THERMODYNAMIC CYCLE

The major assumption made for the SLPP thermodynamic cycle follows directly the description of its operation based on the p - V diagram. It was assumed that the changes of state of the freon vapour follow a cyclic process which resembles the Rankine cycle because it includes two constant pressure processes. However, it also includes two constant vapour quality processes instead of the two constant entropy

1

processes that the actual Rankine cycle includes. This assumption can be clearly visualized with the help of a p-h diagram, figure 2.2.

The processes 2-3 and 4-1 take place at constant vapour quality while 3-4 and 1-2 are at constant pressure and temperature. Under this assumption, the mathematical modelling of the SLPP is simplified. For example, if a constant entropy line was followed from state 4, then the vapour would enter the superheated region, thus increasing very much the complexity of the model. However, experimental p-v diagrams indicate that the cycle is similar to the dotted cycle in figure 2.2.

The p-h diagram for Freon 113 shows that in the area of interest the two constant quality processes can be represented by:

where K'  $_{\rm P}$  and K'  $_{\rm T}$  are constants depending on the dryness fraction of the vapour

For the sake of simplicity, an approximated form of the above equations was introduced:

$$p_{\nu}=K$$
 [2.1]\*

\* Numbers in brackets indicate equations.

$$Tv^{1/2} = K$$
 [2.2]

where the constants K  $_{\underline{P}}$  and K  $_{\underline{T}}$  also depend on the dryness fraction of the vapour.

## 2.2.2. HEAT TRANSFER

There are several modes of heat transfer that take place in the upper part of the SLPP. In particular, there is heat transferred from the evaporator to vapourize the liquid,  $q_{el-v}$ , and heat transfer from the vapour to the condenser,  $q_{cv-1}$ , as a result of condensation. Also, heat is transferred from the evaporator to the vapour directly,  $q_{hv}$ , and from the liquid to the condenser,  $q_{lc}$ . Finally, there is heat transfer from the recondensed vapour to the liquid,  $q_{v-1}$ .

The latter heat transfer rate was assumed to be a certain fraction of  $q_{el-v}$ , which is an exponential function of the depth of the liquid above the evaporator, so that as that depth increases,  $q_{v-1}$  approaches  $q_{el-v}$  asymptotically.

There are other minor heat transfer rates, for example between the liquid surface and the vapour, mainly by radiation and convection, which were considered to be comparatively small with respect to the other modes of heat transfer and

they were therefore neglected.

Effective evaporation takes place due to the difference between  $q_{el-v}$  and  $q_{v-1}$ , so that the mass rate of evaporation,  $M_{evap}$ , is a function of their difference. The vapour condensation rate,  $M_c$ , is a function of  $q_{cv-1}$ . The net vapour generation was assumed to be:

which after algebraic manipulations becomes

where

with

$$B=2.5$$
 cm

It must be noted that the various heat transfer coefficients were initially given values estimated from handbooks. These values were then corrected in order to

calibrate the model (20).

#### 2.2.3. ANALYSIS OF THE FLOW

The flow in the outlet and inlet pipes is a pulsating flow which, under the assumption that at any instant the velocity profiles in each pipe will be the same along the whole length of the pipe, can be considered as a pulsating fully developed flow (20).

Following an analysis for this type of flow according to the geometrical characteristics of the pipes and a Reynolds number specially defined for this purpose (5, 20), the flow can be classified as pulsating laminar flow in wide tubes, where the friction losses can be determined using the D'Arcy-Wiesbach equation:

$$\Delta p = 4 f \frac{L}{fric} - \frac{\rho V^2}{2}$$

$$D = 2$$
[2.5]

Flow analysis of the three liquid columns

The standard method employed was a control volume analysis, using the linear momentum equation. According to this analysis, the resultant force F  $_{\rm R}$  on the particular control volume is considered as the sum of the external forces F  $_{\rm ext}$ , the pressure forces F  $_{\rm p}$ , the shear forces F  $_{\rm s}$  and the body forces F  $_{\rm b}$ .

First, the SLPP was divided into three liquid columns with each one being examined separately.

# a. Main cylinder

The lower boundary of the control volume was located just above the valves where it was assumed that the pressure is uniform. The upper boundary was located low enough so that it would always remain within the liquid column, in order to avoid the problem of a moving control volume. In addition, it was assumed that at the top of the control volume the pressure was uniform and that the mass in the liquid column remained constant. The pressure losses across the diaphragm and due to wall friction were considered to be negligible in comparison to friction in the inlet and outlet pipes. According to a rough estimate, the ratio of the wall friction losses to those in the inlet and outlet pipes was less than 0.02 % of the squared ratio of the respective velocities. According to these considerations, the shear forces in the working tube were taken to be zero. In the absence of other types of forces such as centrifugal and electromagnetic which fall under the general category of external forces, the forces acting on the control volume were:

$$F = -M$$

and

$$F = (p - p)A = v \cdot p \cdot cy1$$

A final assumption was made. It concerned the velocity of the liquid inside the control volume which was considered to be uniform and equal to the velocity of the liquid-vapour interface Y.

This velocity can be related to the outlet and inlet pipe velocities by applying the principle of continuity to the main cylinder:

# b. Outlet pipe

The boundaries of the control volume for the outlet pipe were located just downstream from the outlet valve on the pipe walls and the outlet of the pipe. The forces acting on this control volume are:

$$F = (p - p) A$$
 $p$ 
 $F = -p g(H + L) A$ 
 $f = -(\delta p) + \delta p$ 
 $f = -(\delta p) + \delta p$ 

The friction losses were computed using equation [2.5] while the entry losses associated with the transition from the main cylinder to the outlet valve and the outlet pipe, were

taken to be:

with K fric the pressure loss coefficient,

Combining equations [2.8], [2.9], [2.10] and doing some manipulations, (20), gives:

## c. Inlet pipe

The analysis of the inlet pipe is similar to the outlet pipe; the force equations are:

$$F = (p - p)A$$

$$F = \rho g(H + L)A$$

$$E = (\delta p + \delta p)$$

$$f = (\delta p + \delta p)$$

Here, the exit losses associated with the transition from the inlet pipe through the inlet valve and into the main cylinder were assumed to be double the entry losses (20).

Finally, in much the same way as for the outlet pipe, the following equation was obtained:

$$\begin{pmatrix} M & A & M & A & M \\ \frac{i}{i} & \frac{i}{cy1} & \frac{cy1}{i} \end{pmatrix} \nabla = \begin{pmatrix} \frac{cy1}{cy1} & \nabla & \frac{cy1}{cy1} \\ A & A & A \\ i & cy1 & cy1 \end{pmatrix} \begin{pmatrix} A & A & A \\ cy1 & cy1 & cy1 \end{pmatrix}$$

$$- \rho g(H-L) - (\delta p + \delta p) - \frac{M}{cyr}$$

$$= \frac{1}{cyl} fric exit$$

$$A$$

$$= \frac{1}{cyl}$$

In the above analysis it has been assumed that the external forces are equal to zero.

## 2.2.4. GEOMETRICAL PARAMETERS

## a. Liquid contact areas

In order to calculate the various heat transfer coefficients for the processes taking place in the upper part of the SLPP, the liquid contact areas must be calculated. But both the evaporator and the condenser are of an irregular shape, so that it was necessary to make some assumptions. The respective liquid contact areas were assumed to be uniform in the vertical direction and therefore functions of Y only, the distance of the liquid-vapour interface from the top of the main cylinder. In addition, the upper straight portion of the condenser was taken to be negligible compared to the rest of it.

With these approximations, simple linear equations with respect to Y were obtained for the various liquid contact areas such as the heater-liquid, the condenser-liquid, and also the heater-vapour and the condenser-vapour contact areas (20).

## b. Vapour volume

The specific volume of the vapour must be known in order for the pressure and temperature of the vapour to be determined over a time interval.

For this task, first the volume occupied by the vapour

in the upper part of the SLPP was calculated under the assumption that for both the condenser and the evaporator coils, the total volume of each one is distributed uniformly over its total length. Taking into account the upper straight portion of the heater as well, the volume of the vapour was obtained as a function of Y (20).

Finally, dividing the obtained volume that the vapour occupies by the mass of the vapour yielded its specific volume. Thus the pressure and temperature of the vapour could be determined at any time during the cycle from equations [2.1] and [2.2].

## 2.2.5. HEATER, CONDENSER AND LIQUID FREON TEMPERATURES

Initially the temperature was assumed to be stantaneously the same over the evaporator surface due to the relatively small temperature differences between the evaporator inlet and outlet. This lead to a differential equation which was integrated to give (20):

$$\frac{1}{h} \Delta t \hat{T}_{hi} + \frac{1}{m} \begin{bmatrix} m - m \Delta t \end{bmatrix} \hat{T}_{h}^{\circ} - \frac{1}{m}$$

$$\frac{1}{m} = \frac{1}{m} \begin{bmatrix} m + m \Delta t \end{bmatrix}$$
[2.14]

This equation was used for obtaining the average evaporator temperature at the end of each time step.

In the 10 cm model which was used for the calibration of the computer model, the condenser consisted of a double coil which coiled down and back on itself. Based on that, it was assumed that the condenser surface was at a uniform temperature.

Finally, the constant mixing of the liquid freon in the neighborhood of the heating and condensing coils lead to the assumption that the temperature of the liquid freon is uniform and remains constant.

## 2.2.6. MASS AND ENERGY CONSERVATION

The principles of conservation of mass and energy were applied in order to provide a criterion for checking the validity of the theoretical model.

According to the principle of conservation of mass, the mass of freon evaporated over a cycle must equal the mass of freon condensed over the same cycle. Under the assumption that there are no heat losses through the diaphragm and the main cylinder walls to the surroundings, this reduces to:

$$\int_{\mathbf{q}_{v-1}} dt = \int_{\mathbf{q}_{v}} dt$$
 [2.15]

which was used as a criterion for choosing the constant freon. liquid temperature.

The principle of conservation of energy provided the equation (20):

$$\int_{\mathbf{q}_{b,v}} d\mathbf{t} = \int_{\mathbf{p}_{v}} d\mathbf{v} \qquad [2.16]$$

which was used for the choice of the heat transfer coefficient for the heat transfer between the heater and the vapour.

## 2.2.7. PERFORMANCE CRITERIA

The indicated power is the cyclic integral of the  $p-\Psi$  diagram:

$$\overline{W}_{ind} = \frac{\int (p A Y) dt}{v eff}$$
 [2.17]

The average discharge flowrate is:

$$Q = \frac{\int (A V) dt}{2.18}$$

The power output is a function of the discharge and the pump head:

$$W = \rho g(H - H)Q$$
 [2.19]

The power input is the total rate of heat transfer from the evaporator into the system:

$$q_{tot} = \frac{\int (q_{el-v} + q_{hv})dt}{(2.20)}$$

The indicated and overall efficiencies are:

$$\eta_{ov} = \frac{\varphi}{Q_{tot}}$$
 [2.22]

## 2.3. THE COMPUTER PROGRAM (20)

The main function of the computer program is to solve the system of the four non-linear equations [2.4], [2.7], [2.11] and [2.13]. For this purpose the IMSL subroutine DGEAR was used, which is a predictor-corrector type of differential equation solver. The main program -MAIN- generates time intervals of 0.02 seconds, at the end of which it calls DGEAR. Initially, MAIN allows 6 seconds for the initial transition to settle out, using assumed input data for the mass of the vapour M v and the position of the liquid-vapour interface.

The program engages an iterative computation of the freon liquid temperature T  $_{\rm L}$ . An initial guess value for T  $_{\rm L}$  is used. Then the computation runs for four or five cycles until, with the aid of a secant method iterative scheme, convergence is achieved. Then, a final round of computation is employed in order to compute the various performance criteria

that characterize one cycle.

In general, MAIN first sets the initial conditions and the time intervals. For this purpose, it utilises DEFCON, a subroutine which computes the program constants, mainly geometric. Then MAIN sets the initial position of the liquid-vapour interface at the bottom of the heater. With this position as input data, subroutine VANDA computes the various contact areas as well as the volume of the freon vapour.

Next, DGEAR solves the system of differential equations with the aid of two subroutines, FCN and FCNJ. FCN computes the rate of change of the state variables and determines the position on the p-h diagram while FCNJ computes the 4x4 Jacobian matrix of partial derivatives for the system in question.

After DGEAR has yielded the new values of M , ,V , ,V , ,n and Y, first MAIN checks the stopping condition, in other words, whether the model has been led to a simulated stall. This condition requires that there must not be any flow at all for the last 0.5 seconds. If the stalling condition is not satisfied, the average heater temperature is computed in THNEW. Then MAIN checks if initial transient has been settled out. If this is the case, the program proceeds. If not, it takes the computations back to DGEAR again.

Now subroutine CYCLE is called, which compares the new

value of the vapour pressure to the old one and identifies one cycle. Then it computes the performance criteria and checks if convergence has been achieved for this value of T L. For this purpose, equation [2.15] is used. If the final value of T L has been reached, control is transferred to MAIN, which, with the aid of subroutines OUTPUT and FINAL prints out the results engaging also the McGill University Fortran subroutine PLOT1 which draws the required graphs. If however, convergence has not yet been achieved, CYCLE utilizes a secant iterative scheme to obtain a new value for T L. The computations are then taken back to the step where DEFCON computes the initial values for a new round of computations.

A listing of the program is presented in Appendix 2.

The computer program was used to run several tests on the theoretical model. The results obtained from these tests could be used in two ways. First, they would show the extent to which each parameter has an effect on the performance of the SLPP and indicate the range of each parameter where optimization of the SLPP can be pursued. Then, the experimental testing of the SLPP, which would be more limited in extent, could be focused on the appropriate parameter variations. Second, the theoretical results could be compared with those obtained experimentally to determine the limitations of the theoretical model. It must be noted that the theoretical model was based on empirical data obtained from tests on a 10 cm model.

The parameters that were varied can be divided into two categories. First, parameters that are associated with the hot and cooling water flows through the SLPP, such as the hot water inlet temperature T  $_{\rm h\, I}$ , the hot water mass flowrate m  $_{\rm h}$  and the cooling water temperature T  $_{\rm c}$ . Second, parameters that have to do with the geometry of the SLPP, especially the heat exchangers. These were the surface area of the lower part of the heater A  $_{\rm h\, b}$ , the distance of the heater and the condenser from the top of the cylinder L  $_{\rm h}$  and L  $_{\rm c\, t}$ 

respectively, and the thickness of the heater L  $_{\rm th}$ . Each of these parameters was tested for different values of the total head while the rest of the parameters were kept constant. The outlet head was varied from 1.0 to 2.5 m while the inlet head was kept constant at 1.5 m.

The theoretical results obtained from each run are presented and interpreted in terms of the theoretical model in a qualitative way. Some minor modifications had to be incorporated to the original program to allow for some of the geometrical variations, notably in altering the scale size.

The performance of the model is presented in terms of the discharge and the efficiency versus the total head. The power output is not plotted because it can be expressed as a function of the discharge and the total head.

\*\*\*

## 3.1. RESULTS ON THE 10 CR MODEL

#### 3.1.1. HOT WATER INLET TEMPERATURE

T  $_{\rm h\, i}$  was varied in a range between 71 and 93°C. The results are in figures 3.1 and 3.2. The discharge and the efficiency of the model increase as T  $_{\rm h\, i}$  increases.

The average heater temperature T  $_h$  is a function [2.14] of the hot water inlet temperature T  $_h$  is a function [2.14] of the hot water inlet temperature T  $_h$  is that an increase in T  $_h$  i results in an increase of T  $_h$ . The heat transfer rates from the heater to the vapour q  $_h$  v and to the liquid q  $_{el-v}$  both increase with T  $_h$ . The effect of increasing q  $_{el-v}$  is to increase both the mass rate of evaporation M  $_e$  and the heat input to the model. The former results in increasing the rate of producing vapour in the upper part of the working tube and therefore decreasing its specific volume since the volume of the vapour has remained unchanged. Thus the pressure of the vapour is increased [2.1] leading to an increase in the outlet velocity [2.11]. Following V  $_o$ , the discharge [2.18] will also increase and with it the power output [2.19]. The overall efficiency will also increase through [2.22] despite the fact that an increase in T  $_h$  i increases the total heat input.

## 3.1.2. HOT WATER MASS FLOWRATE

 $\mathfrak{m}_h$  was tested for different values in a range that is within the limits of the actual models. The results are shown in figures 3.3 and 3.4. It can be seen that for the variations of  $\mathfrak{m}_h$  considered, the discharge increased slightly at the higher heads with a small overall increase in the efficiency.

The average temperature of the heater T  $_h$  is also a function of the hot water mass flowrate [2.14] but the functional relationship here is not very strong so that when  $\mathfrak{m}_h$  is increased T  $_h$  will increase only slightly. Through T  $_h$ , the variations of  $\mathfrak{m}_h$  lead to the same effects that were discussed previously for an increase in T  $_{h_1}$ .

## 3.1.3. COOLING WATER TEMPERATURE

T  $_{\rm c}$  was varied between 10 and 27°C. Figures 3.5 and 3.6 show that increases of T  $_{\rm c}$  have the inverse effect on the discharge while the efficiency increases as T  $_{\rm c}$  increases. In addition, at the higher values of T  $_{\rm c}$  the model stalls.

When T  $_{\rm c}$  is increased the heat transfer rate from the vapour to the condenser q  $_{\rm c\,v^{-1}}$  will drop so that the mass rate of condensation M  $_{\rm c}$  decreases. On the other hand, the liquid temperature T  $_{\rm L}$  will increase with T  $_{\rm c}$  leading to a drop in

per since it is a function of the temperature difference between the heater and the liquid. This will result in decreasing the mass rate of evaporation M. Also, as a result of the decrease in q. el-v., the hot water outlet temperature will increase so that the heat input to the model will decrease. This decrease of both M. and M. results in decreasing the mass of the vapour per cycle in the working tube [2.3] which, as it was discussed before, will lead to a decrease in the discharge and therefore in the power output. However, the decrease of the heat input is larger compared to that of the power output (Table 3, Appendix 1.1) and this has the net effect of increasing the efficiency.

As a consequence of the above, higher values of  $\mathbf{T}_{\,\mathrm{c}}$  will result in smaller condensation and evaporation rates so that the model eventually will stall.

# 3.1.4. SURFACE AREA OF THE LOWER PART OF THE HEATER

The results obtained by varying A  $_{\rm h,b}$ , figures 3.7 and 3.8 show that both the discharge and the overall efficiency are increased as A  $_{\rm h\,b}$  increases. In addition, they show that for small values of A  $_{\rm h\,b}$  the model will not operate.

When the surface area of the lower part of the heater is increased, the contact area of the heater with the liquid is increased correspondingly, resulting in an increase of

q elev . Thee discharge and the efficiency will therefore increase following the effects that were previously discussed.

It must be noted that the size of the working tube imposes a limitation on how much A hb can be increased.

## 3.1.5. DISTANCE OF THE HEATER FROM THE TOP

The results obtained when L  $_{\rm h}$  was varied are in figures 3.9 and 3.10. They exhibit the trend of improving performance with smaller values of L  $_{\rm h}$ .

Small values of L h means that the evaporator is brought closer to the top of the cylinder. But since the location of the evaporator determines the position around which the oscillations of the liquid vapour interface take place, the interface will also be brought closer to the top of the cylinder. The volume of the vapour as well as its specific volume will therefore decrease resulting in an increase of the vapour pressure which leads to an increase of the outlet velocity V ([2.kl]) and thus of the discharge and the overall efficiency. In other words, there will be less inactive vapour volume at the top of the working tube.

The increase of V or results in an increase of the amplitude of the oscillations through [2.7], figure 3.11, because the surface areas involved remain constant. At the same time, the frequency remains practically constant, figure

3.12.

It must be noticed however, that before L h was able to reach its limiting value of 0.0 cm, the model started predicting negative values of the distance Y between the liquid-vapour interface and the top of the cylinder. This happened at 0.63 cm from the top, and it is probably due to the prediction of very large amplitudes in this case, as the trend of figure 3.11 implies, because the computer program does not allow for restrictions of the amplitude at heater positions close to the top of the working tube.

## 3.1.6. DISTANCE OF THE CONDENSER FROM THE TOP

The results obtained from varying  $L_{ct}$  are in figures 3.13 and 3.14. They show that the performance of the model increases as the condenser is lowered, i.e.  $L_{ct}$  increases. However, as  $L_{ct}$  is increased beyond 2.5 cm the model will not operate at the higher heads.

when the distance of the top of the condenser from the top of the working tube L  $_{\rm ct}$  is increased, the theoretical model predicts no change in the vapour volume, since it is not a function of L  $_{\rm ct}$  (20). However, the contact area of the vapour with the condenser decreases, while that of the liquid with the condenser increases, thus increasing the mass of the vapour at the top of the working tube [2.4]. Therefore, the

specific volume of the vapour decreases leading to an increase of the vapour pressure through [2.1]. As a result, the outlet velocity will increase [2.11] as well as the amplitude [2.7], (figure 3.15), while, following the increase in V , the discharge will increase too [2.18], together with the power output [2.19].

The decrease in the condensation rate M  $_{\rm c}$  that is brought about by the decrease in the vapour-condenser contact area, will eventually result to decrease the evaporation rate, through the conservation of mass principle [2.15], decreasing the heat input to the model. Since there is a decrease in the heat input and an increase in the power output (Table 6, Appendix 1.1), the efficiency increases. But the more L  $_{\rm ct}$  is increased, the more M  $_{\rm c}$  will decrease and consequently, at the higher values of L  $_{\rm ct}$  the model will be unable to overcome the higher heads and it will stall.

## 3.1.7. THICKNESS OF THE HEATER

The variations of the heater thickness L th show that the discharge and the efficiency of the model increase as the thickness of the evaporator is decreased, figures 3.16 and 3.17.

When the evaporator is thicker, the liquid remains in contact with it for a longer time period. But since the

surface area and the temperature difference have not changed, the heat transfer rate from the evaporator to the liquid and consequently the mass rate of evaporation remain unchanged. However, now evaporation occurs over a longer time period. That means that although the vapour pressure has not changed, it remains longer at the same level. But the computer program identifies the transition to the subsequent stages of the SLPP cycle by means of the pressure changes in order to determine the time period of the cycle. Because of this, now the time period of the cycle will be increased, or the frequency will be decreased (figure 3.18). As a result, the discharge will decrease [2.18] together with the power output and the efficiency.

Varied together with its diameter in order to keep the surface area constant. Therefore increasing the thickness of the heater resulted in a heater with smaller diameter as well. This however introduced another effect, namely that of varying the heater diameter. In order to separate the two effects, the results on the performance of two heaters with the same diameter but with different thicknesses are compared in figure 3.19. It can be seen that although in this case the thicker heater has also a larger surface area, the discharge and the efficiency are decreased. This justifies the previous discussion, indicating that the increase in the thickness is

the dominant effect.

In all the previous results there is a clear trend of decreasing discharge with increasing total head. In the theoretical model this effect comes from equation [2.11], where it can be seen that an increment of the outlet head H owill result in decreasing the outlet velocity V or and therefore the discharge of the model.

Figure 3.20, based on the results obtained from the tests on T  $_{\rm h\, i}$  variations, shows the power output plotted against the overall efficiency  $_{\rm h\, i}$ . It can be seen that p  $_{\rm o}$  increases proportionally to  $_{\rm h\, i}$ .

An observation of the tabulated results shows that when the rest of the parameters are kept constant, the power output tends to increase together with the total head  $\Delta H$ . But the discharge decreases with  $\Delta H$  so that the effect of  $\Delta H$  on p o is more dominant than that of the discharge.

## 3.2. SCALING

Another set of results was obtained by varying the scale size of the SLPP. The intention was to explore the performance of the SLPP when its size is varied, something that would be difficult to do experimentally because it would require the construction of several models. For this purpose the program was scaled geometrically. This was done by introducing a scale factor "f" as the ratio of the diameter of the model over the diameter of the reference model which was 10 cm. All the qeometric parameters were multiplied with f to the appropriate power; that is to say, lengths were multiplied with the scale factor in its first power, surfaces with f2 etc. Other parameters that were associated with the geometry of the SLPP were also scaled accordingly. Such parameters were the volume of the freon in the main cylinder which was multiplied with  $\hat{f}^3$ and the hot water mass flowrate which was scaled proportionally to the cross-sectional area change of the heater coil. The inlet and outlet heads and tube lengths and diameters were not scaled.

The tests were carried out for scale factors from 0.8 to 1.3. The results obtained are shown in figures 3.21 and 3.22. It can be seen that the discharge increases with the scale factor while the efficiency does the opposite.

Figure 3.23 shows the amplitude plotted against the scale factor for three different total heads. The amplitude decreases with the total head while, taking into account the acceptable roundoff errors, it remains almost constant for the different scale factors. Since the amplitude remains constant, the trend of increasing outlet velocity with increasing scale factor will occur through [2.7]. This is because the effective cross-sectional area of the main cylinder increases proportionally to f' while the cross-sectional area of the outlet pipe is not scaled. The outlet velocity is not increased proportionally to f2 however, because [2.8] adjusts it in order to take into account the friction losses which, according to the D'Arcy-Wiesbach equation [2.5], are proportional to  $V^2$  . The outlet velocity therefore will increase as the scale factor increases, but less than would be expected due to increased friction losses. The discharge and the power output will increase proportionally to V . .

Figure 3.24 shows that the frequency decreases with increasing scale factor. From [2.4] it can be seen that the mass of the vapour at the top of the working tube is proportional to f<sup>2</sup> so that the specific volume of the vapour is varied proportionally to f and the pressure of the vapour is varied inversely proportional to f [2.1]. Therefore, when f>1, the vapour pressure decreases while when f<1, it increases. The changes in p v in the theoretical model

determine the time period of the cycle so that, when f>l this time period will increase, i.e. the frequency will decrease.

On the other hand, f>l results in increasing the heat transfer surfaces so that the heat input to the model is increased proportionally to f<sup>2</sup>, that is more than the power output is increased. The net result of this is to decrease the overall efficiency with increasing scale factors.

Interest was focused on scale factors larger than unity despite the lower efficiencies because of practical considerations for the construction of an actual model utilizing thermal syphon forces. A working tube diameter of 14 cm which corresponds to a scale factor of 1.375 was chosen.

Using this value of f, another set of tests was carried out on the same parameters that were tested before, in order to enable a direct comparison with the experimental results that would be obtained.

These results are presented in figures 3.25 to 3.36. Except for the expected upwards shifting of the discharge and the downwards shifting of the overall efficiency, the same trends as before are exhibited in all the results; sometimes the trends are more pronounced, as is the case for T  $_{\rm c}$ , figures 3.29 and 3.30, and L  $_{\rm ct}$ , figures 3.35 and 3.36, where the model stalls at smaller distances of the condenser from

the top of the cylinder. Also, the model again started giving negative values of Y as L  $_{\rm h}$  was decreased, but this time this effect appeared on values of L  $_{\rm h}$  below 5.9 cm. The heat input remained always high despite the reductions in T  $_{\rm h\,i}$ ,  $\dot{\rm m}$   $_{\rm h}$  and A  $_{\rm h\,b}$  and decreased only when the thickness of the evaporator was decreased. Finally, the model did not operate at all at total heads higher than 3.5 m.

Two models were built and tested experimentally. The first one, with a tube diameter of 14 cm was designed to allow for the vertical position of the heater and condenser to be varied. The second one did not have an internal condenser coil. The tube diameter was 12.7 cm to provide the same working vapour volume as the first. The condenser and heater were fixed. The model was made of copper and condensation occurred on the inside surface of the working tube.

The main reason why these two models were chosen to be larger than the previous one, was the minimum size of the evaporator coils required for the thermal syphon effect.

For both models the working fluid that was used was Refrigerant 113 (Freon 113).

#### 4.1. LABORATORY FACILITIES

A schematic of the experimental set-up in the laboratory is shown in figure 4.1. The variable input head consisted of a bucket supplied with an overflow drain, which was fastened to a stand so that it could be set at different levels. The make-up water entered the bucket directly from the main water line. The variable output head consisted of a pulley and rope system with which the outlet pipe could be elevated at different heights. The maximum suction and discharge heads obtainable were 1.5 m and 2.5 m respectively, so that the maximum total head was physically limited to 4.0 m.

The discharge was measured by collecting the outlet water in a weigh tank over a time period that was measured with a stop watch.

The hot water was heated in a separate tank by means of an electric heater supplied with a rheostat to control the temperature. With the help of a 1/4 hp gear-type rotary pump, it was circulated in a closed loop, passing through a calibrated rotameter, a valve to control the mass flowrate, the evaporator coil and back to the heated reservoir tank.

The cooling water entered from the main water line, passed through a valve to control the mass flowrate, a rotameter, the condenser and then discharged to the drain in an open loop system. The cooling water temperature was not

controlled.

The temperatures were measured using chromel-constantan thermocouples placed at the inlets and outlets of the condenser and the evaporator and were recorded on a digital Omega meter to the nearest  $\pm$  0.5°C.

A pressure transducer placed at the top of the main cylinder measured the pressure of the vapour. For the volume of the vapour, it was preferred to have it measured in real time instead of the previous method which consisted in recording the pressure on a chart recorder and taking a series of photographs of the chart recorder and the liquid level position together. For this reason considerable effort was devoted to the development of such a device that would measure the volume of the vapour or the position of the liquid-vapour interface.

Resistive type devices to measure the height of the interface between the Freon 113 liquid and vapour were unsuccessful due to the insignificant change in resistance between the two phases. Other systems for measuring a liquid height such as capacitive type, resistance across a "hot wire", photosensors and doppler were rejected in favour of measuring the pressure variations due to a change in height of the liquid column.

Figure 4.2 shows how the pressure transducers and instrumentation were set up. Only one additional tap was

required in the working tube below the liquid level for the condifferential pressure transducer. The output from the differential transducer and the output from the original total vapour pressure transducer were recorded directly on an oscilloscope, or x-y plotter, to obtain the p - V diagrams.

Both transducers were installed above the working tube. The lower line of the differential transducer was filled with liquid Freon 113. A light oil was used in the upper lines of both transducers with a thin diaphragm to separate the oil from the Freon 113 vapour at the top of the working tube in order to avoid gas compression.

Despite these precautions, problems occurred when the check valves opened and closed. Upon closing of a valve a pressure pulse was sent through both pressure lines at different rates which caused the differential transducer to give a "jittery" output, figure 4.3. Mechanical and electrical dampers were introduced to attenuate the "jitters" but too much damping reduced the time response of the system severely. A compromise was made resulting in typical p - V diagrams as shown in figure 4.3.

A static test calibration for the liquid height showed a Freon 113 level sensitivity of 0.000841 v/cm. This sensitivity gave excessively high dynamic amplitudes due to the influence of the pressure pulses from the check valves. The pressure pulses from the check valves varied with the pump head and the

p - V system had to be calibrated dynamically.

#### 4.2. 14 cm DIAMETER SLPP

A scaled drawing of the 14 cm diameter model is shown in figure 4.4. As it was mentioned before, this model was designed with a variable geometry so that the positions of the evaporator and the condenser could be adjusted freely. For this purpose swage locks were used for fastening the evaporator and condenser inlet and outlet pipes to the top cover plate of the tube.

For the condenser, in contrast to the previous 10 cm circular model, only one coil was used which was mounted at the top of the tube by two straight pieces of pipe, so that pressure losses could be minimized. In this way, the cooling water could enter the condenser from the top and flow downwards, or the reverse. The heating coil was built in such a way so that the hot water could flow either from the center to the periphery or the reverse. Outside the tube the inlets and outlets of the condenser and the evaporator could be easily switched.

Finally, as an alternative to the water supply of the condenser, water could be bled off the discharge pipe of the SLPP to enter the condenser.

#### 4.2.1. RESULTS

The parameters that could be varied in this model were the distances of the evaporator and condenser from the top of the cylinder, the hot and cooling water mass flowrates and the hot water inlet temperature. Initially the evaporator was located at a distance of 6 cm from the top and the condenser was at the top of the cylinder. The flowrates were set at average values and the hot water inlet, temperature at approximately 80°C. Then, each one of the parameters was tested separately starting from the cooling water flowrate  $\hat{\textbf{m}}$  . Following this, the hot water mass flowrate,  $\hat{\textbf{m}}$  , the hot water inlet temperature T h, the position of the evaporator L  $_{\rm h}$  and finally the position of the condenser L  $_{\rm ct}$ was varied. After each test was completed, the best value for the corresponding parameter was chosen and was kept constant for the rest of the tests. At each set of tests, the performance characteristics were obtained at half meter increments of the discharge head, from 1.0 to 2.5 m, for three different suction heads, 0.5, 1.0 and 1.5 m. The cooling water inlet temperature for all the tests was 18±3°C.

The results obtained with different cooling water flowrates  $\mathfrak{m}_c$  are shown in figure 4.5. In the figure, the dashed lines indicate the region within which all the results

are scattered in a way that no general trend can be observed. The three solid lines indicate the average discharge for low, medium and high cooling water flowrates. The pump reached a total head of 3.5 m before stalling, with flowrates between 0.033 and 0.060 kg/s and a total head of 3.0 m for the lower ones. A cooling water flowrate of 0.033 kg/s was maintained through the remaining tests in an effort to keep the cooling water needs of the SLPP at low levels, even though better performance was obtained at higher values of m .

Figure 4.6 shows how the performance varies with different hot water flowrates m h . There is a general trend of increasing discharge and therefore power output as m h increases, especially at the lower suction heads. The model reached a maximum total head of 3.5 m with all the flowrates tested except the lowest one, with which it reached a total head of 3.0 m. A hot water mass flowrate of 0.048 kg/s was decided to be maintained constant for the rest of the tests although the SLPP operated better at higher flowrates. This was done because it was not expected to be possible to achieve higher hot water flowrates when the thermal syphon effect would be implemented.

The performance of the SLPP was obtained at three different temperatures, 70°C, 80°C and 90°C (figure 4.7). At

70°C, the discharge was low and the model reached a maximum total head of only 2.5 m. At 80°C the results were better and the pump reached a total head of 3.5 m before stalling, while at 90°C the pump did not stall even at the maximum total head of 4.0 m obtainable in the laboratory. However, despite this clear trend of increasing discharge, efficiency and power output with the hot water inlet temperature, a temperature of 80°C was chosen to be kept constant for the hot water inlet for the rest of the tests, because it is the highest practical temperature that can be obtained from a flat plate solar collector, i.e. without too low a collector efficiency.

The results obtained from locating the evaporator at different distances from the top of the cylinder are shown in figure 4.8. They show that when the evaporator is placed too close, at 5.0 cm from the top, the pump stalls at low total heads. The best performance was obtained with the evaporator at 6.0 cm from the top of the working tube, where the pump reached a maximum total head of 3.5 m. At larger distances from the top -7.0 cm- the discharge is lower again. The distance of 6.0 cm from the top was therefore maintained as the optimum for the heater.

The different distances of the condenser from the top of the cylinder were tested under two conditions, namely with and without insulation outside the inlet and outlet tubes of the evaporator. The results (figure 4.9) showed that the discharge decreased as the condenser was moved away from the top. It can also be seen that when insulation was used the performance of the model was better than when no insulation was used.

However, when the condenser was placed the closest to the top, the opposite was found to occur. The total head at which the pump stalled decreased as the distance of the condenser from the top increased. Finally, it was decided to keep the condenser as close as possible to the top of the cylinder

Another series of tests was carried out that concerned the direction of the flow in the condenser and the evaporator. The way the SLPP was installed, the cooling water entered the condenser at the bottom and left it from the top while the hot water entered the evaporator at its periphery and left from the center. By switching the inlets and outlets, the flow direction was reversed. This was done first in the condenser, then in the evaporator and finally in both so that all the possible combinations were tested.

The results obtained are in figure 4.10 and they show that the SLPP performed better when the hot water was entering the heater at its periphery than at its center. They also show (Table 20, Appendix 1.2) that the SLPP performed better when the cooling water was entering the condenser at its top

than at its bottom, with the exception of the bottom-periphery configuration which gave higher discharge at the lower heads. However, the top-periphery configuration was chosen as the optimum mainly because it gave higher efficiencies while, in terms of the discharge, it was close to the bottom-periphery configuration, especially at the medium and higher total heads. The highest total head that was achieved was 3.5 m and it occurred with a suction head of 1.0 m.

One final test was carried out using the alternative supply of cooling water for the condenser. Water was bled off the discharge pipe and was allowed to pass through the condenser coils. The results obtained (figure 4.11) showed a poorer performance of the SLPP than when the water was coming directly from the main. The poor performance is associated with the very low pulsating mass flowrates of cooling water that were achieved. Also, in many instances the pump could not start at all because initially there was no flow in the discharge pipe and therefore there could be no cooling water flow. It was noticed however, that the cooling water flow was periodic following the periodic flow in the discharge pipe. Also it was observed that the flow in the condenser had a phase difference of 180° with the oscillations inside the In other words, when the liquid freon was going up and evaporation was taking place, there was practically no cooling water flow.

The discharge and the power output reached their overall maximum values of 0.33 kg/s and 7.2 W respectively, when the hot water inlet temperature was set at 90°C. The maximum value of 0.65 % for the efficiency was achieved with a cooling water flowrate of 0.053 kg/s. Typically, the discharge varied between 0.17 and 0.32 kg/s, the efficiency between 0.4 and 0.61 % and the power output between 4.0 and 5.6 W.

Figure 4.12 shows the variation of the efficiency and the power output for the three different hot water inlet temperatures where the close correlation between those two performance characteristics can be observed.

Effort was given to prevent air from leaking in the working tube. Such leakage was observed initially so that the top cover plate had to be sealed better, especially at the places where the inlet and outlet pipes of the evaporator and the condenser were passing through. Nevertheless, many times after the end of an experiment it was observed that a gas belt of small thickness was at the top of the working tube. This gas could be either air that had leaked in during the experiments or freon vapour that was not condensed.

Finally, it must be noticed that the uppermost position the condenser could reach when it was pulled up, was taken as

the zero position of the condenser. However, due to the bends of its inlet and outlet pipes, the condenser was actually at about 1 cm below the top of the cylinder.

The percentage error in the test results is due mainly to the inability to control the cooling water and hot water inlet temperatures which varied by ±3°C and ±2°C respectively, over a time period. The measurements of pump heads and discharge are accurate to within 0.01 m and 0.001 kg/s. The efficiency is calculated with the total heat input which is obtained from the hot water flowrate and the temperature drop in the evaporator. These values were measured to within 1% and 5% error. The large error in the temperature difference is due to the accuracy of measuring the temperatures to the nearest 0.5°C and the small temperature difference of about 10°C across the evaporator. The net result is a possible 15% to 20% error in the efficiency.

## 4.3. 12.7 cm DIAMETER SLPP

A scaled drawing of the 12.7 cm model is shown in figure 4.13. This model was designed with a fixed geometry. Major modifications however were introduced in the design of the evaporator and the condenser.

In order to minimize the pressure losses in the evaporator, it was made with a fabricated central portion (figure 4.13) and the inlet and outlet pipes passed through the side of the main cylinder. The diameter of the heating pipe was doubled but it was also slightly flattened in order to keep the heater as thin as possible.

ĵ

For the condenser, a design completely different from the previous models was implemented. The condensing coil was eliminated and instead surface condensation was incorporated on the inner surface of the working tube which for this reason was made of copper. A cheese cloth was placed around the outside surface of the tube and was kept moist by running cold water over it.

Due to the elimination of the condensing coil, the diameter of the main tube was reduced from 14 cm to 12.7 cm in order to keep constant the cross-sectional area of the vapour.

Finally, the total height of the main tube was reduced.

#### 4.3.1. RESULTS

This model was tested with three different cooling water mass flowrates, four hot water mass flowrates and three hot water inlet temperatures. These were the only parameters that could be varied in addition to the suction and discharge heads. Each cooling water mass flowrate was tested with all

the four hot water mass flowrates.

Figures 4.14 and 4.15 show the results obtained for the first two cooling water mass flowrates. A total head of 2.0 m was reached while no general trend can be identified. Figure 4.16 shows the results from the test on the third cooling water flowrate, the highest one, with which the SLPP reached a total head of 3.0 m. The performance is comparatively better than the two previous tests and a trend of increasing discharge with increasing hot water mass flowrate can be observed. In all these tests the hot water inlet temperature was kept at approximately 80°C.

Figure 4.17 shows the results obtained from varying the hot water inlet temperature while the cooling and hot water flowrates were kept constant at 0.060 kg/s and 0.034 kg/s respectively. The model reached a total head of 2.5 m before stalling. These results show the opposite trend of the 14 cm model, in other words, increasing discharge with decreasing inlet temperature of the hot water.

The pump did not operate at suction heads larger than 0.5 m. The discharge and the power output reached their maximum values of 0.230 kg/s and 3.38 W respectively with the  $_{\rm c}$  =0.060 kg/s and the  $_{\rm h}$  =0.151 kg/s while the maximum value of 0.65% for the efficiency was reached with the  $_{\rm c}$  =0.040 kg/s and again the  $_{\rm h}$  =0.151 kg/s. Typically the discharge varied between 0.08 and 0.20 kg/s, the power output between 1.0 and

3.2 W and the efficiency between 0.34 and 0.62 %. In general, the performance of the 12.7 cm diameter model was poor compared with the 14 cm diameter model. It must be noted also that 0.060 kg/s which is the optimum value of the cooling water mass flowrate for this model, was the maximum value used on the previous model while the optimum value of 0.151 kg/s for the hot water mass flowrate is more than double the maximum value of the same parameter used on the previous model.

Because of the poor performance of this model, wooden beads were introduced in the cylinder above the evaporator in an effort to reduce the heat transfer between the evaporator and the vapour. Even though low mass flowrates were used for the hot water, no improvement in the performance was observed, (figure 4.18).

Finally, it was noticed that the surface of the working tube at the level of the evaporator was much warmer than the rest of the working tube surface. It was noted that the evaporator inlet and outlet tubes were not insulated completely from the sides of the working tube.

Some difficulties were experienced with small leaks at the lead soldered and epoxied joints while the silver soldered joints held up well.

## CHAPTER 5: DISCUSSION OF THE RESULTS

The results obtained from running the computer model and testing the two experimental models have been presented in the two previous chapters. In this chapter these results will be compared in order to determine qualitative trends and deviations between the test results and the theoretical results from the same test on different models.

First the results from tests that were carried out both theoretically and experimentally will be examined in order to point out possible disagreements between the theoretical and the experimental results. Then the results from the tests on parameters that were tested only theoretically will be discussed. It must be noticed that the theoretical interpretation of these results has already been given in the second chapter, so that here these results will be examined from a physical point of view. Finally, the tests for which only experimental results are available will be discussed.

### 5.1. HOT WATER MASS FLOWRATE

The experimental results obtained on variations of the hot water flowrate  $m_h$  in the 14 cm plastic model show (figure 4.6) a trend of increasing discharge with increasing  $m_h$ . This was expected since the hot water is associated with the heat input to the system so that it increases together with  $m_h$ . This results in vapourizing a larger mass of liquid, thus increasing the vapour pressure at the top of the working tube. As a consequence the momentum transferred to the water columns of the inlet and outlet pipes will be higher, resulting in increasing the discharge.

In the corresponding theoretical results however, this trend is very subtle. Here the discharge increases only slightly with increasing  $\mathfrak{m}_h$ . This is due to the fact that in the theoretical model the hot water flowrate is taken into account only in computing the average heater temperature, as it was discussed in section 3.1.2, and the significance of  $\mathfrak{m}_h$  in the corresponding formula is rather small, so that the theoretical model is not very sensitive in changes of  $\mathfrak{m}_h$ . This effect, combined with the assumption made that the heater is at an instantaneously uniform temperature, results in computing an almost constant heat input to the model when  $\mathfrak{m}_h$  is varied.

The same effect appears on the efficiency as well. The

theoretical efficiency remains practically constant for different hot water flowrates. The experimental results however show that the efficiency attains its maximum values at the medium hot water flowrates. This is reasonable because at the lower flowrates where the heat input is lower, the discharge and the power output are also low resulting in low efficiencies. On the other hand, at the higher flowrates, although the power output is increased, the significant increase of the heat input results in lowering the efficiency again, so that the optimum hot water flowrates are the medium ones.

In the 12.7 cm copper model the hot water mass flowrate variations were tested for three different cooling water mass flowrates, figures 4.14, 4.15, 4.16. The results from the two lower cooling water flowrates show the opposite trend from the previous model, while at the highest cooling water flowrate the results show the same trend that was observed in the plastic model. These controversial results indicate that the surface condensation on the inner surface of the working tube which was implemented in this model results in low condensation rates. As a consequence, although the rate of evaporation is increased due to higher hot water flowrates, the condensation rate is insufficient to condense the vapour which remains at the top of the working tube, thus damping the oscillations of the liquid column.

Only the highest of the three cooling water flowrates provides a sufficient condensation rate. In this case however, even at a hot water flowrate double the maximum tested on the 14 cm model, the discharge is lower than that of the previous model. A possible explanation is that due to the smaller mass of the liquid column in the copper model because of the decrease in its height, less momentum is transferred to the inlet and outlet columns.

# 5.2. HOT WATER INLET TEMPERATURE

The experimental results obtained from varying the hot water inlet temperature T  $_{\rm h\,i}$  on the 14 cm plastic model (figure 4.7) show the trend of increasing discharge with increasing T  $_{\rm h\,i}$ , in agreement with the theoretical predictions.

Physically this is expected since the higher temperatures of the hot water inlet tend to increase the pressure of the vapour at the top of the cylinder. This is because a higher T hi will result in increasing the heat input and therefore the evaporation rate while the temperature of the vapour will also increase due to direct heat transfer between the evaporator and the vapour, as it was discussed in section 3.1.1 in terms of the theoretical model. The increase in the vapour temperature will result in increasing the

condensation rate so that the momentum transferred to the inlet column will be higher. Also, as a result of the increase in vapour pressure, higher momentum will be transferred to the outlet column as well.

The efficiency is also observed to increase with increasing T hi , a result which is consistent with the higher Carnot efficiency associated with higher operating temperatures.

The results obtained from the same test on the 12.7 cm model (figure 4.17) again show the opposite trend from the plastic model, in other words the discharge decreases as T  $_{\rm h\,i}$  is increased. This must be attributed to the low condensation rates that are associated with this model, as was discussed before.

## 5.3. HEATER POSITION

The experimental tests on the 14 cm plastic model when the distance of the heater from the top of the cylinder L  $_{\rm h}$  was varied, show (figure 4.8) that the optimum performance of the SLPP can be attained at L  $_{\rm h}$  =6.0 cm while for values of L  $_{\rm h}$  both higher and lower than 6.0 cm, the discharge is lower.

Referring to the theoretical results on the scaled model, these agree with the experimental ones for values of L  $_{\rm h}$  larger than 6.0 cm, where both experiments and theory

indicate that the discharge will decrease with increasing L<sub>h</sub>. This is reasonable since the lowering of the evaporator will also lower the mean position of the liquid-vapour interface and thus will increase the volume of the vapour, resulting in decreasing its pressure, i.e. increasing the dead or non-reactive vapour space.

However, for values of L h smaller than 6.0 cm, it is expected physically that the resulting small distances of the mean position of the liquid vapour interface from the top of the cylinder will tend to limit the amplitude of the oscillations of the liquid freon resulting in a damping of its motion. The theoretical model did not predict this effect. However, as was discussed before, as L h approaches its limit, the computer model computes very small vapour volumes and ends up giving negative results, so that no theoretical predictions can be obtained in this area.

The overall efficiency followed the trends of the discharge in both the theoretical and experimental results since the variations of L h did not produce any significant change in the heat input to the SLPP.

The distance of the evaporator from the top of the cylinder was not varied in the 12.7 cm copper model due to its fixed geometry.

#### 5.4. CONDENSER POSITION

The experimental results obtained from the 14 cm plastic model when the distance of the condenser from the top of the cylinder L  $_{\rm ct}$  was varied, show (figure 4.9) that the discharge decreases as L  $_{\rm ct}$  is increased. This contradicts the results from the theoretical model which predicted the opposite, in other words that the discharge would increase with increasing L  $_{\rm ct}$ . Both experiments and theory agree however that when L°  $_{\rm ct}$  is increased beyond a limit the SLPP stalls.

As the condenser is moved lower from the top, an increasing portion of it is immersed in the liquid permanently, because the amplitude is not so large as to expose the whole condenser to the vapour when the liquid-vapour interface moves downwards. Therefore the surface area available for heat transfer between the vapour and the condenser decreases thus decreasing the condensation rate.

In the theoretical model it has been assumed that the condenser is at a uniform and constant temperature. This assumption, combined with the larger amplitudes that the theoretical model computed, resulted in estimating that for small values of L  $_{\rm ct}$  the decrease in the condensation rate has a smaller effect compared to that for larger values of L  $_{\rm ct}$ .

In the experimental model however, as it was discussed in the previous chapter, the condenser was not at a uniform

temperature. The cooling water entered the condenser at its bottom and left it from its top, creating a temperature gradient along the condenser. Due to this gradient, the temperature difference between the condenser and the vapour was largest in the area of the bottom of the condenser and was decreasing towards the top.

On the other hand, the smaller amplitudes that occurred in the experimental model, resulted in having a large portion of the condenser immersed in the liquid, when the condenser was moved downwards. Therefore the condensation rate was decreased more in the experimental than in the theoretical model when L ct was increased. As a consequence the discharge also decreased.

The efficiency followed the trends of the discharge in both the theoretical and the experimental results because there were no important changes in the heat input to the SLPP.

These tests were not carried out on the 12.7 cm copper model because of its fixed geometry.

In all the previous results it can be seen that the theoretical model predicted the discharge and the efficiency of the SLPP to be higher than actually found in the experimental tests.

Apart from the experimental errors involved in the test

results, especially in the calculation of the efficiency, there are sources of energy loss that were not taken into account in the theoretical model. Such sources are the heat losses of the main cylinder of the SLPP to the surroundings, especially through the top cover plate which was made of steel instead of plastic and therefore had a higher thermal conductivity. Also the pressure losses due to the irregular motion of the polyethylene diaphragm and the friction losses on the inner walls of the main cylinder were not taken into account.

The pressure losses due to friction in the suction and discharge pipes as well as those due to the opening and closing of the valves were taken into account in the theoretical model. The values of the corresponding friction factors however, were calibrated using earlier experimental results from the 10 cm diameter plastic model. Since the discharge as well as the velocities in the inlet and outlet pipes of the 14 cm diameter model are greater than those of the older model, it is possible that the friction factors would need to be calibrated again and that in its present condition the theoretical model underestimates the various friction losses of the 14 cm diameter SLPP.

Finally, another factor that may have altered the performance of the experimental model was the presence of a rather small amount of air or freon vapour at the top of the

working cylinder, as it was discussed in the previous chapter.

It is possible that the gas had formed an inert belt at the top of the cylinder which acted as a damper on the oscillations inside the cylinder.

In the above quantitative comparisons only the results on the 14 cm plastic model were referred to, because the design of this model is closer to the assumptions made in the theoretical model.

# 5.5. CONDENSER TEMPERATURE

The average temperature of the condenser was introduced as a constant in the theoretical model under the assumption that it remains constant through the cycle. It was varied only in the computer model because, as it was discussed in the previous chapter, in the experimental models there was no control over the cooling water inlet temperature.

The results obtained have shown (figures 3.29, 3.30) that the discharge will tend to decrease with increasing T  $_{\rm c}$  while the efficiency will tend to increase.

An increase of the cooling water inlet temperature will result in decreasing the rate of condensation so that the discharge will be expected to decrease. Furthermore, if T  $_{\rm c}$  were allowed to go even higher the significant decrease of the condensation rate would result in stalling the SLPP.

The efficiency would also be expected to decrease in agreement with the decrease in the Carnot efficiency, when T c is increased. That is because the power output would decrease following the trend of the discharge while there should be no significant effect on the heat input. On the other hand, the theoretical model predicts the opposite, namely that the heat input will decrease more than the work output when T c is increased, resulting in an increase of the efficiency.

## 5.6. EVAPORATOR DIMENSIONS

The surface area of the lower part of the heater A  $_{\rm h\,b}$  as well as its thickness L  $_{\rm t\,h}$  are also parameters that were tested only on the computer model. It was not practical to construct several heaters of different sizes and to test them experimentally.

The results showed (figures 3.31, 3.32) that both the discharge and the efficiency would increase with increasing A  $_{\rm hb}$ . Physically this is to be expected since an increase in A  $_{\rm hb}$  would also result in an increase in evaporation rate.

There are two ways to increase the surface area of the evaporator. Either its diameter or its thickness could be increased. There is however a limit in increasing the diameter of the evaporator, since its maximum diameter is determined by the diameter of the condensing coil. Also, it is not desired

to have the evaporator very close to the condenser in order to avoid direct heat losses.

On the other hand, the results obtained on the theoretical model have shown (figures 3.33, 3.34) that increasing the thickness of the evaporator will result in decreasing the discharge and the efficiency of the SLPP. This is reasonable because the major disadvantage of the SLPP is that in some intervals of the cycle evaporation and condensation overlap and thus counteract each other. Therefore ideally the evaporator should be as thin as possible so that evaporation could take place over a small interval of the cycle.

# 5.7. COOLING WATER MASS FLOWRATE

The cooling water mass flowrate was tested only in the two experimental models. In the theoretical model it was not introduced as a parameter because it was assumed that the condenser was at a constant and uniform temperature.

The results obtained in the 12.7 cm diameter copper model showed (figures 4.14, 4.15, 4.16) that the lower cooling water flowrates were insufficient for the operation of the SLPP and that the discharge and the efficiency increased as the flowrates increased. However, the results obtained on the 14 cm diameter plastic model showed (figure 4.5) that the

SLPP was not very sensitive to changes of the cooling water flowrates, with the exception of the lowest two, for which the SLPP stalled at relatively lower total heads.

An increase of the cooling water flowrate results in an increase of the condensation rate of the vapour and the discharge of the SLPP, implying an increase of the frequency. This is indicated mainly by the results from the copper model while on the plastic model it can be observed only in the two lowest cooling water flowrates.

At this point it must be noticed that in both models the same cooling water flowrates were used. The difference in the performance between them indicates that the condensation arrangement was more efficient for the plastic model, as was discussed previously. It also indicates that beyond a limit the increase in the condensation rate cannot increase the discharge anymore. This limit is determined by the evaporation rate, because it determines the amount of the vapour that is produced at the top of the working tube.

### 5.8. REVERSING THE FLOWS

The effect of reversing the flows of the hot and the cooling water in the SLPP was tested in the 14 cm model as described in the previous chapter. The results showed (figure 4.10, table 20) that the top-periphery was the optimum of the

four possible combinations of the condenser and heater inlets.

The direction of the flow in the evaporator or the condenser effects the temperature gradient along them. When the cooling\_water enters the condenser at its top, the temperature difference between the condenser and the vapour is larger at this higher portion of the condenser than at its lower portion. Since the latter is immersed in the liquid for a large part of the cycle it would be advantageous to have a small temperature difference between this part of the condenser and the liquid in order to minimize the heat that the condenser extracts from the liquid. Thus the upper portion of the condenser plays a more important role in the condensation process and there should be therefore a higher temperature difference between this part of the condenser and the vapour. The reverse flow in the condenser would result in extracting more heat from the liquid and less from the vapour because by the time the cooling water would come to condense the vapour, its temperature would already have risen.

However, at the lower heads which are associated with larger amplitudes, it is advantageous to have the cooling water entering the condenser at its bottom, because in this case the area below the evaporator is covered better when the liquid-vapour interface moves downwards exposing the lower part of the condenser to the vapour. This advantage is cancelled at the higher heads as was discussed before.

Nevertheless, even at the lower heads, there is an amount of heat lost to the condenser through the liquid, as the lower efficiencies in this case imply.

When the hot water enters the evaporator at its periphery, the outer coils will be at a higher temperature. In this area however, the liquid is at a lower temperature because it is in contact with the condenser, so that a higher temperature difference exists between the evaporator and the liquid, which increases the evaporation rate. On the other hand, when the flow is reversed, the opposite will happen and the high temperature coils will be those in the center where the liquid is at a higher temperature so that the evaporation rate is lower. For this reason, it is advantageous to implement this alternative for the hot water inlet.

The above results have shown the effects that the temperature gradients and their directions along the condenser and the evaporator have on the performance of the SLPP. It can be seen how the experimental model deviates from the theoretical one, where it has been assumed that the condenser is at a constant uniform temperature while the evaporator is at an instantaneously uniform temperature.

#### 5.9. ALTERNATIVE COOLING WATER SUPPLY

The final test that was carried out on the 14 cm model

was to use the alternative supply of cooling water by bleeding off the discharge pipe, instead of connecting with the main water line. The results obtained showed (figure 4.11) a poor performance. It was noticed however, that the faow in the condenser was pulsating, because the flow in the discharge pipe itself is pulsating. Furthermore, it had a phase difference of 180° from the oscillations of the liquid column inside the working tube. That is, when the liquid-vapour interface was moving up and evaporation began, there was little flow in the condenser. The reason is that there is no flow in the discharge pipe, since at this stage suction occurs. Therefore the condensation rate during this phase of the cycle is significantly decreased. This provides a means to offset the major disadvantage (21) of the SLPP, namely that during this phase of the cycle, evaporation and condensation take place simultaneously. In order to implement, this alternative however, first two problems have to be solved. First, the low cooling water flowrate causing a low condensation rate which is the main reason for the poor results of this configuration. Second, the difficulty in starting the SLPP because initially there is no flow in the discharge pipe and therefore no flow in the condenser.

A possible way to overcome this problem could be to connect the outlet of the condenser to the suction pipe, so that the low pressure during suction could drive the cooling

water, thus smoothing its flow when the SLPP is started.

In combining the SLPP with a solar collector for heating the water that flows through the evaporator, consideration must be given to the arrangement of the piping circuit as well as the collector itself.

The nature of the future applications for the SLPP requires that it operate as an autonomous unit. In order to avoid the need of an auxiliary energy source, the hot water is to be circulated between the collector and the SLPP naturally, that is by utilizing thermosyphon forces in the system.

In a thermosyphon system the driving force for the circulation of the fluid is the density difference between the inlet and the outlet of the collector, caused by heating the fluid in the collector. Such a system requires no pumps or controls and is fundamentally simpler to design. The only requirements for proper functioning are that relatively larger piping must be used to avoid excessive pressure losses while special attention must be given to the various sources of pressure drop due to friction in the circuit (22). The thermal syphon forces will balance the friction forces to adjust the flow rate accordingly.

This chapter analyzes the implementation of thermosyphon flow in the SLPP, taking into account the requirements of the

system in terms of pressure drops. Then, using experimental data for solar collectors that were made available by the Canadian Solar Industries Association Inc., a solar collector is selected for operating with the SLPP.

#### 6.1. THERMOSYPHON HEAD

The typical arrangement of the SLPP-collector — installation is shown in figure 6.1.a. The water leaves the collector (point 2) and goes to the SLPP (point 3) through the connecting pipe. There it gives off heat to the working fluid of the SLPP and then it returns to the collector (4-1), where it is reheated.

In the pipeline 2-3 the water is hot and therefore its density is small, while in the pipeline 4-1 it is cold and has a larger density. Assuming that:

- i) the temperature distribution of the water along the collector and the evaporator coil is linear, and
- ii) there are no heat losses in the connecting pipes, then the temperature distribution of the water can be plotted as a function of position in the system, figure 6.1.b (23).

If it is further assumed that the relationship between the specific gravity S of the water and its temperature is linear (23) due to the relatively small temperature difference between 1 and 2, then figure 6.1.b also represents the distribution of the specific gravity in the system. The thermosyphon head due to the specific gravity difference between the two legs of the pipe circuit will be equal to the area 1234:

$$h_{T} = \frac{1}{2} (S_{2} - S_{1}) [(h_{1} - h_{1}) + (h_{1} - h_{1})]$$
(6.1)

The specific gravity is defined as the ratio of the density of water in a given temperature over its density at 4°C (24). Therefore it is dimensionless and thus the thermosyphon head is obtained in metres.

In order to generalize [6.1] it is better to approximate the relationship between specific gravity and temperature, using a parabolic function (23):

$$S=At^2+Bt+D$$
 [6.2]

where the constants A,B,D are (23):

so that [6.1] becomes:

$$h_{T} = \frac{1}{2} (t_{2} - t_{1})(2At_{B} + B)[(h_{3} - h_{2}) + (h_{4} - h_{1})]$$
[6.3]

with

In [6.3], h  $_1$  can be taken equal to zero, considering the ground as the reference level.  $h_{\tilde{w},2}$  depends on the length and tilt of the particular solar collector and can therefore be considered as a constant for a given collector and location. Furthermore, from figure 6.1, h  $_3$  is equal to h  $_4$ . Finally, using the data from the previous chapters, the average temperature t  $_m$  of the hot water in the evaporator, can be set as a constant at 75°C. Therefore, only two independent parameters remain in [6.3], namely the temperature difference  $\Delta T$  between the inlet and outlet of the evaporator, and the distance of the top of the SLPP from the top of the collector  $\Delta h = h_1 - h_2$ .

The thermosyphon head was obtained by varying  $\Delta T$  between 5°C and 20°C and  $\Delta h$  between 0.25 m and 3.5 m. It must be noticed that 0.25 m is the minimum height of the SLPP above the collector, due to the SLPP's own height. The results are

shown plotted in figure 6.2. As it was expected from [6.3], the thermosyphon head varies linearly with  $\Delta T$  and  $\Delta h$ . Also, it can be seen that the thermosyphon head is in the order of millimetres.

Finally it must be noticed that the SLPP is expected to operate even if it is elevated to such heights above the ground. It will operate under these conditions provided that the inlet and outlet pipes are below the water surfaces of the inlet and outlet reservoirs and the maximum distance between the two reservoirs is less than 4.0 m.

## 6.2. FRICTION HEAD

In order to achieve thermosyphon flow, the thermosyphon head h  $_{\rm T}$  must be equal to the friction head loss h  $_{\rm f}$  in the hot water circuit (23) for the required flow rate:

$$h_{\tau} = h_{\tau \ f \ r \ i \ c} \qquad [6.4]$$

In order to calculate the friction head, the system of figure 6.1 can be divided into three sections, the pipe circuit, the evaporator coil and the collector. Each of these sections will be examined separately. The total friction head can then be obtained as the sum of the friction heads in each of these sections as a function of flowrate.

# 6.2.1. PIPE CIRCUIT

In order to determine the head loss due to friction in the pipe circuit, the D'Arcy-Wiesbach equation was used:

$$h_{fric} = \frac{f l u^2}{2 g d}$$
 [6.5]

When the flow is laminar, i.e. Re<2300, the friction factor f in [6.5] can be determined as:

while for turbulent flow f must be obtained from the Moody diagram (25).

The Reynolds number can be expressed in terms of the mass flowrate and the pipe diameter as

In order to keep the friction head low, the most simple arrangement of the pipes is preferred, as shown in figure 6.1. This pipe circuit however includes five 90° bends. These are taken into account by adding to the total pipe length 1 in

[6.5] the equivalent length which compensates the resistance due to the behds (25). It must be noticed that the pipe circuit may include three bends instead of five, in the case of a specially designed SLPP where the evaporator inlet and outlet pipes would be passing through the working tube instead of the top cover plate.

A relative radius ratio of 6 for the bends and a relative roughness of 0.0015 for the pipes, [6.5] was used to yield the friction head for different values of the pipe diameter d and the mass flowrate m. This procedure was repeated for different overall pipe lengths, corresponding to different heights of the SLPP above the collector. The results are shown in figure 6.3. It must be noticed that in this figure, the friction head has been non-dimensionalized by dividing by the total pipe length, including the equivalent length for the bends. Therefore, upon using this diagram, the pipe length must be calculated and the equivalent length due to the bends must be added to it.

In figure 6.3, the behavior of the curves for small values of the pipe diameter, is due to the transition from laminar flow, which is dominant at higher values of the pipe diameter, to turbulent. For values of the diameter below 1 in., as the mass flowrate increases the flow leaves the laminar regime and enters the transition zone, to enter finally the turbulent regime at the highest flowrate, where

the largest deviation is observed.

#### 6.2.2. EVAPORATOR COIL

The friction head in the evaporator coil was calculated following a method suggested in (25). The evaporator coil was approximated with successive 180° bends, each having a relative radius larger than that of the previous one by 0.5. The total resistance of each bend was calculated in terms of equivalent length of pipe, taking into account the resistances due to curvature and length. Then, the calculated equivalent lengths were summed up and finally, the total friction head in the evaporator coil was determined again using the D'Arcy-Wiesbach equation. The friction factors were determined in the same way as before.

The friction head in the evaporator coil was obtained for different values of the coil pipe diameter and the mass flowrate of the water. The results are shown plotted in figure 6.4. Except for the curve on the lowest flowrate, the other curves present a discontinuity for medium values of the coil diameter. This is due to the discontinuity in the friction factors in this area, because there the flow is in the transition zone between the laminar and turbulent flow regimes. This discontinuity does not appear in the curve on the lowest flowrate as it remains laminar.

## 6.2.3. SOLAR COLLECTOR

For the solar collector, it was preferred to use experimental data on existing solar collectors instead of attempting to estimate theoretically the friction head, since the designs of solar collectors vary greatly.

Experimental data on several flat plate collectors were made available from the Canadian Solar Industries Association Inc. Some of those collectors were discarded in view of their range of operating temperatures, which did not fit the requirements of the SLPP. The three that remained, were the Nortec TD 1000, the Solcan 3001 and the Thermo-Solar SCIM & CIM.

The friction heads for each one of them are shown plotted in figure 6.5, for different values of the mass flowrate. As it can be seen in the figure, only the friction head of the Nortec TD 1000 is in the same order of magnitude as the thermosyphon head that the SLPP installation can provide, as it was previously discussed. Therefore, from the collectors for which experimental data were available, only this one can be considered as compatible to the SLPP.

The results presented in figures 6.2 to 6.5 can be used, incorporating a trial and error procedure, in order to

determine the height above the collector in which the SLPP must be positioned, together with the necessary diameters of the heating coil and the connecting pipe, so that thermosyphon flow of a desired flowrate can be achieved. This is illustrated in the following example.

From figure 6.3, for a pipe diameter of 1 inch (0.0254 m) and a hot water flowrate of 0.05 kg/s, the non-dimensional friction losses are 0.000054. Anticipating a height of 1.5 m of the SLPP above the collector, the length of the connecting pipe is 6.469 m while the equivalent length of the bends is 2.286 m, giving a total pipe length of 8.755 m. Multiplying this by the non-dimensional friction losses, yields the friction losses for the pipe circuit, which are 0.000473 m.

From figure 6.4, the friction losses of the heating coil are 0.0009 m, for a diameter of 0.75 inches (0.019 m) and the same hot water flowrate as above.

From figure 6.5, the friction losses of the Nortec TD 1000 collector are 0.015 kPa or 0.00153 m, using again the same hot water flowrate.

The total friction loss in the system therefore adds up to 0.0029 m. Now, in figure 6.2, this corresponds to a position of the SLPP at 1.5 m above the collector, taking into account a 10°C temperature difference between the collector inlet and outlet.

### 6.3. SIZE OF SOLAR COLLECTOR

Following the previous discussion, the size of the solar collector that is required to provide the necessary heat input to the SLPP can now be estimated using the available data for the Nortec TD 1000 collector. This is a liquid flat plate collector, single glazed, with standard dimensions 2.17 x 0.9 m and an absorber area of 1.73 m<sup>2</sup> (26).

The area of the collector was estimated using the formula (29):

$$Q = \eta G A \qquad [6.7]$$

where Q  $_{\rm u}$  is the required useful gain of the collector, which is:

$$Q = m c (T - T)$$
 [6.8]

In [6.7],  $n_c$  is the efficiency of the collector which is determined experimentally,  $A_c$  is the area of the collector and  $G_T$  is the incident radiant energy on the tilted plane of the collector. Equating the right-hand sides of equations [6.7] and [6.8] gives:

From the experimental results on the SLPP the mass flowrate  $m_h$  was 0.05 kg/s while the temperature difference between the inlet and the outlet of the evaporator was 10°C.

The incident radiant energy G  $_{\rm T}$  was estimated at 900 W/m². It must be noticed however, that for a particular application, a detailed analysis would be needed, based on meteorological data for the particular location, which would take into account the monthly and daily variation of the incident insolation (29).

Using the value 900 W/m² for G<sub>T</sub> and estimating the average ambient air temperature at 10°C, the efficiency of 45 % for the collector was obtained from the experimental data, figure 6.6 (26). Since it was assumed that there are no heat losses in the connecting pipes, the water outlet temperature of the evaporator (70°C) is the inlet temperature in the collector.

With these values, [6.9] yielded an area of 5.16 m<sup>2</sup> for the collector, which corresponds to three collectors of net absorber area 1.73 m<sup>2</sup> each, with the dimensions of the collector given in (26). These collectors will have to be connected in parallel. In this case, the hot water flowrate will have to be divided by three, therefore reducing further the friction losses in the collector.

### 6.4. EXPERIMENTAL TESTS

Prior to the inalysis presented above, some experimental testing was carried out at the Brace Research Institute, in order to test the thermosyphon capabilities of a solar panel.

For this purpose, a simple parallel tube heat exchanger was constructed. The solar panel available was a 1.765 m<sup>2</sup> FIRRA Tech Inc. model 78101-8. The apparatus (figure 6.7) included a manometer, a calibrated flowmeter and a digital thermometer with thermocouples located at the three positions indicated in the figure.

The best results were obtained at noon of July 3, 1984, after three days of testing. They showed that the FIRRA solar panel could provide the thermosyphon head necessary for driving the flow in the heat exchanger, with a mass flowrate of 0.007 kg/s for the water, and inlet and outlet temperatures of 49°C and 69°C respectively. The pressure drop was measured to be 7 inches (0.178 m).

It can be seen that this solar panel cannot match with the SLPP. The reasons are that both the hot water flowrate and the inlet temperature are lower than those required for the operation of the SLPP, while the temperature drop between the heater inlet and outlet is higher, i.e. this solar panel cannot meet the thermal requirements of the SLPP. Also, in the light of the previous analysis it can be seen that the pressure drop of the solar panel is very high and combined with the friction losses in the heating coil would probably make the operation of the SLPP impossible at higher flowrates and lower temperature drops.

# 7.1. CONCLUSIONS

The major conclusions that can be drawn from this thesis are:

- i) The theoretical model predicts correctly qualitative trends on the performance of the SLPP, with the exception of the positions of the evaporator and the condenser. It cannot be used for quantitative predictions.
- ii) The efficiency of the 14 cm diameter model remained low, at about 0.5 %.
- iii) The surface condensation which was implemented on the 12.7 cm diameter model, proved to be insufficient, this being the main reason for the low performance of the model.
  - iv) The circulation of the hot water by thermosyphon forces is feasible, but the system must be matched between the solar panel and SLPP.

## 7.2. RECOMENDATIONS FOR FUTURE WORK

There are a few points that should be examined by a future researcher in this field. These are:

- i) The computer model should be recalibrated taking into account the changes in the size of the SLPP, so that it will be able to give quantitative predictions on the performance of the SLPP. Also, attention should be given to the behavior of the model when some parameters approach their limiting values.
- ii) An experimental model with tube diameter less than 10 cm, i.e. scale factor less than unity, should be constructed and tested in order to check the theoretical predictions of high efficiencies for small scale factor values.
- iii) The SLPP should be integrated with a solar collector in order to test experimentally the operation of the system when thermosyphon forces are incorporated.

## REFERENCES

- 1. M. N. Bahadori, "Solar Water Pumping", Solar Energy Conversion - An Introductory Course (edited by A. E. Dixon and J. D. Leslie), August 1978.
- 2. M. Vergnet, "The Utilization of Solar Energy for Pumping Water in Developing Countries", Appropriate Technologies for Semi-Arid Areas: Wind and Solar Energy for Water Supply, West Berlin Conference Report.
- 3. Sir William Halcrow and Partners in Association with Intermediate Technology Development Group Ltd., "Small-Scale Solar-Powered Irrigation Pumping Systems, Technical and Economic Review", World Bank Publication (UNDP Project GLO/78/004), London, Sept. 1981.
- 4. J. T. Pytlinski, "Solar Energy Installations for Pumping Irrigation Water", Solar Energy Vol. 21, pp. 255-262, May 1978.
- 5. C. D. West, "Liquid Piston Stirling Engines", Van Nostrand Reinhold Co., 1983.
- 6. C. L. Murphy, "Review of Liquid Piston Pumps and their Operation with Solar Energy", ASME 79-SOL-4, Dec. 1978.
- 7. R. S. Soin, I. M. Prasad, D. P. Rao and K. S. Rao, "Development and Performance of Solar Water Pumps", Brace Research Institute File No. X:16:10, Nov. 1976.
- 8. D. P. Rao and K. S. Rao, "Solar Water Pump for Lift

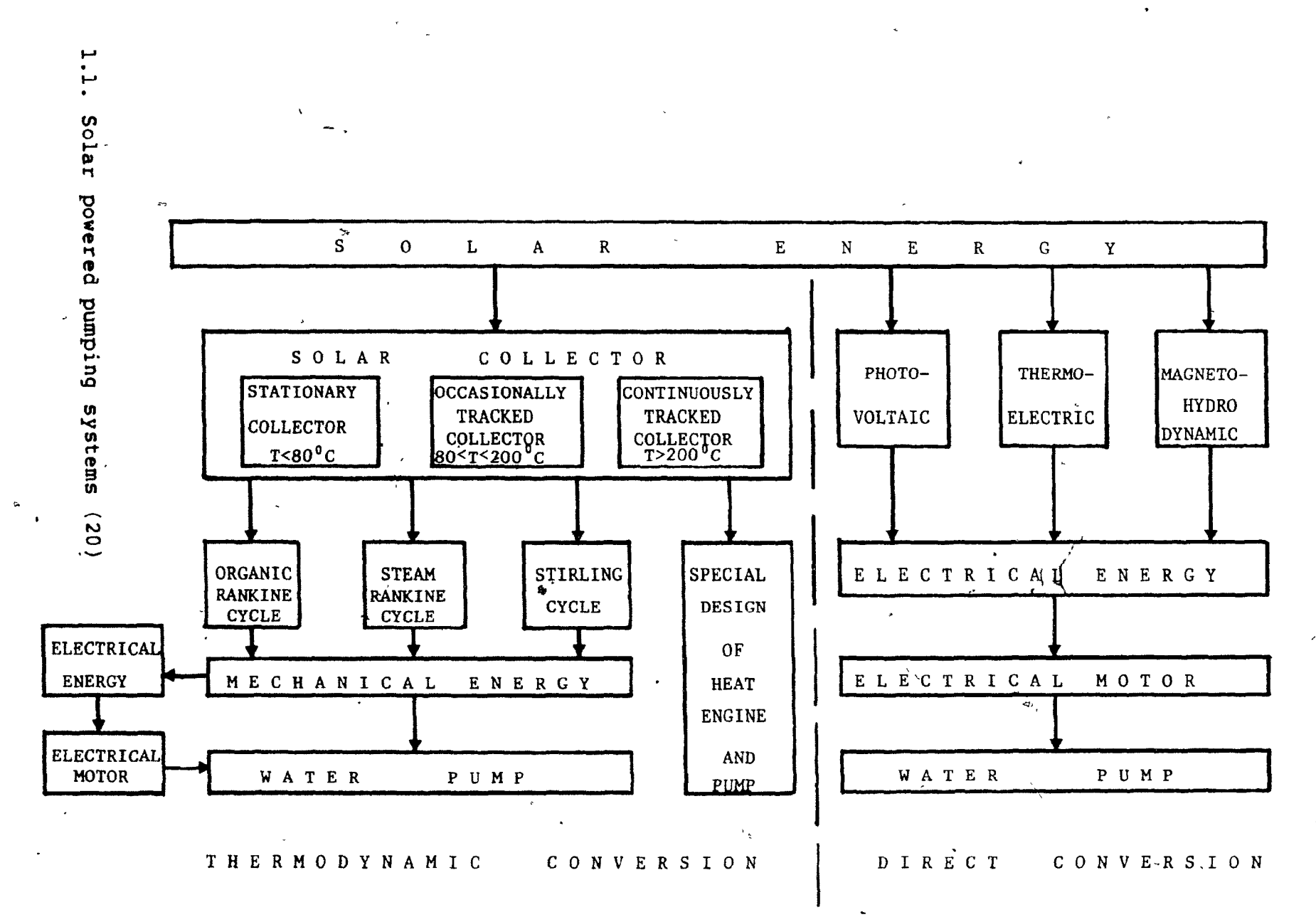
- Irrigation", Solar Energy, Vol. 18, pp. 105, 1976.
- T. H. Lambert, "The Design of a Solar-Powered Water Pump",
   ASME Old Guard Contest, New York, Dec. 1978.
- 10. F. Farlan, "Oscillations of a Liquid in a Tube Caused by Constant Application of Heat", McGill University, Dept. of Mechanical Engineering, B. Sc. (Honours) Thesis, April, 1978.
- 11. S. Dyck, W. Green and C. Noble, "A Study of a Fluidyne Heat Engine", McGill University, Dept. of Mechanical Engineering, Final Year Project, April, 1976.
- 12. R. Findlay and P. Hook, "Fluidyne Engine", McGill University, Dept. of Mechanical Engineering, Final Year Project, April, 1977.
- 13. K. Winters, "Flash Boiling Steam Pump", McGill University, )
  Dept. of Mechanical Engineering, M. Sc. Thesis, May, 1977.
- 14. R. Marie and K. Little, "Further Developments of the Liquid Piston Pump", McGill University, Dept. of Mechanical Engineering, Final Year Project, April, 1980.
- 15. C. L. Murphy, "A Solar Liquid Piston Pump", Solwest 80 Conference Proceedings, pp. 499-502, August 1980.
- 16. J. G. Gerakis, "Modified Liquid Piston Pumps", McGill University, Dept. of Mechanical Engineering, Final Year Project, July, 1980.
- 17. C. L. Murphy, "Optimizing the Performance of a Solar Liquid Piston Pump", Proceedings of the ASME Solar

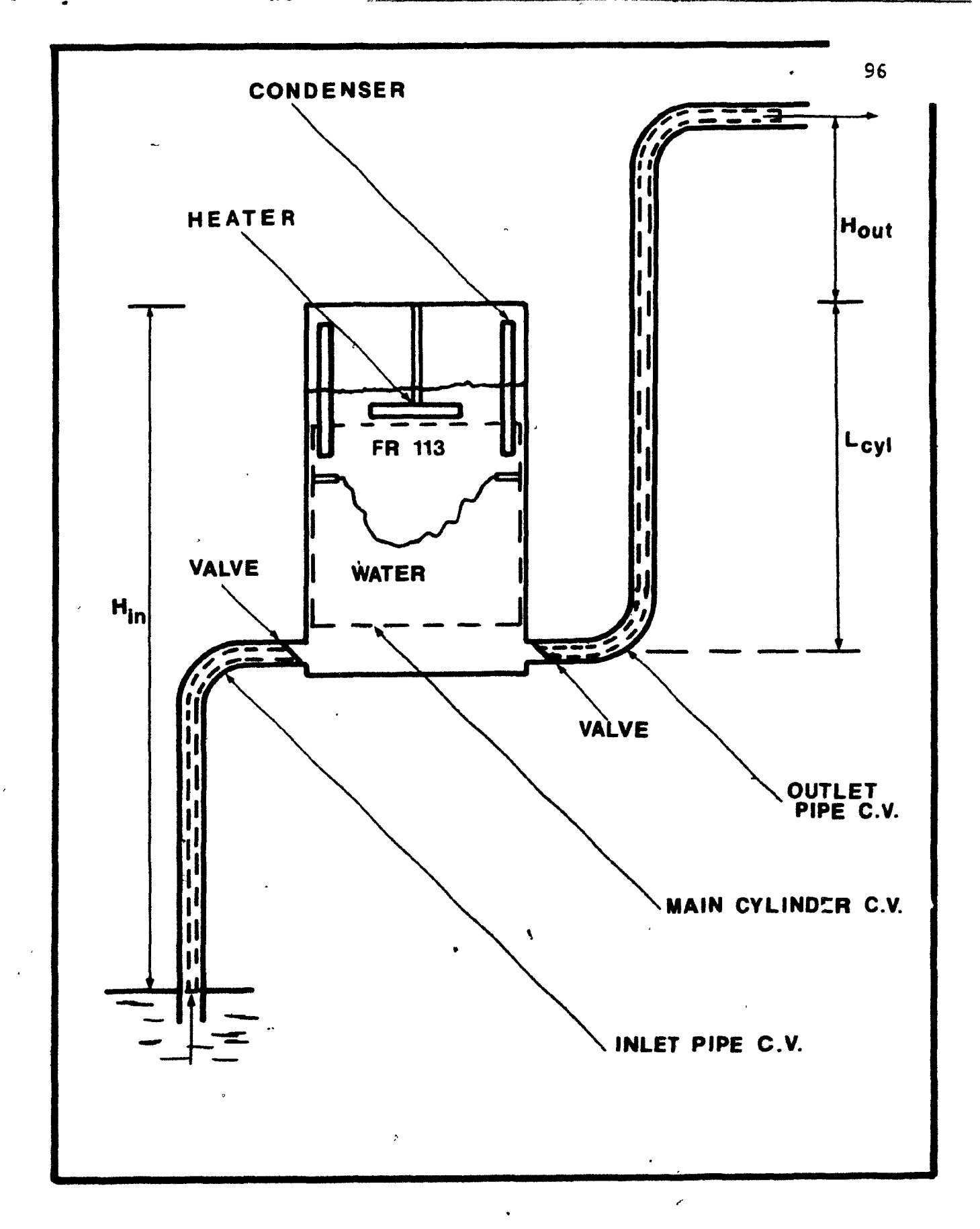
- Division Third Annual Conference.
- 18. D. Barry, R. Dunkley and P. Gohier, "Performance Analysis of a Liquid Piston Pump", McGill University, Dept. of Mechanical Engineering, Final Year Project, February, 1981.
- 19. G. Ho and C. Thomas, "Liquid Piston Pump 3", McGill University, Dept. of Mechanical Engineering, Final Year Project, July, 1982.
- 20. A. Brew-Hammond, "Performance Characteristics and Computer Modelling of a Solar Liquid Piston Pump", McGill University, Dept. of Mechanical Engineering, Masters Thesis, January, 1984.
- 21. C. L. Murphy, A. Brew-Hammond, "Modelling the Performance Characteristics of a Solar Liquid Piston Pump", Proceedings of the ASME Solar Energy Division Sixth Annual Conference, April, 1984.
- 22. J. F. Kreider, F. Kreith, "Solar Heating and Cooling", McGraw-Hill Book Co., 1975.
- 23. D. J. Close, "The Performance of Solar Water Heaters with Natural Circulation", Solar Energy Vol. 6 No. 1, p. 33, 1962.
- 24. V. L. Streeter, E. B. Wylie, "Fluid Mechanics", McGraw-Hill Book Co., 1981.
- 25. Crane Co., "Flow of Fluids", Crane Technical Paper No. 410, 1957.

- 26. Nortec Solar Industries'Inc., "Nortec TD 1000, Liquid Flat Plate Collector", Canadian Solar Industries Association Inc., May, 1981.
- 27. Solcan Ltd., "Solcan 3001, Liquid Finned Tube Collector", Canadian Solar Industries Association Inc., October, 1983.
- 28. Petro-Sun International Inc., "Thermo-Solar SCIM & CIM, Glazed Liquid Flat Plate Collector", Canadian Solar Industries Association Inc., May, 1983.
- 29. J. A. Duffie, W. A. Beckman, "Solar Engineering of Thermal Processes", John Wiley & Sons, 1980.

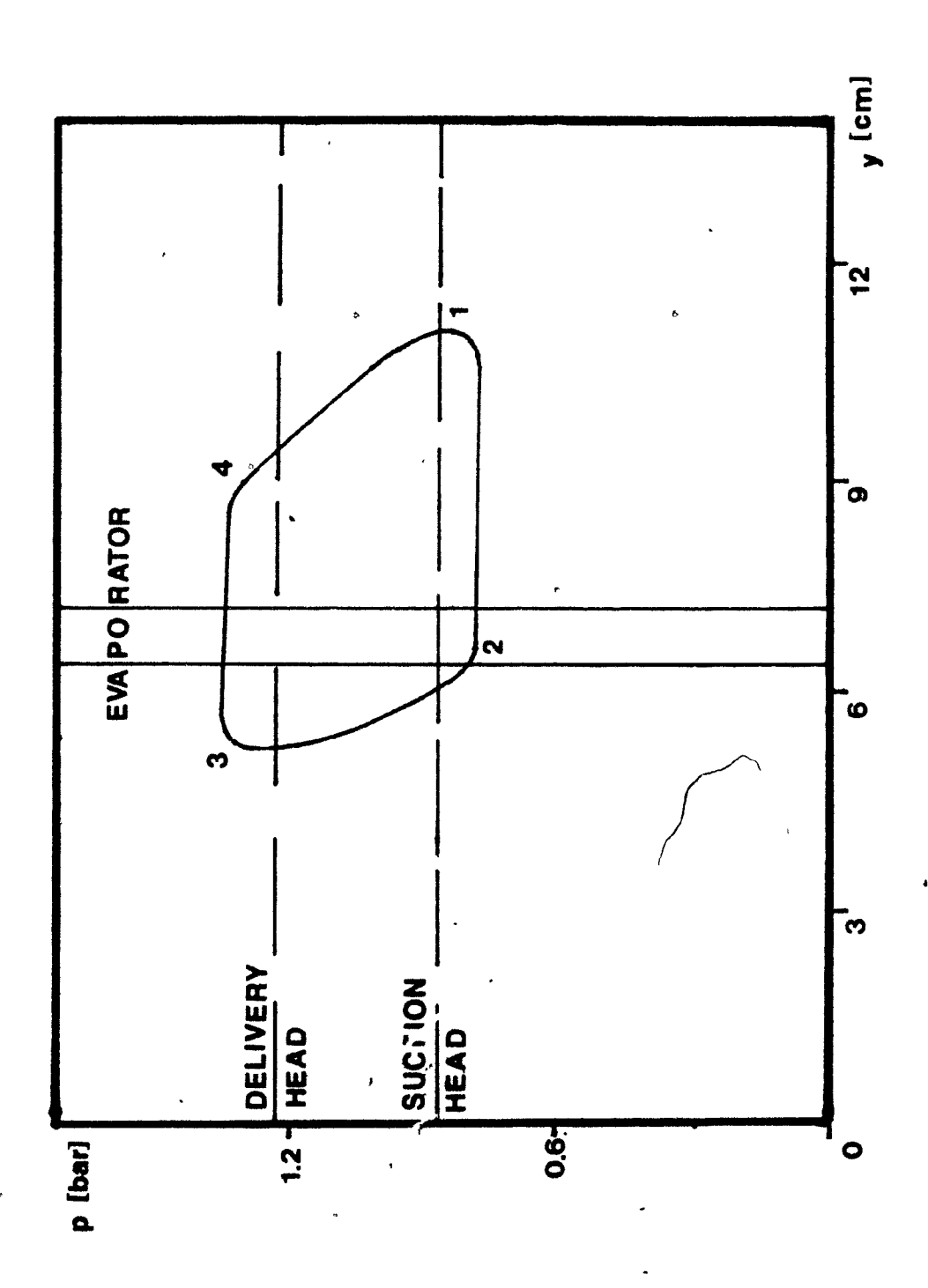
12.3

FIGURES



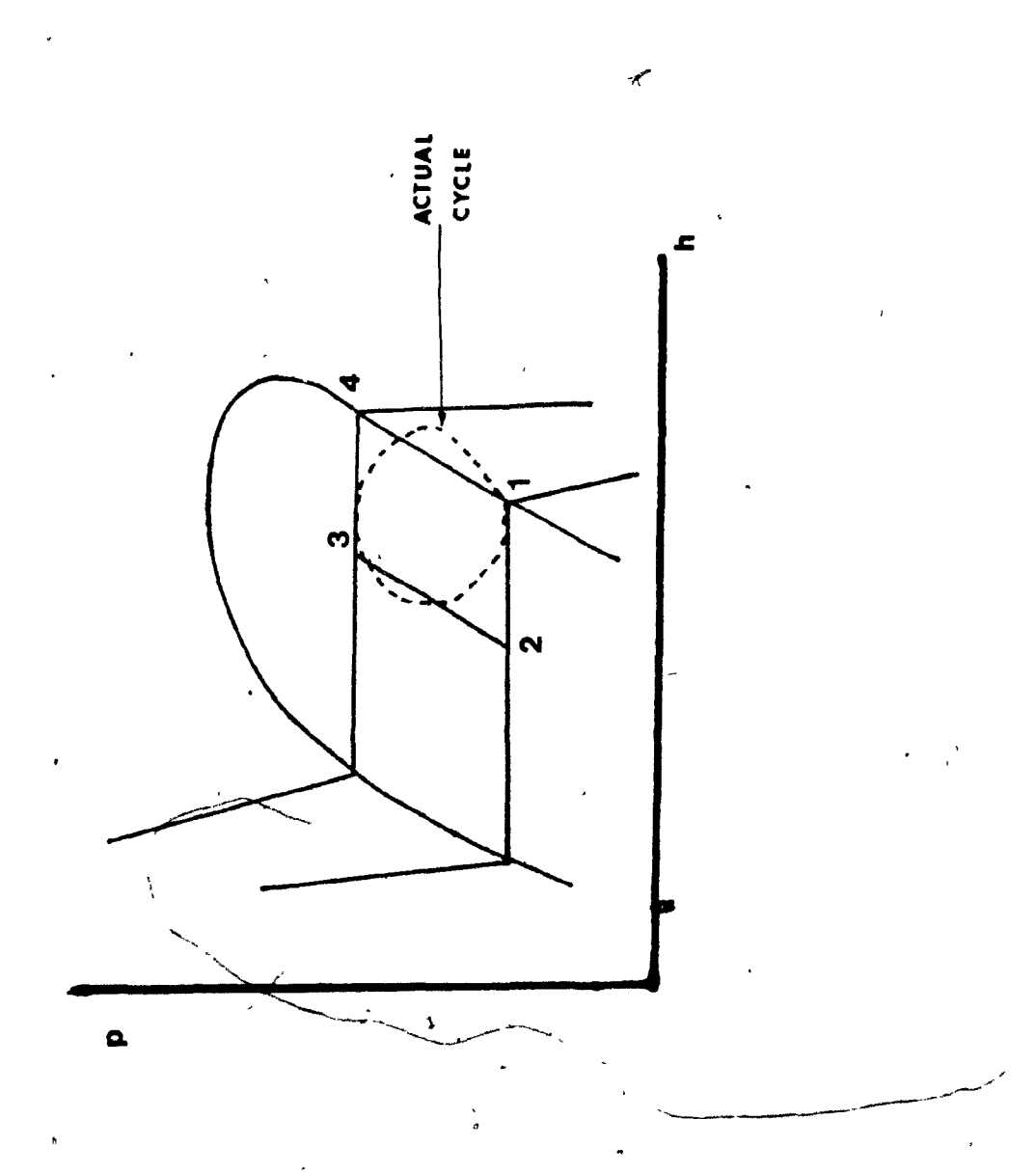


1.2. Schematic of a SLPP (20)



2.1. Theoretical  $p-\nu$  diagram for the SLPP (20)

i



2.2. Theoretical and experimental p-h diagrams for the SLPP (20)  $\,$ 

(





4.0

3.0-

T<sub>hi</sub> (°C)

0 71

Δ 77

**B2** 

**88** 

<u> 4</u> 93

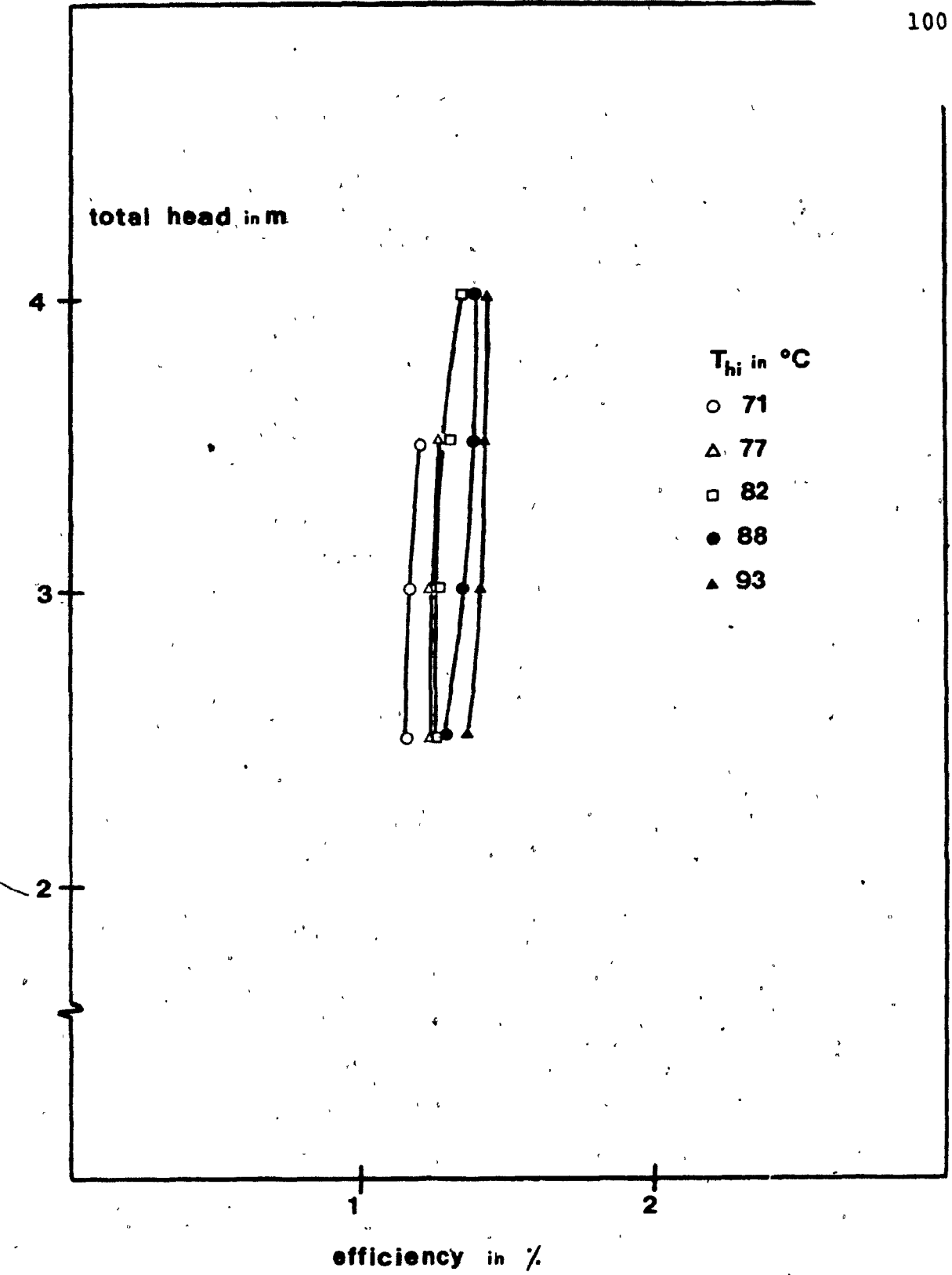
2.0

 $\dot{m}_{h} = .017 \text{ (kg/s)}$ 

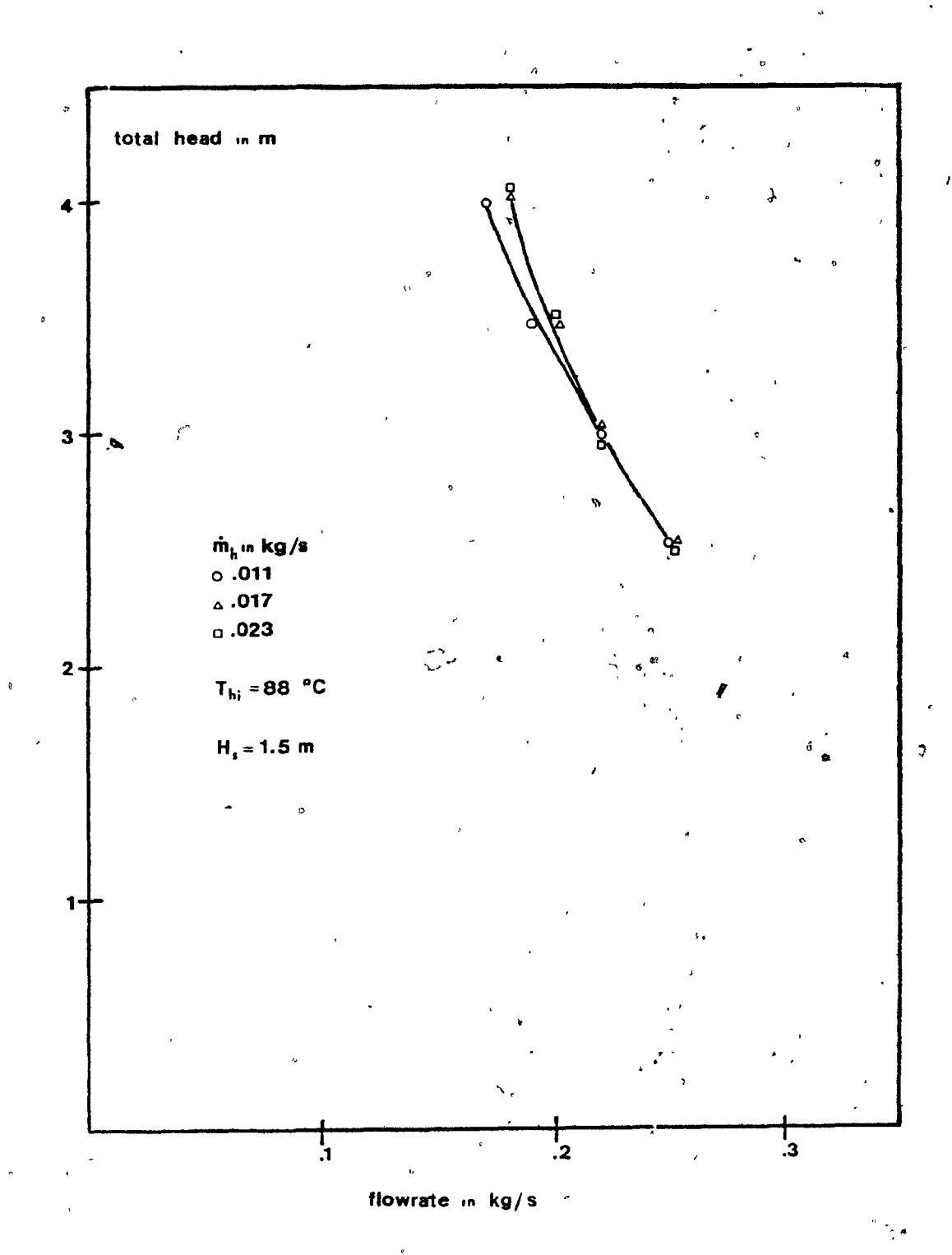
 $H_s = 1.5 \text{ (m)}$ 

flowrate (kg/s)

3.1. Flowrate vs Total head (var. T )



3.2. Efficiency vs Total head (var. T )



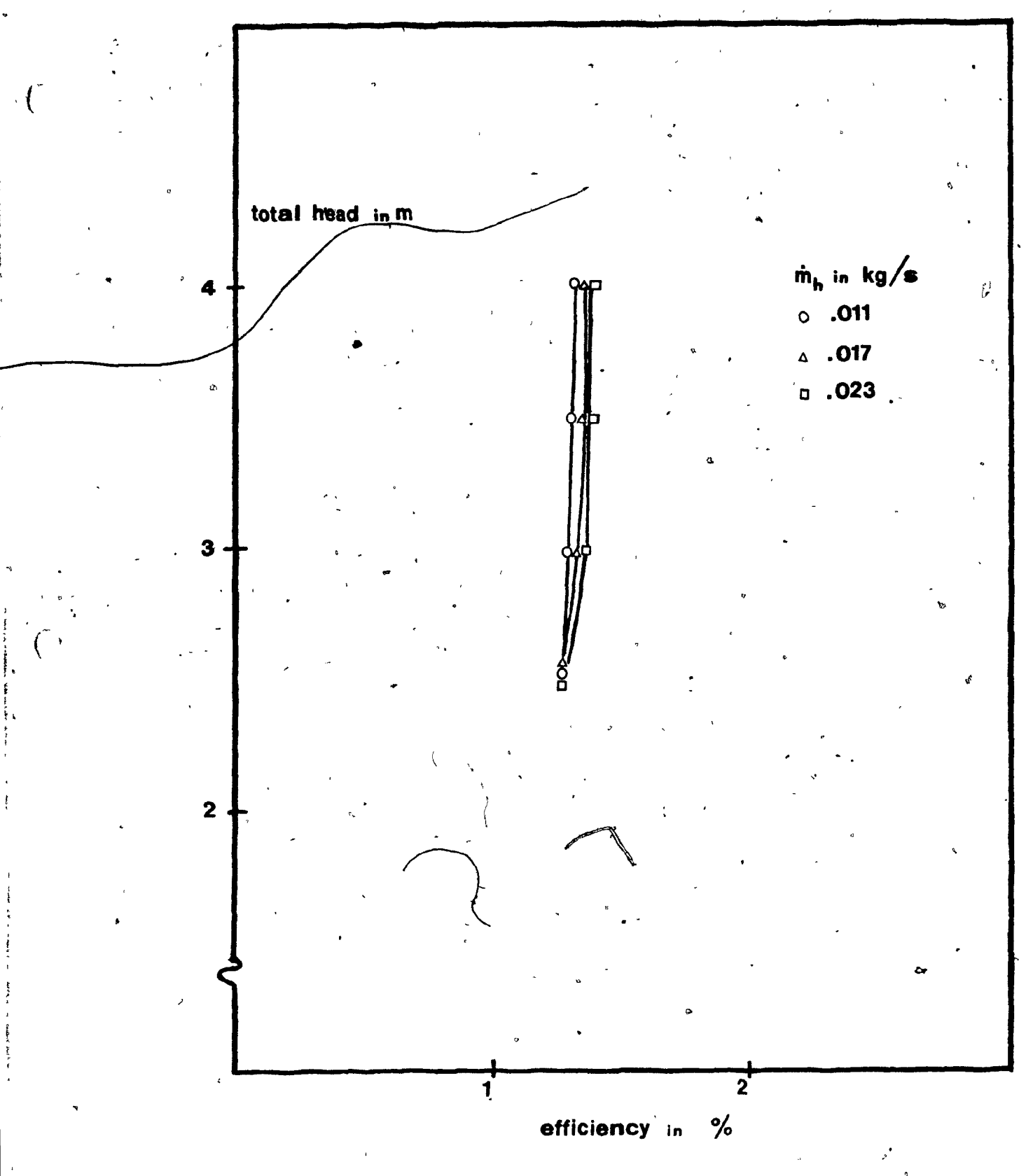
3.3. Flowrate vs Total head (var.  $m_h$ )

. ,

.

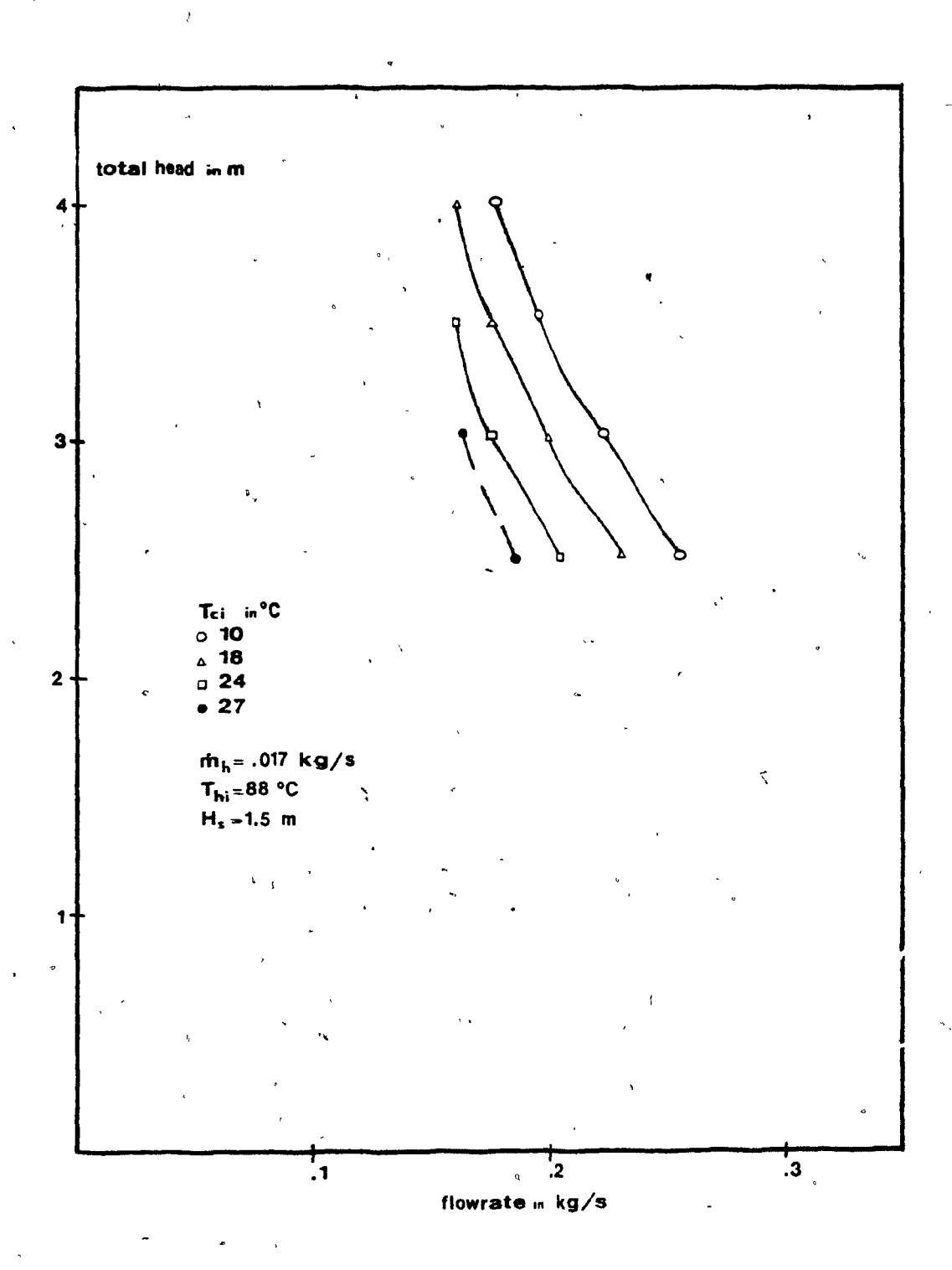
\

1



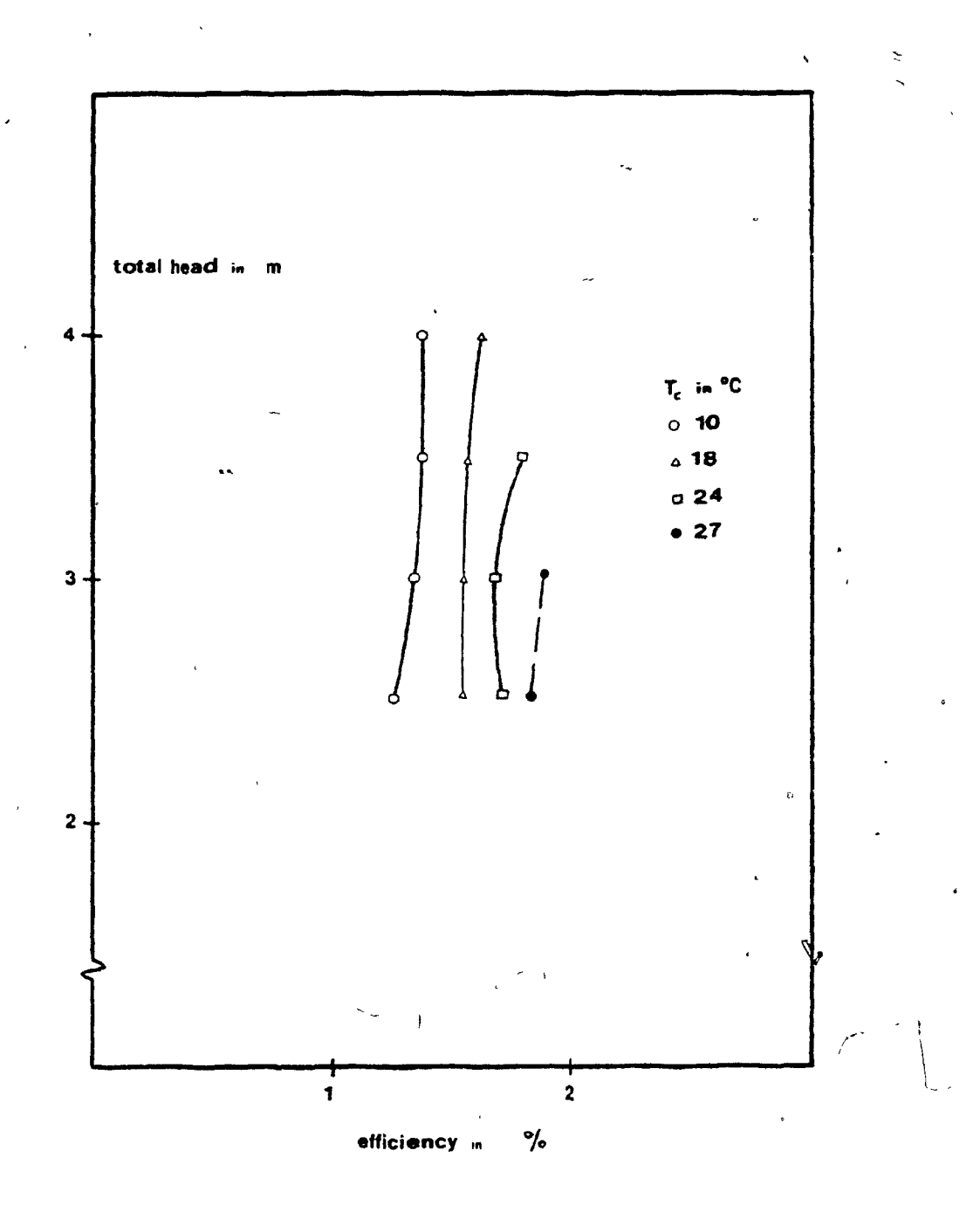
3.4. Efficiency vs Total head (var. m )

Λ



3.5. Flowrate vs Total head (var. T)

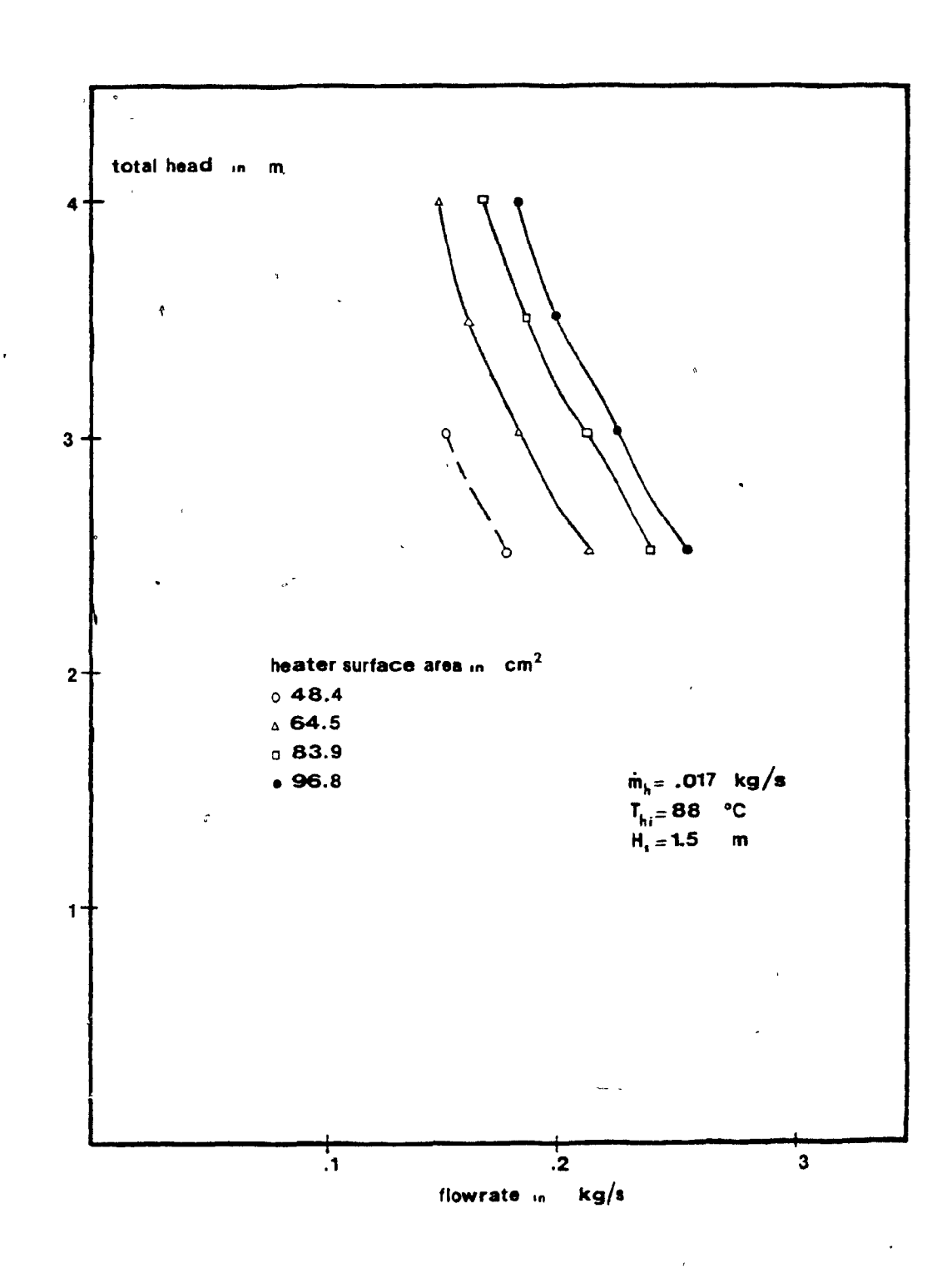
الخرا



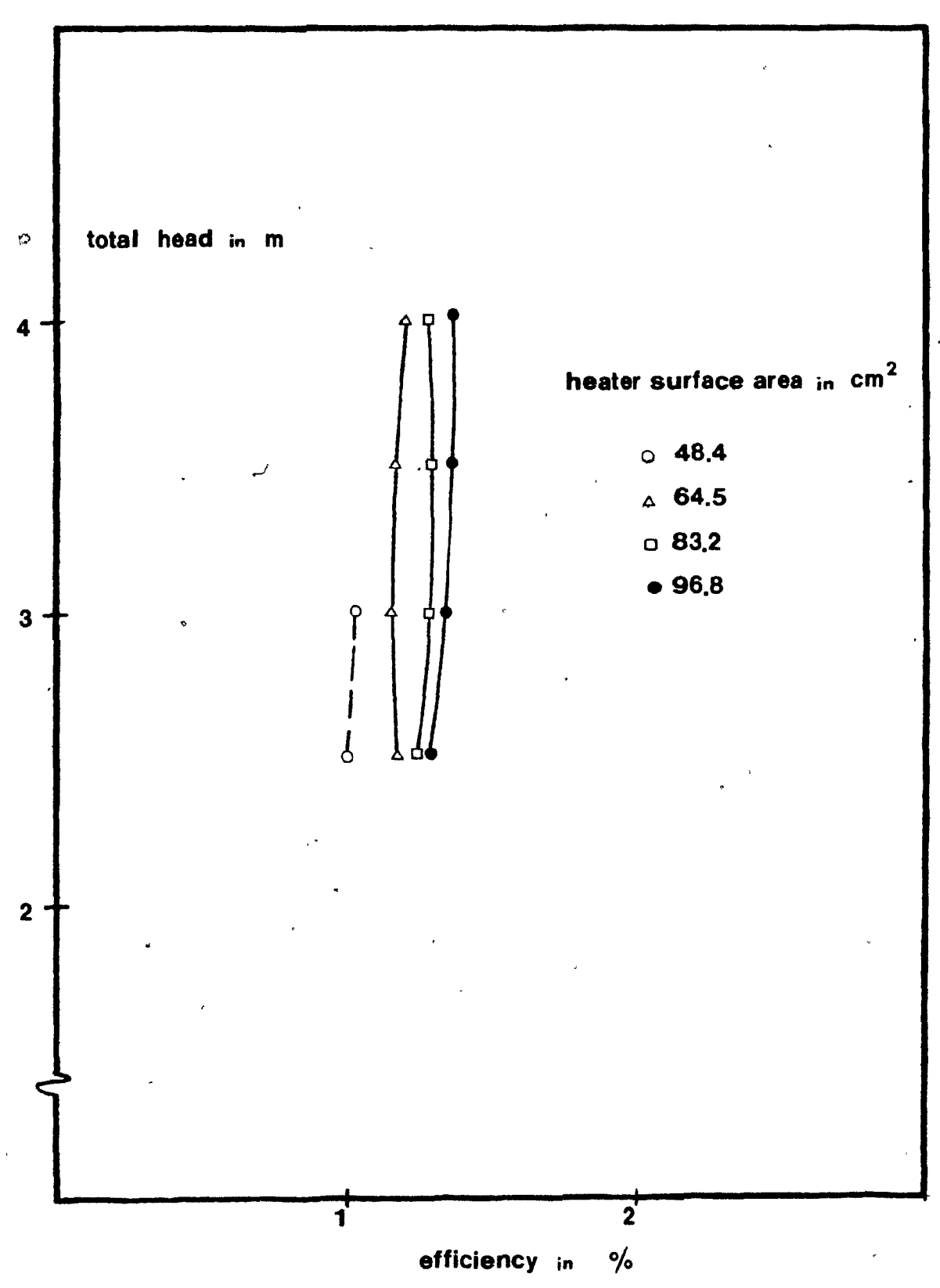
3.6. Efficiency vs Total head (var. T )

.

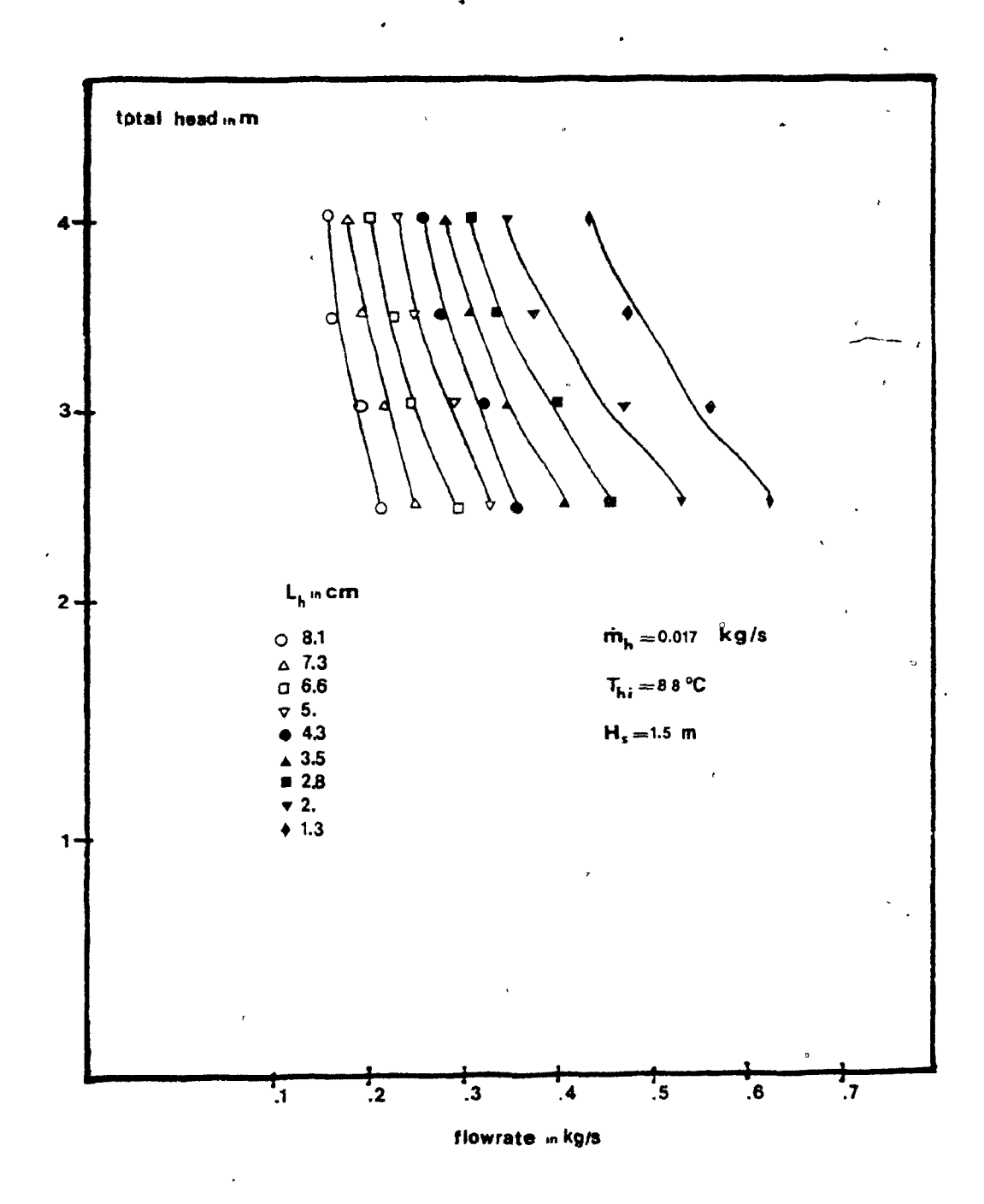
-----



3.7. Flowrate vs Total head (var. A )

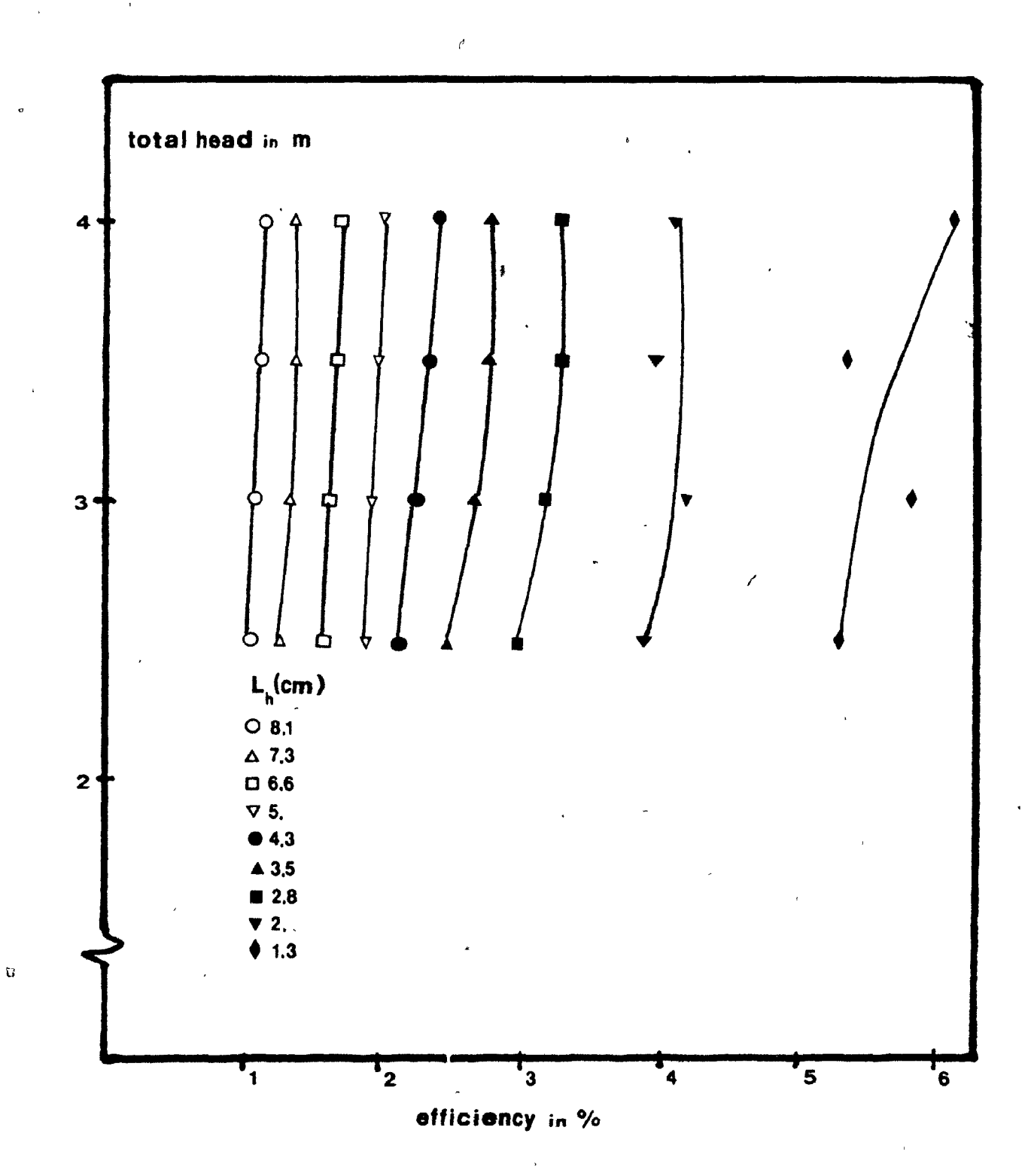


3.8. Efficiency vs Total head (var.  $A_{hb}$ )



3.9. Flowrate vs Total head (var.  $L_h$ )

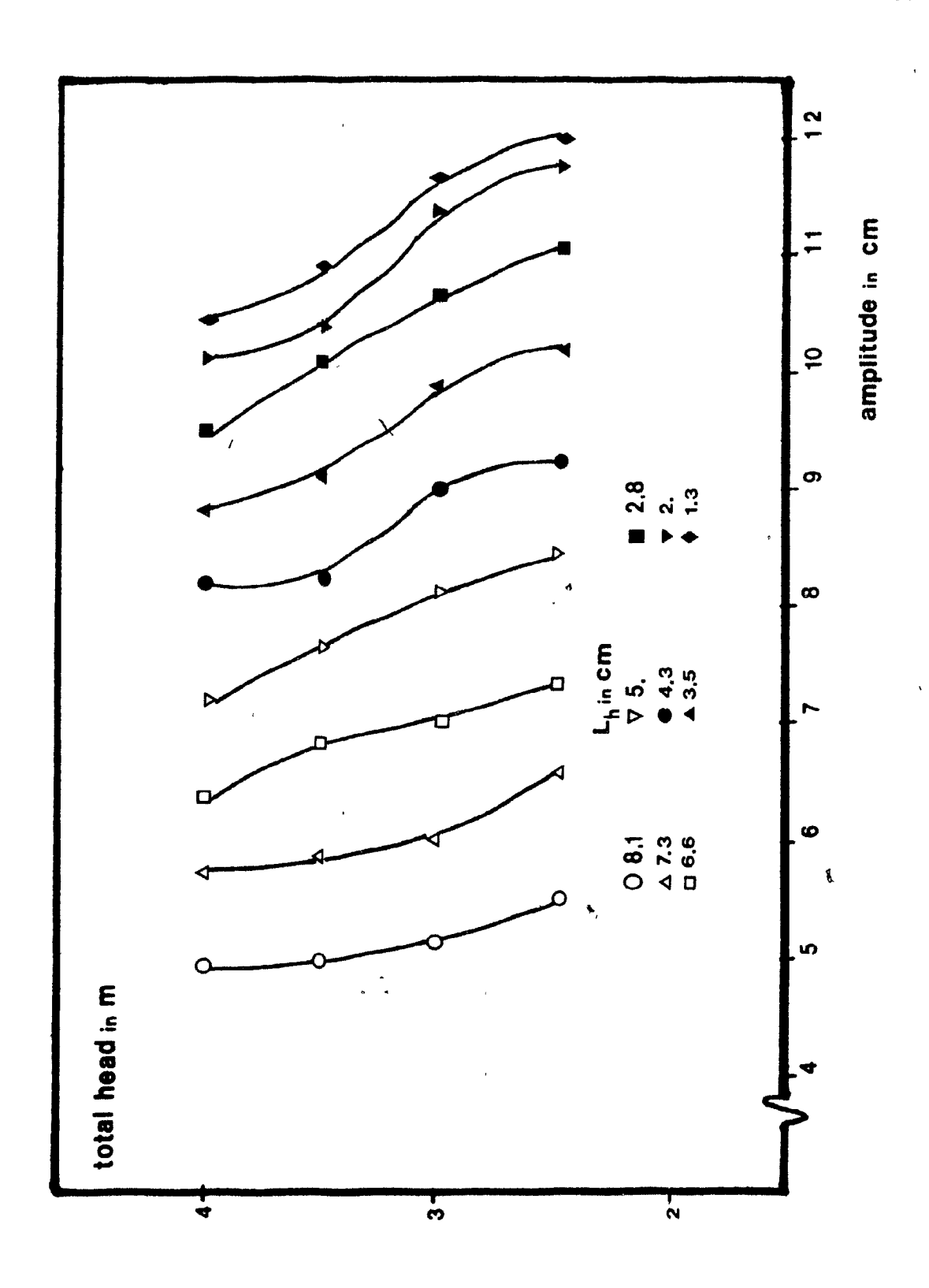
ø



3.10. Efficiency vs Total head (var. L)

-----

---



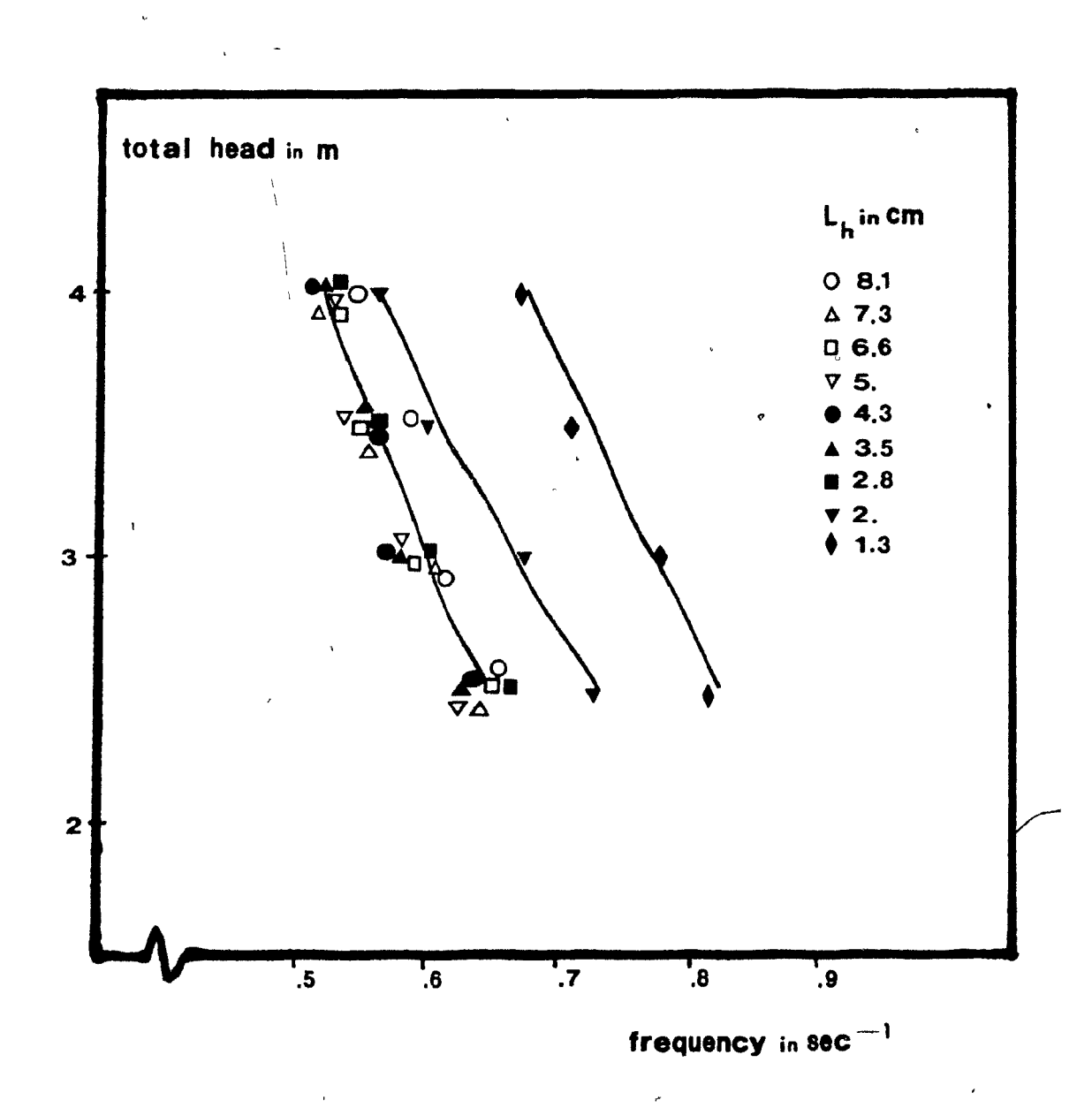
3.11. Amplitude vs Total head (var.  $L_h$ )

...

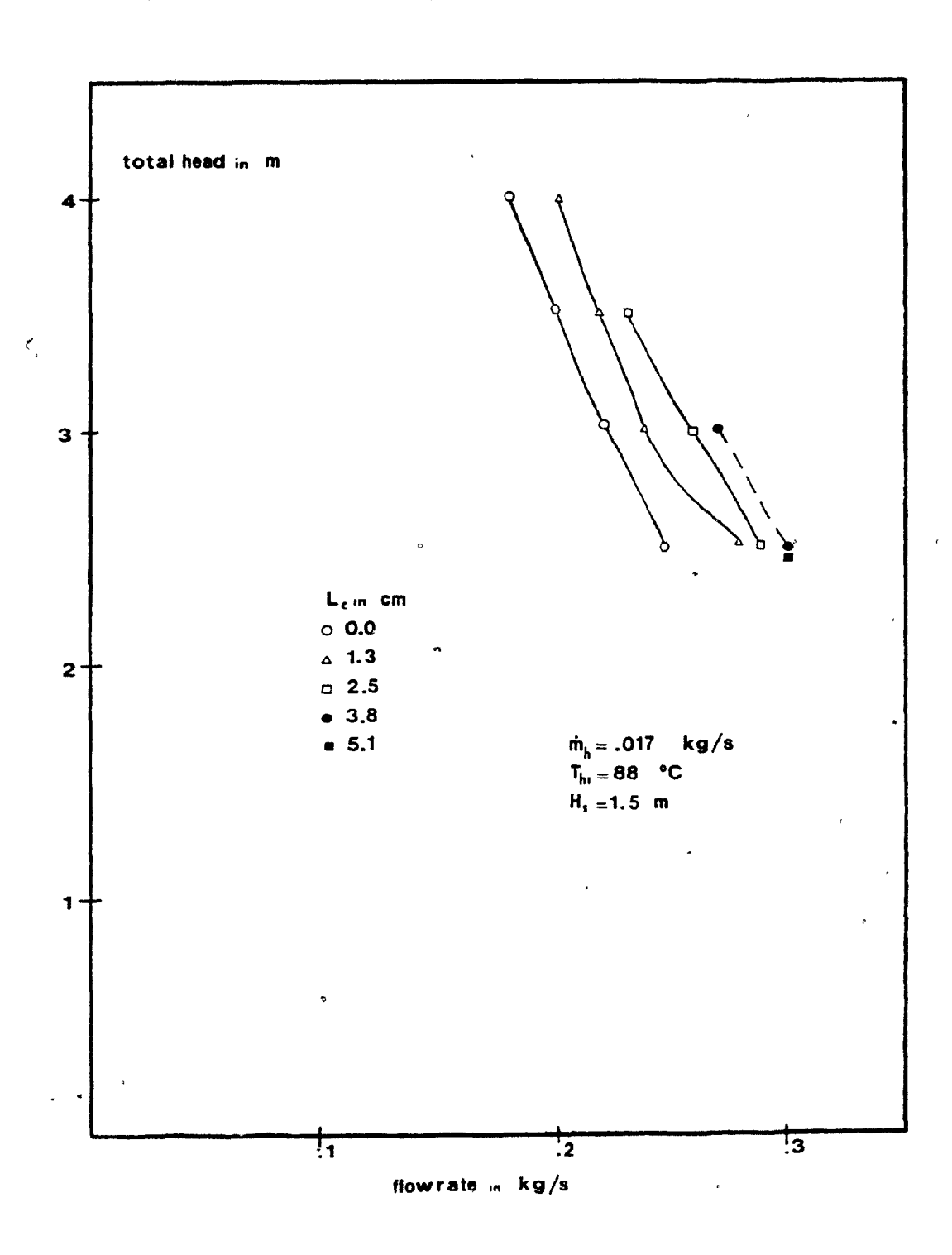
.

•

. . .



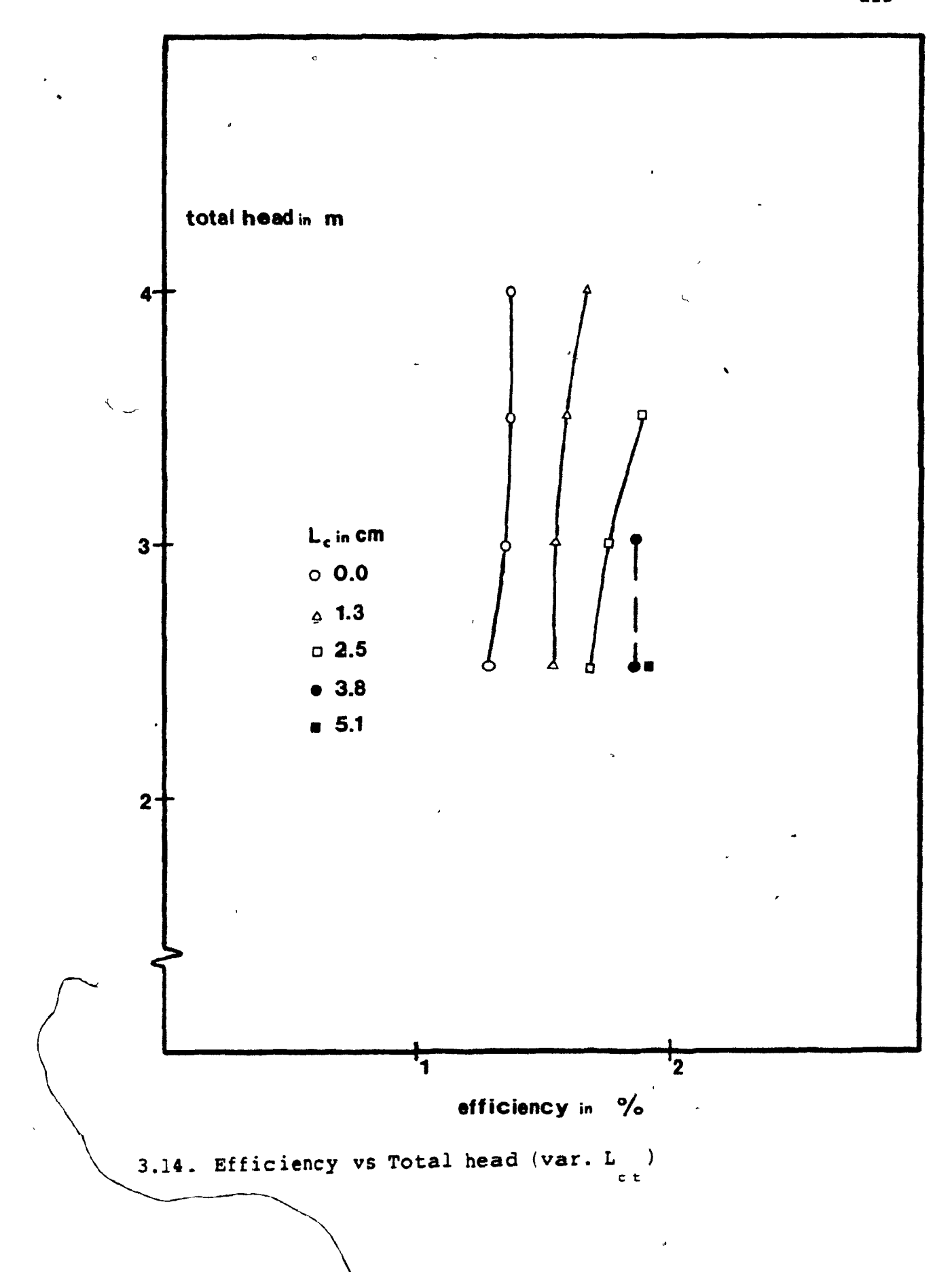
3.12. Frequency vs Total head (var.  $L_h$ )



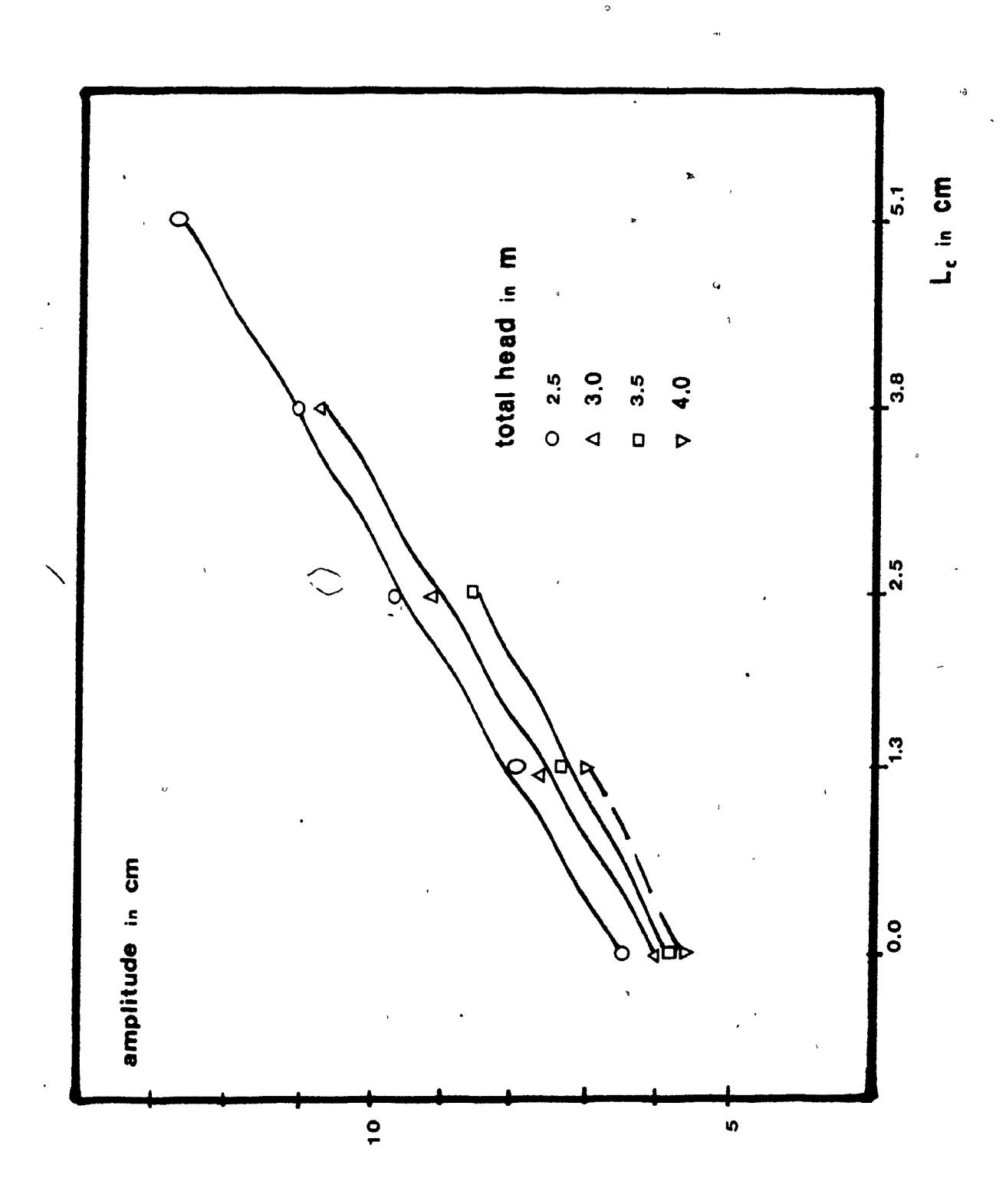
3.13. Flowrate vs Total head (var.  $L_{ct}$ )

Of the Salaran and Salaran and

٠ -



1\_

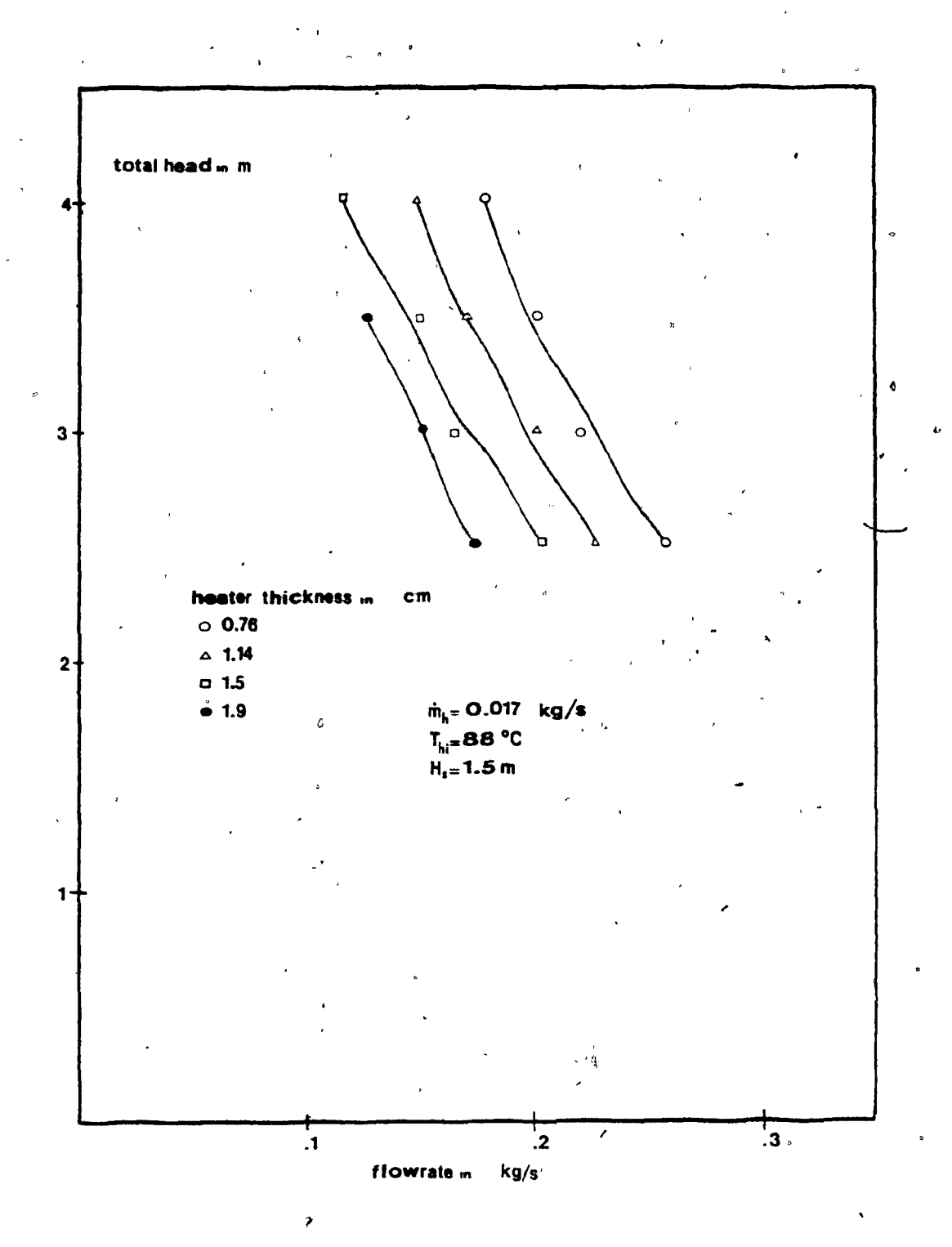


3.15. Amplitude vs L (var. total head)

•

...

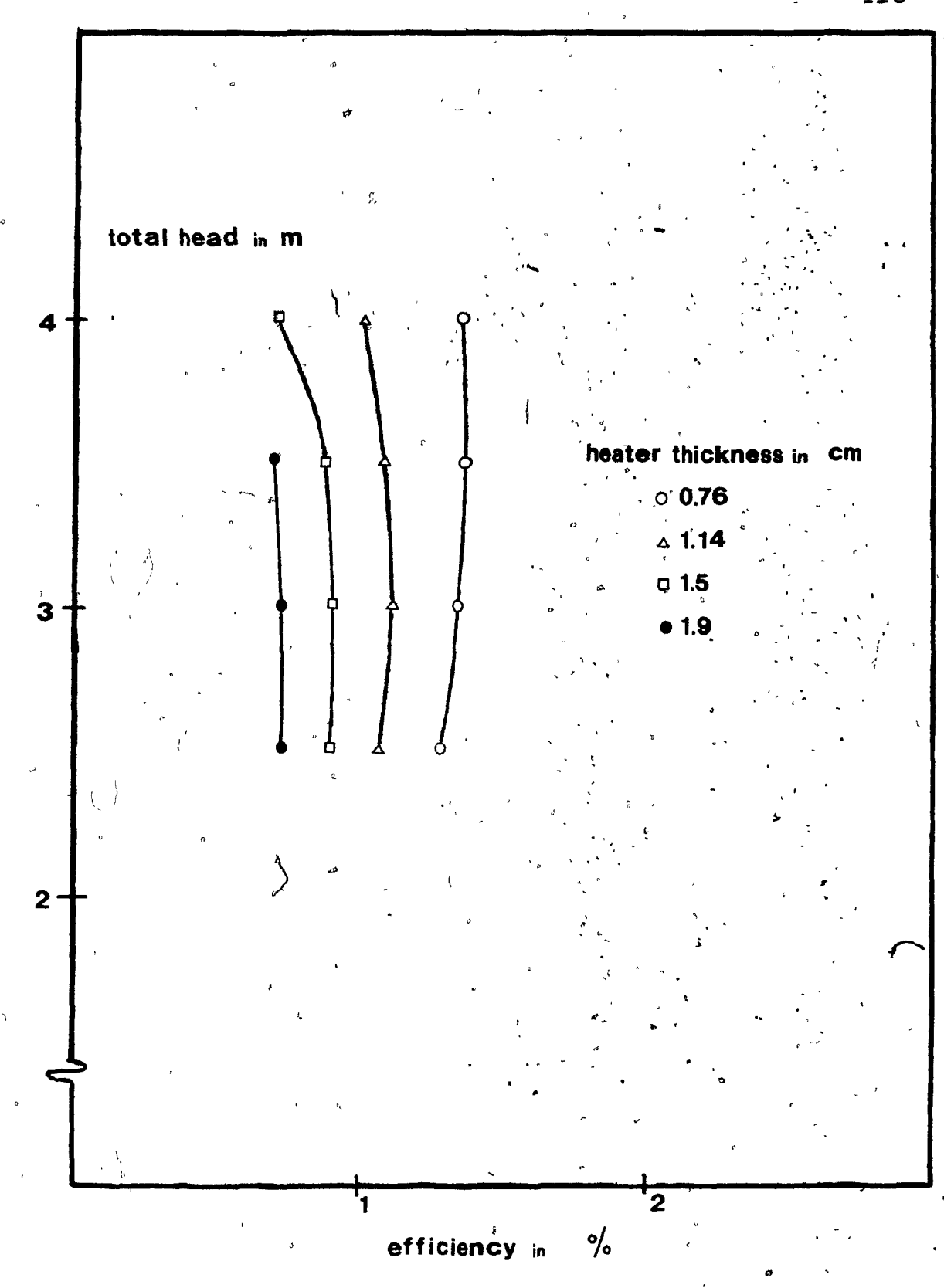
---



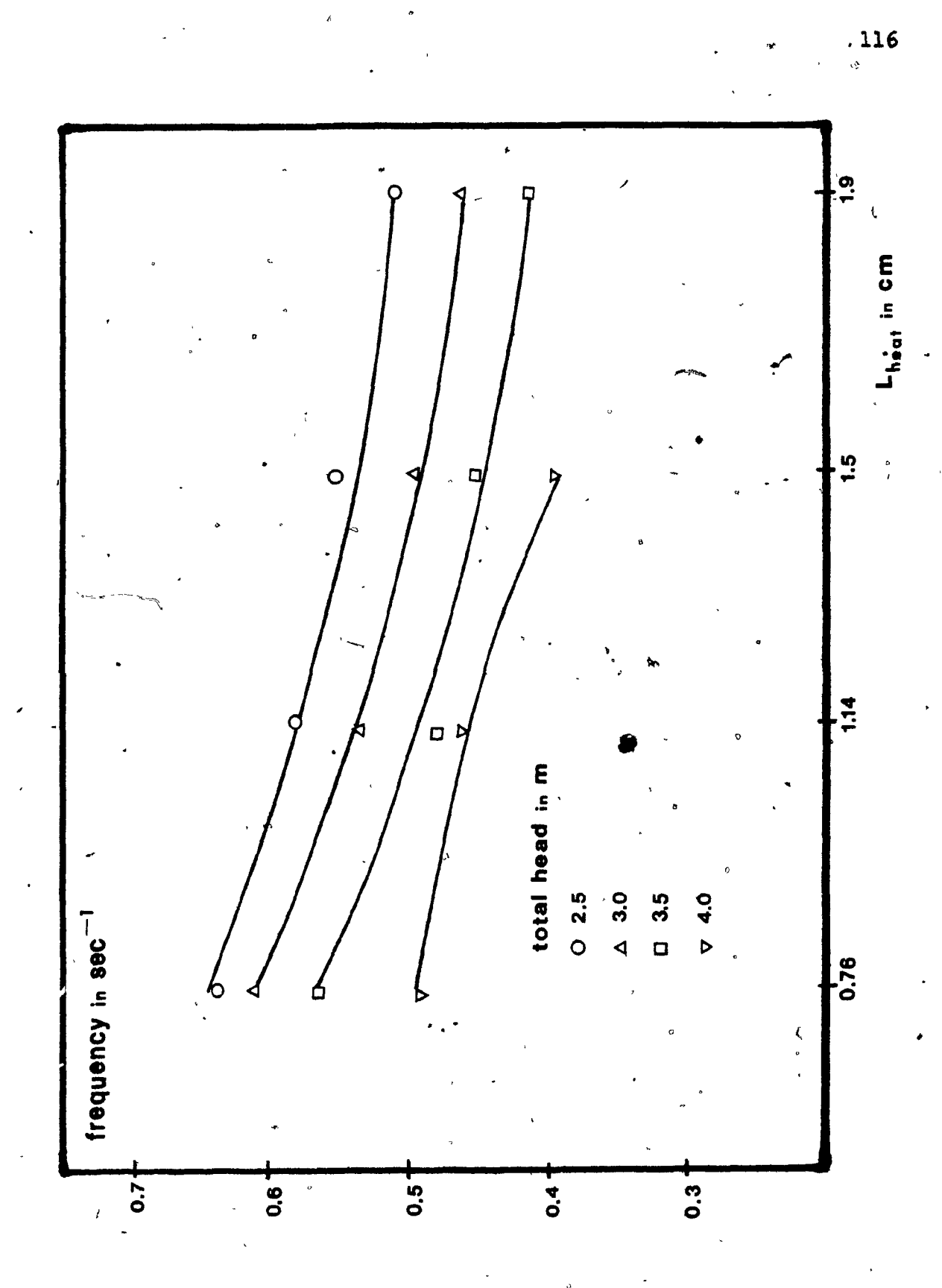
3.16. Flowrate vs Total head (var. L h

\_\_\_\_\_

\_\_\_ 2 -\_

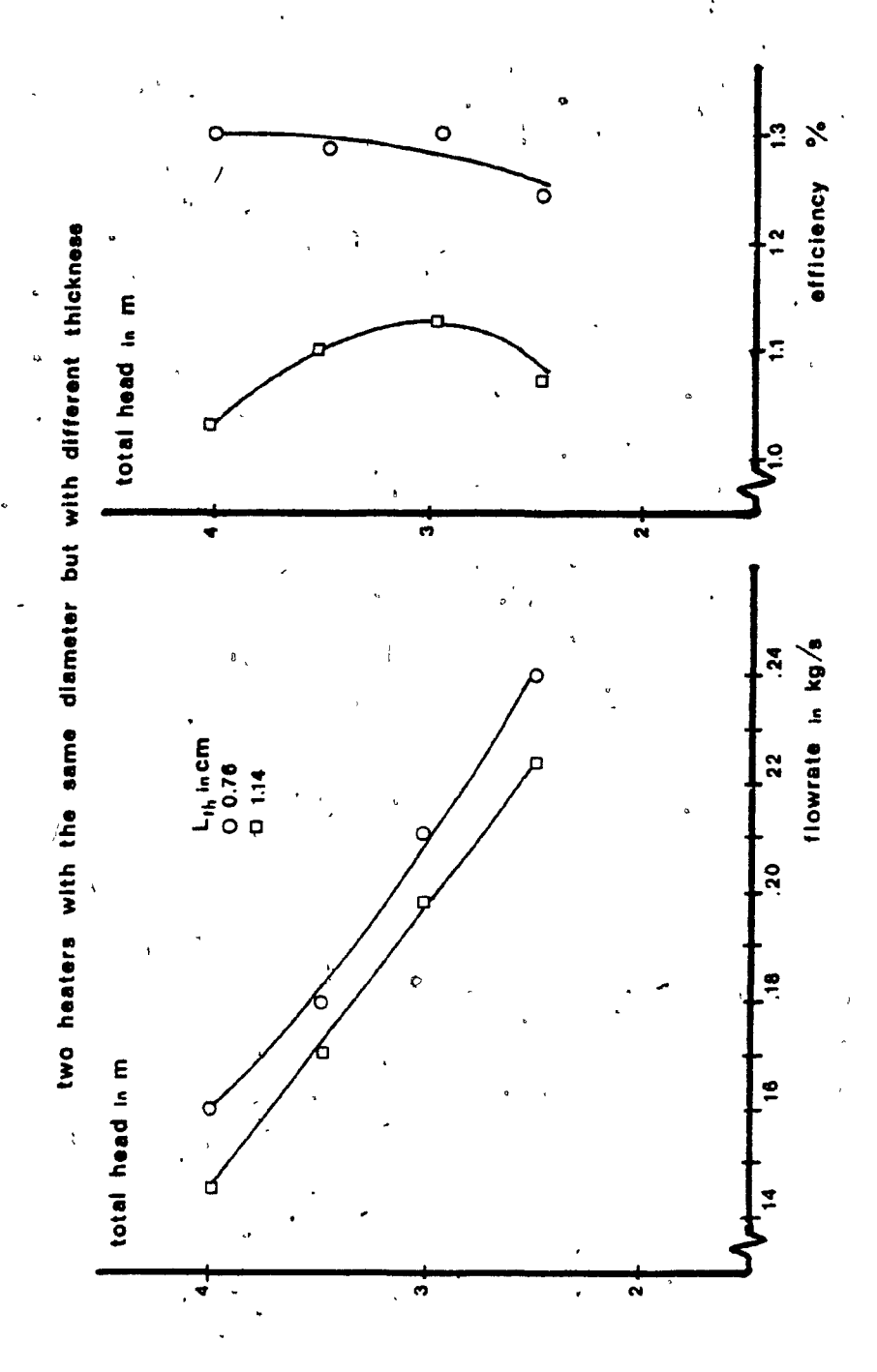


3.17. Efficiency vs Total head (var. L )



3.18. Frequency vs L (var. total head)

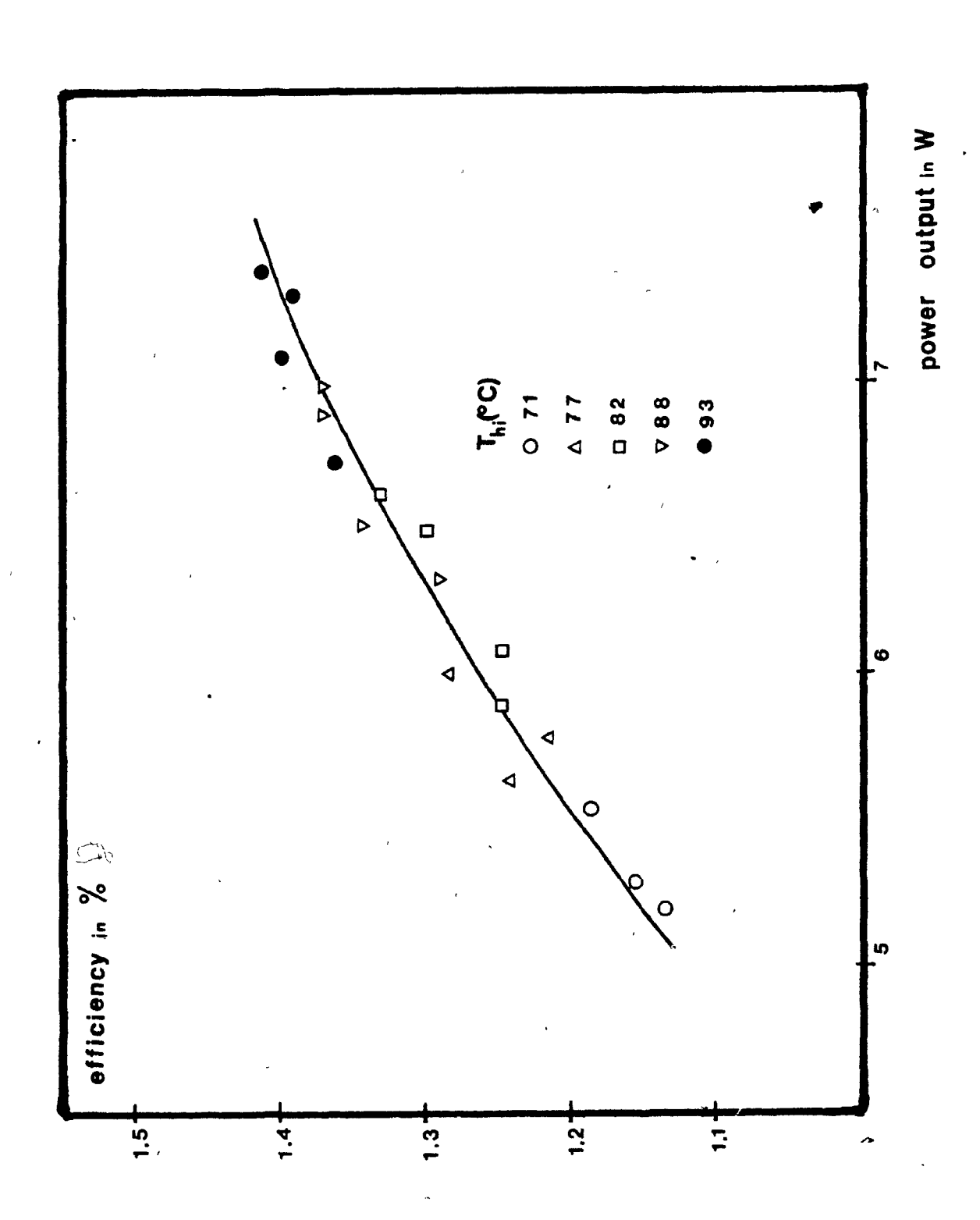
0)



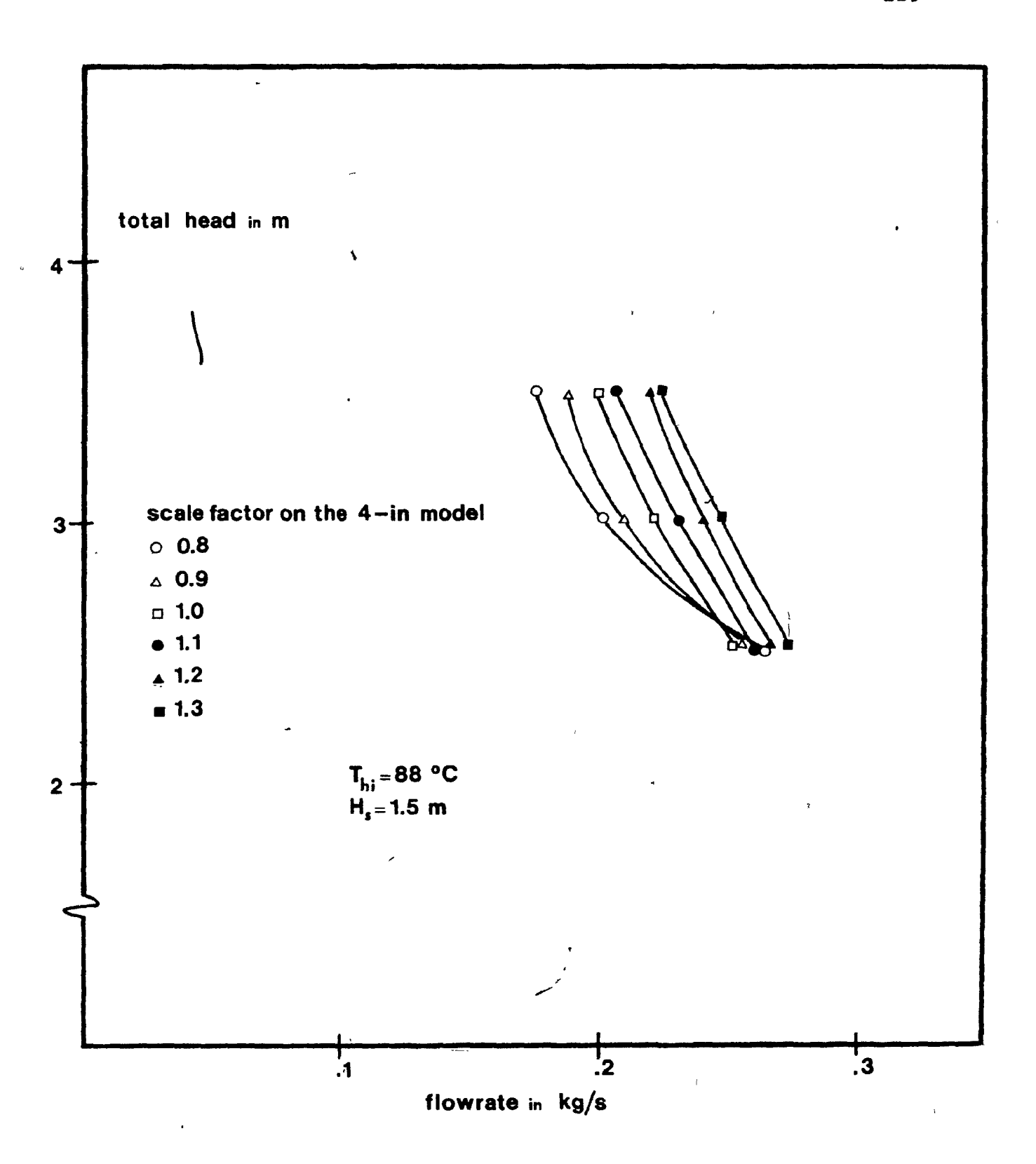
3.19. Flowrate and Efficiency vs Total head (var. L )

(`)

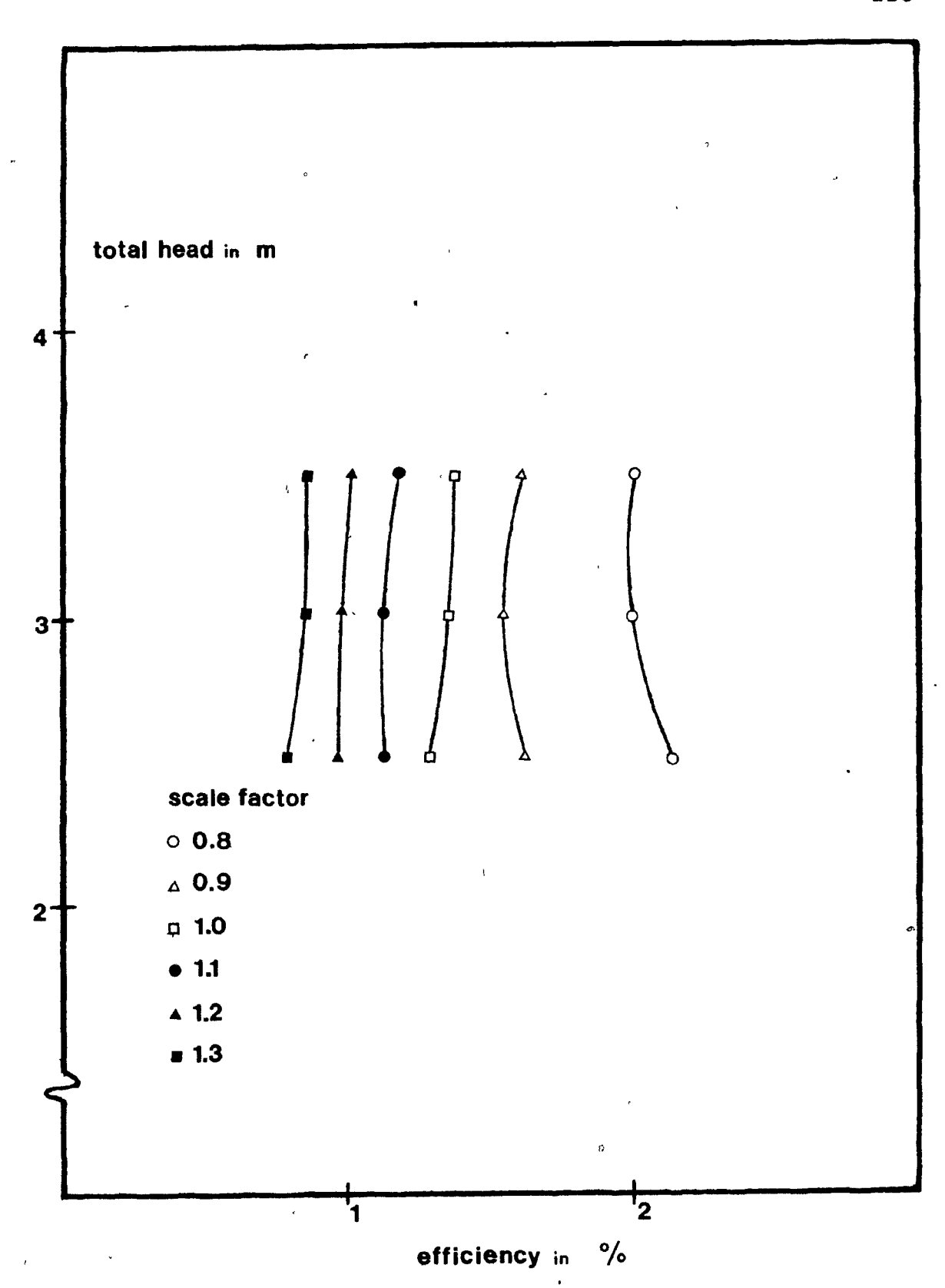
\_\_\_\_



3.20. Efficiency vs Power output (var.  $T_{hi}$ )



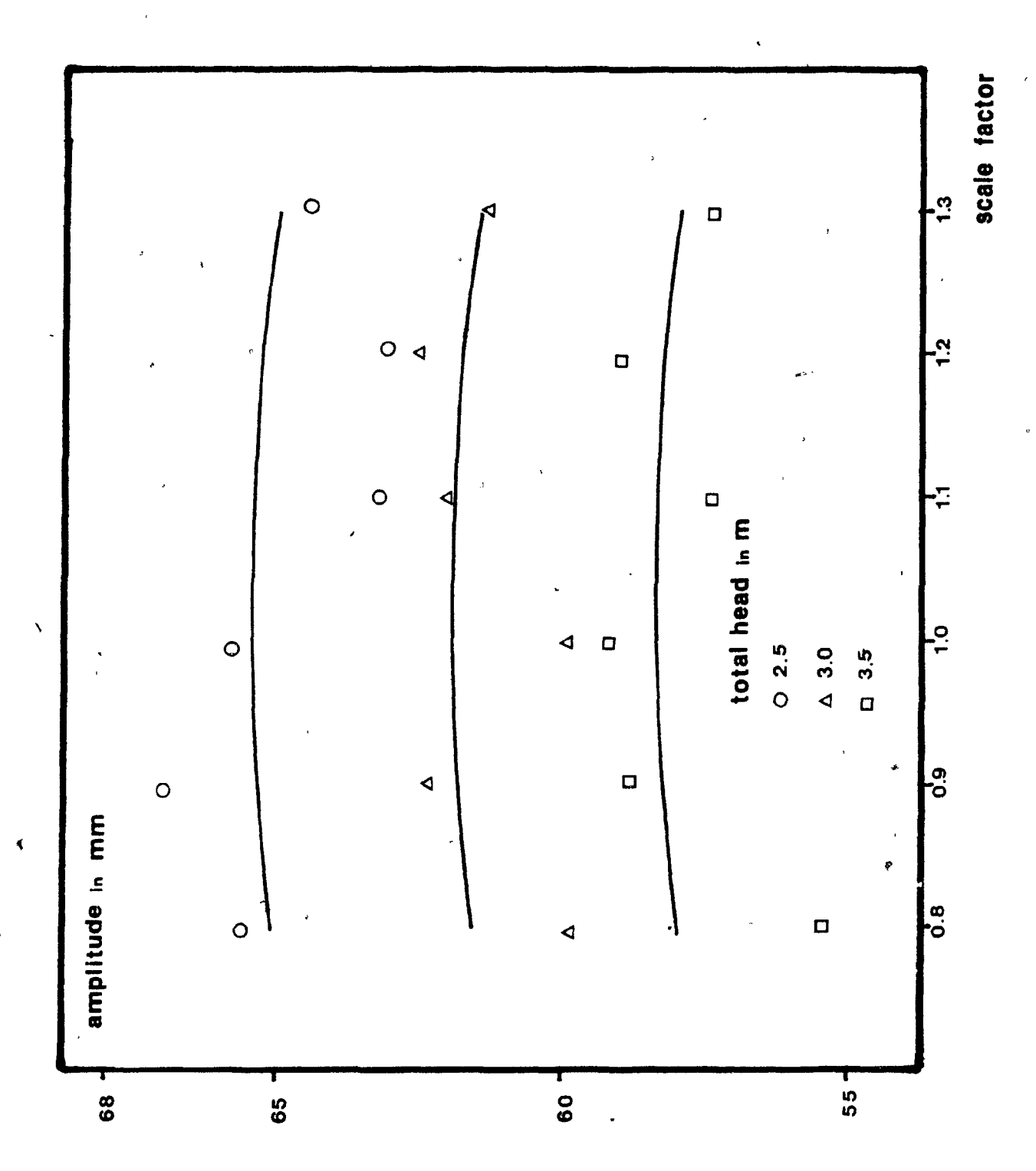
3.21. Flowrate vs Total head (var. scale factor)



3.22. Efficiency vs Total head (var. scale factor)

ŧ

• -

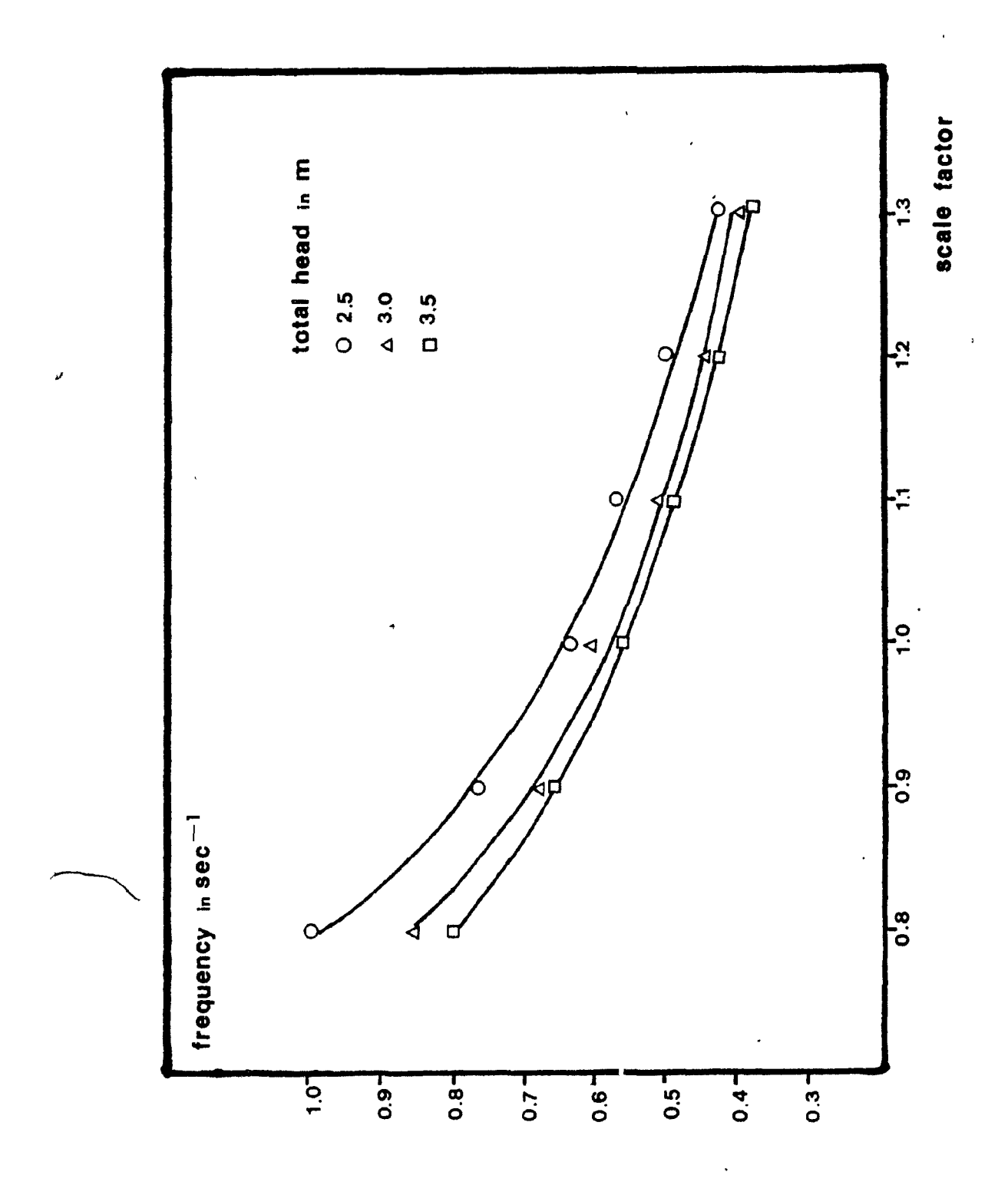


3.23. Amplitude vs Scale factor (var. total head)

a

,

١,



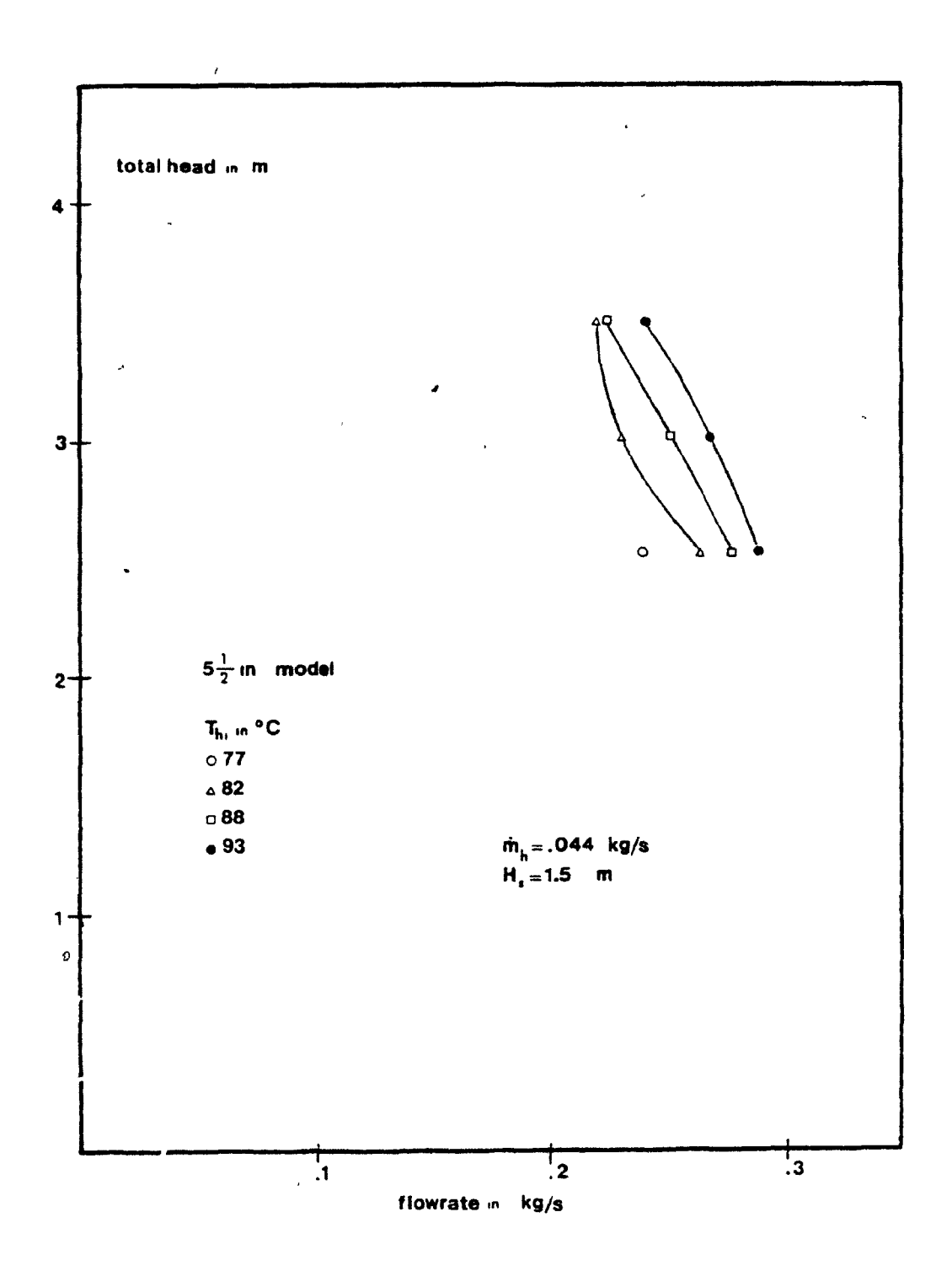
3.24. Frequency vs Scale factor (var. total head)

-----

----

.

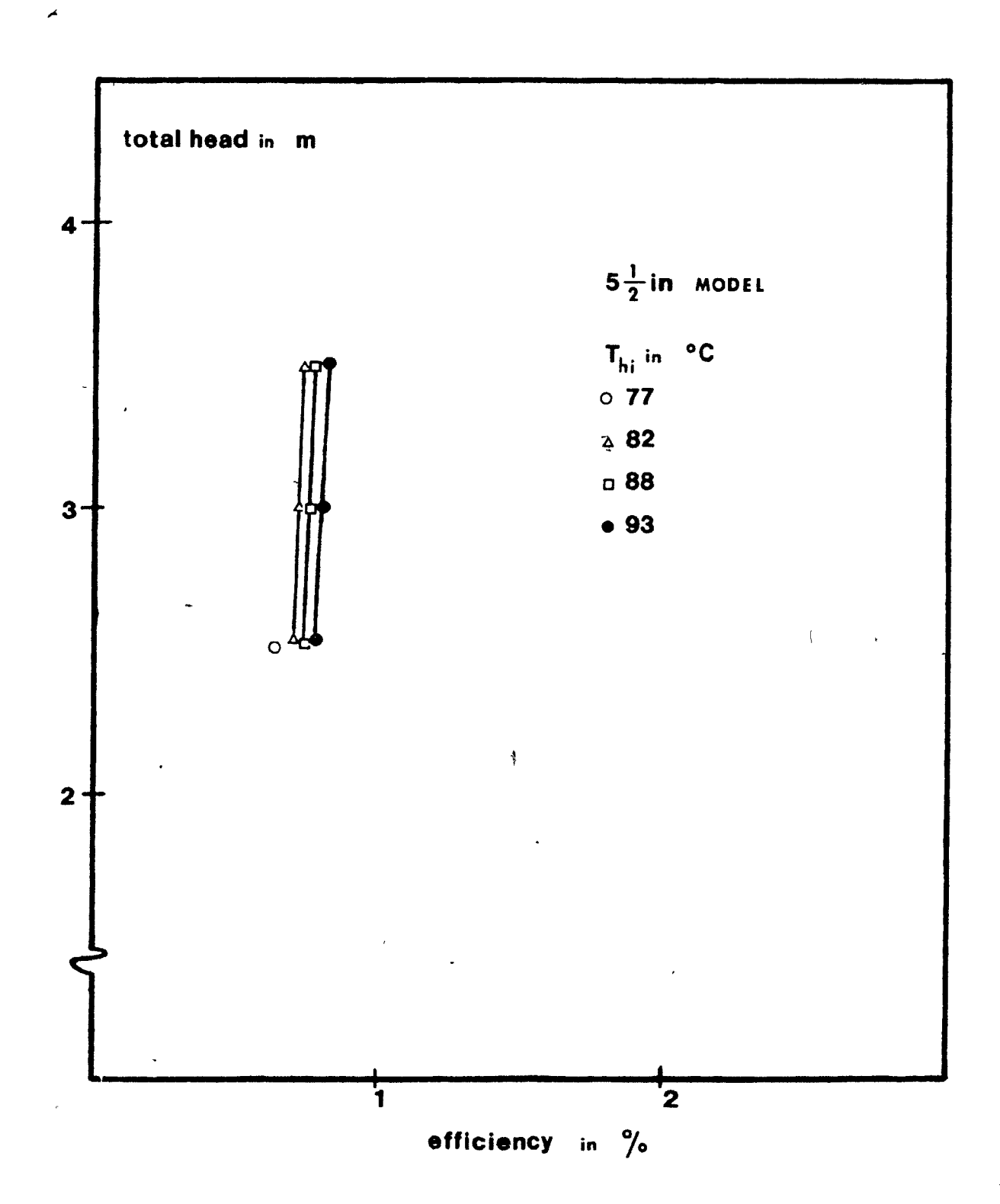
-



3.25. Flowrate vs Total head (var. T -scaled model)

managana ik dinakkangangangangangangangangan arawa

\_\_\_\_

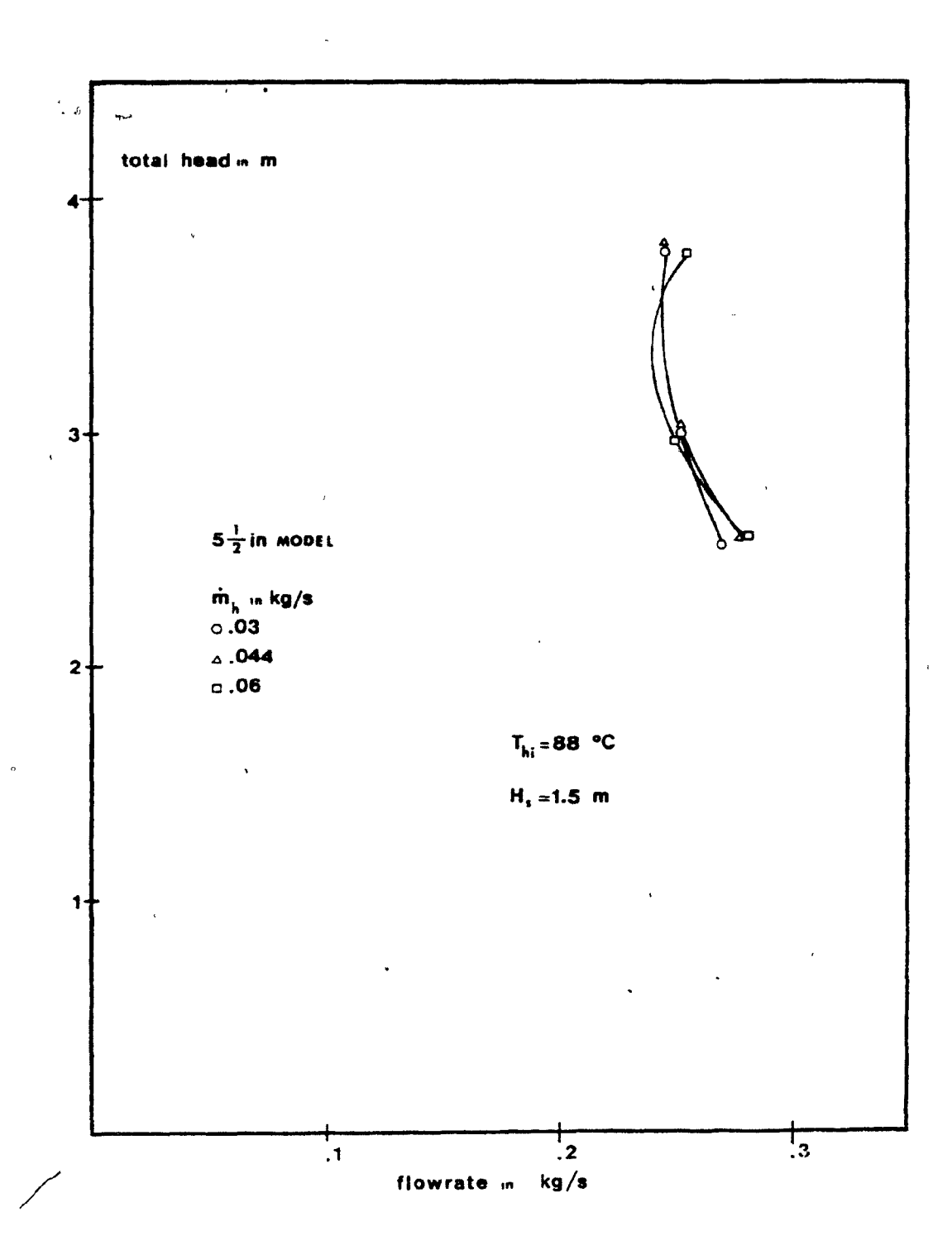


3.26. Efficiency vs Total head (var. T  $_{h i}$  -scaled model)

.... . .

erentaria e e

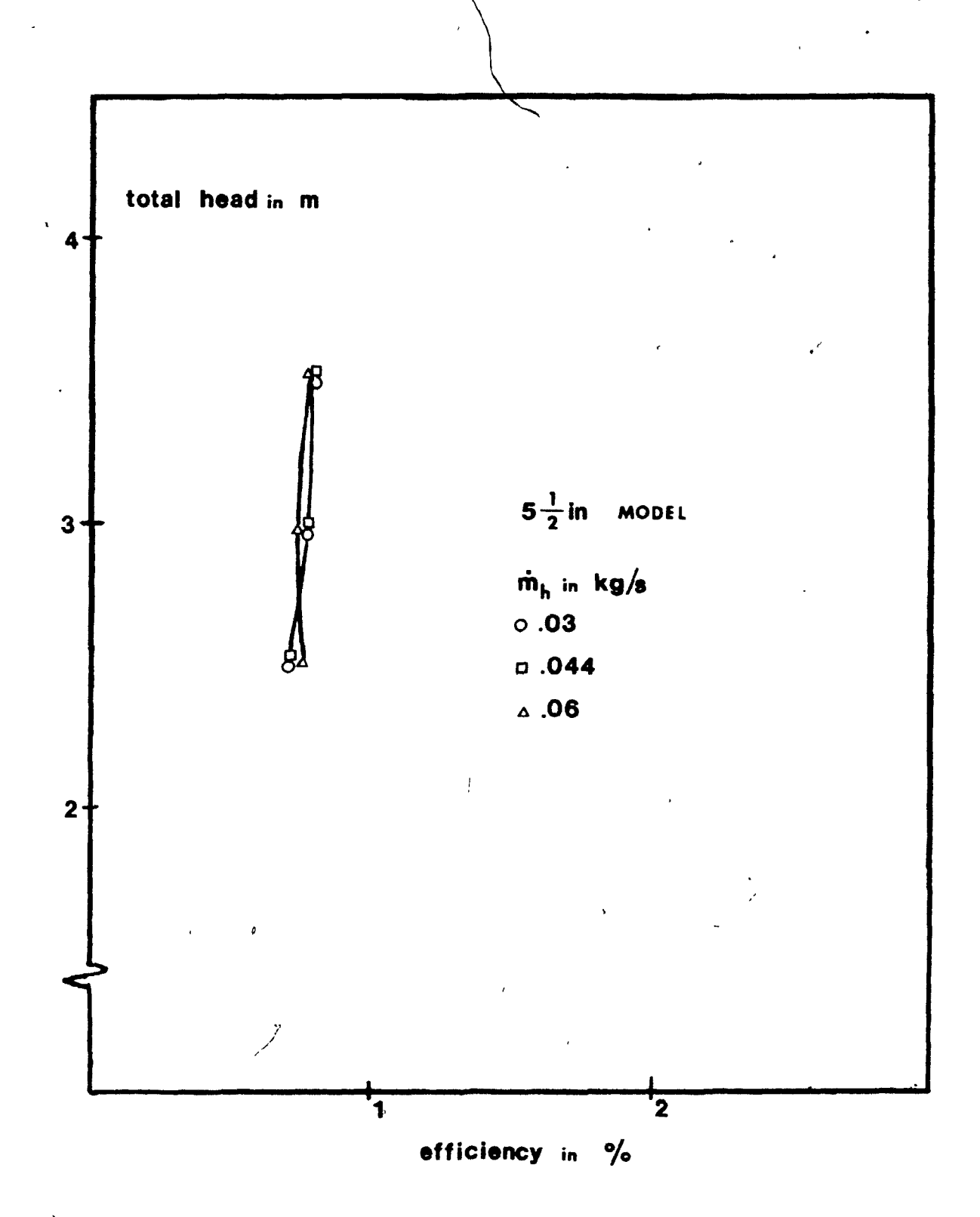
----



3.27. Flowrate vs Total head (var. m -scaled model)

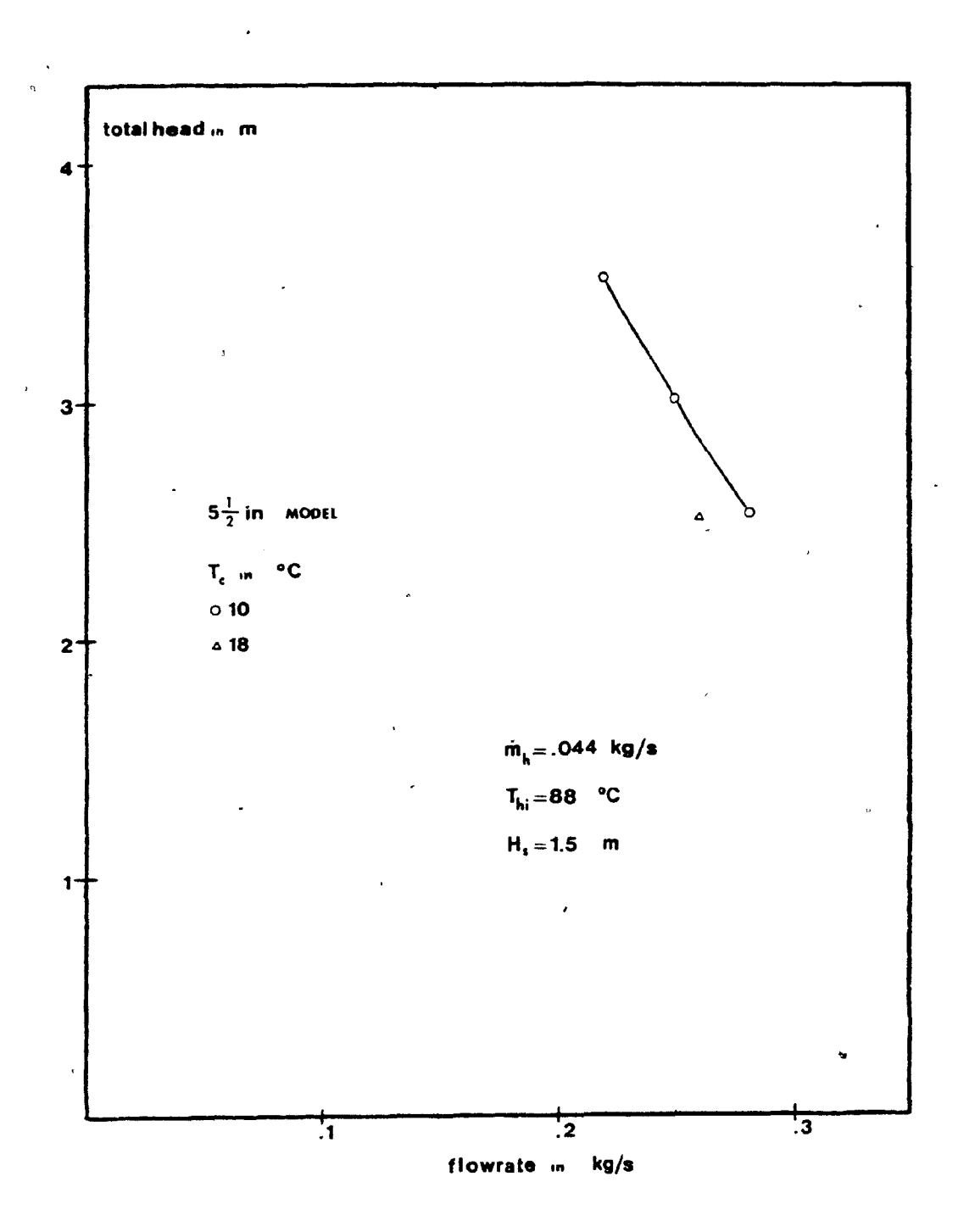
(

and the second s



3.28. Efficiency vs Total head (var. m -scaled model)

75 30



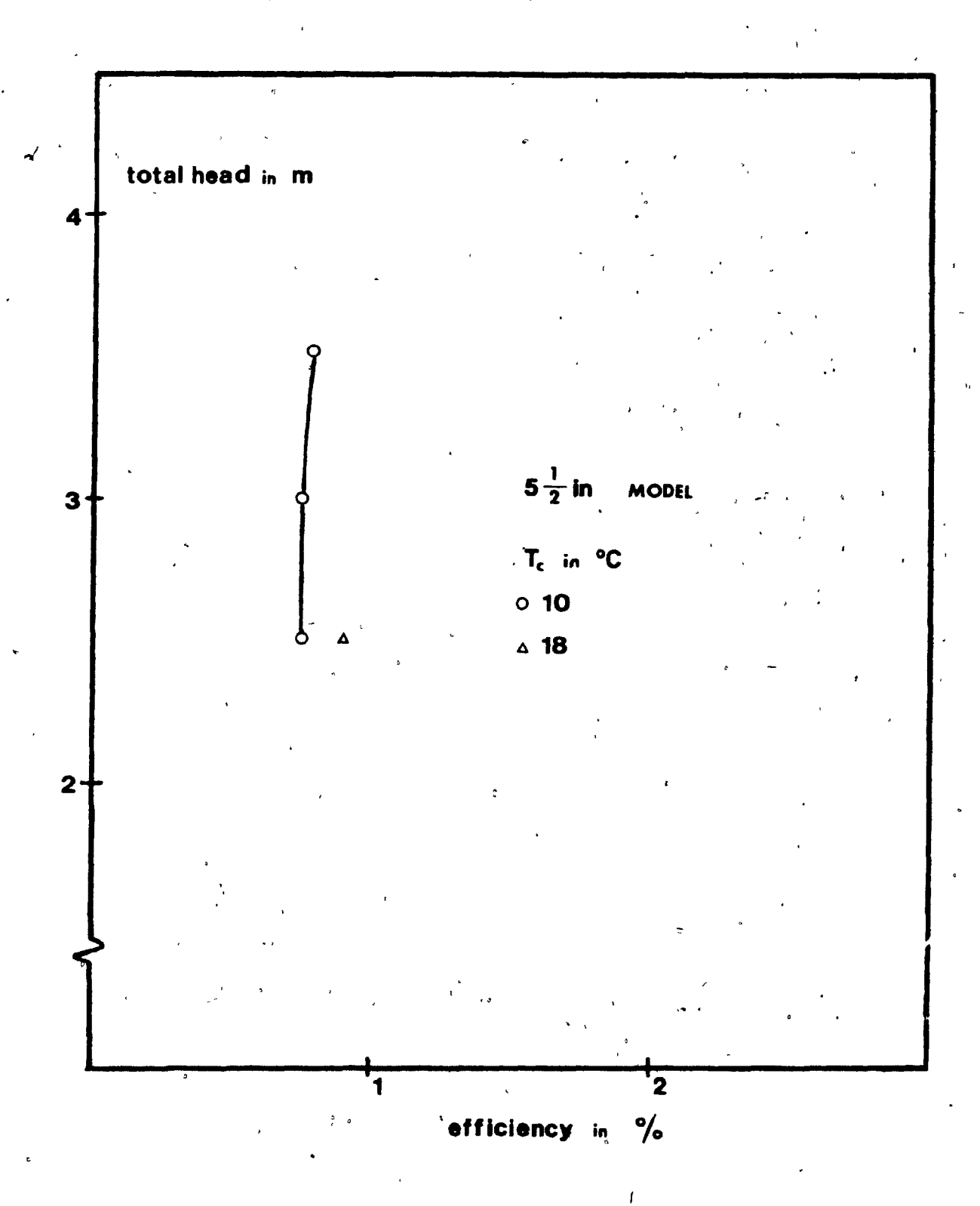
3.29. Flowrate vs Total head (var. T -scaled model)

\_ -

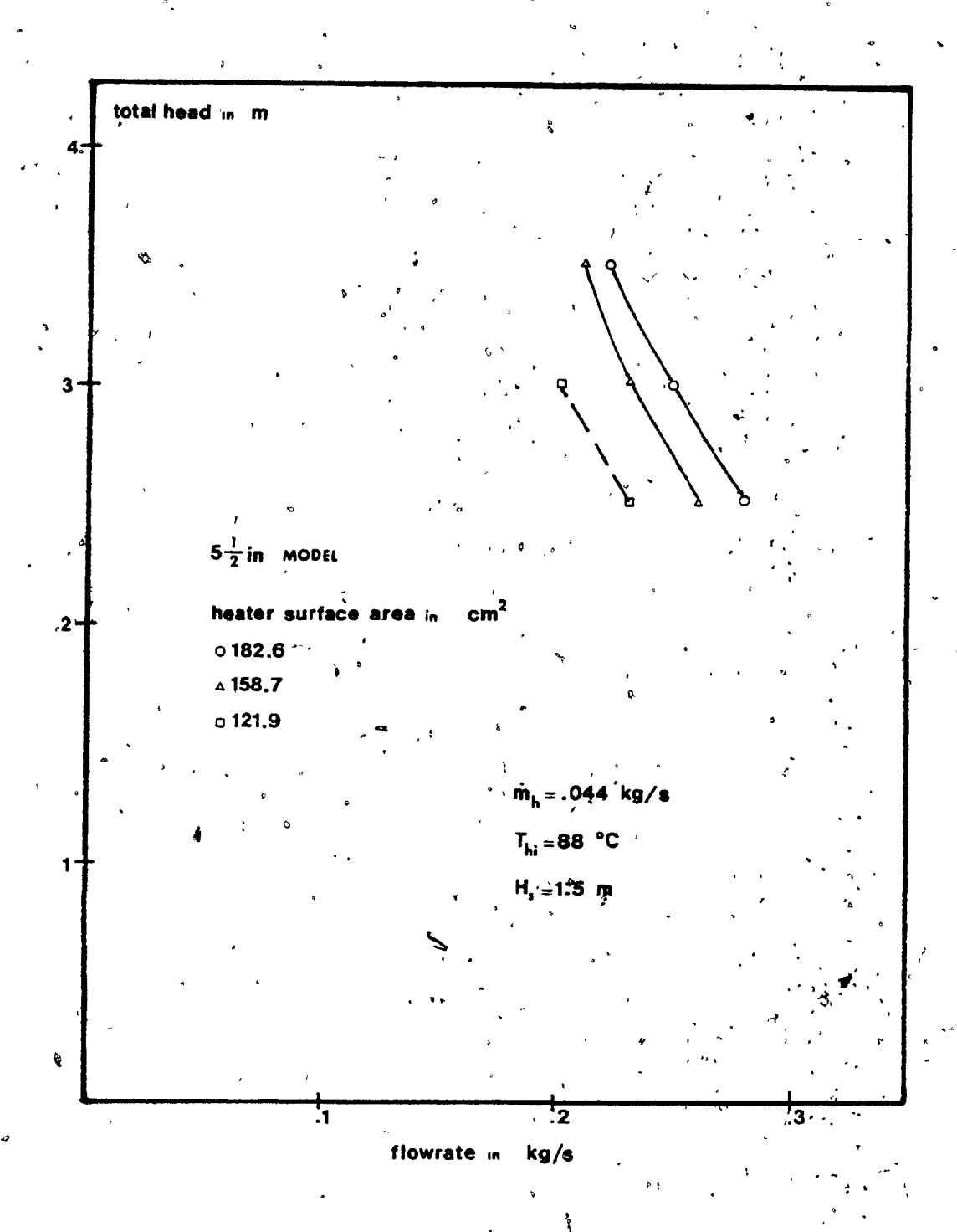
and the second s

.

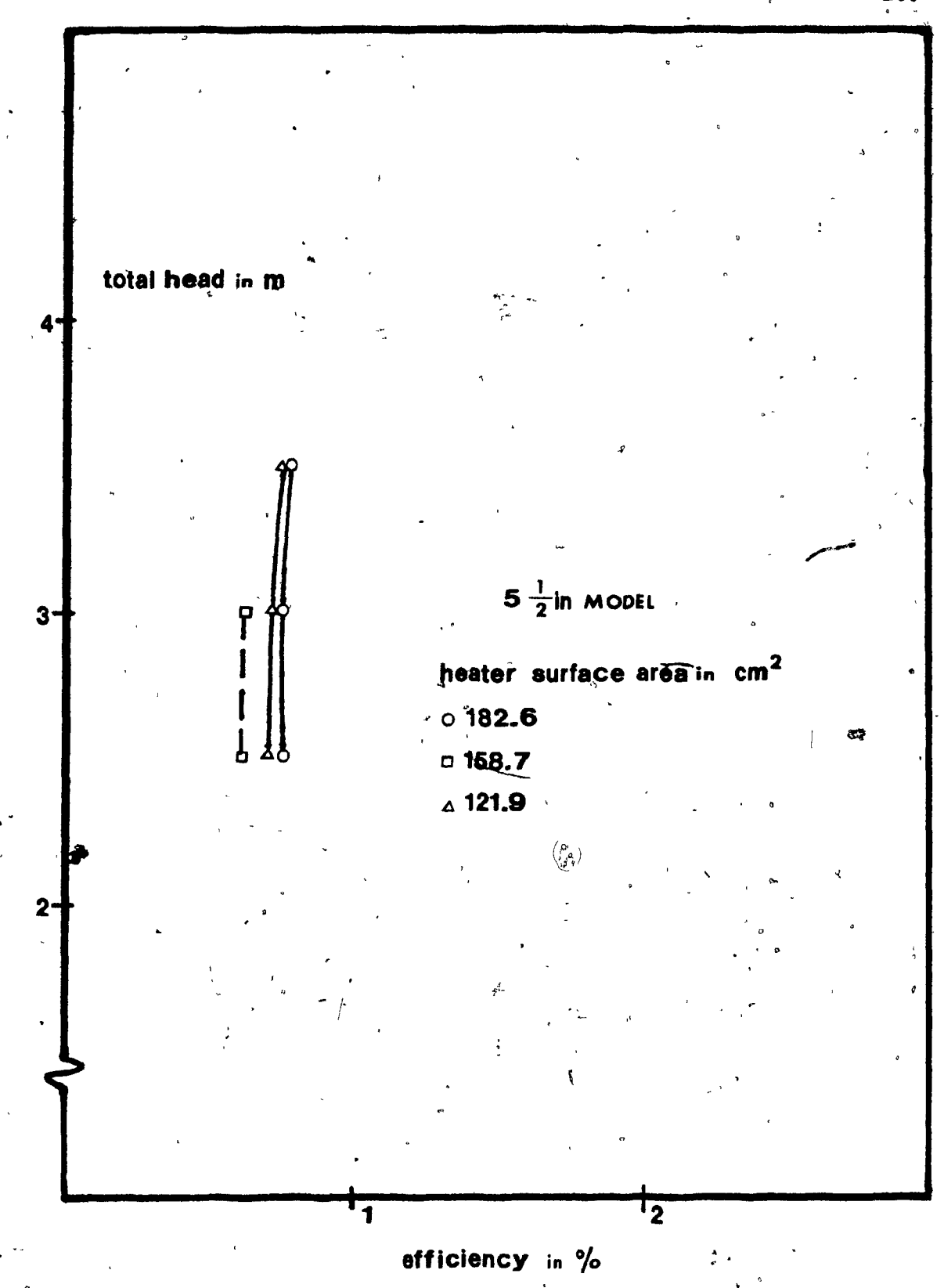
A---



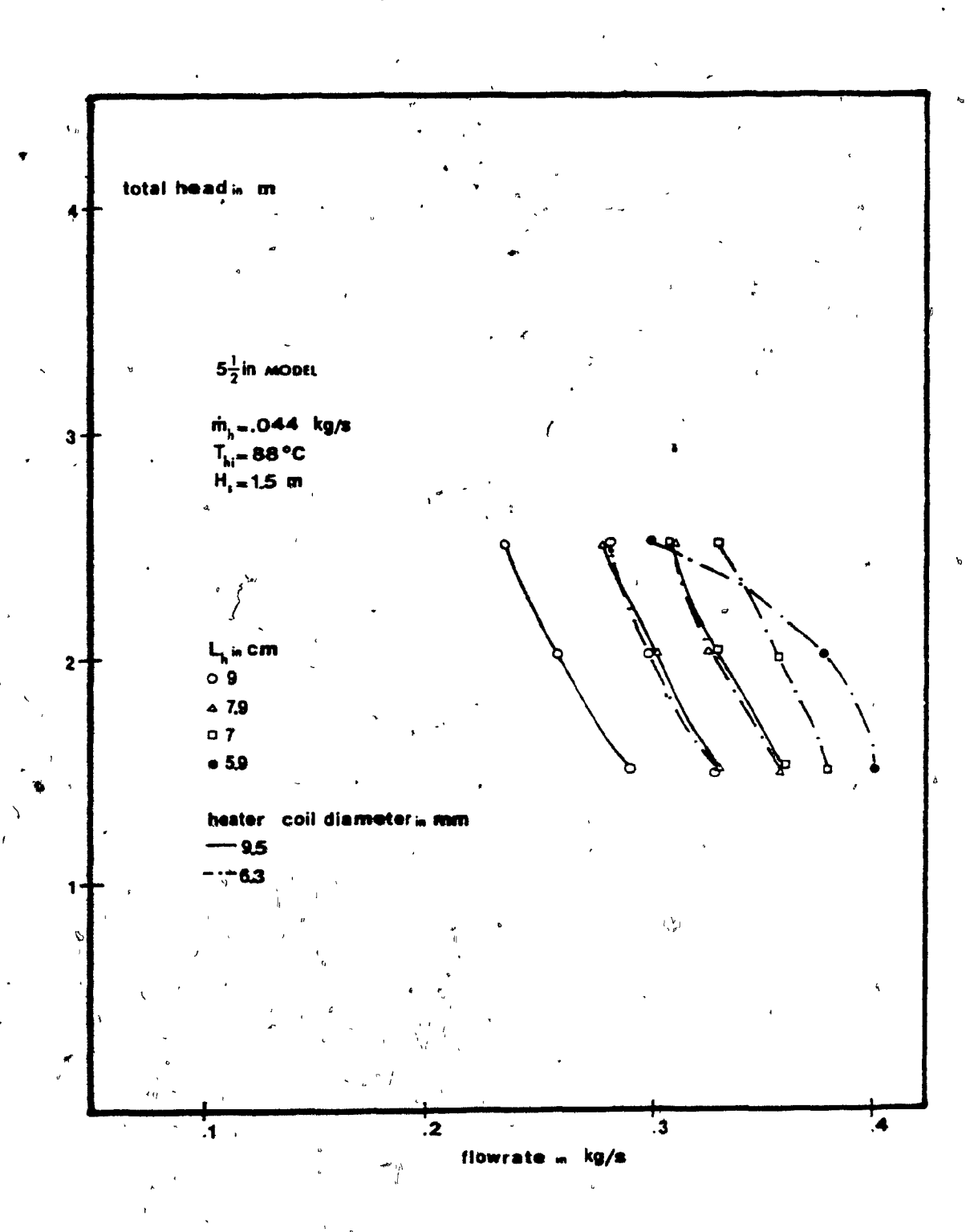
3.30. Efficiency vs Total head (var. T\_-scaled model)



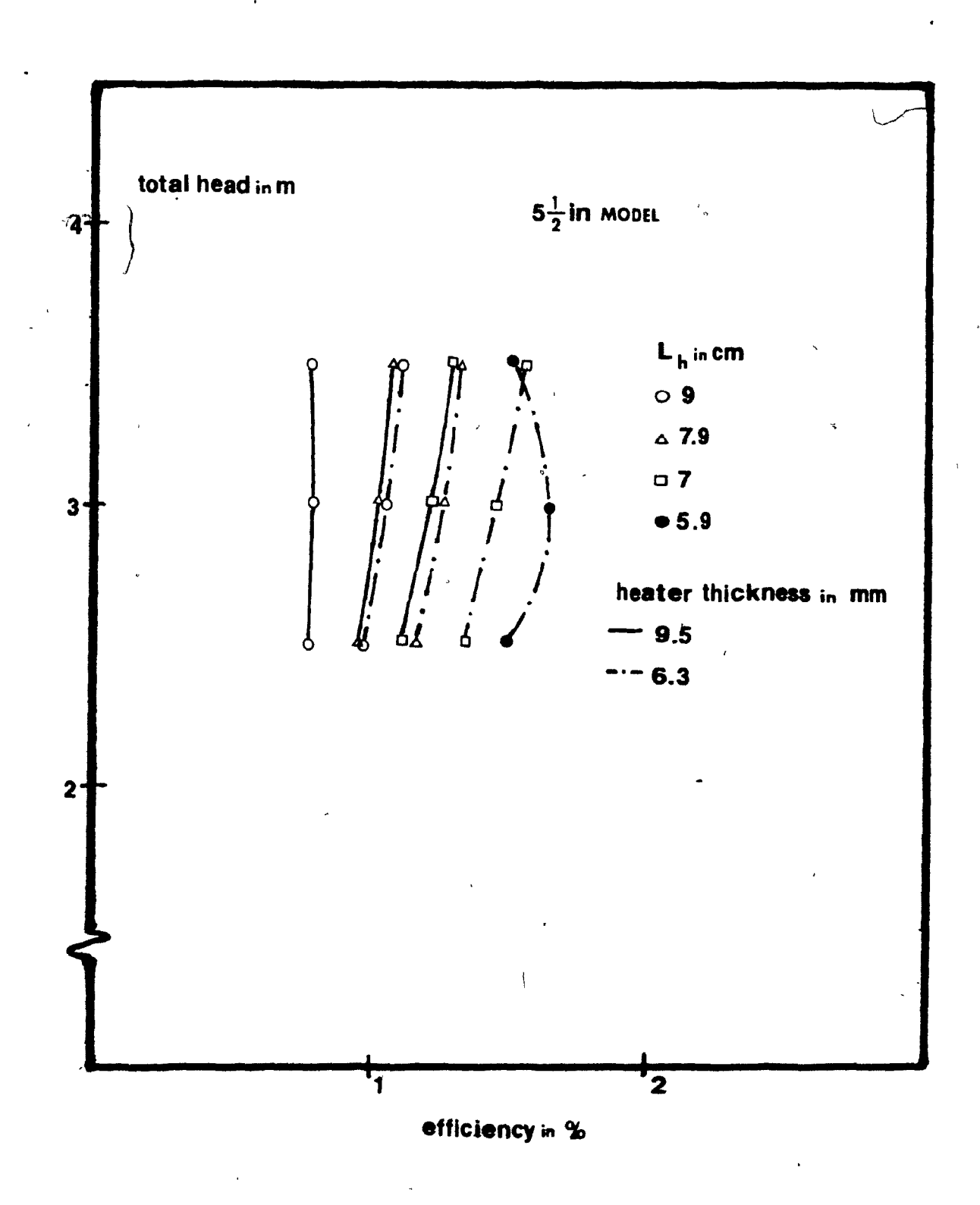
3.31. Flowrate vs Total head (var. A -scaled model)



3.32. Efficiency vs Total head (var. A -scaled model)



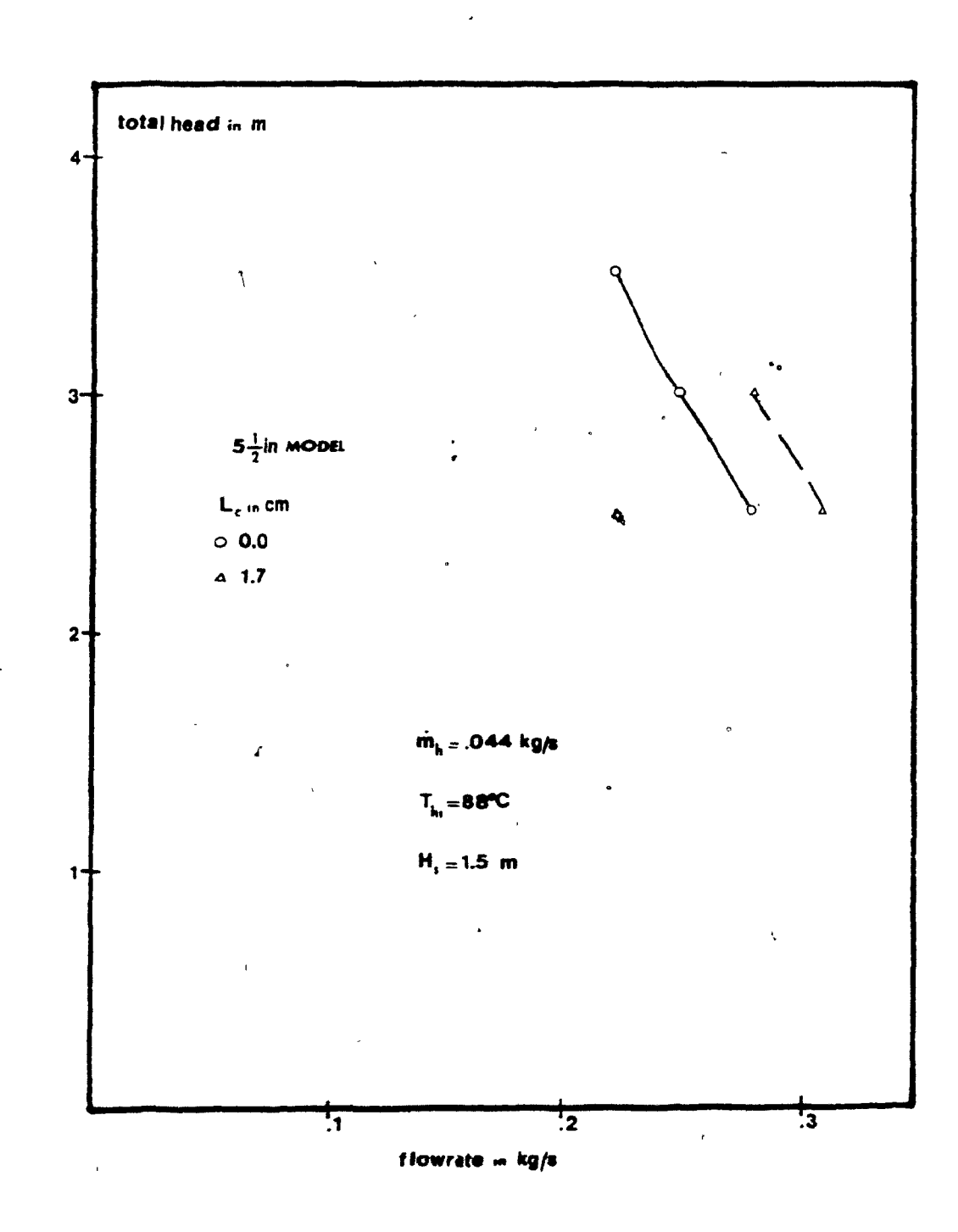
3.33. Flowrate vs Total head (var. L and L -scaled model)



3.34. Efficiency vs Total head (var. L and L -scaled model)

-

.

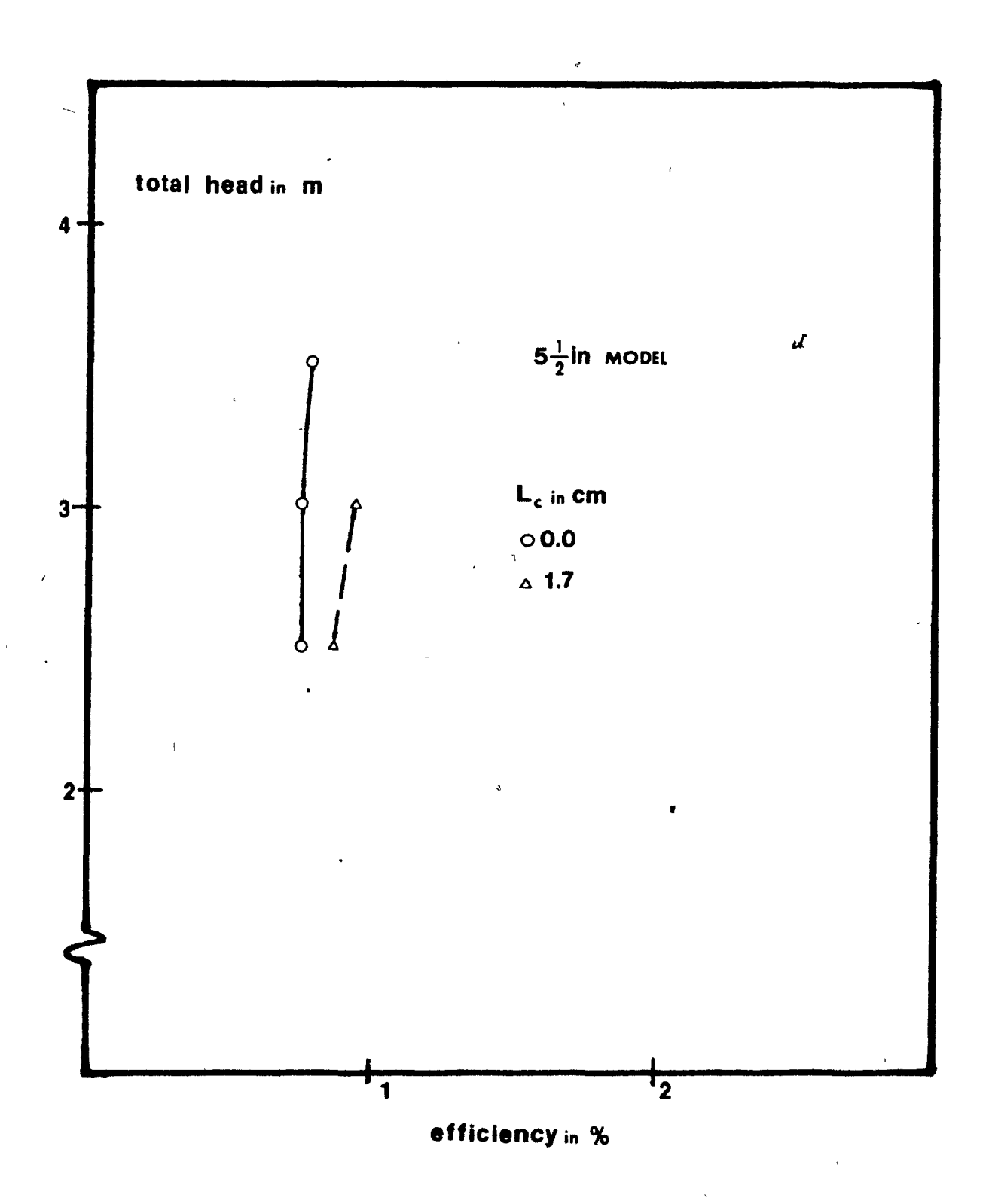


3.35. Flowrate vs Total head (var. L -scaled model)

 $\vartheta'_{\mathfrak{u}}$ 

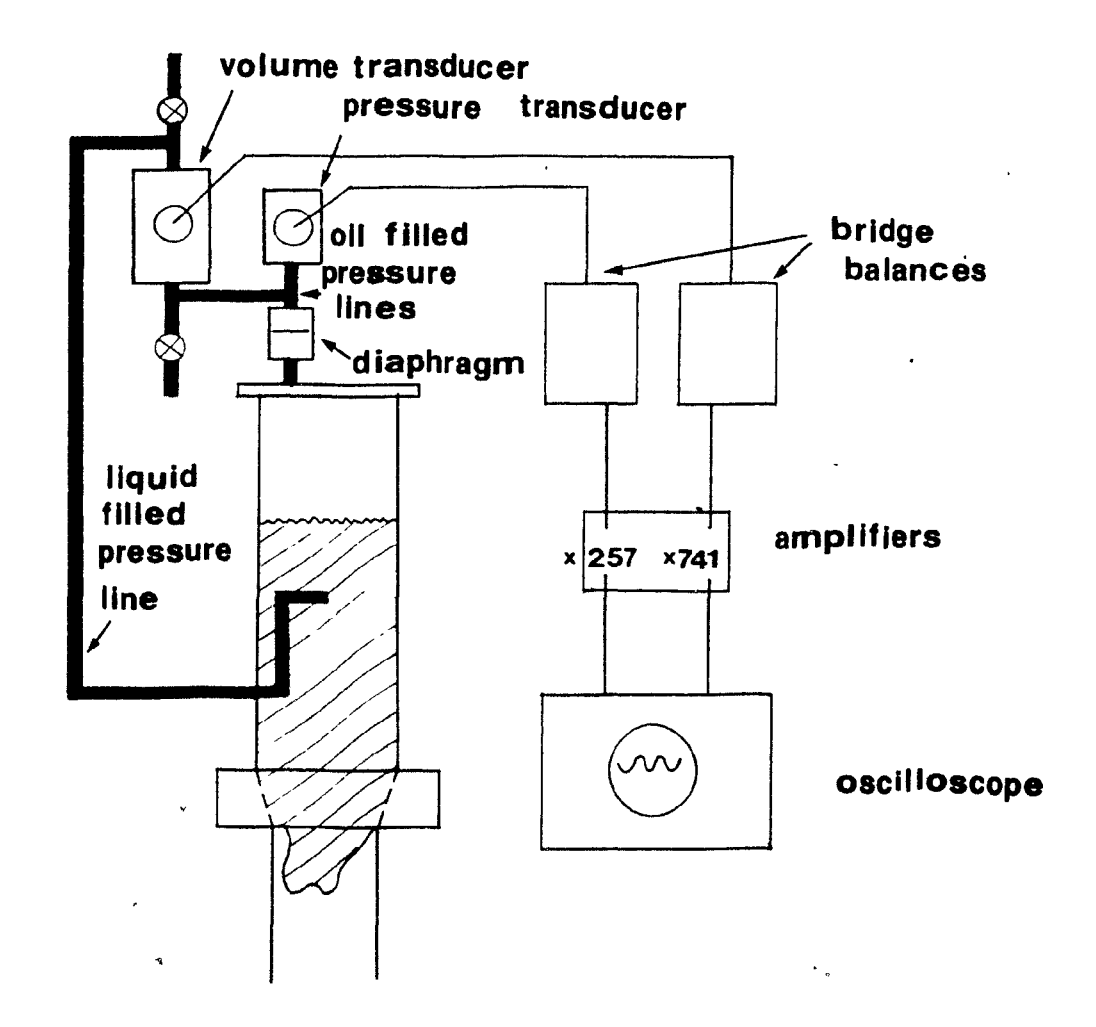
*d* 

. .

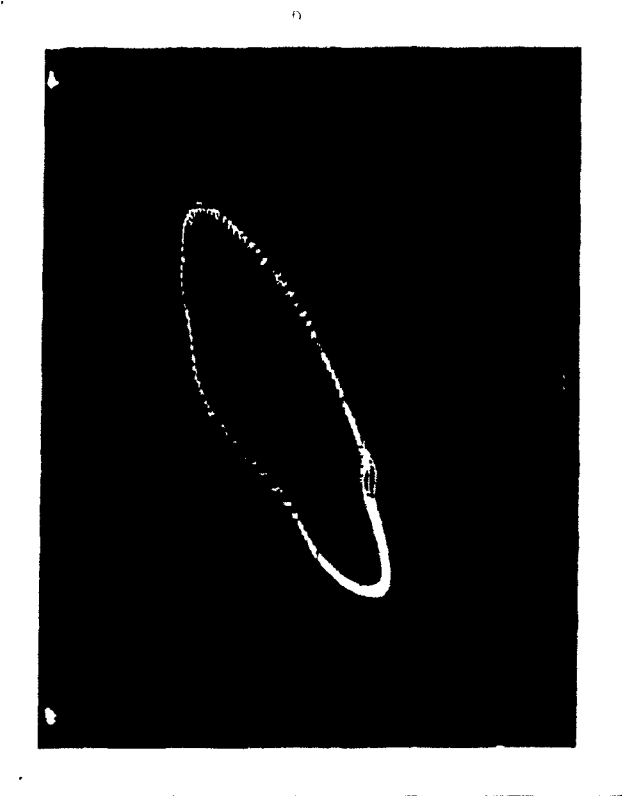


3.36. Efficiency vs Total head (var. L -scaled model)

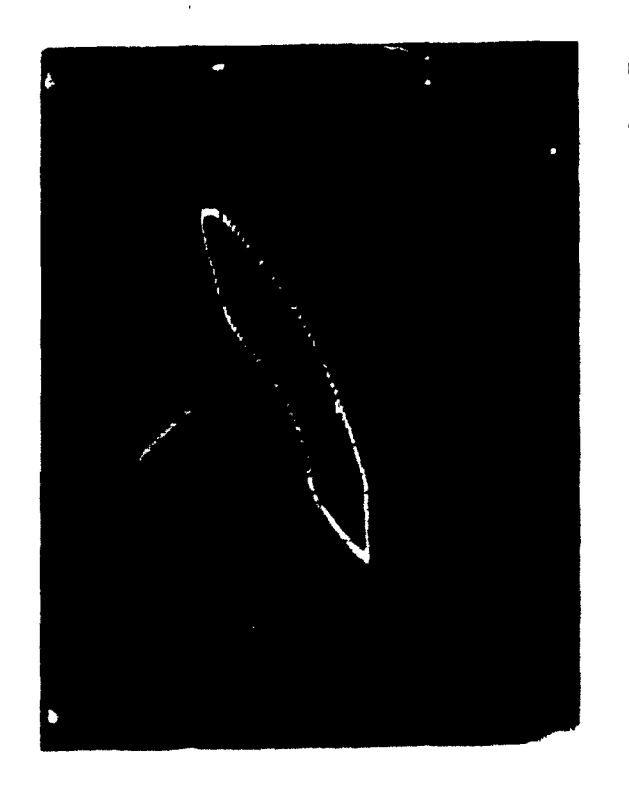
\_\_\_\_



4.2. Instrumentation set-up for pressure-volume diagrams

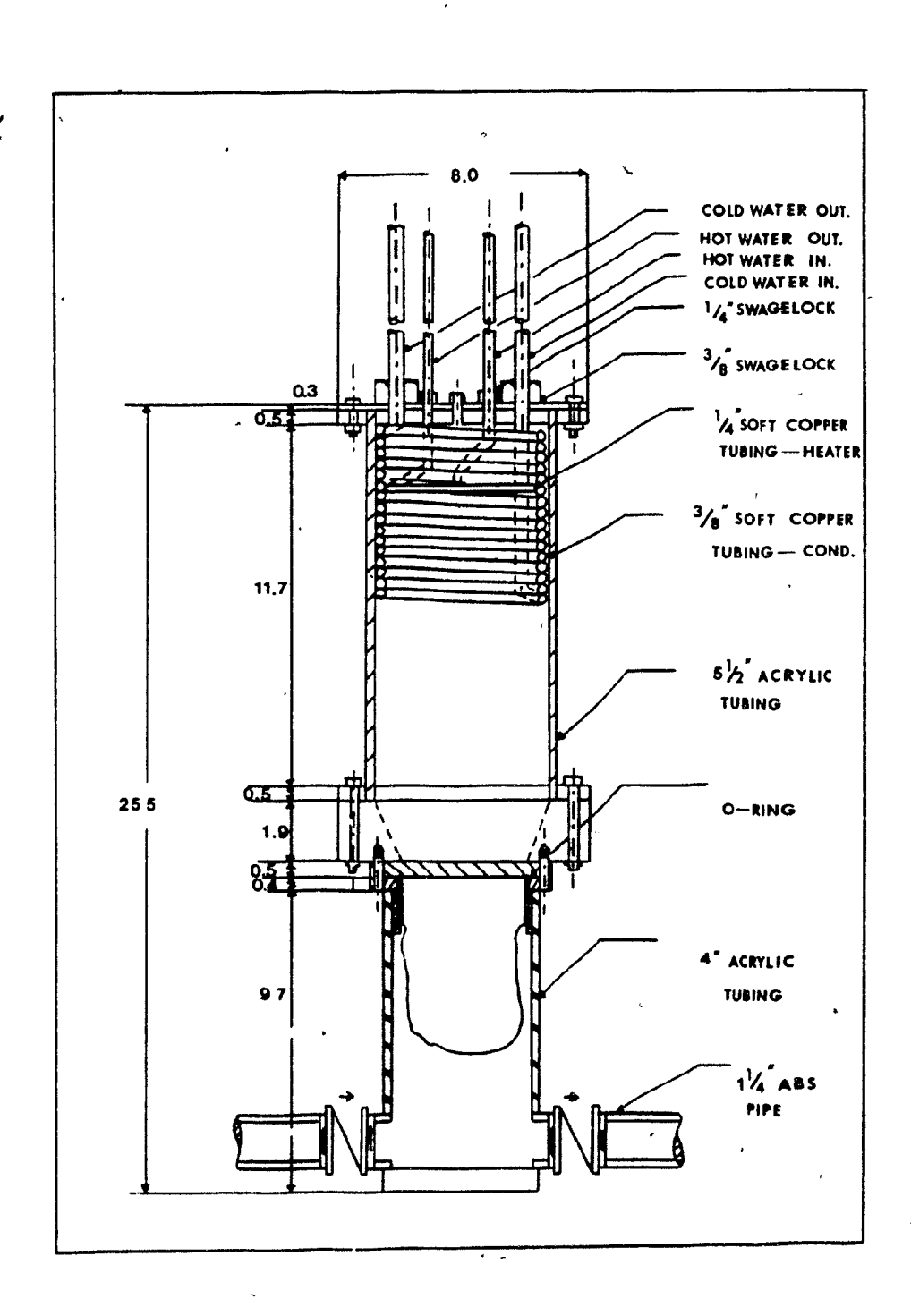


H<sub>s</sub> = 1.5 m H<sub>o</sub> = 1.0 m frequency = 0.497 Hz amplitude = 4.4 cm power = 3 W

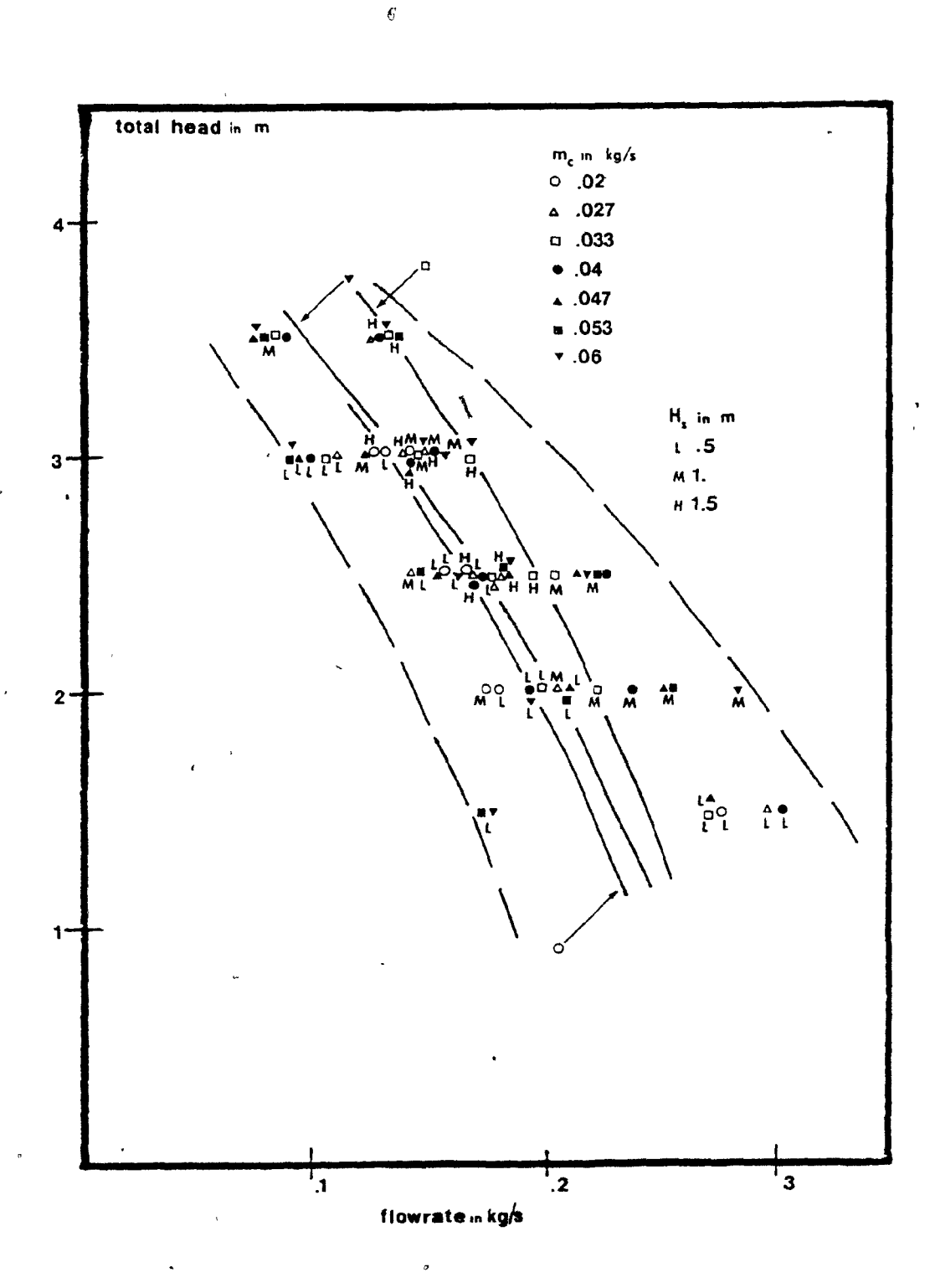


H<sub>s</sub> = 0.5 m H<sub>o</sub> = 2.5 m frequency = 0.413 Hz amplitude = 3.3 cm power = 3.4 W

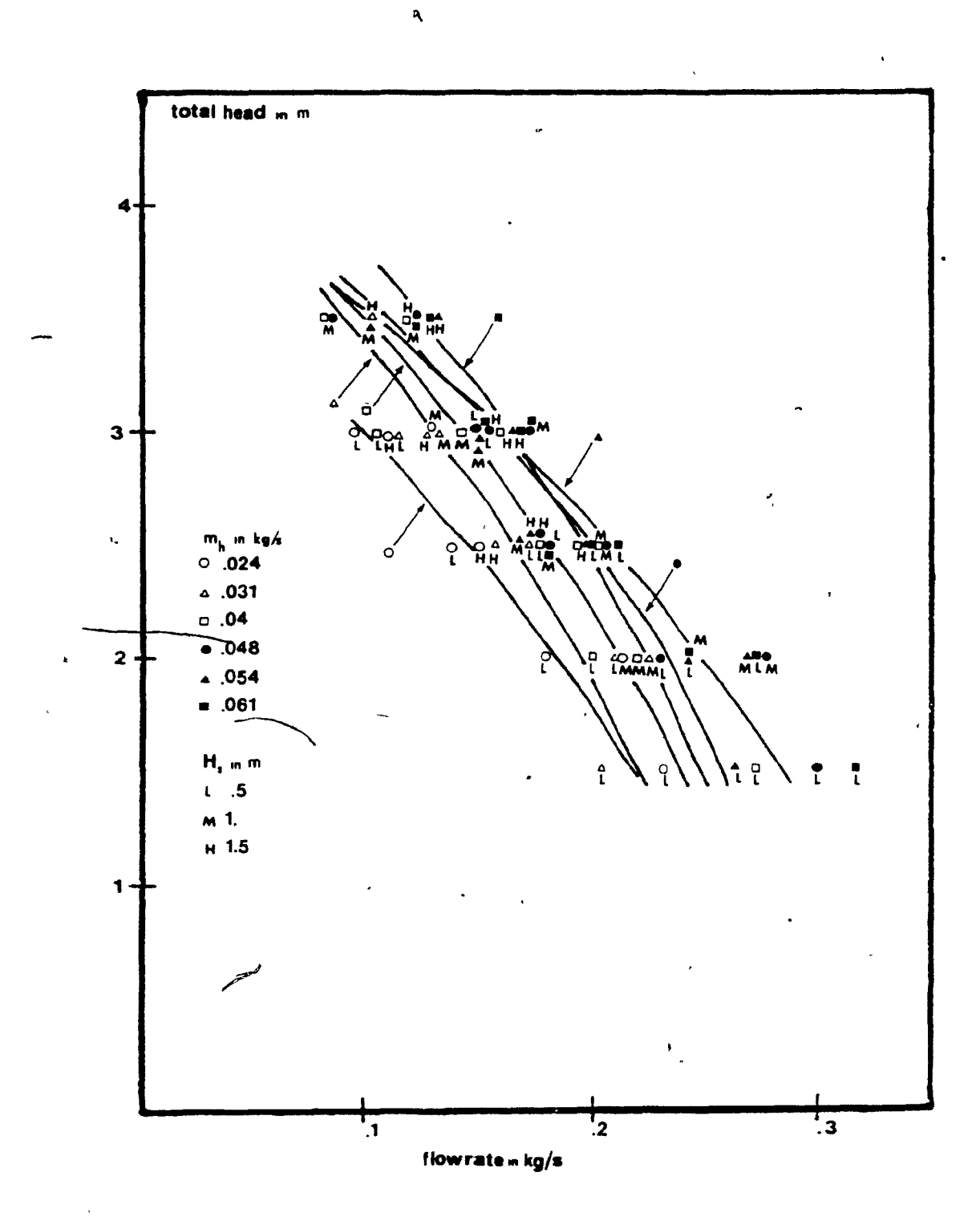
4.3. Typical pressure-volume diagram



4.4. Assembly drawing to scale of 14 cm SLPP

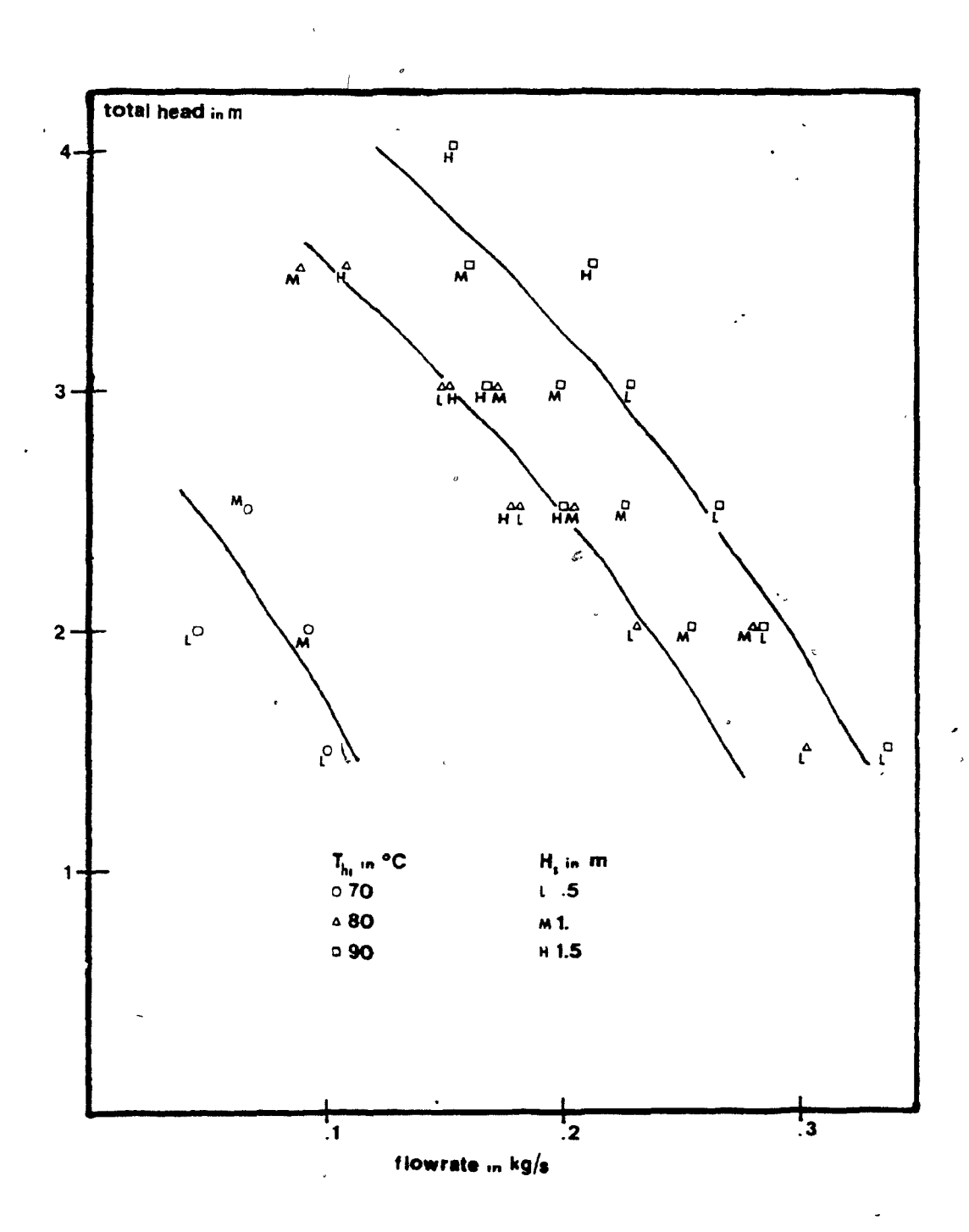


4.5. Flowrate vs Total head (var. m -14 cm SLPP)

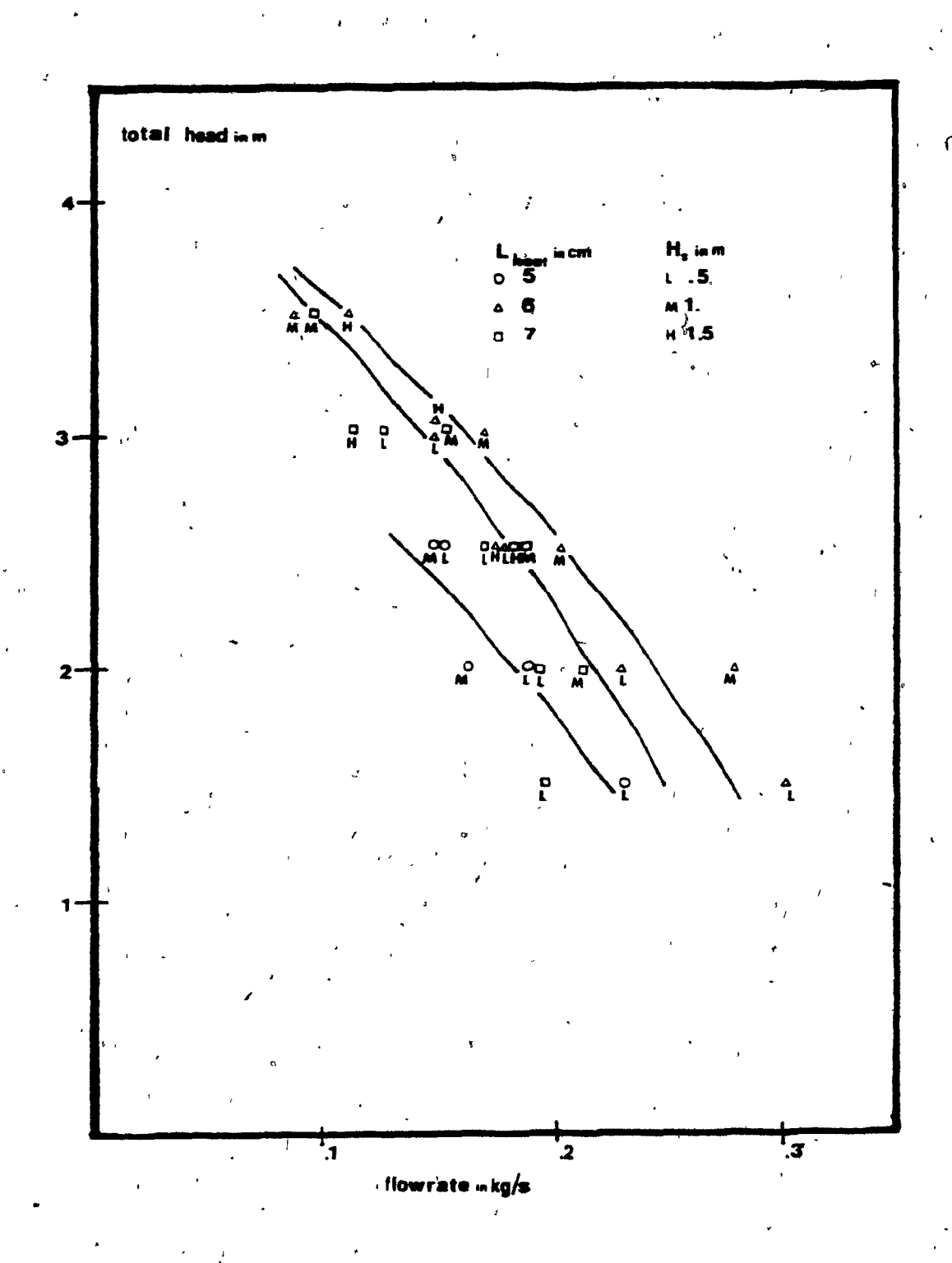


4.6. Plowrate vs Total head (var. m -14 cm SLPP)

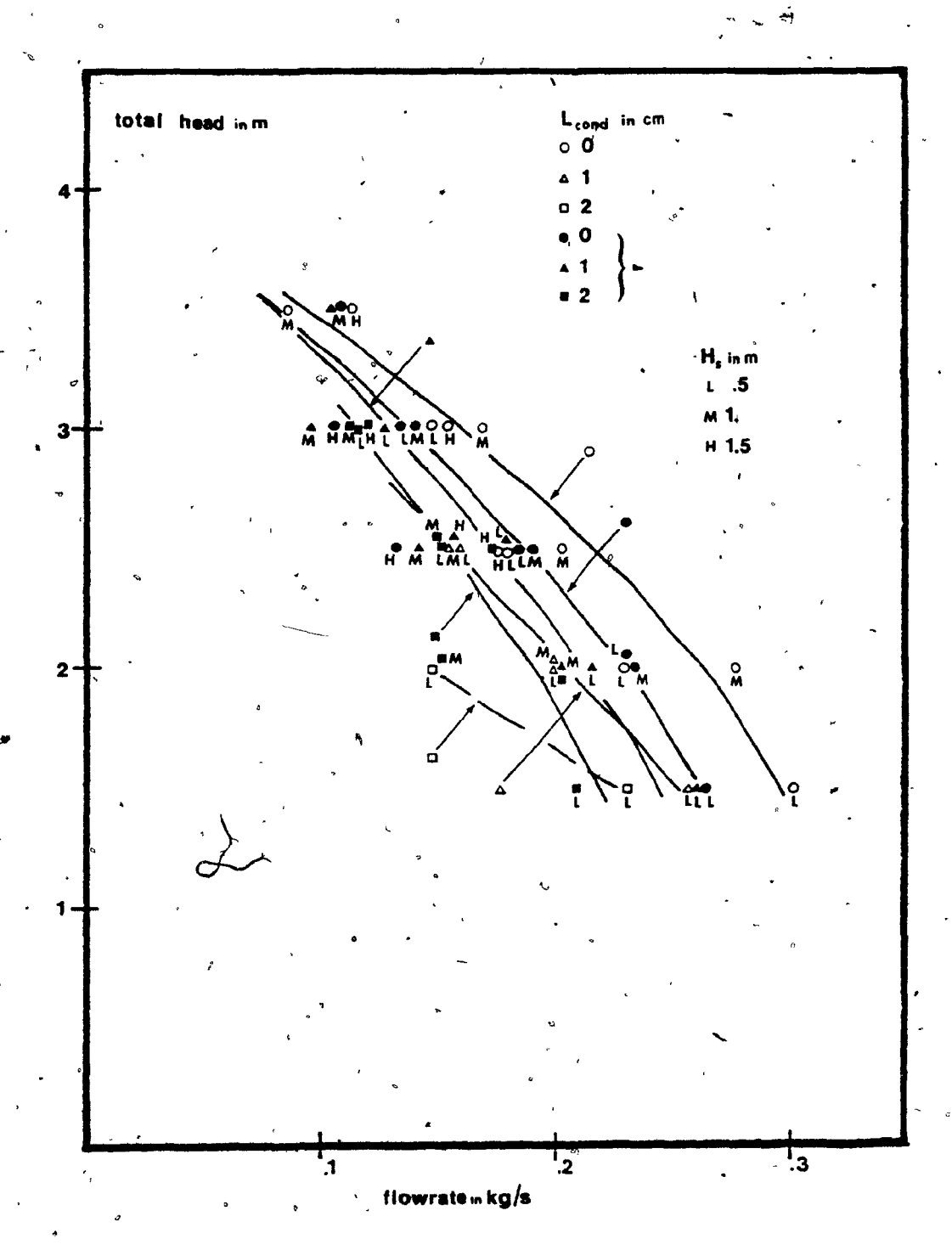
The statement of the state of t



4.7. Flowrate vs Total head (var. T -14 cm SLPP)

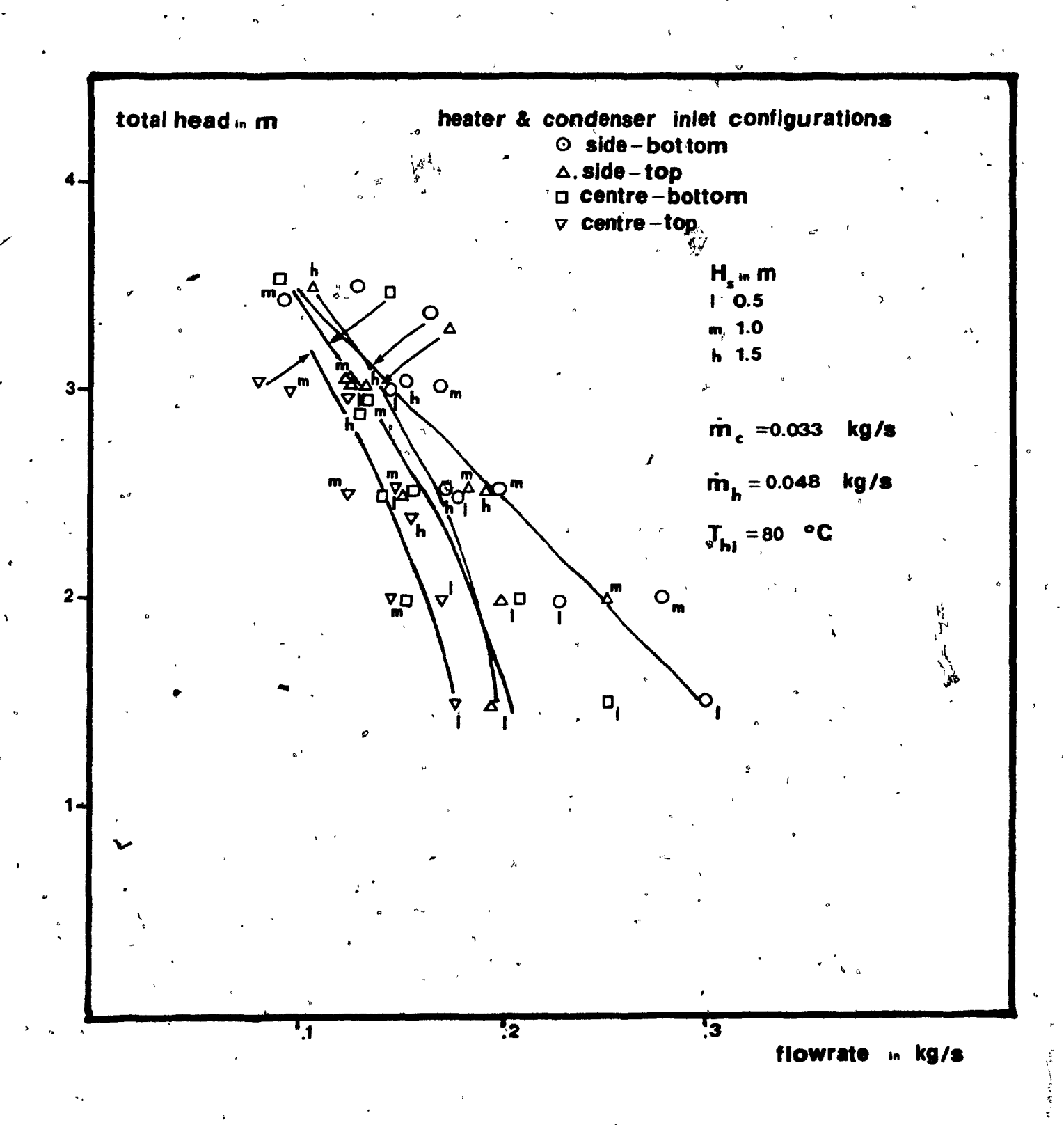


4.8. Flowrate vs Total head (var. L -14 cm SLPP)



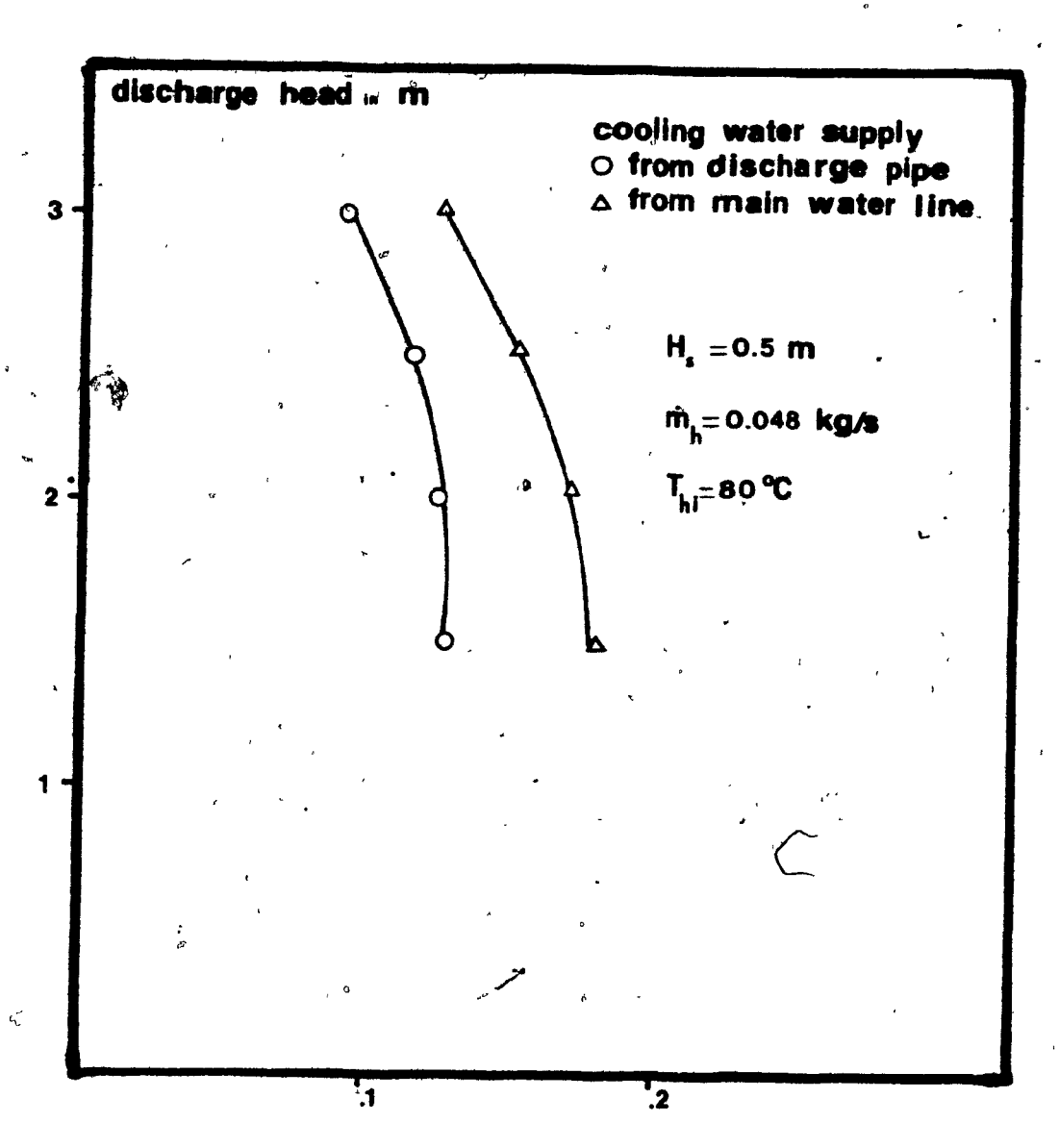
heater inlet and autlet tubes insulated

4.9. Flowrate vs Total head (var. L -14 cm SLPP)



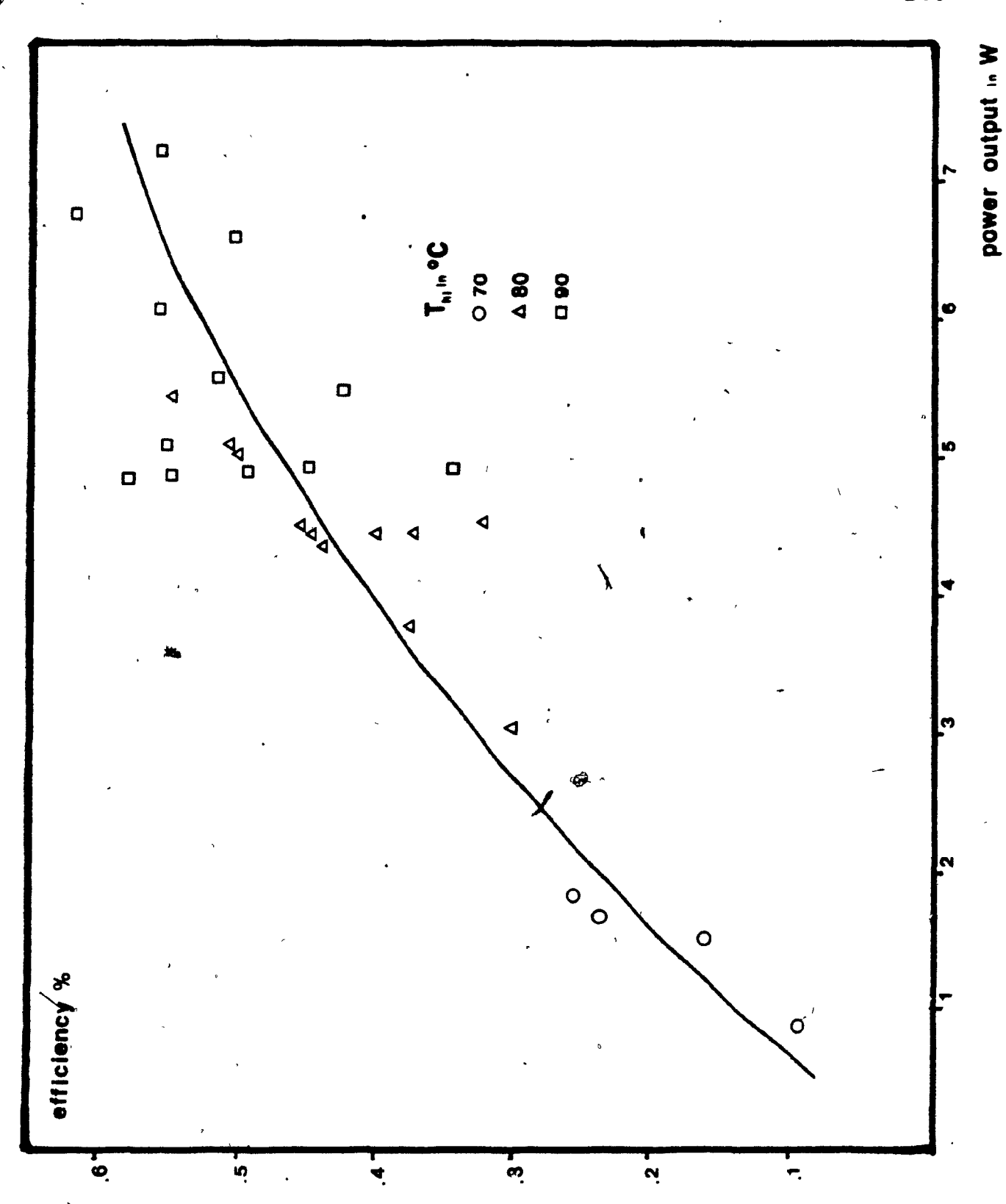
4.10. Flowrate vs Total head (var. in- and outlet conf. -14 cm , SLPP)

O



flowrate in kg/s

4.11. Flowrate vs Discharge head (alt. cooling water supply)



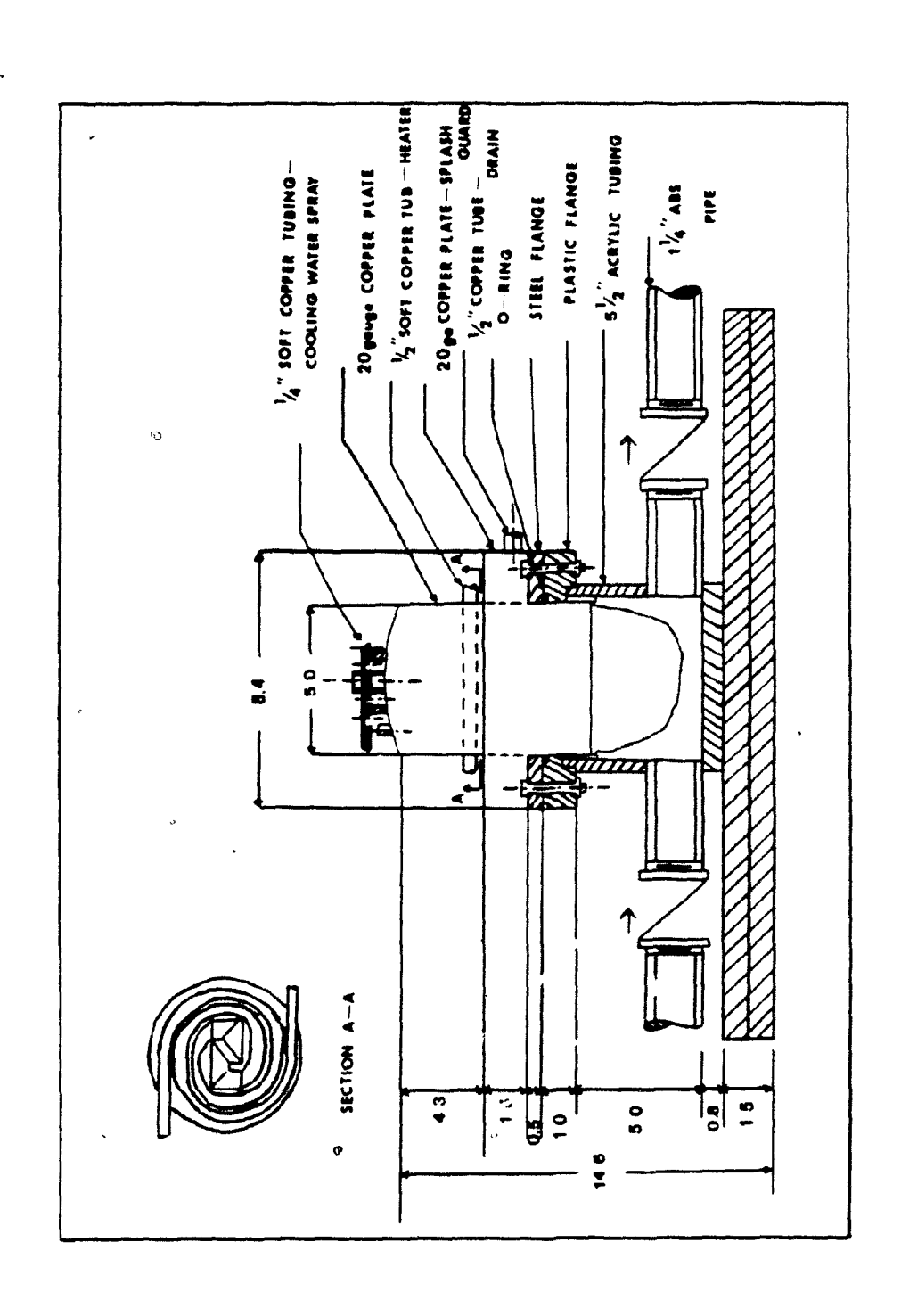
4.12. Efficiency vs Power output (var. T -14 cm SLPP)

, ,

•

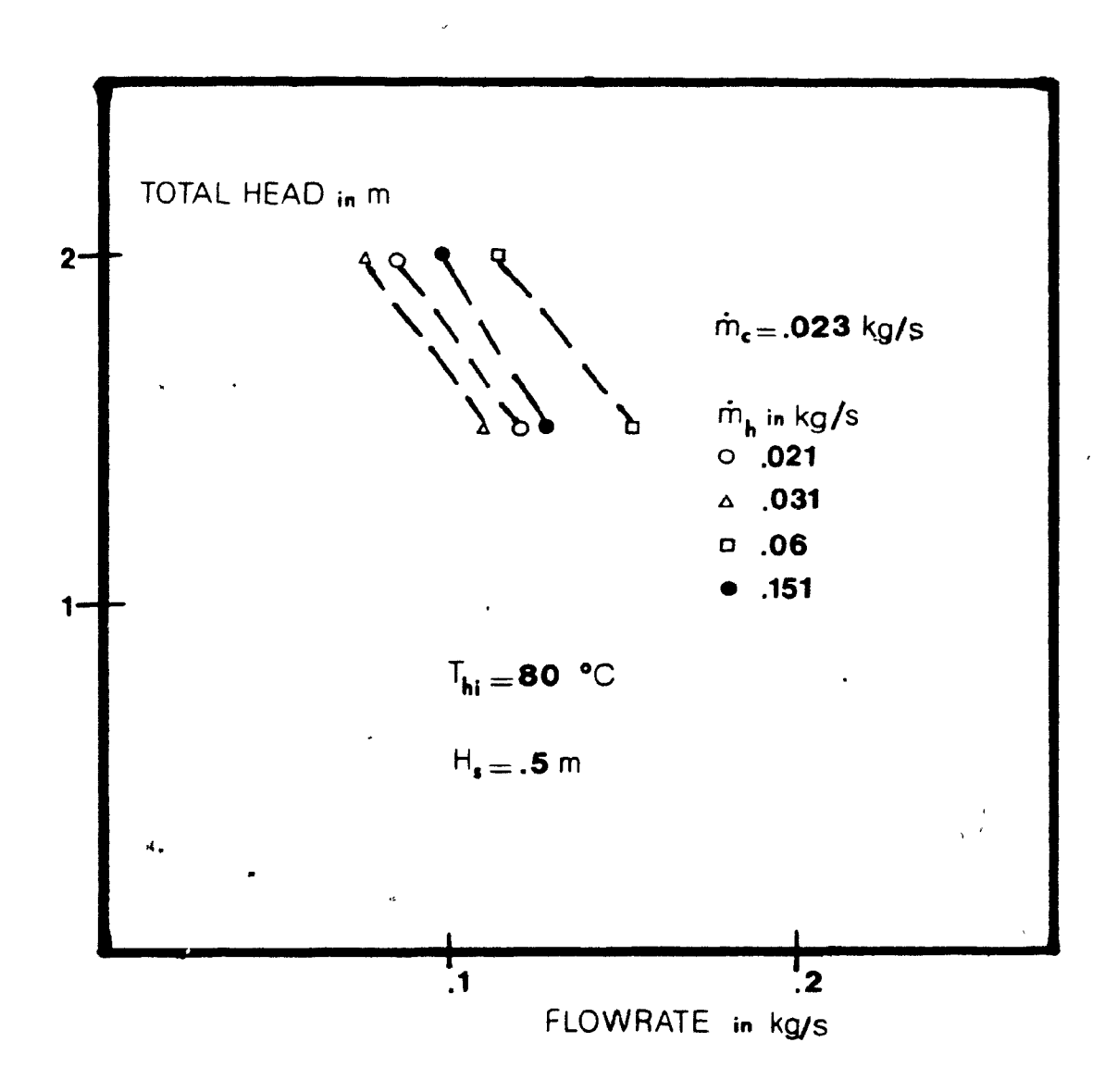
. . . .

•

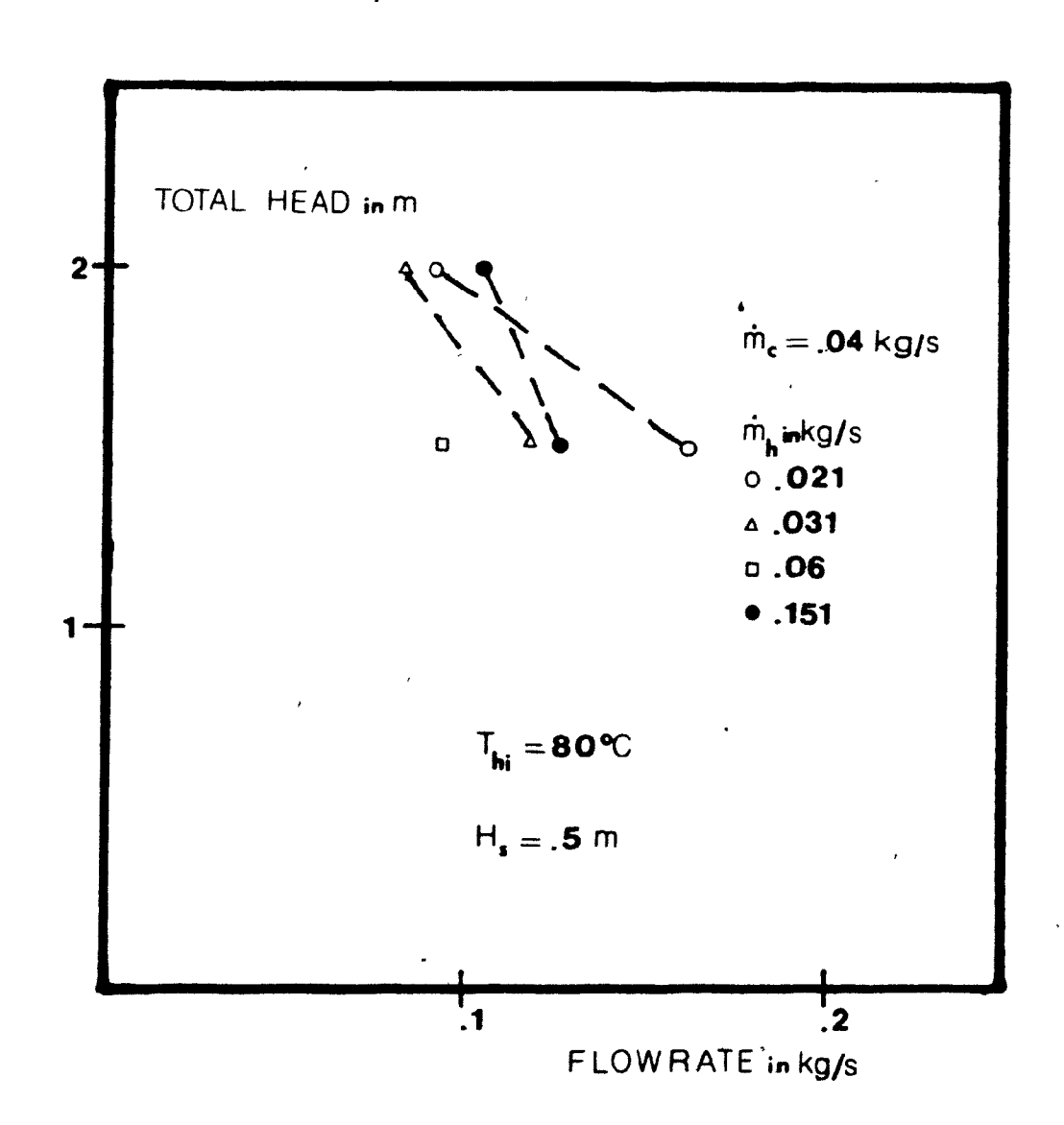


4.13. Assembly drawing to scale of 12.7 cm SLPP

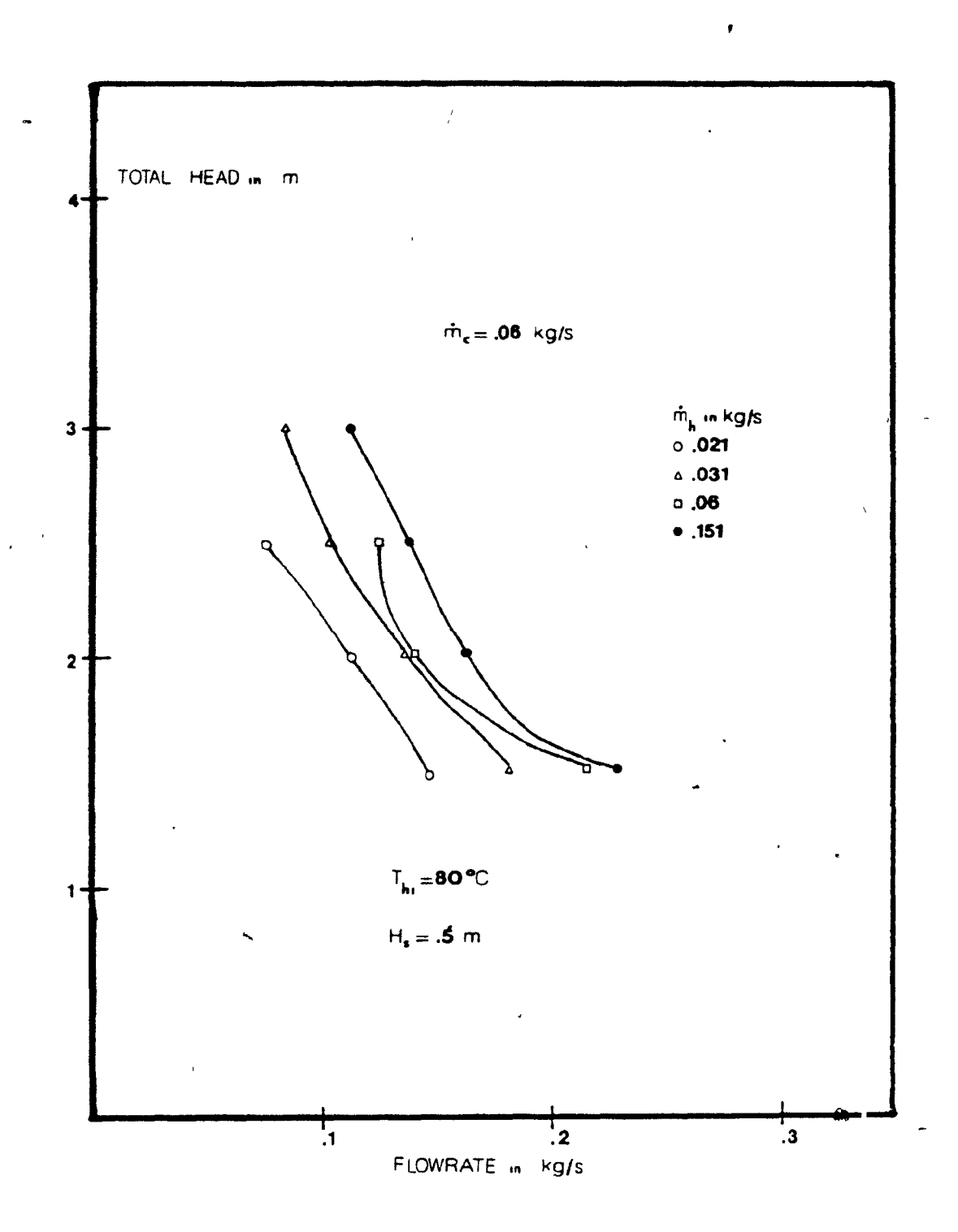
١.



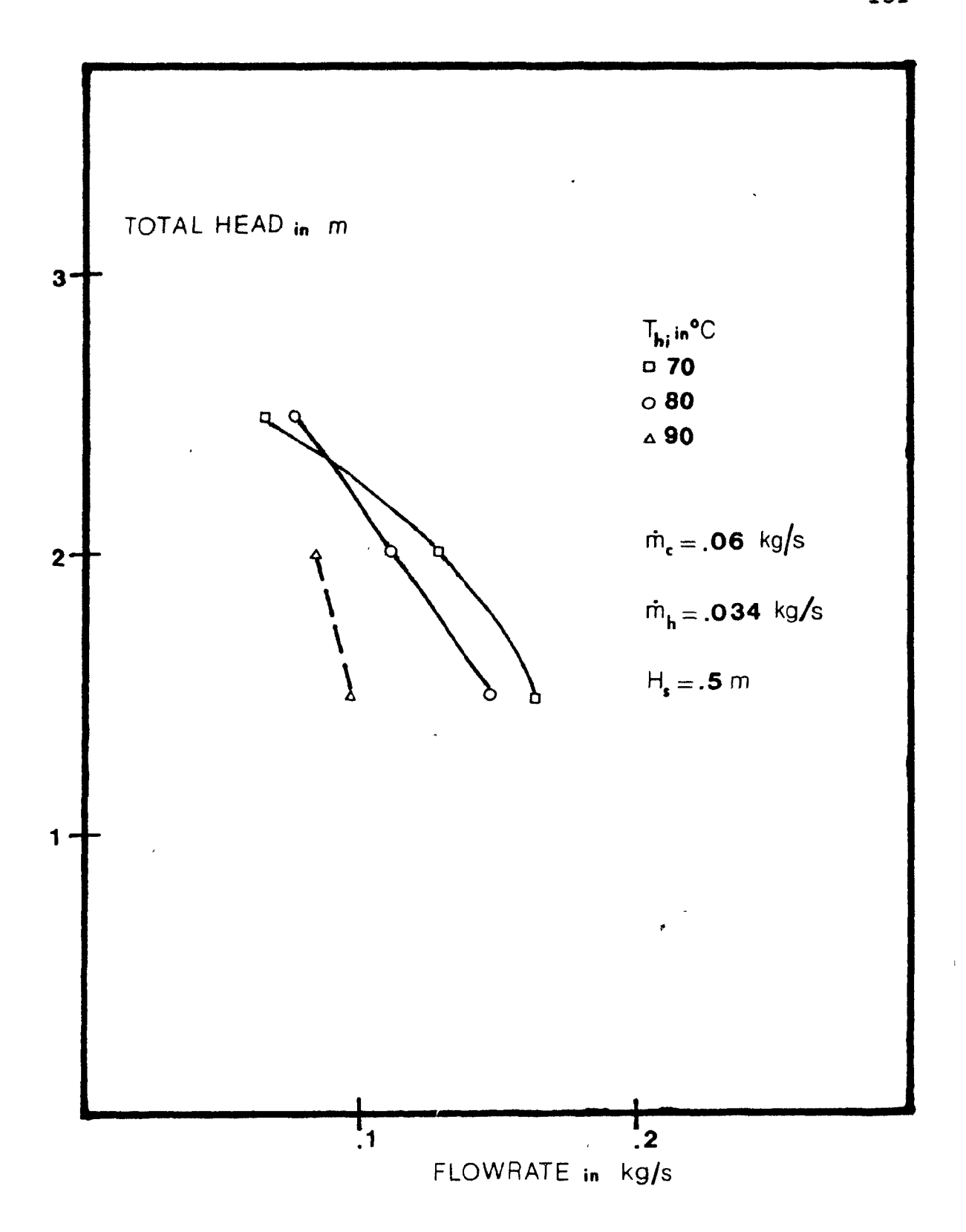
4.14. Flowrate vs Total head (var. m and m -12.7 cm SLPP)



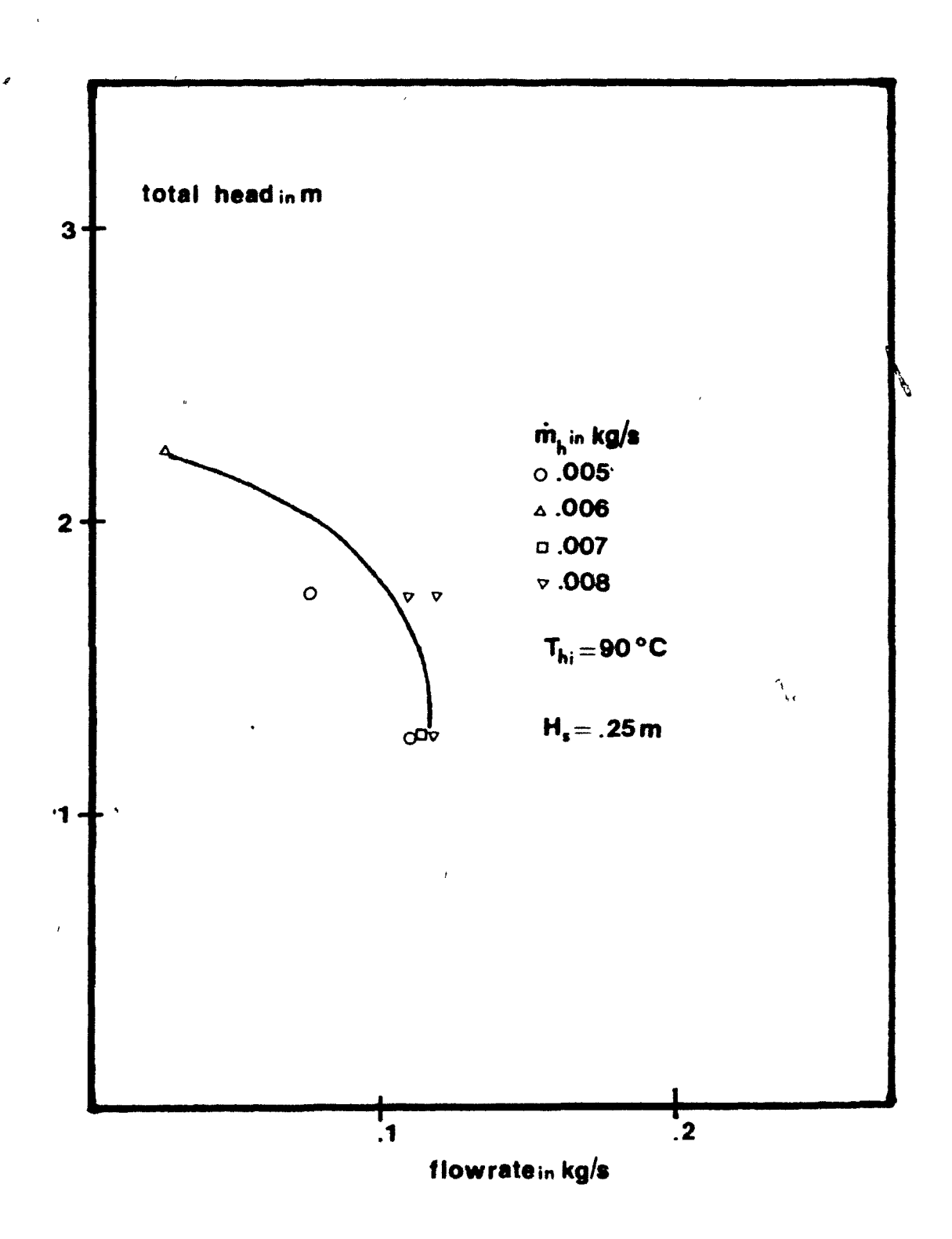
4.15. Flowrate vs Total head (var. m and m -12.7 cm SLPP)



4.16. Flowrate vs Total head (var. m and m -12.7 cm SLPP)

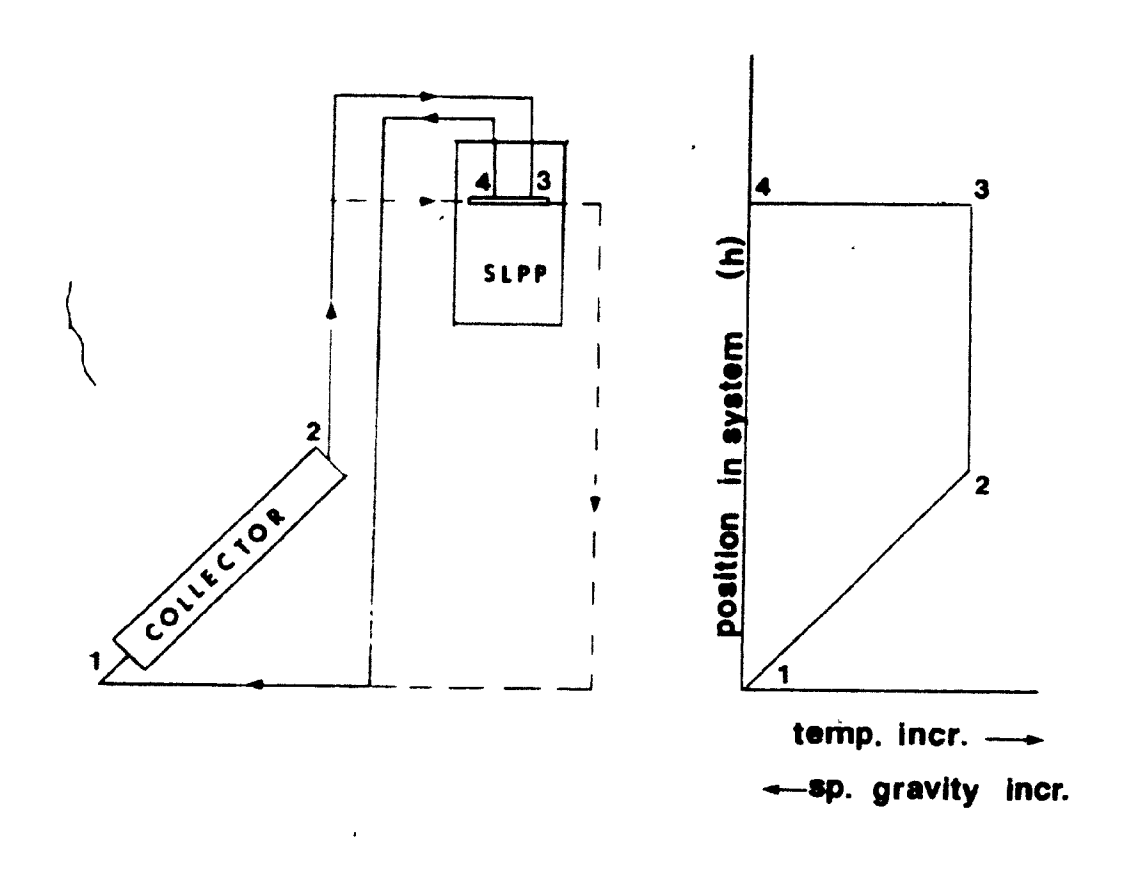


4.17. Flowrate vs Total head (var. T -12.7 cm SLPP)



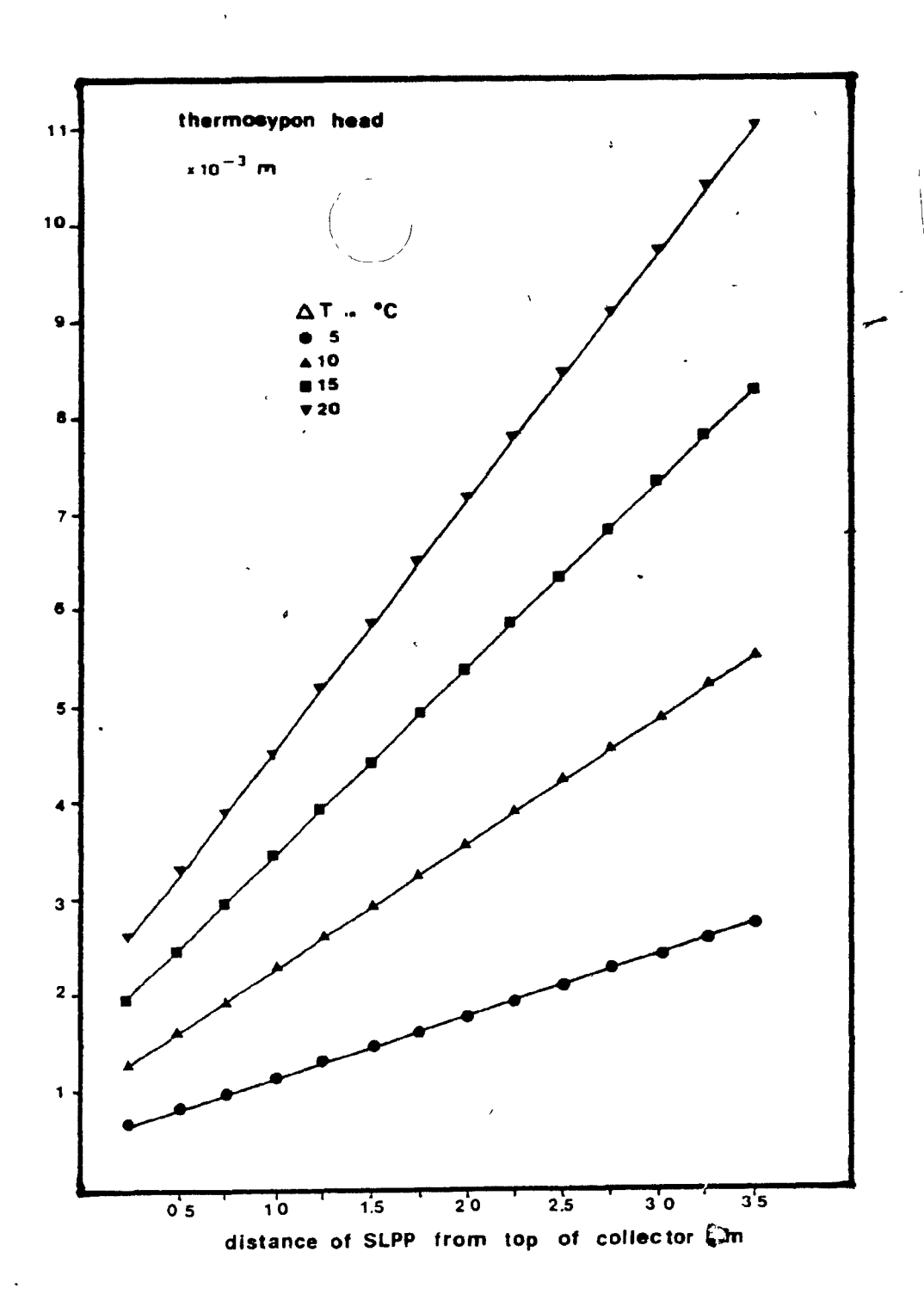
4.18. Flowrate vs Total head (var. m -12.7 cm SLPP)

and a supplemental problem of the state of t



6.1. Schematic of the SLPP-collector installation

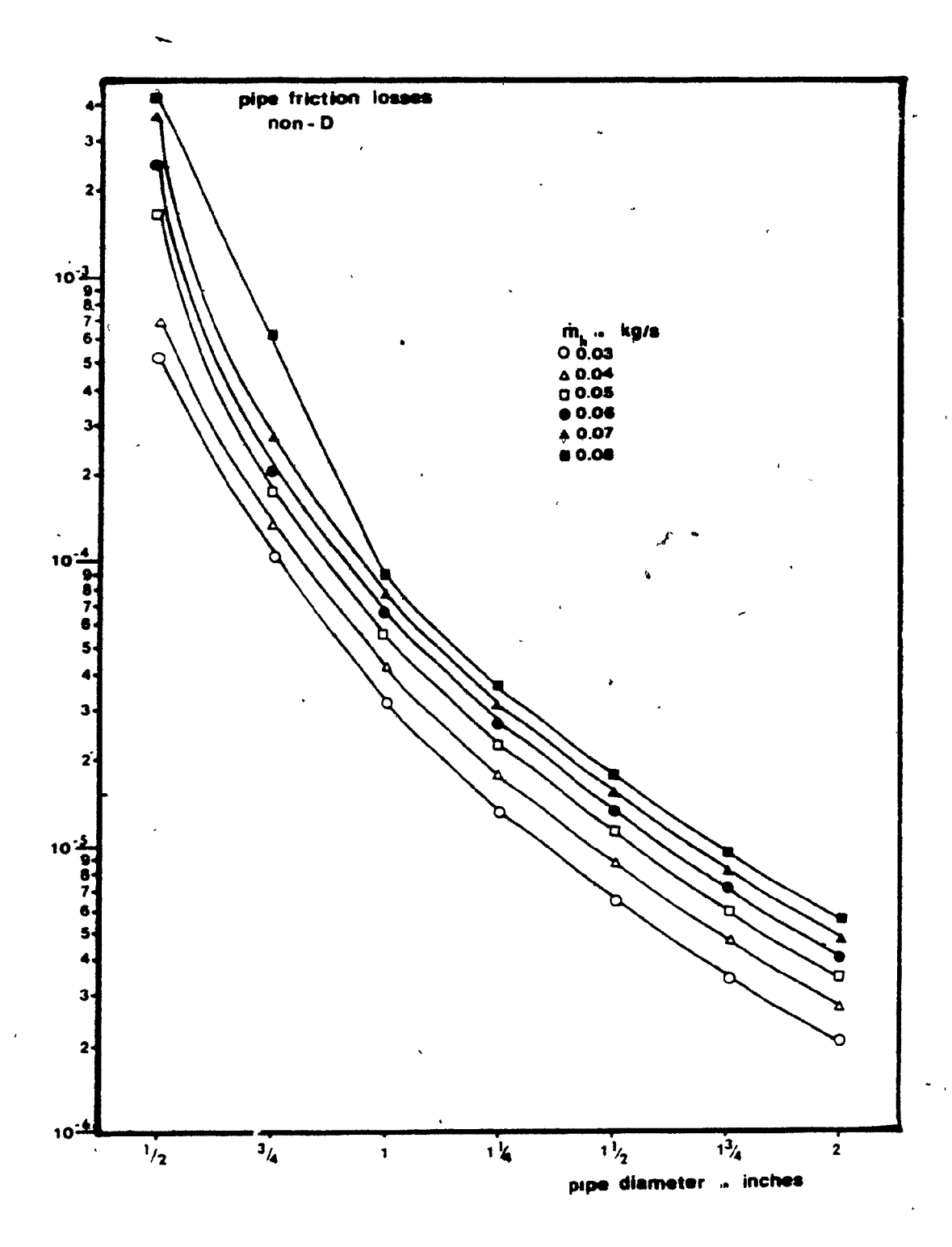
1\_



6.2. Thermosyphon head

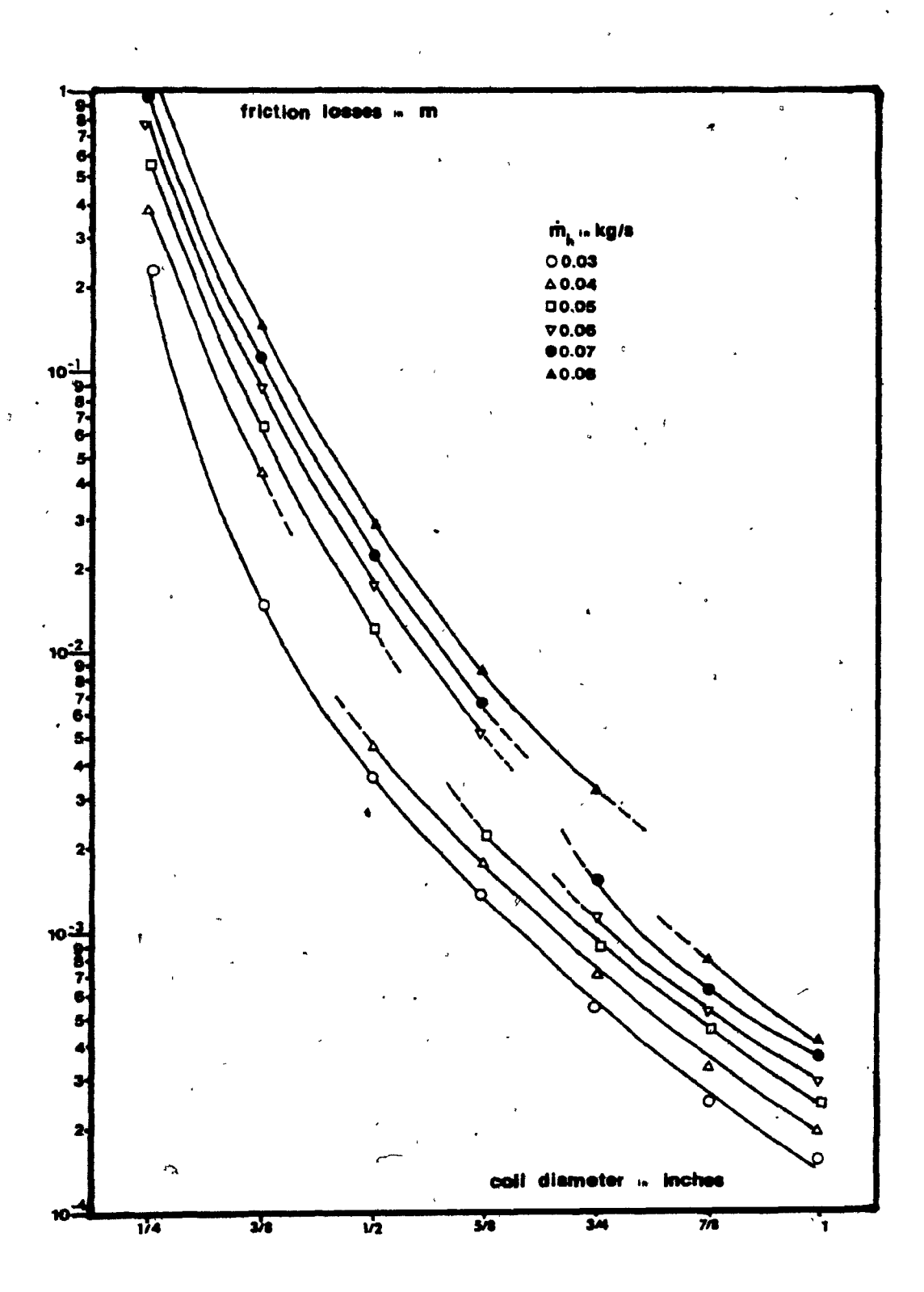
----

-

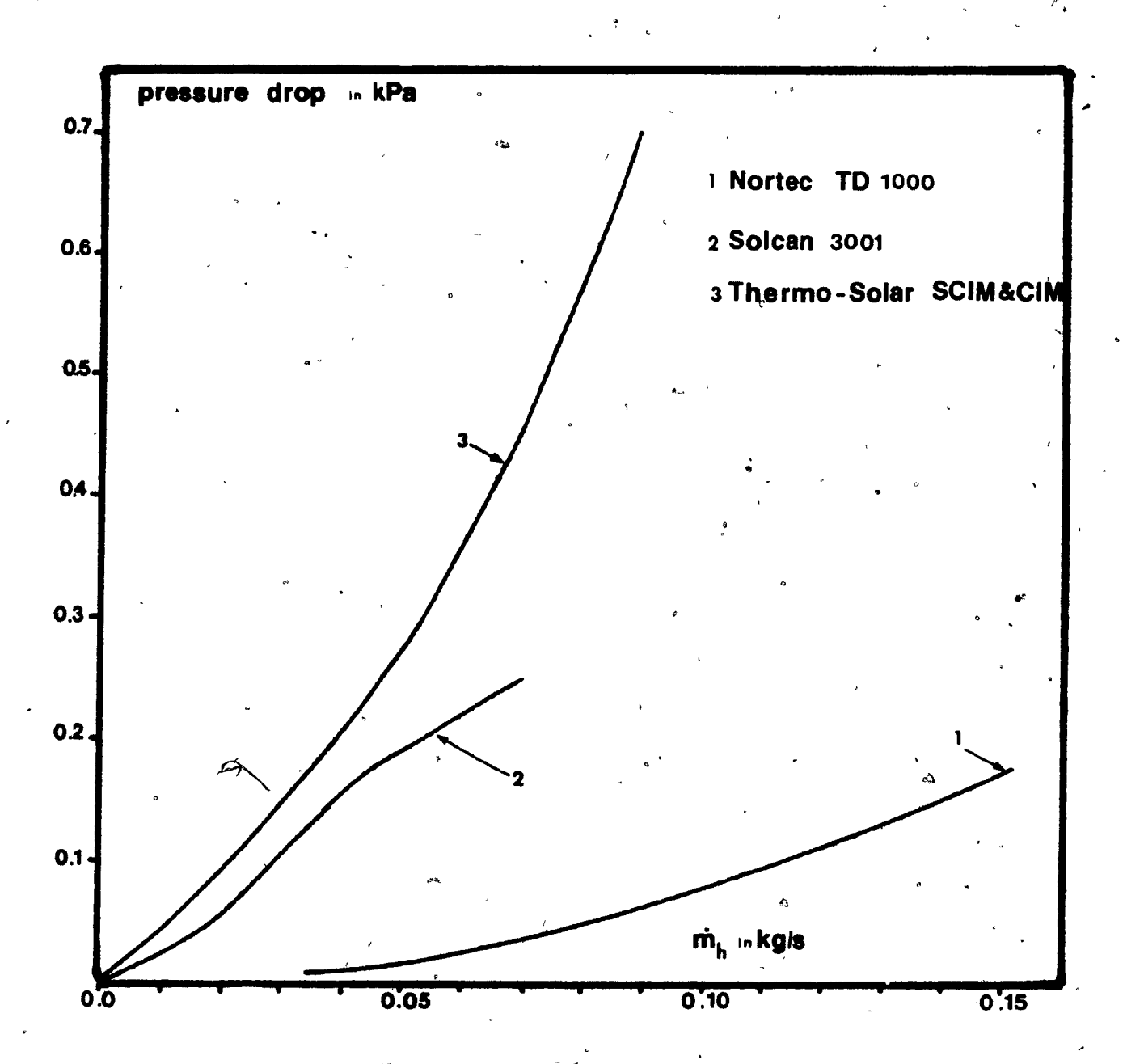


6.3. Friction losses in pipe circuit (non-D)

١..

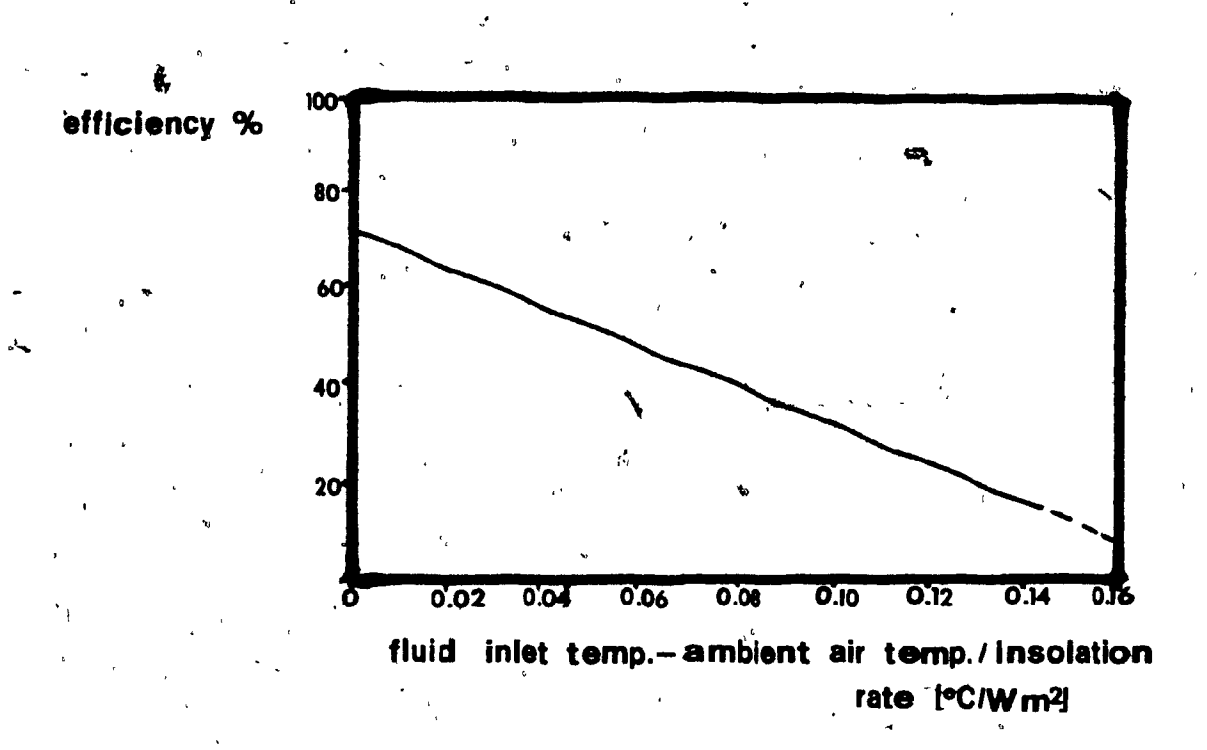


6.4. Priction losses in coil

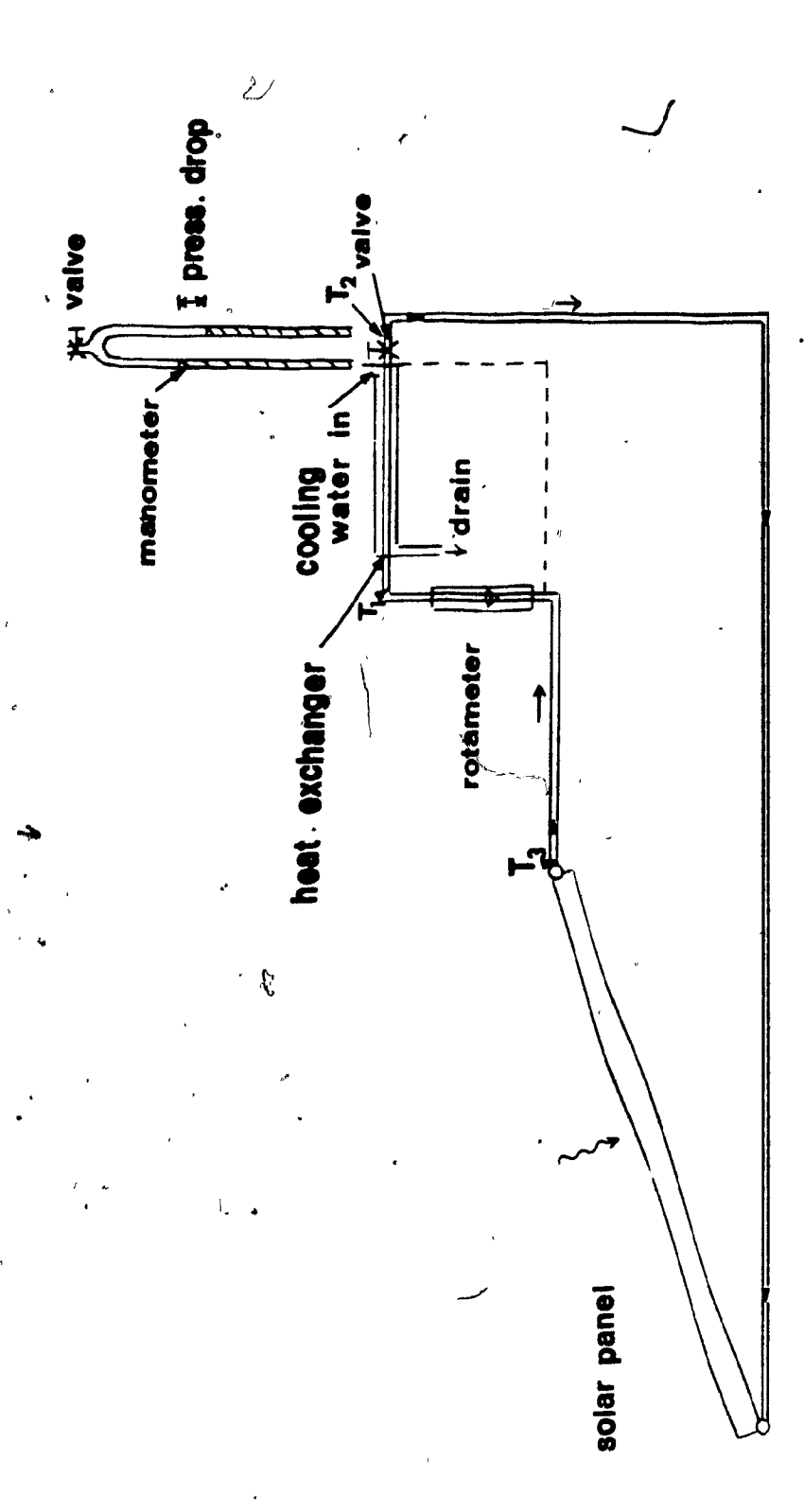


6.5. Friction losses in solar collectors (26, 27, 28)

D



6.6. Collector efficiency curve (26)



6.7. Thermal syphon heat exchanger

1

|---

\_\_\_\_

,

1.1. THEORETICAL RESULTS

```
ΔН
                                 Pout
                         q
   h i
(°C)
                        (W)
                                (W)
         (m)
             (kg/s)
                                        (%)
                                                       . 5 .
71
        2.5
             0.21
                      455.0
                              5.192
                                      1.14
              0.18
         3.0
                      455.9
                              5.27
                                      1.16
                              5.512
         3.5
              0.158
                      460.8
                                      1.19
 77
        2.5
              0.23
                      454.6
                              5.65
                                      1.24
                      474.6
         3.0
              0.193
                              5.8
                                      1.22
         3.5
              0.173
                      467.7
                              6.01
                                      1.28
                              5.9
 82
        2.5
              0.237
                      473.0
                                      1.25
        3.0
              0.204
                      487.0
                              6.08
                                      1.25
        3.5
              0.186
                      497.1
                              6.48
                                      1.3
              0.17
                      496.3
                                      1.33
        4.0
                              6.62
88
        2.5
              0.255
                      490.0
                              6.34
                                      1.29
        3.0
              0.219
                      488.4
                              6.54
                                      1.34
        3.5
              0.199
                      503.8
                              6.92
                                      1.37
              0.176
                      509.0
                              6.99
                                      1.37
        4.0
              0.27
                              6.73
93
        2.5
                      494.4
                                      1.36
              0.24
                      505.5
                              7.1
                                      1.4
        3.0
             0.209 523.7
        3.5
                              7.29
                                      1.39
        4.0 0.186 523.8
                              7.38
                                      1.41
                  L = 6.6 \text{ cm} L = 0.0 \text{ cm}
 h = 0.017 \text{ kg/s}
                                             H = 1.5 m
                                 ct
1. Variation of T
```

ф d	ΔΗ	Q	${\tt q}_{_{\rm i}}$	p out	η
(kg/s)	(m)	(kg/s)	(W)	(W)	(%)
0.011	2.5 3.0 3.5 4.0	0.25 0.22 0.19 0.17	480.7 497.2 506.8 524.4	6.2 6.5 6.7 6.9	1.29 1.3 1.33 1.33
0.017	2.5 3.0 3.5 4.0	0.25 0.22 0.20 0.18	490.0 488.4 504.0 521.2	6.3 6.5 6.9 7.1	1.29 1.34 1.37
0.023	2.5 3.0 3.5 4.0	0.25 0.22 0.20 0.18	492.0 492.0 504.6 518.0	6.3 6.7 7.0 7.2	1.29 1.37 1.38 1.39

T = 88 °C L = 6.6 cm L = 0.0 cm H = 1.5 m

2. Variation of m

<b>T</b> ,	ΔН	Q	q	p	η
( oC )	(m)		1	out (W)	(%)
<del>\ \ \ /</del>	\ 111 /	(10)	(44)		(107
10		0.219 0.199		6.54 6.92	1.29 1.34 1.37 1.37
18	3.5	0.229 0.200 0.175 0.16	386.6 390.7	6.08	1.54 1.55 1.56 1.62
24		0.174 0.160	309.0 312.7		1.7 1.67 1.78
27	2.5 3.0 3.5	0.164	263.7	4.6 4.9	1.8
<pre>h = 0. 3. Vari</pre>		g/s T of T		L =6.6	cm 1
A	ΔΗ	Q	<b>q</b>	p	η

A h b	ΔΗ	Q	٩ <sub>١</sub>	Pout	η				
(cm²)	(m)	(kg/s)	(W)	(W)	(६)				
48.4	2.5 3.0 3.5 4.0	0.15 STALL	434.3 ED	4.4 4.5	1.01				
64.5	3.0 3.5	0.18 0.16	460.7	5.4 5.4 5.7 5.8					
83.9	3.0 3.5	0.21 0.18	480.0	6.0 6.3 6.4 6.5	1.3				
96.8	3.0	0.22 0.20	488.4	6.3 6.5 6.9 7.1	1.34		o.		-
h = 0	.017 k	g/s T		$L_{h} = 7.3$		=0.0	cm	H =1.5	m

4. Variation of A

```
L
        ΔН
                       g,
                      (W)
                              (W)
                                      (暑)
(cm)
        (m)
             (kg/s)
                            15.64
 1.27
        2.5
               0.63
                     296.8
                                      5.27
        3.0
               0.57
                     292.9 17.06
                                      5.82
               0.48
        3.5
                     314.0 16.78
                                      5.34
                             17.75
               0.44
                     288.3
        4.0
                                      6.16
 2.0
        2.5
               0.54
                     341.3
                             13.5
                                      3.9
               0.48
                             14.4
                                      4.2
        3.0
                     342.2
        3.5
               0.38
                     332.3
                             13.4
                                      4.0
        4.0
               0.35
                     335.4
                             13.9
                                      4.1
                                      3.0
 2.8
        2.5
               0.46
                     377.9
                            11.6
               0.40
                     377.2
                            12.0
                                      3.2
        3.0
               0.34
        3.5
                     368.3
                            12.0
                                      3.3
               0.31
        4.0
                     371.9
                            12.3
                                      3.3
               0.41
        2.5
                                      2.5
 3.5
                     405.1
                             10.1
               0.35
        3.0
                     393.8
                             10.6
                                      2.7
        3.5
               0.31
                     388.7
                             10.9
                                      2.8
               0.28
        4.0
                     402.1
                             11.3
                                      2.8
                              9.0
 4.3
        2.5
               0.36
                     419.6
                                      2.15
                              9.5
        3.0
               0.32
                     420.7
                                      2.25
        3.5
               0.28
                     417.5
                              9.8
                                      2.35
        4.0
               0.26
                     429.5
                             10.3
                                      2.4
                                      1.87
 5.0
        2.5
               0.33
                     439.1
                              8.2
               0.29
                              8.6
                                      1.92
        3.0
                     448.0
               0.25
                     453.2
                              8.8
                                      1.94
        3.5
        4.0
               0.23
                     446.9
                              9.2
                                      2.07
        2.5
               0.29
                              7.2
 6.6
                     456.6
                                      1.58
               0.25
        3.0
                     467.8
                              7.5
                                      1.6
               0.23
        3.5
                     481.4
                              8.0
                                      1.66
               0.20
        4.0
                     476.2
                              8.1
                                      1.7
 7.3
        2.5
                              6.3
               0.25
                     489.8
                                      1.29
               0.22
                              6.5
        3.0
                     488.4
                                      1.34
               0.20
                     503.8
                              6.9
                                      1.37
        3.5
               0.18
        4.0
                     521.2
                              7.1
                                      1.37
8.1
        2.5
               0.21
                     516.4
                              5.3
                                      1.03
        3.0
               0.19
                     530.2
                              5.6
                                      1.06
               0.17
                     548.8
                                      1.09
        3.5
                              6.0
               0.16
                     579.6
                              6.5
                                      1.12
        4.0
  h = 0.017 \text{ kg/s} T = 88 °C L = 0.0 cm H = 1.5 m
                 h i
5. Variation of L
```

\_ 1

L	ΔH	Q	ď	p out	η
(cm)	( m )	(kg/s)	(W)	(W)	(%)
0.0	2.5 3.0 3.5 4.0	0.25 0.22 0.20 0.18	490.0 488.4 504.0 521.2	6.34 6.5 6.9 7.1	1.29 1.34 1.37 1.37
1.3	2.5 3.0 3.5 4.0		452.2 472.4 482.0 481.0	6.9 7.2 7.6 8.0	1.53 1.53 1.57 1.66
2.5	2.5 3.0 3.5 4.0	0.26	440.0 444.4 441.4 ED	7.3 7.8 8.2	1.67 1.76 1.87
3.8	2.5 3.0 3.5 4.0			7.5 8.0	1.85
5.1	2.5 3.0 3.5 4.0	0.30 STALL STALL STALL	ED	7.5	1.90

m = 0.017 kg/s T = 88 °C L = 6.6 cm H = 1.5 m 6. Variation of L

L t h	ΔН	Q	g 1	p out	'n
(cm)	(m)_	(kg/s)	(W)	(W)_	( <u>ዬ</u> )
0.76	2.5	0.255	490.0	6.34	1.29
	3.0	0.219	488.4	6.54	1.34
	3.5	0.2	503.8	6.92	1.37
	4.0	0.176	509.0	6.99	1.37
1.14	2.5	0.224	515.8	5.57	1.08
	3.0	0.198	522.0	5.9	1.13
	3.5	0.17	542.0	5.97	1.10
	4.0	0.145	557.0	5.8	1.03
1.5	2.5	0.201	543.6	5.0	0.92
	3.0	0.168	563.5	5.01	0.89
	3.5	0.15	584.8	5.23	0.89
	4.0	0.114	633.3	4.54	0.72
1.9	2.5	0.175	584.8	4.35	0.74
	3.0	0.15	597.8	4.5	0.74
	3.5	0.127	625.2	4.43	0.71

m = 0.017 kg/s T = 88 °C L = 6.6 cm L = 0.0 cm H = 1.5 m

7. Variation of L

f	ф h	L h	ΔН	Q	ď	p •ut	η
(-)	(kg/s)	(kg/s)	(m)	(kg/s)	(W)	(W)	(%)
0.8	0.011	5.3	2.5	0.266	313.0	6.63	2.12
			3.0 3.5	0.203 0.174	306.2 302.6	6.07 6.06	1.98 2.00
0.9	0.014	5.9	2.5 3.0 3.5	0.257 0.209 0.187	396.1 406.4 406.8	6.4 6.25 6.5	1.61 1.54 1.60
1.0	0.017	6.6	2.5 3.0 3.5	0.255 0.219 0.199	489.8 488.4 503.8	6.34 6.5 6.9	1.29 1.34 1.37
1.1	0.020	7.2	2.5 3.0 3.5	0.26 0.23 0.206	580.1 610.2 609.3	6.5 6.8 7.2	1.12 1.12 1.18
1.2	0.025	7.9	2.5 3.0 3.5	0.27 0.24 0.217	699.4 737.1 746.8	6.7 7.14 7.5	0.96 0.97 1.01
1.3	0.029	8.6	2.5 3.0 3.5	0.272 0.248 0.222	854.4 862.7 879.1	6.8 7.4 7.7	0.79 0.86 0.88
	T =88	°C	L =0.0	cm	H =1	.5 m	

8. Variation of scale factor

```
ΔН
 h 1
(°C)
                             (W)
        (m) (kg/s)
                     (W)
                                    (%)
 71
        2.5
             STALLED
        3.0
            STALLED
        3.5
             STALLED
        4.0
             STALLED
 77
        2.5
             0.24 919.0 5.9 0.64
        3.0
             STALLED
        3.5
             STALLED
        4.0
             STALLED
                           6.6
                                 0.71
 82
        2.5
             0.265 925.0
        3.0
             0.23
                    963.6
                           6.9 0.72
                    983.0
        3.5
             0.21
                            7.3
                                   0.74
        4.0
             STALLED
 88
        2.5
             0.28
                    936.2
                            7.0
                                   0.75
        3.0
             0.25
                   984.6
                            7.4
                                   0.75
             0.22 1004.0
                            7.8
        3.5
                                   0.78
        4.0
             STALLED
 93
        2.5
            0.29
                  966.0
                           7.3
                                 0.76
        3.0
            0.27 998.0
                           8.0 0.80
        3.5
            0.24 1017.0
                            8.4
                                   0.83
        4.0 STALLED
 h = 0.044 \text{ kg/s} L = 9.1 \text{ cm} L = 0.0 \text{ cm} H = 1.5 \text{ m}
9. Variation of T (scaled model)
  ιħ
                Q
         \Delta H
                       q
                              р
                                     η
                               out
                      (W)
                              (W)
         (m) (kg/s)
0.030
         2.5 0.27
                      951.2
                             6.8
                                    0.72
         3.0 0.25
                             7.5
                                    0.78
                      963.0
         3.5 0.22
                      981.6
                             7.9
                                    0.80
         4.0
             STALLED
0.044
         2.5 0.28
                      936.2
                             7.0
                                   0.75
                                   0.75
         3.0 0.25
                     984.6
                             7.4
         3.5 0.22
                     1004.0
                             7.8
                                    0.78
         4.0 STALLED
0.060
         2.5 0.28
                      954.5
                             6.9
                                    0.73
         3.0 0.25
                      983.2
                             7.5
                                    0.77
         3.5 0.23
                     1005.0
                             7.9
                                    0.79
         4.0 STALLED
 T = 88 °C L = 9.1 cm L = 0.0 cm H = 1.5 m
  h i h
                   ct
10. Variation of m
                     (scaled model)
```

1

```
q<sub>i</sub>
 C 1
                           (W)
                                   (%)
                    (W)
(°C)
           (kg/s)
       (m)
                           7.0
                                0.75
                  936.9
            0.28
10
       2.5
                                 0.75
                  984.6
                           7.4
       3.0
            0.25
            0.22 1004.0
                           7.8
                                 0.78
       3.5
       4.0
            STALLED
            0.26 724.9 6.5 0.90
18
       2.5
        3.0
            STALLED
        3.5
             STALLED
        4.0
            STALLED
        2.5
            STALLED
24
        3.0
            STALLED
            STALLED
        3.5
            STALLED
        4.0
 m = 0.044 \text{ kg/s} T = 88 °C L = 9.1 cm L = 0.0 cm H = 1.5 m
11. Variation of T (scaled model)
                             pout
        ΔΗ
               Q
                     q
 A
 hЬ
                            (W)
                    (W)
                                 ( % )
(cm<sup>2</sup>)
        (m) (kg/s)
                  936.2 7.0 0.75
        2.5 0.28
182.6
        3.0 0.25 984.6 7.4 0.75
             0.22 1004.0
                            7.8
                                  0.78
        3.5
             STALLED
        4.0
                           6.5
                                  0.70
                    932.5
158.7
        2.5
             0.26
             0.23
                    954.0
                           7.0
                                  0.73
        3.0
                            7.4
                                  0.76
                    973.6
        3.5
             0.21
             STALLED
        4.0
                           5.7
                                  0.62
                    905.5
121.9
        2.5
            0.23
                          5.9 0.62
        3.0
            0.20
                    940.0
        3.5 STALLED
        4.0 STALLED
 m = 0.044 kg/s T = 88 °C L = 9.1 cm L = 0.0 cm H = 1.5 m
12. Variation of A (scaled model)
```

h b

ΔΗ

Fire

L h	L th	ΔН	Q	ď	p out	η
(cm)	(mm)	(m)	(kg/s)	(W)	(W)	(%)
				•		
9.0	9.5	2.5 3.0 3.5	0.29 0.258 0.236	911.2 949.7 965.6	7.29 7.7 8.23	0.80 0.81 0.85
7.9		2.5 3.0 3.5	0.33 0.302 0.278			0.96 1.03 1.09
7.0		2.5 3.0 3.5	0.36 0.33 0.308	796.4 818.1 825.5	9.9	1.12 1.21 1.30
9.0	6.3	2.5 3.0 3.5	0.33 0.30 0.28	836.5 854.9 869.1	8.24 9.0 9.7	0.98 1.05 1.12
7.9		2.5 3.0 3.5	0.36 0.33 0.31	771.5 792.6 788.2		1.17 1.25 1.37
7.0		2.5 3.0 3.5	0.38 0.36 0.33	706.8 739.4 748.5	9.5 10.7 11.7	1.35 1.44 1.56
5.9		2.5 3.0 3.5	0.40 0.38 0.297	673.3 683.0 684.4	10.0 11.3 10.3	1.48 1.65 1.51

m = 0.044 kg/s T = 88 °C L = 0.0 cm H = 1.5 m 13. Variation of L = 0.0 and L = 0.0 (scaled model)

L	ΔΗ	Q	g .	p	η
(cm)	(m)	(kg/s}	i (W)	out (W)	(%)
<b>,,,</b> ,,,,,,,,,,,,,,,,,,,,,,,,,,,,,,,,,	<u> </u>	<u> </u>			( 10 /
0.0	2.5 3.0 3.5 4.0	0.28 0.25 0.22 1 STALLE		7.0 7.4 7.8	0.75 0.75 0.78
1.7	2.5 3.0 3.5 4.0	0.31 0.28 STALLE STALLE		7.7 8.4	0.88 0.96
3.5	2.5 3.0 3.5 4.0	STALLE STALLE STALLE STALLE	D D		٠

 $\frac{h}{h} = 0.044 \text{ kg/s}$ T =88 °C L =9.1 cm H =1.5 m

14. Variation of L (scaled model)  $\sim$ 

	th c	H	ΔН	Q	<b>q</b>	p out	n
)	(kg/s)	(m)	(m)	(kg/s)_	(W)	(W)	( % )
	0.020	0.5	1.5 2.0 2.5 3.0	0.279 0.174 0.164 0.131	1003.2 836.0 919.6 836.0	4.1 3.4 4.1 3.9	0.4 0.4 0.44 0.47
		1.0	2.0 2.5 3.0 3.5	0.180 - 0.144 STALLEI	668.8 - 836.0	3.5	0.52
	,	1.5		0.169 0.128 STALLEI	668.8 D	4.1 3.8	0.49
	0.027	0.5	2.0	0.298 0.206 0.171 0.113		4.4 4.0 4.2 3.3	0.4 0.43 0.42 0.36
	_	1.0	3.0 3.5	0.206 0.144 0.149 STALLEI	752.4 836.0	4.3 3.5 4.4	0.43 0.46 0.52
	,	1.5	3.0	0.182 0.144 STALLEI	∕ <del>83</del> 6.0 D	4.5 4.2	0.49 0.50
	0.033	0.5	1.5 2.0 ° 2.5 3.0	0.199	1003.2 1003.2 1003.2 1003.2	4.0 3.9 4.4 3.2	0.39 0.39 0.44 0.32
		1.0	2.5 3.0	0.223	836.0 836.0 1003.2 919.6	4.4 5.0 4.3 2.9	0.52 0.59 0.42 0.31
		1.5	3.0 3.5	0.196 0.168 0.121 STALLE	1003.2 836.0 836.0	4.8 4.9 4.1	0.48 0.58 0.49
	0:040	0.5	2.0 2.5	0.173	1086.8 1086.8 1003.2 1003.2	4.5 3.8 4.2 2.9	0.41 0.35 0.42 0.29

15. Variation of th (14 cm model)

----

```
2.0
2.5
        1.0
                    0.239
                              836.0
                                       4.7
                                               0.56
                    0.225
                             1003.2
                                       5.5
                                               0.55
                   0.144
                                               0.42
               3.0
                             1003.2
                                       4.2
               3.5
                    0.084
                             1003.2
                                       2.9
                                               0.29
        1.5
               2.5
                    0.172
                             1086.8
                                       4.2
                                               0.38
               3.0
                    0.154
                             1003.2
                                       4.5
                                               0.45
                    0.130
               3.5
                              919.6
                                       4.4
                                               0.48
               4.0
                    STALLED
0.047
        0.5
               1.5
                    0.273
                             1086.8
                                       4.0
                                               0.37
               2.0 0.209
                             1003.2
                                       4.1
                                               0.41
                             1086.8
               2.5
                    0.158
                                       3.9
                                               0.36
                     0.095
                                               0.26
               3.0
                             1086.8
                                       2.8
        1.0
               2.0
                     0.252
                              836.0
                                       4.9
                                               0.56
                                       5.2
               2.5
                    0.214
                                               0.52
                             1003.2
                    0.124
                                       3.7
                                               0.37
               3.0
                             1003.2
               3.5
                    0.077
                             1003.2
                                               0.26
                                       2.6
                                               0.42
        1.5
               2.5
                     0.187
                             1086.8
                                       4.6
                                               0.51
               3.0
                    0.145
                              836.0
                                       4.3
               3.5
                                               0.51
                     0.126
                              836.0
                                       4.3
               4.0
                    STALLED
0.053
        0.5
               1.5
                    0.173
                             1003.2
                                       2.5
                                               0.25
               2.0
                     0.208
                             1086.8
                                       4.1
                                               0.38
                                               0.36
               2.5
                    0.146
                             1003.2
                                       3.6
                                               0.24
               3.0
                    0.094
                             1170.4
                                       2.8
        1.0
               2.0
                    0.252
                             1086.8
                                       4.9
                                               0.45
               2.5
                    0.221
                                               0.65
                              836.0
                                       5.4
                                       4.2
                    0.145
               3.0
                             1003.2
                                               0.42
               3.5
                    0.079
                                       2.7
                             1003.2
                                               0.27
               2.5
                             1003.2
        1.5
                    0.179
                                       4.3
                                               0.43
               3.0
               3.5
                              836.0
                                       4.7
                                               0.56
                    0.136
               4.0
                    STALLED
Q.060
        0.5
               1.5
                    0.178
                                       2.6
                                               0.28
                              919.6
               2.0
                    0.194
                                               0.35
                             1086.8
                                       3.8
               2.5
                    0.168
                             1003.2
                                               0.41
                                       4.1
               3.0
                    0.093
                                       2,7
                                               0.25
                             1086.8
                                               0.56
        1.0
               2.0
                    0.285
                             1003.2
                                       5.6
               2.5
                    0.221
                             1003.2
                                       5.4
                                               0.54
               3.0
                    0.156
                             1086.8
                                       4.5
                                               0.41
               3.5
                    0.077
                             1003.2
                                       2.6
                                               0.26
                                               0.41
        1.5
               2.5
                    0.184
                             1086.8
                                       4.5
                    0.169
               3.0
                              836.0
                                       5.0
                                               0.60
                                               0.50
               3.5
                    0.133
                              919.6
                                       4.6
               4.0
                    STALLED
```

 $f_h = 0.040 \text{ kg/s}$  T = 78 °C L = 6.0 cm L = 0.0 cm h ct 15. Variation of fh (14 cm model - continued)

, <b>m</b>	H	ΔН	Q	g ,	Pout	ŋ
(kg/s)		(m)	(kg/s)	(W)	(W)	(%)
0.024	0.5	1.5 2.0 2.5 3.0	0.234 0.179 0.140 0.100		3.4 3.5 3.4 2.9	0.48 0.39 0.35 0.34
: <del> </del>	1.0	2.0 2.5 3.0 3.5	0.218 	852.7 - 752.4 D	4.3 - 3.9	0.50 - 0.52
	1.5	2.5 3.0 3.5 4.0	0.150 0.111 STALLE STALLE		3.6 3.3	0.42 0.47
0.031	0.5	1.5 ,2.0 2.5 3.0	0.211	974.0	3.0 4.1 4.2 3.4	0.35 0.42 0.43 0.32
	1.0	2.0 2.5 3.0 3.5	0.228 0.135 STALLE	974.0 - 843.9	4.5 - 4.0	0.46
,	1.5	2.5 3.0 3.5 4.0			3.9 3.8 3.6	0.40 0.45 0.39
0.040	0.5 ,	1.5 2.0 2.5 3.0	0.273 0.199 0.181 0.110	1006.9 1006.9 1006.9 1006.9	4.0 3.9 4.4 3.2	0.40 0.39 0.43 0.32
	1.0	2.0 2.5 3.0 3.5	0.204		5.0 4.3	0.52 0.59 0.42 0.30
	1.5	2.5 3.0 3.5 4.0		839.3 839.3	4.8 4.9 4.1	0.47 0.58 0.49
0.048	0.5	1.5 2.0 2.5 3.0	0.231 0.183	1404.5 1203.8	4.4 4.5 4.5 4.4	0.44 0.32 0.37 0.40

16. Variation of the (14 cm model)

```
995.4
        1.0
                     0.280
                                         5.5
                                                 0.55
               2.0
                              995.4
                                         5.0
               2.5
                     0.206
                                                 0.50
               3.0
                     0.172
                              995.4
                                         5.0
                                                 0.51
                     0.089
                              995.4
               3.5
                                         3.0
                                                 0.31
                              995.4
        1.5
              2.5
                     0.179
                                         4.4
                                                 0.44
               3.0
                     0.153
                              995.4
                                         4.5
                                                 0.45
               3.5
                     0.111
                              995.4
                                         3.8
                                                 0.38
               4.0
                     STALLED
0.054
        0.5
               1.5
                     0.265
                             1009.6
                                         3.9
                                                 0.38
               2.0
                     0.244
                             1009.6
                                         4.8
                                                 0.47
               2.5
                             1234.0
                     0.202
                                         4.9
                                                 0.40
                     0.152
                             1121.8
                                                 0.40
               3.0
                                         4.5
                             1009.6
               2.0
                     0.270
                                         5.3
                                                 0.52
        1.0
               2.5
                     0.171
                              785.3
                                         4.2
                                                 0.53
                     0.154
                             1009.6
                                         4.5
                                                 0.45
               3.0
               3.5
                     0.105
                              897.5
                                         3.6
                                                 0 40
               2.5
                                                 0.54
        1.5
                     0.174
                              785.3
                                         4.3
               3.0
                                         4.9
                     0.166
                             1121.8
                                                 0.43
               3.5
                     0.135
                              897.5
                                         4.6
                                                 0.52
               4.0
                     STALLED
0.061
        0.5
               1,5
                     0.317
                             1137.6
                                         4.7
                                                 0.41
               2.0
                     0.273
                             1137.6
                                         5.4
                                                 0.47
               2.5
                     0.214
                             1264.0
                                         5.3
                                                 0.41
               3.0
                     0.157
                             1137.6
                                         4.6
                                                 0.40
                     0.245
                                         4.8
        1.0
               2.0
                             1137.6
                                                 0.42
                                         4.2
                                                 0.47
               2.5
                     0.171
                              884.8
                     0.174
               3.0
                             1011.2
                                         5.1
                                                 0.50
                     0.123
                             1011.2
                                         4.2
                                                 0.41
               3.5
                             1137.6
               2.5
                     0.193
                                         4.7
                                                 0.41
        1.5
                                         5.0
                                                 0.43
               3.0
                     0.169
                             1137.6
               3.5
                     0.133
                             1137.6
                                         4.6
                                                 0.40
               4.0
                     STALLED
```

m = 0.033 kg/s T = 80 °C L = 6.0 cm L = 0.0 cm m = 0.0 cm l6. Variation of m = 0.04 cm model - continued)

A

	T hi	H	ΔH	Q	q i	p	η
	(°C)	(m)	(m)	(kg/s)	(W)	(W)	(୫)
	<b>70</b>	0.5	1.5 2.0 2.5 3.0	0.101 0.45 STALLED STALLED	895.9 895.9	2.0	0.17 0.10
	,	1.0	2.0 2.5 3.0 3.5	0.092 0.068 STALLED STALLED	696.8 696.8	1.8	0.26
		1.5	2.5 3.0 3.5 4.0	STALLED STALLED STALLED STALLED		•	•
Ų	80	0.5	1.5 2.0 2.5 3.0	0.231 0.183	995.4 1393.6 1194.5 1094.9	4.5 4.5 4.5 4.5	0.45 0.32 0.37 0.40
	×.	1.0	2.5	0.280 0.206 0.172 0.089	995.4 995.4 995.4 995.4	5.5 5.0 5.0 3.0	0.55° 0.50 0.51 0.31
		1.5	2.5 3.0 3.5 4.0	0.179 0.153 0.111 STALLED	995.4 995.4 995.4	4.4 4.5 3.8	0.44 0.45 0.38
	90	0.5		0.282 0.268	1393.6 1294.0 1294.0 1094.9	4.9 5.5 6.6 6.8	0.35 0.43 0.51 0.61
		1.0	3.0	0.228 0.199	1094.9	5.9 4	0.50 0.51 0.49 0.51
	•	1.5	3.0 3.5	0.211	1094.9 1294.3	4.9 5.0 7.3 - 6.1.	0.45 0.56
	<b>.</b> _ (	<b>1</b> 022	h /	± -0 049	h a /a	T -6 0 am	r ~0 0 cm

m = 0.033 kg/s m = 0.048 kg/s L = 6.0 cm L = 0.0 cm local local

¥

L	H	ΔH	Q '	q <sub>i</sub> .	i	p out	η .		<	iş.
(cm)	(m)	(m)	(kg/s).	(W)	(1	W)	(8)			
5.0	0.5	1.5 2.0 2.5 3.0	0.229 0.190 0.155 STALLED	995.4 995.4 895.9	3	.4 .7 .8	0.34 0.37 0.42	'	-	
	1.0	2.0 2.5 3.0 3.5	0.163 0.151 STALLED STALLED			.2	0.40			•
	1.5	2.5 3.0 3.5 4.0	STALLED STALLED STALLED STALLED	) 					3	o
<sub>_</sub> 6.0	0.5	1.5 2.0 2.5 3.0	0.183	995.4 1393.6 1194.5 1094.9	4 4	.4 25 .5 .4	0.45 0.32 0.37 0.40	2		
	1.0	2.0 2.5 3.0 3.5	0.280 0.206 0.172 0.089	995.4 995.4 995.4 995.4	5 5	.5 .0 .0	0.55 0.50 0.50	) )		
	1.5	2.5 3.0 3.5 4.0	0.179 0.153 0.111 STALLED	995.4 995.4	4	.4 .5 .8	0.44 0.45 0.38	5	t	- Ç
7.0	0.5	1.5 2.0 2.5 3.0		796.3 796.3 1094.9 1194.5	3 4	.9 .8 .2 .8	0.38 0.48 0.38 0.32	3 3		
	1.0	2.5 3.0	0.214 0.190 0.153 0.100	995.4 995.4	4	.2 .6 .5	0.47	7 5		
4	1.5.	3.0 3.5	0.185 0.115 STALLED STALLED	995.4	3	.5 .4	0.45		2	
ф =	0.033	kg/s	m = 0.048	kq/s	8= T	0 °C	L =	=0.0	CM	

m = 0.033 kg/s m = 0.048 kg/s m = 0.0

L	Н	ΔН	Q	q ´	p	η
ct (cm)	s (m)	(m)	(kg/s)	i (W)	οú t (₩)	(%)
			•			
0.0	0.5	1.5 2.0 2.5 3.0	0.302 0.231 0.183 0.151	995.4 1393.6 1194.5 1094.9	4.4 4.5 4.5 4.4	0.45 0.32 0.37 0.40
·	1.0	2.0 2.5 3.0 3.5	0.280 0.206 0.172 0.089	995.4 995.4 995.4 995.4	5.5 5.0 5.0 3.0	0.55 0.50 0.51 0.31
ρ,	1.5	2.5 3.0 3.5 4.0	0.179 0.153 0.111 STALLE	995.4 995.4 995.4	4.4 4.5 3.8	0.44 0.45 0.38
1.0	0.5	1.5 2.0 2.5 3.0	0.258 0.199 0.161 STALLE	995.4 995.4 	3.8 3.9 3.9	0.38 0.39 0.44
	1.0	2.0 2.5 3.0 3.5	0.199 0.156 STALLES		3.9 3.8	0.35 0.42
ç	1.5	2.5 3.0 3.5 4.0	STALLEI STALLEI STALLEI STALLEI	D D .		

19. Variation of L (14 cm model)

O

.

-

- -- -- --

```
3.0
                   0.137
                            995.4
                                      4.0
                                              0.40
      1.0
             2.0
                   0.231
                            995.4
                                      4.5
                                              0.45
             2.5
                   0.191
                            895.9
                                     · 4.7
                                              0.52
             3.0
                   0.141
                            895.9
                                      4.1
                                              0.46
                   0.112
             3.5
                            796.3
                                      3.8
                                              0.48
             2.5
                                      3.3
      1.5
                   0.135
                            696.8
                                              0.47
             3.0
                   0.107
                            796.3
                                      3.1
                                              0.39
             3.5
                   STALLED
             4.0
                   STALLED
1.0 * 0.5
                            995.4
            1.5
                   0.261
                                      3.8
                                              0.38
            2.0
                   0.217
                           1094.9
                                      4.2
                                              0.39
            2.5
                   0.181
                           1094.9
                                      4.4
                                              0.40
             3.0
                   0.130
                            995.4
                                      3.8
                                              0.38
      1.0
            2.0
                   0.201
                            895.9
                                      3.9
                                              0.44
             2.5
                   0.146
                            696.8
                                      3.6
                                              0.51
            3.0
                   0.097
                            696.8
                                      2.8
                                              0.41
            3.5
                   0.107
                           1393.6
                                      3.7
                                              0.26
      1.5
            2.5
                   0.159
                            895.9
                                      3.9
                                              0.43
            3.0
                   STALLED
            3.5
                   STALLED
            4.0
                   STALLED
2.0 * 0.5
                            796.3
            1.5
                   0.211
                                      3.1
                                              0.39
                            696.8
            2.0
                   0.202
                                      3.98
                                              0.56
            2.5
                   0.153
                            895.9
                                      3.7
                                              0.42
            3.0
                   0.117
                            895.9
                                      3.5
                                              0.38
     1.0
            2.0
                   0.151
                            796.3
                                      2.9
                                              0.37
            2.5
                   0.152
                            895.9
                                      3.7
                                              0.41
            3.0
                   0.115
                            895.9
                                      3.4
                                              0.38
            3.5
                   STALLED
     1.5
            2.5
                   0.178
                            895.9
                                      4.3
                                              0.48
            3.0
                   0.120
                            995.4
                                      3.5
                                              0.35
            3.5
                   STALLED
            4.0
                   STALLED
                  h = 0.048 \text{ kg/s}
h = 0.033 \text{ kg/s}
                                     =80 °C L =6.0 cm
                   h
                                    h i
```

0.0 \* 0.5

19. Variation of L

1.5

2.0

2.5

0.265

0.231

0.186

995.4

995.4

1094.9

3.9

4.5

4.5

0.39

0.45

0.41

(14 cm model - continued)

<sup>\*</sup> Heater inlet and outlet tubes insulated.

H	ΔН	ı, <b>Q</b>	${\tt q}_{_{\bf i}}$	, p	η	
(m)	(m)	(kg/s)	(W)	(W)	(%)	
0.5	1.5 2.0 2.5 3.0	0.256 0.212 0.161 0.135	796.3 796.3 796.3 796.3	3.7 4.1 3.9 3.9	0.47 0.52 0.50 0.50	BOTTOM - CENTER
1.0	2.0 2.5 3.0 3.5	0.158 0.141 0.113 0.089	696.8 696.8 597.2 695.2	3.1 3.4 3.3 3.1	0.44 0.50 0.56 0.38	
1.5	2.5 3.0 3.5 4.0	STALLED STALLED STALLED STALLED				?
0.5	1.5 2.0 2.5 3.0	0.18 0.17 0.15 0.13	796.3 796.3 796.3 796.3	2.7 3.3 3.7 3.8	0.34 0.41 0.47 0.48	TOP - CENTER
1.0	2.0 2.5 3.0 3.5	0.15 0.13 0.10 STALLED	597.2 597.2 597.2	3.0 3.3 2.9	0.50 0.55 0.49	
1.5.	2.5 3.0 3.5 4.0	0.16 0.13 STALLED STALLED	796.3 796.3	4.0 3.7	0.50 0.47	^
0.5	1.5 2.0 2.5 3.0	0.183	995.4 1393.6 1194.5 1094.9	4.4 4.5 4.5 4.4	0.45 0.32 0.37 0.40	BOTTOM - PERIPHERY
1.0	2.0 2.5 3.0 3.5	0.280 0.206 0.172 0.089	995.4 995.4 995.4 995.4	5.5 5.0 5.1 3.1	0.55 0.51 0.51 0.31	
1.5	2.5 3.0 3.5 4.0	0.179 0.153 0.111 STALLED	995.4 995.4 995.4	4.4 4.5 3.8	0.44 0.45 0.38	<i>c</i> ,

<sup>20.</sup> Switching the inlets and outlets of the evaporator and the condenser (14 cm model)

```
0.192
0.5
       1.5
                       895.9
                                 2.8
                                        0.31
                                                   TOP - PERIPHERY
              0.199
                                 3.9
                                        0.43
        2.0
                       895.9
        2.5
              0.159
                       895.9
                                 3.9
                                        0.43
        3.0
              0.131
                       895.9
                                 3.8
                                        0.43
1.0
                       895.9
        2.0
              0.252
                                 4.9
                                        0.55
        2.5
              0.187
                       895.9
                                 4.6-
                                        0.51
        3.0
              0.127
                                        0.42
                       895.9
                                 3.7
        3.5
              0.114
                       895.9
                                 3.9
                                        0.43
                                        0.53
1.5
        2.5
                                 4.7
              0.193
                       895.9
        3.0
              0.132
                       995.4
                                 3.9
                                        0.39
        3.5
              STALLED
              STALLED
        4.0
```

m (ave.)	H	ΔH	Q	ď	p out	n
(kg/s)	(m)	(m)	(kg/s)	(W)	(W)	(१)
0.0083 0.012 0.014 0.0155	0.5	1.5 2.0 2.5 3.0	0.13 0.12 0.11 0.09	497.7 497.7 497.7 597.2	1.8 2.1 2.3 2.2	0.37 0.42 0.47 0.37
,	1.0	2.0 2.5 3.0 3.5	STALLI STALLI STALLI STALLI	ED ED		est .
	1.5	2.5 3.0 3.5 4.0	STALLI STALLI STALLI STALLI	ED ED		

h = 0.048 kg/s T = 80 °C L = 6.0 cm

21. Alternative cooling water supply (14 cm model)

\_\_\_

th c	<b>t</b> h	ΔH	Q	q	p out	'n
(kg/s)		(m)	(kg/s)	(W).	(W)	(왕)
0.060	0.021		0.148 0.113 0.076 STALLEI	398.2 442.4	2.2 2.2 1.9	0.55 0.56 0.43
a	0.031	2.5 2.0 2.5 3.0	0.182 0.137 0.103 0.084	518.3 499.3 453.5 873.8	2.7 2.7 2.5 2.5	0.52 0.52 0.56 0.54
,	0.060	2.0	0.217 0.141 0.124 STALLEI	632.0 748.9	3.2 2.7 3.0	
	0.151	1.5 2.0 2.5 3.0	0.230 0.162 0.138 0.113	948.0		0.53 0.33 0.53 0.35
0.040	0.021	1.5 2.0 2.5 3.0	0.163 0.093 STALLEI			0.60
	0.031	1.5 2.0 2.5 3.0	0.119 0.082 STALLEI	388.7 )	1.7	0.45
	0.060	2.0	0.094 STALLEI STALLEI STALLEI	)	1.4	0.36
	0.151	1.5 2.0 2.5 3.0				
0.023	0.021	1.5 2.0 2.5 3.0	0.121 0.085 STALLEI STALLEI		1.8	0.40
,			•	~		

22. Variation of m and m (12.7 cm model)

 $T_{h i} = 80$  °C  $H_{s} = 0.5$  m

22. Variation of h and h (12.7 cm model - continued)

T hı	ΔH	, <b>Q</b>	g ,	p out	η
(°C)	(m)	(kg/s)	(W)	(W)	<u>(왕)</u>
70	1.5 2.0 2.5 3.0	0.166 0.129 0.064 STALLE	497.9 568.8 639.9 D	2.4 2.5 1.6	0.49 0.44 0.25
80	1.5 2.0 2.5 3.0	0.148 0.113 0.078 STALLE	445.6 497.7 355.5 D	2.2 2.2 1.9	0.49. 0.45. 0.54
90	1.5 2.0 2.5 3.0	0.098 0.085 STALLE STALLE		1.4 1.7	0.34 0.47

m = 0.060 kg/s m = 0.034 kg/s m = 0.5 m23. Variation of m = 0.034 kg/s m = 0.5 m

\_\_\_\_

1,

,

APPENDIX 2

COMPUTER PROGRAM LISTING

```
MAIN PROGRAM TO SIMULATE THE SLPP - ABEEKU BREW-HAMMOND - 14/6/83
      EXTERNAL FCN, FCNJ
      COMMON
              /GEAR/DUMMY(48), SDUMMY(4), I DUMMY(38)
      COMMON
              /DEF/VOUTDO, VINDO, DELT, PVAP, TVAP, PPREV, TPREV, SPVOL, TH, TL
              /DEF/NSAVE, NPV, IPHASE, ISPV, IPTEST, NI, ITL, NPRINT, SCALE
C
      REAL*8 VOUTDO, VINDO, DELT, T, TEND, PVAP, TVAP, PPREV, TPREV, SPVOL, TH, TL
      REAL*8 PD(4,4),YV(4),YVDOT(4),H,TOL,WK(88),DUMMY,TSTART,VAR
      REAL*4 SDUMMY
      DIMENSION IWK(4)
   STATE VARIABLES AND UNITS
  1 - MASS OF VAPOUR (LBS)
    - OUTPUT PIPE VELOCITY (IN/SEC) =VE OUT
   3 - INPUT PIPE VELOCITY (IN/SEC) = VE IN
   4 - LIQUID LEVEL BELOW TOP OF CULINDER (IN)
  OTHER PARAMETERS AND UNITS
  SPECIFIC VOLUME (LBM/FT**3)
  TEMPERATURE (DEGREES FARENHEIT)
  PRESSURE (PSI)
      NPRINT = 1
     ASSUMED RANKINE-LIKE CYCLE WITH SATURATED VAPOUR AND X=F(LHTOP)****
        DO 9999 NRUN = 40,100,20
CC
        INRUN = 10 - NRUN
        VAR = FLOAT(NRUN)
C
  HERE TO INTERPOLATE FOR FREON LIQUID TEMPERATURE
      TL = 116.0
      ITL = 1
      ISTALL = 0
1000 CONTINUE
      NSAVE = 0
      NPV = 12
      IPHASE = 1
      IPTEST = 1
      NI = 1
      N = 4
      T = 0.
      TFIN = 16.
      TSTART = 6.
      DELT = 0.02
      TZFLOW = 0.
      H = 0.0001
      TOL = 0.0001
      METH = 1
     MITER = 1
      INDEX = 1
```

NOW CALCULATE SUBROUTINE CONSTANTS AND DEFINE INITIAL CONDITIONS

```
TEND = 0.
                 CALL DEFCON (VAR, YV)
                 CALL FCN (N, TEND, YV, YVDOT)
                WRITE (6,1100)
C1100 FORMAT(//// ,' SEC',T11,'MDOT',T22,'VOUTD',T33,'VIND',T44,'YDOC 1 T55,'TVAP',T66,'TH',T77,'SPVOL',T88,'VOUT',T99,'VIN',T110,'Y',C' 1 T121,'PVAP')
                                                          SEC',T11,'MDOT',T22,'VOUTD',T33,'VIND',T44,'YDOT',
                 WRITE (6,2300) T, (YVDOT(K), K=1,4), TVAP, TH, SPVOL, (YV(K), K=2,4), PVAP
        NOW START DGEAR
   2000 TEND = {}^{\circ}T + DELT
                 ISPV = -1
                 CALL DGEAR (N, FCN, FCNJ, T, H, YV, TEND, TOL, METH, MITER, INDEX, IWK, WK, IER)
                 IF (IER .EQ. 0) GO TO 2200
       HERE TO PRINT OUT IF IER NOT = 0
                WRITE (6,2100) T,H,DUMMY(8), IER, (IDUMMY(J), J=6,8)
   2100 FORMAT( ' IER > 0',3G15.8,5I10)
                 IF (IER .GT. 128) GO TO 9999
   2200 CONTINUE
                CALL FCN(N, TEND, YV, YVDOT)
              WRITE (6,2300) TEND, (YVDOT(K), K=1,4), TVAP, TH, SPVOL, <math>(YV(K), K=2,4), TVAP, TH, SPVOL, (YV(K), K=2,4), TVAP, TYAP, TH, SPVOL, (YV(K), K=2,4), TVAP, TYAP, 
              1 PVAP
C2300 FORMAT( 1x, F5.2, 11G11.4)
       RESET VALUES OF VOUTDO, VINDO, PPREV AND TPREV
                VOUTDO = YVDOT(2)
                                 = YVDOT(3)
                VÍNDO
                PPREV = PVAP
                TPREV = TVAP
        TEST FOR VARIOUS STOPPING CONDITIONS
                IF (YV(2) . GT. 0. . OR. YV(3) . GT. 0.) GO TO 3100
                TZFLOW = TZFLOW + DELT
                IF (TZFLOW.LT. 0.5) GO TO 3200
C HERE IF THERE HAS BEEN NO FLOW IN OR OUT FOR 0.5 SEC; ASSUME STALL
                WRITE (6,3000) TEND, YV(4), PVAP
   3000 FORMAT(/// ,' STALL ASSUMED: TIME = ',F5.2,',
                          PRESSURE = ',G12.4)
                GO TO 9999
   3100 \text{ TZFLOW} = 0.
  3200 CONTINUE
       TEST FOR NEGATIVE MVAP OR Y
                IF (YV(1) .LE. 0.) GO TO 3209.
                IF (YV(4) .LE. 0.) GO TO 3209
                GO TO 3400 -
   3209 WRITE (6,3300)
   3300 FORMAT(
                                     ' NEGATIVE MVAP OR Y').
                STOP
23400 CONTINUE
```

CALCULATE THE NEW HEATER TEMPERATURE

```
CALL THNEW
   HERE WHILE WAITING FOR INITIAL TRANSIENT TO SETTLE OUT
      IF (TEND .LT. TSTART) GO TO 2000
   IDENTIFY ONE CYCLE AND CALCULATE THE PERFORMANCE CRITERIA
  AND PARAMETERS IN THE CONSERVATION EQUATIONS
      CALL CYCLE
   RESET TIME
      T = TEND
   CHECK IF FREON LIQUID TEMPERATURE HAS BEEN DETERMINED
      IF (IPHASE .EQ. 7) GO TO 1000
C
   CHECK IF CYCLE IS COMPLETE
C
      IF (IPHASE .EQ. 6) GO TO 6100
C
   HERE IF CYCLE IS NOT COMPLETE; CHECK IF TIME IS UP
      IF (TEND .LT. TFIN) GO TO 2000
      WRITE (6,6000)TFIN
 6000 FORMAT(
              ' CONVERGENCE WAS NOT ACHIEVED IN', G12.4, 'SECS')
      GO TO 9999
 6100 CONTINUE
   PLOT THE FINAL RESULTS
      CALL OUTPUT
 9999 CONTINUE
      CALL FINAL
      STOP
      END
MULTIPLE ENTRY SUBROUTINE FOR SLPP SIMULATION
      SUBROUTINE DEFCON (VAR, YV)
              /DEF/VOUTDO, VINDO, DELT, PVAP, TVAP, PPREV, TPREV, SPVOL, TH, TL
      COMMON
      COMMON
              /DEF/NSAVE, NPV, I PHASE \ I\SPV, I PTEST, NI, ITL, NPRINT, SCALE
              /VA/LHTOP, LHEAT, LHBOT, LCTOP, LCOND, LCBOT, AHBOT, AHEAT, ACYL
      COMMON
              /VA/ACCOIL, ACOND, DAHDY, DACDY, VOL, DVOLDY, C6, C7, C8, C9, C10
      COMMON
      COMMON
              /VA/C11,C12,C13,C14,C15,C16,C37,C38,C39,Y
      REAL*8 VOUTDO, VINDO, DELT, T, TEND, PVAP, TVAP, PPREV, TPREV, SPVOL, TH, TL
      REAL*8 LHTOP, LHEAT, LHBOT, LCTOP, LCOND, LCBOT, AHBOT, AHEAT, ACYL
      REAL*8 ACCOIL, ACOND, DAHDY, DACDY, VOL, DVOLDY, C6, C7, C8, C9, C10
      REAL*8 C11,C12,C13,C14,C15,C16,C37,C38,C39,Y,FRIC
      REAL*8 PD(4,4),YV(4),YVDOT(4),VAR,TERM,QEVAP,QHEATO,THONEW
      REAL*8 YI1(150),YI2(150),YI3(150),YI4(150),YI5(150),YI6(150)
      REAL*8 Y17(150),Y18(150),Y111,Y112,Y113,Y114,Y115,Y116,Y117,Y118
      REAL*4 Y1(400), Y2(400), Y3(400), Y4(400), Y5(400), Y11(150), Y22(150)
      REAL*4 Y33(150),Y44(150),Y55(150),Y66(150),Y77(150),Y88(150)
```

```
REAL*4 YB(20), YC(20), YD(20), YE(20), YF(20), YG(20), YH(20)
      REAL*8 YA(20), TOTHED
C
      REAL*8 AHUP, AHBU, AOUT, AIN, DCYL, DOUT, DIN, LOUT, LIN, LCYL, HOUT, HIN
      REAL*8 VHUP, VHBOT, VCCOIL, MASSH, MHRATE, MEVAP, MCOND, SPVOLS, KP, KT
      REAL*8 TC, THI, HEVAP, HHV, HCOND, HLC, HFG, MVAP, VOUT, VIN, MEVAPT
      REAL*8 MDOT, VOUTD, VIND, YDOT, INDEFF, ROFRE, ROWAT, GRAV, MU, MCONDT
      REAL*8 C1,C2,C3,C4,C5,C17,C18,C19,C20,C21,C22,C23,C24,C25,C26
      REAL*8 C27,C28,C29,C30,C31,C32,C33,C34,C35,C36,DTDM,DTDY,INDPOW
      REAL*8 LFRE, LWAT, KFRICT, TL1, TL2, FTL1, FTL2, TTWO, TFOUR, PTWO, PFOUR
      REAL*8 C1H, C2H, CVH, SCALE
C
      DATA LOUT/200./,LIN/200./,HOUT/40./,HIN/-60.0/
      DATA DOUT/1.5/, DIN/1.5/
      DATA ROFRE/1.425E-04/, ROWAT/0.933E-04/, GRAV/386./, PATMOS/14.7/
      DATA HEVAP/14.E-04/,HHV/0.07E-04/,HCOND/0.6E-04/,HLC/1.150E-04/
      DATA HFG/63./, CP/1./, MU/1.45E-08/, PI/3.1416/
      DATA THI/190.0/,TC/50./,KFRICT/10./,FRIC/0.025/
C
      DCAL
             = 3.9375
      AHUP
             = 4.
      VHUP
             = 0.255
      VHBOT =
               0.925
      VCCOIL= 11.74
      MHRATE= 0.0352
      VOLFRE= 122.
C
      LHTOP = 0.8
      LHEAT = 0.3
      LCTOP = 0.0
C
      LCBOT = 4.75
      LCOND = 4.75
      LCYL = 25.
      AHBOT = 15.
      ACCOIL= 100.
C
   SCALING
      SCALE=1.375
      DCYL=DCYL*SCALE
      AHUP=AHUP*(SCALE**2)
      VHUP=VHUP*(SCALE**3)
      VHBOT=VHBOT*(SCALE**3)
      VCCOIL=VCCOIL*(SCALE**3)
      LHTOP=LHTOP*SCALE
      LHEAT=LHEAT*SCALE
      LCTOP=LCTOP*SCALE
C
      LCBOT=LCBOT*SCALE
      LCOND=LCOND*SCALE
      LCYL=LCYL*SCALE
      AHBOT=AHBOT*(SCALE**2)
      ACCOIL=ACCOIL*(SCALE**2)
      MHRATE=MHRATE*(SCALE**2)
      VOLFRE=VOLFRE*(SCALE**3)
```

```
C
             = VAR
      HOUT
             = VAR
C
       LOUT
C
              = THI
       TH
       THONEW = THI
       QHEATN = 0.
       IPV = 1
C
            = PI * DOUT**2/4.
       AOUT
             = PI * DIN**2/4.
       AIN
             = PI *'DCYL**2/ 4.
       ACYL
       LHBOT = LHTOP + LHEAT
       LCOND = LCBOT - LCTOP
C
       LCBOT = LCTOP + LCOND
       LFRE = VOLFRE/ ACYL
       LWAT = LCYL - LHTOP - LFRE
       CVH = 0.
       C1 = LHTOP/(2.6*SCALE)
       C2 = LCOND/ (4.75*SCALE)
C1H=LHEAT/(.3*SCALE)
       C2H=AHBOT/(15.*SCALE)
 C
              = AHUP * Cl
       AHUP
              = AHUP + AHBOT
       AHBU
       ACCOIL = ACCOIL * C2
              = VHUP * Cl
       VHUP
       VCCOIL = VCCOIL * C2
       VHBOT = VHBOT * ClH * C2H
       MASSH = (VHUP + VHBOT) * ROWAT * GRAV
 С
            = VCCOIL/ LCOND
       C3
            =- VHUP/ LHTOP
       C4
            = VHBOT/ LHEAT
       C5
            = ACYL - C3
       C6
            = C6 - C4
       C7
            = C6 - C5
       C8
            = ACYL - C4
       C9
       C10 = ACYL - C5
 С
       IF (LCTOP.EQ.O.) GO TO 2001
       CVH=LCTOP*C9
  2001 Cll = (LHTOP-LCTOP) * C7+CVH
       C12 = C11 + .LHEAT * C8
       Cl3 = Cl2 + (LCBOT - LHBOT) * C6
        C14 = (LCBOT-LCTOP) * C7 + CVH
        C15 = C14 + (LHTOP - LCBOT) * C9
        C16 = C15 + (LHBOT - LHTOP) * C10
 С
        C17 = MHRATE * CP * DELT
        C18 = C17/2.
        C19 = MASSH * CP/ 2. - C18
        C20 = C17 + C19
```

```
C
      C21 = HEVAP/HFG
      C22 = HCOND/HFG
C
      C23 = AOUT / ACYL
      C24 = AIN / ACYL
      C25 = AOUT / AIN
C
      C26 = KFRICT * ROWAT/ 2
      C27 = 2. * ROWAT * FRIC
      C28 = C27 * LOUT / DOUT
      C29 = ROFRE * LFRE + ROWAT * LWAT
      C30 = C29 * C24
      C31 = C29 * C23
      C32 = (ROFRE*LFRE - ROWAT*(HOUT + LHTOP + LFRE)) * GRAV - PATMOS
      C33 = ROWAT * LOUT + C31
      C34 = PATMOS - (ROFRE*LFRE - ROWAT*(HIN + LHTOP + LFRE)) * GRAV
      C35 = C27 * LIN / DIN
      C36 = ROWAT * LIN + C30
C
      C37 = AHUP/ LHTOP
      C38 = AHBOT/ LHEAT
      C39 = ACCOIL/ LCOND
C
      C40 = C26 + C28
      C41 = 2. * C40 / C33
С
      C42 = 2. * C26 + C35
      C43 = 2. * C42/ C36
   WRITE DIMENSIONAL PARAMETER VALUES
      WRITE (6, 2010)
                       LHTOP, LHEAT, LHBOT, AHUP, AHBOT, AHBU, VHUP, VHBOT,
     1 MASSH, MHRATE
 2010 FORMAT('1',' HEATER PARAMETERS: LHTOP, LHEAT, LHBOT, AHUP, AHBOT, AHBU,
     1 VHUP, VHBOT, MASSH, MHRATE', /, 10G12.4, //)
      WRITE (6, 2020) LCTOP, LCOND, LCBOT, ACCOIL, VCCOIL
               ' CONDENSER PARAMETERS: LCTOP, LCOND, LCBOT, ACCOIL, VCCOIL',
 2020 FORMAT(
     1 /,5G12.4,//)
      WRITE (6,2025) HEVAP, HHV, HCOND, HLC FORMAT( ' HEAT TRANSFER COEFFICIENTS: HEVAP, HHV, HCOND, HLC', /,
 2025 FORMAT(
     1 4G12.4,//)
      WRITE (6,2030) HOUT, HIN, KFRICT FORMAT( 'INLET AND OUTLET HEADS: HOUT, HIN, KFRICT', /, 3G12.4, //)
      WRITE (6,2040) LCYL, LOUT, LIN, LFRE, LWAT, DCYL, DOUT, DIN, ACYL, AOUT,
     1 AIN
2040 FORMAT( ' MISCELLANEOUS PARAMETERS: LCYL, LOUT, LIN, LFRE, LWAT,
     1 DCYL, DOUT, DIN, ACYL, AOUT, AIN', /, 11G12.4, //)
      WRITE (6,2050) C1,C2,C3,C4,C5,C6,C7,C8,C9,C10,C11,C12,C13,C14,C15,
     1 C16,C17,C18,C19,C20,C21,C22,C23,C24,C25,C26,C27,C28,C29,C30,C31,
     1 C32,C33,C34,C35,C36,C37,C38,C39,C40,C41,C42,C43
2050 FORMAT( ' CONSTANT VALUES: C1,C2,C3,C4,C5,C6,C7,C8,C9, C10,C11,
     1 C12,C13,C14,C15,C16,C17,C18,C19,C20,C21,C22,C23,C24,C25,C26,C27'
          C28,C29,C30,C31,C32,C33,C34,C35,C36,C37,C38,C39,C40,C41,C42,
```

```
1 C43',/,4(11G12.4,/),//)
  NOW CALCULATE THE INITIAL CONDITIONS ASSUMING THAT THE FREON
  LIQUID-VAPOUR INTERFACE IS ALREADY AT THE LEVEL OF THE HEATER
  WITH AN ARTIFICIALLY HIGH PRESSURE IN THE VAPOUR
     PVAP
            = - C32 + 2.
     PPREV = PVAP + 1.
            = 33.6/ PVAP
      SPVOL
            = 171.1/ DSQRT(SPVOL)
     TVAP
     Y '= LHBOT
      CALL VANDA
      YV(.1)
            = VOL/ SPVOL/1728.
      YV(2)
            = 20.
      YV(3)
            = 0.
     YV(4)
            = LHBOT
     VOUTDO = 50.
     VINDO = 0.
     KP = 33.6
     KT = 171.1
     RETURN
C
ENTRY FOR D/DT CALCULATIONS
     ENTRY FCN(N, TEND, YV, YVDOT)
C
     MVAP = YV(1)
     VOUT = YV(2)
     VIN = YV(3)
          = YV(4)
C
  HERE TO CALCULATE LIQUID CONTACT AREAS AND VAPOUR SPECIFIC VOLUME
     CALL VANDA
     SPVOL = VOL/ MVAP/ 1728.
     GO TO (3010, 3020, 3030, 3040), IPV
  ASSUME VAPOUR IS INITIALLY SATURATED
3009 \text{ KP} = 33.6
     KT = 171.1
3010 PVAP = KP/ SPVOL
     TVAP = KT/ DSQRT(SPVOL)
     IF (PPREV .LT. PVAP) IPV = 2
     IF (IPV .NE. 2) GO TO 3050
     PTWO = PPREV
     TTWO = TPREV
3020 IF (Y .LT. LHTOP) GO TO 3021
     PVAP = PTWO
     TVAP = TTWO
     GO TO 3050
3021 IF (ISPV .EQ. 1) IPV = 3
     PPREV = PPREV - 5.
```

```
KP = PVAP * SPVOL
     KT = TVAP * DSQRT(SPVOL)
 3030 \text{ PVAP} = \text{KP/ SPVOL}
     TVAP = KT/DSQRT(SPVOL)
      IF (PPREV.GT. PVAP) IPV = 4
     IF (IPV .NE. 4) GO TO 3050
C
     KP = PPREV
     KT = TPREV
     PFOUR = PPREV
     TFOUR = TPREV
     SPVOLS = 33.6/ PPREV °
C
 3040 IF (SPVOL .GT. SPVOLS) GO TO 3041
     PVAP = PFOUR
     TVAP = TFOUR
     GO TO 3050
 3041 \text{ IF (ISPV .EQ. 1) IPV = 1}
     'PPREV = PPREV + 5.
     GO TO 3009
 3050 CONTINUE
C
 PROCEED WITH ACTUAL D/DT CALCULATIONS
     TERM = Y - LHBOT
     TERM = DEXP(TERM)
     QEVAP = TERM * AHEAT * HEVAP * (TH - TL)
     MEVAP = QEVAP/ HFG
     MCOND = (ACCOIL - ACOND) * C22 * (TVAP - TC)
     MDOT = MEVAP - MCOND
C
     VOUTD = (PVAP - C40 * VOUT**2 + C30 * VINDO + C32) / C33
  OUTLET VALVE CONTROL
     IF (VOUT .LE. 0. .AND. VOUTD .LT. 0.) VOUTD = 0.
C
     VIND = (C34 - PVAP - C42 * VIN**2 + C31 * VOUTDO)/ C36
  INLET VALVE CONTROL
     IF (VIN .LE. 0. .AND. VIND .LT. 0.) VIND = 0.
C
  DVOLDY IS EQUAL TO THE EFFECTIVE CROSS-SECTIONAL AREA
     YDOT = (VOUT * AOUT - VIN * AIN)/ DVOLDY
CC
     WRITE (6,3060) VOUT, VIN, AOUT, AIN, ACYL, DVOLDY, YDOT
3060 FORMAT( ' VOUT, VIN, AOUT, AIN, ACYL, DVOLDY, YDOT =', 7G12.4)
     YVDOT(1) = MDOT
     YVDOT(2) = VOUTD
     YVDOT(3) = VIND
     YVDOT(4) = YDOT
C
     RETURN
C ENTRY TO CALCULATE PARTIAL DERIVATIVES
```

```
ENTRY FCNJ(N, TEND, YV, PD)
C
      MVAP = YV(1)
      VOUT = YV(2)
      VIN = YV(3)
           = YV(4)
   INITIALIZE PARTIALS TO ZERO
      DO 4005 I=1,4
      DO 4005 J=1,4
 4005 PD(I,J) = 0.
   PVAP AND TVAP PARTIALS
      IF (IPV .EQ. 2 .OR. IPV .EQ. 4) GO TO 4010
      DPDM = KP/VOL/1728.
      DPDY = - KP * MVAP / (VOL / 1728.) **2 * DVOLDY / 1728.
      DTDM = MVAP * VOL / 1728.
      DTDM = KT/ 2./DSQRT(DTDM)
      DTDY = MVAP/(VOL/1728.)**3
      DTDY = -KT * DSQRT(DTDY) / 2. * DVOLDY / 1728.
     GO TO 4020
 4010 \text{ DPDM} = 0.
      DPDY = 0.
      DTDM = 0.
      DTDY = 0.
 4020 CONTINUE
   PARTIAL OF MOOT WRT MVAP
      PD(1,1) = - (ACCOIL - ACOND) * C22 * DTDM
C
   PARTIALS OF MDOT WRT VOUT AND VIN = 0
   PARTIAL OF MDOT WRT Y
      PD(1,4) = TERM * (AHEAT + DAHDY) * C21 * (TH - TL)
      PD(1,4) = PD(1,4) + (DACDY*(TVAP-TC) - (ACCOIL-ACOND)*DTDY)*C22
   COMPUTE PARTIALS OF VOUTD ONLY WHEN VOUT > 0
      IF (VOUT .LE. 0.) GO TO 4030
      PD(2,1) = DPDM/C33
      PD(2,2) = - C41 * VOUT
   PARTIAL WRT VIN = 0
C
      PD(2,4) = DPDY/C33
   COMPUTE PARTIAL OF YDOT WRT VOUT ONLY WHEN VOUT > 0
      PD(4,2) = AOUT/DVOLDY
 4030 CONTINUE
   COMPUTE PARTIALS OF VIND ONLY WHEN VIN > 0
      IF (VIN .LE. 0.) GO TO 4040
      PD(3,1) = - DPDM/ C36
   PARTIAL WRT VOUT = 0
      PD(3,3) = - C43 \times VIN
      PD(3,4) = - DPDY/C36
C
```

```
COMPUTE PARTIAL OF YDOT WRT VIN ONLY WHEN VIN > 0
     PD(4,3) = -AIN/DVOLDY
 4040 CONTINUE
C
   OTHER PARTIALS OF YDOT = 0
C
     RETURN
ENTRY TO COMPUTE PERFORMANCE CRITERIA AND PARAMETERS IN THE
   CONSERVATION EQUATIONS FOR ONE CYCLE
     ENTRY CYCLE
     NPREV = NSAVE
     NSAVE = NSAVE + 1
C
   SAVE THE VARIABLES FOR TIME BASED PLOTTING
     Y1(NSAVE) = YVDOT(1)
     Y2(NSAVE) = VOUT
     Y3(NSAVE) = VIN
     Y4(NSAVE) = Y
     Y5(NSAVE) = PVAP
     IF (NSAVE .EQ. 1) RETURN
     IF (IPV .NE. 2 .AND. IPTEST .EQ. 1) RETURN
     IPTEST = -1
   THE FOLLOWING SECTION AVALYSES ONE CYCLE
     GO TO (5100, 5200, 5300, 5400, 5500), IPHASE
   HERE WAITING FOR BEGINNING OF CYCLE
 5100 IF (IPV" .EQ. 3) GO TO 5110"
     YI1(1) = AHEAT * (TH - TL)
     YI2(1) = (1. - TERM) * AHEAT * (TH - TL)
    "YI3(1) = (ACCOIL - ACOND) * (TVAP - TC)
     YI4(1) = (AHBU - AHEAT) * (TH - TVAP)
     YI5(1) = PVAP \cdot * DVOLDY * YVDOT(4)
     YI6(1) = VOUT
     YI7(1) = ACOND * (TL - TC)
     YI8(1) = THONEW
     Tl
            = TEND
     PCHECK = PVAP
     PMAX
            = PVAP
     PMIN
            = PVAP
     XAMY
            = Y
     MINY
            = Y
     RETURN
C
  HERE IF BEGINNING OF CYCLE IS FOUND
 5110 IPHASE = 2
     GO TO 5600
C
 5200 IF (IPV .EQ. 3) GO TO 5600
   HERE IF ANOTHER MAXIMUM OR MINIMUM IS FOUND
C
     IPHASE = 3
   DETERMINE ACTUAL PMAX OR PMIN
```

```
IF (PVAP .GT. PCHECK) PMAX = PVAP
      IF (PVAP .LT. PCHECK) PMIN = PVAP
      GO TO 5600
 5300 IF (IPV .EQ. 4) GO TO 5600
   HERE IF SECOND HALF OF CYCLE IS FOUND
      IPHASE = 4
      GO TO, 5600
C
 5400 IF (IPV .EQ. 1) GO TO 5600
   HERE IF FINAL MAXIMUM OR MINIMA IS FOUND
      IPHASE = 5
   CHECK PMAX OR PMIN
      IF (PVAP .GT. PMAX) PMAX = PVAP
   IF (PVAP .LT. PMIN) PMIN = PVAP CONVERGENCE TEST
      PCON = PVAP - PCHECK
      PCON = ABS(PTEST)
      IF (PCON .LT. 1.E-02) GO TO 5600
      IPHASE = 1
      NPV = 13
      NI = 1
      GO TO 5100'
C
 5500 IF (IPV .EQ. 2) GO TO 5600
      IPHASE = 6
      TCYCLE = TEND - T1 - DELT
      FREQ = 1./TCYCLE
      GO TO 5700
C
   DETERMINE YMAX AND YMIN
 5600 \text{ IF } (Y .GT. YMAX) YMAX = Y
      IF (Y .LT. YMIN) YMIN = Y
C
   STORE VARIABLES FOR INTEGRATION
      NI = NI + 1
      YII(NI) = AHEAT * (TH - TL)
      YI2(NI) = (1. - TERM) * AHEAT * (TH - TL)
      YI3(NI) = (ACCOIL - ACOND) * (TVAP - TC)
      YI4(NI) = (AHBU - AHEAT) * (TH - TVAP)
      YI5(NI) = PVAP * DVOLDY * YVDOT(4)
      YI6(NI) = VOUT
      YI7(NI) = ACOND * (TL - TC)
      YI8(NI) = THONEW
   SAVE VARIABLES FOR Y BASED PLOT
      NPV = NPV + 1
      Y11(NPV) = YVDOT(1)
      Y22(NPV) = HEVAP * YI1(NI)
      Y33(NPV) = HEVAP * YI2(NI)
      Y44(NPV) = Y
      Y55(NPV) = PVAP
```

```
Y66(NPV) = Y22(NPV) - Y33(NPV)
      Y77(NPV) = HCOND * YI3(NI)
      Y88(NPV) = TH
      RETURN
C
   PERFORM THE INTEGRATIONS
 5700 \text{ YIII} = 0.
      YII2 = 0.
      YII3 = 0.
      YII4 = 0.
      YII5 = 0.
     \cdot YII6 = 0.
      YII7 = 0.
      YII8 = 0.
C
      NIM = NI - 1
      DO 5710 I = 2,NIM
      YII1 = YII1 + YI1(I)
      YII2 = YII2 + YI2(I)
      YII3 = YII3 + YI3(I)
      YII4 = YII4 + YI4(I)
      YII5 = YII5 + YI5(I)
      YII6 = YII6 + YI6(I)
      YII7 = YII7 + YI7(I)
 5710 \text{ YII8} = \text{YII8} + \text{YI8}(I)
      YIII = YIII + .(YII(1) + YII(NI))/ 2.
      YII2 = YII2 + (YI2(1) + YI2(NI))/2.
      YII3 = YII3 + (YI3(1) + YI3(NI))/2.
      YII4 = YII4 + (YI4(1) + YI4(NI))/2.
      YII5 = YII5 + (YI5(1) + YI5(NI))/2.
      YII6 = YII6 + (YI6(1) + YI6(NI))/2.
С
   NOW PROCEED WITH PERFORMANCE CRITERIA AND CONSERVATION EQUATIONS
      MEVAPT = C21 * (YIII - YII2)
      MCONDT = C22 * YII3
      FACTOR = DELT * 1054.35/ TCYCLE
             = HHV * YII4 * FACTOR
             = HEVAP * YIIl * FACTOR + QHVT
      POWIN
              = HLC *, YII7 * FACTOR
      OLCT
             = HEVAP * YII2 * FACTOR
      QVCLT
C
  DETERMINE FREON LIQUID TEMPERATURE
      GO TO (5711, 5712), ITL
 5711 FTL1 = QVCLT - QLCT
      FTLlA = DABS(FTL1)
      IF (FTL1A .LT. 10.) GO TO 5713
      TLl = TL
      TL = 1.30.
      TL2 = TL
      ITL = 2
      IPHASE = 7
      WRITE (6,5714) TL1,QVCLT,QLCT
```

```
5712 \text{ FTL2} = \text{QVCLT} - \text{QLCT}
      FTL2A = DABS(FTL2)
      IF (FTL2A .LT. 10.) GO TO 5713
   NOW INTERPOLATE FOR NEW FREON LIQUID TEMPERATURE
      TL = (TL1 * FTL2 - TL2 * FTL1) / (FTL2 - FTL1)
      TL1 = TL2
      FTL1 = FTL2
      TL2 = TL
      IPHASE = 7
      WRITE (6,5714) TL1,QVCLT,QLCT
      RETURN
 5713 CONTINUE
 5714 FORMAT( / ,' INACCURATE FREON LIQUID TEMPERATURE OF',G12.4,
     1 'USED IN ABOVE CALCULATIONS; REPEAT',/,' QVCLT, QLCT =',
     1 2G12.4,///)
C
   CONTINUE WITH PERFORMANCE CRITERIA AND CONSERVATION EQUATIONS
              = YMAX - YMIN
      OCTOT
             = QLCT + HCOND * YII3 * FACTOR
      PDVWRK = YII5 * DELT * 0.1131
      INDPOW = PDVWRK/ TCYCLE
      AVFLOW = AOUT * YII6 * DELT/ TCYCLE * 60./ 1728.
      POWOUT = AVFLOW * (HOUT - HIN) * ROWAT * GRAV * 3.258
      INDEFF = INDPOW/ POWIN
             = POWOUT/ POWIN
      THOC = (DELT * YII8 / TCYCLE - 32.) / 1.8
      THIC = (THI - 32.) / 1.8
      THC = (THIC + THOC)/2.
      FLOWSI = AVFLOW * 0.4719
      PMAXSI = PMAX * 0.0689
      PMINSI = PMIN * 0.0689
      YMAXSI = YMAX * 2.54
      YMINŚI = YMIN * 2.54
      AMPSI
             = YMAXSI - YMINSI
      TOTHED = (HOUT - HIN)/40.
      YA(NPRINT) = TOTHED
      YB(NPRINT) = FREQ
      YC(NPRINT) = AMPSI
      YD(NPRINT) = FLOWSI
      YE(NPRINT) = POWIN
      YF(NPRINT) = INDPOW
      YG(NPRINT) = POWOUT
      YH(NPRINT) = OVEFF
      NPRINT = NPRINT + 1
      WRITE (6,5720)
C5720 FORMAT( '
                 SEC',T11,'MDOT',T22,'VOUTD',T33,'VIND',T44,'YDOT',
     1 T55, 'TVAP', T66, 'SPVOL', T77, 'MVAP', T88, 'VOUT', T99, 'VIN', T110, 'Y',
C
     1 T121, 'PVAP', ///)
C
      WRITE (6,5721)
C5721 FORMAT( 5X,'TH',8X,'MSEVAP',14X,'MVCL',16X,'MEVAP',15X,'MCOND')
```

```
WRITE (6,5722) (Y88(I),Y22(I),Y33(I),Y66(I),Y77(I),I=13,100)
C5722 FORMAT( 5X,F5.2,4G20.8)
      WRITE (6,5800) T1,TCYCLE,FREQ,PMIN,PMAX,YMIN,YMAX,AMP,AVFLOW
5800 FORMAT(/// ,' TEST CYCLE STARTED AT T =',G12.4,',
                                                              DURATION = '.
                   FREQUENCY = 1
     1 Gl2.4,'
     1 G12.4, 'SEC', /, 'MIN PRESSURE =',G12.4, 'MAX PRESSURE =',G12.4, 1 'PSI', /, 'MIN LEVEL =',G12.4,' MAX LEVEL=',G12.4,' AMPLITUDE=',
     1 G12.4, 'INCHES', /, ' AVERAGE FLOW =', G12.4, 5X, 'CU. FT./MIN.')
      WRITE (6,5810) PMINSI, PMAXSI, YMINSI, YMAXSI, FLOWSI
 5810 FORMAT(/,' IN METRIC UNITS',/,' MIN PRESSURE =',G12.4,
1 'MAX PRESSURE =',G12.4,'BAR',10X,'MIN LEVEL =',G12.4,'
1 'MAX LEVEL =',G12.4,'CM',/,' AVERAGE FLOW =',G12.4,5X,
     1 'LITRES/SEC.',//)
WRITE (6,5815) THIC, THOC, THC
 5815 FORMAT( ' INLET HOT WATER TEMP = ',G12.4,
     1 'OUTLET HOT WATER TEMP = ',G12.4,' AVERAGE HEATER TEMP =
     1 G12.4.//)
      WRITE (6,5816) TL
 5816 FORMAT( / , ' FREON LIQUID TEMPERATURE =',G12.4,//)
      WRITE (6,5820) POWIN, INDPOW, POWOUT, INDEFF, OVEFF
.5820 FORMAT(/ ,' HEAT INPUT POWER =',G12.4,'INDICATED POWER
                                                 WATTS',/,26X,
     1 G12.4,5X,'OUTPUT POWER =',G12.4,'
     1 'INDICATED EFFICIENCY =',G12.4,5%,'OVERALL EFFICIENCY
     1 G12.4,/)
      WRITE (6,5825)
 5825 FORMAT( /, ' THE FOLLWING PARAMETERS IN THE INTEGRAL EQUATIONS',
     1 'ARE IN JOULES AND POUNDS')
      WRITE (6,5830) QCTOT, QVCLT, QLCT, MEVAPT, MCONDT, QHVT, INDPOW
     FORMAT( ' QCTOT =',G12.4,/,' QVCLT =',G12.4,' QLCT =',G12.4,/,
1 ' MEVAPT =',G12.4,'MCONDT =',G12.4,/,' QHVT =',G12.4,
 5830 FORMAT(
           INDPOW = ', G12.4,/)
      RETURN
ENTRY TO CALCULATE NEW HEATER TEMPERATURE
      ENTRY THNEW
      THOOLD = THONEW
      QHEATO = QHEATN
      QHEATN = QEVAP + (AHBU - AHEAT) * HHV * (TH - TVAP)
              = DELT * (QHEATO + QHEATN)/ 2.
      THONEW = (C17 * THI + C19 * THOOLD - QDEL) / C20
      TH
              = \langle THI + THONEW \rangle / 2.
      RETURN
ENTRY TO PLOT VARIABLES
      ENTRY OUTPUT
      NC = 100
   INSERT THE BORDERLINE POINTS FOR THE 'P-V' AND MOOT-Y PLOTS
      DO 6110 I=1,7,2
 6110 \ Y55(I) = 0.
      DO 6120 I=2,8,2
```

```
6120_{1}Y55(I) = 25.
     \text{Y55(9)} = \text{-C32}
      Y55(10) = Y55(9)
      Y55(11) = C34
      Y55(12) = Y55(11)
      DO 6130 I = 1.4
      \mathbf{J} = \mathbf{I}_0 + \mathbf{1}_1
      Y11(I) = -0.25E-01
 6130 \text{ Y11(J)} = 0.5E-01
      DO 6131 I = 9,12
 6131 \text{ Yll}(I) = 0.
      DO 6140 I = 1,11,2
      J = I + 1
      Y22(I) = 0.5E-01
 6140 \ Y22(J) = 0.
      DO 6150 I = 1,12
      Y33(I) = Y22(I)
      Y66(I) = Y22(Y)
 6150 \text{ Y}77 \& I) = \text{Y}22(I)
      Y44(1) = 0.
      44(2) = 0.
      Y44(3) = LHTOP
      Y44(4) = LHTOP
      Y44(5) = LHBOT
      Y44(6) = LHBOT
      Y44(7) = 6.*SCALE
      Y44(8) = 6.*SCALE
      Y44(9)
              = 0.
      Y44(10) = 6.*SCALE
      Y44(11) = 0.
      Y44(12) = 6.*SCALE
      DO 6160 I=1,NPV
C6160 WRITE (6,6170) Y44(I), Y55(I), I
 6170 FORMAT( 3G20.4)
      CALL PLOT1 (Y44, Y55, NPV, NC)
      CALL PLOT1 (Y44, Y11, NPV, NC)
      CALL PLOT1 (Y44, Y22, NPV, NC)
      CALL PLOT1 (Y44, Y33, NPV, NC)
      CALL PLOT1 (Y44, Y66, NPV, NC)
      CALL PLOT1 (Y44, Y77, NPV, NC)
C
      RETURN
ENTRY TO PRINT SUMMARY OF RESULTS
      ENTRY FINAL
      NPRIÑT = NPRINT - 1
      WRITE (6, 6171) HIN
 6171 FORMAT('1'
                  ,' SUMMARY OF RESULTS FOR SUCTION HEAD =
```

```
1 G12.4,///,T7,'TOTAL HEAD',
1 'T21,'FREQ',T33;'AMPSI',T44,'AV.FLOW',T57,'HEAT.IN',T68,'IND.POW',
1 T80,'POW.OUT',T92,'OV.EFF'
      DO 6172 I = 1 WPRINT
      WRITE (6,6178) YA(I),YB(I),YC(I),YD(I),YE(I),YF(I),YG(I),YH(I)
 6172 CONTINUE
 6173 FORMAT( //
                /,-5X,8G12.4)
      RETURN
      END
SUBROUTINE VANDA
   SUBROUTINE TO CALCULATE THE · LIQUID CONTACT AREAS, THE FREON VAPOUR
  VOLUME AND THEIR PARTIAL DIFFERENTIALS
      COMMON
              /VA/LHTOP, LHEAT, LHBOT, LCTOP, LCOND, LCBOT, AHBOT, AHEAT, ACYL
      COMMON
               /VA/ACCOIL, ACOND, DAHDY, DACDY, VOL, DVOLDY, C6, C7, C8, C9, C10
      COMMON
               /VA/C11,C12,C13,C14,C15,C16,C37,C38,C39,Y
C
      REAL*8 LHTOP, LHEAT, LHBOT, LCTOP, LCOND, LCBOT, AHBOT, AHEAT, ACYL
      REAL*8 ACCOIL, ACOND, DAHDY, DACDY, VOL, DVOLDY, C6, C7, C8, C9, C10
      REAL*8 Cl1, Cl2, Cl3, Cl4, Cl5, Cl6, C37, C38, C39, Y
      IF (Y .GE. LHBOT) GO TO 1020
      IF (Y .GE. LHTOP) GO TO 1010
      AHEAT = AHBOT + C37 * (LHTOP - Y)
      DAHDY = - C37
      GO TO 1030
 1010 AHEAT = AHBOT - C38 * (Y - LHTOP)
      DAHDY = -C38
      GO TO 1030
 1020 \text{ AHEAT} = 0.
      DAHDY = 0.
1030 CONTINUE
      IF (Y .GE. LCBOT) GO TO 1050
      IF (Y..GE. LCTOP) GO TO 1040
      ACOND = ACCOIL
      DACDY = 0.
      GO TO 1060
 1040 \text{ ACOND} = \text{ACCOIL} - \text{C39} * (Y - \text{LCTOP})
      DACDY = - C39
      GO TO 1060
1050 ACOND = 0.
      DACDY = 0.
1060 CONTINUE
      IF (LCBOT .LE. LHTOP) GO TO 1160
      IF (LCBOT .GE. LHBOT) GO TO 1120
      WRITE (6,1110)
1110 FORMAT( /, 'LHTOP < LCBOT < LHBOT')
      STOP
1120 IF (Y .GE. LCBOT) GO TO 1150
```

IF (Y .GE. LHBOT) GO TO 1140

```
IF (Y.GE. LHTOP) GO TO 1130
      IF (Y.GE.LCTOP) GO TO 1125
      VOL=Y*C9
      DVOLDY=ACYL
 1125 VOL = Y \times C7
      DVOLDY = C7
      RETURN
 1130 VOL = Cll + (Y - LHTOP) * C8
      DVOLDY = C8
      RETURN
 1140 VOL = C12 + (Y - LHBOT) * C6
DVOLDY = C6
      DVOLDY = C6
      RETURN
 1150 VOL = C13 + (Y - LCBOT) * ACYL
      DVOLDY = ACYL
      RETURN
 1160 IF (Y .GE. LHBOT) GO TO 1190
      IF (Y .GE. LHTOP) GO TO 1180
      IF (Y .GE. LCBOT) GO TO 1170
      IF (Y.GE.LCTOP)GO TO 1165
      VOL=V*C9
      DVOLDY=ACYL
 1165 \text{ VOL} = Y * C7
      DVOLDY = C7
      RETURN
 1170 VOL = C14 + (Y - LCBOT) * C9
      DVOLDY = C9
      RETURN
 1180 VOL = C15 + (Y - LHTOP) * C10
      DVOLDY = C10
      RETURN
 1190 VOL = C16 + (Y - LHBOT) * ACYL
      DVOLDY = ACYL
      RETURN
      END
//GO.SYSIN DD *
```

COS INFORMATION 5647 FERRIER MONTREAL QUEBEC (514)738-2191 COS COS INFORMATION 5647 FERRIER MONTREAL QUEBEC (514)738-2191 COS COS INFORMATION 5647 FERRIER MONTREAL QUEBEC (514)738-2191 COS COS INFORMATION 5647 FERRIER

DATE 21 JUL 85 AT 23 54:48

DEPARTMENT 17\*

JOB ID: 4601 · REPORT NO 3

FILE ID . SIMPLEX HOLES

INPUT PROCESSING TIME: 00:01 05

DUTPUT PROCESSING TIME: 00:02 45

REPORT COMPLETION CODE: O

PAGES TO BIN 328

PAGES TO TRAY

PAPER PATH HOLES 3

LINES PRINTED. 6292

TAPE MOUNTS: 1

BLOCKS READ 85

BLOCKS SKIPPED: O

RECORDS READ 10720

DUDE RECORDS READ. 2

MAXIMUM COPY COUNT 1

OVERPRINTS 201

COLLATE ' YES

SF/MF. MULTI

SIMPLEX/DUPLEX

SIMPLEX

JDE, JDL USED

C516,17FC

ACCTINFO.

JOB 5728/CXP3SCR2/CXP3000 /21 55.27 H 21 JUL 85/

INITIAL FONT LIST.

OMT 10S

QMT 10B

(DJDE MODIFIED)

INITIAL FORM LIST

-NONE

INITIAL CME LIST:

-NONE

COS INFORMATION 5647 FERRIER MONTREAL QUEBEC (514)738-2191 COS

START | 1T/JOB 5728/CXP3SCR2/CXP3000 /21 55.27 H 21 JUL 85/ DJDE 0 (=('>>>> PLAIN PAPER ??' ) , ; 'DJDE JDE = A002, JDL=17FA, COPIES = 1 , END ;

> BLANK PAGE PAGE EN BLANC

PAGE EN BLANG

\*\*\*\*\*\*\*\*\*CXP3SCR2\*\*\*\*000000 \*\*\*\*JOB 5728\*\*\*\*\*\*\*\*\*\*\*\*\*

COS INFORMATION 5647 FERRIER MONTREAL QUEBEC (514)738-2191 COS COS INFORMATION 5647 FERRIER MONTREAL QUEBEC (514)738-2191 COS COS INFORMATION 5647 FERRIER MONTREAL QUEBEC (514)738-2191 COS COS

DATE: 21 JUL 85 AT 23:55:54

DEPARTMENT 17\*

JOB ID 4601 REPORT NO 4

FILE ID: SIMPLEX.HOLES

INPUT PROCESSING TIME 00:00.07

OUTPUT PROCESSING TIME: 00:00.01

REPORT COMPLETION CODE. O

PAGES TO BIN: 4

PAGES TO TRAY

PAPER PATH HOLES:

LINES PRINTED: 76

TAPE MOUNTS

BLOCKS READ. O

BLOCKS SKIPPED

RECORDS READ:

DJDE RECORDS READ 2

MAXIMUM COPY COUNT 1

OVERPRINTS .

COLLATE YES

SF/MF. MULTI

SIMPLEX/DUPLEX SIMPLEX

JDE, JDL USED · A002, 17FA

ACCTINFO: JOB 5728/CXP3SCR2/CXP3000 /21.55.27 H 21 JUL 85/

INITIAL FONT LIST. 1624BL

1624EL

(DUDE MODIFIED)

INITIAL FORM LIST -NONE

INITIAL CME LIST - NONE

COS INFORMATION 5647 FERRIER MONTREAL QUEBEC (514)738-2191 COS COS INFORMATION 5647 FERRIER MONTREAL QUEBEC (514)738-2191 COS COS INFORMATION 5647 FERRIER MONTREAL QUEBEC (514)738-2191 COS COS INFORMATION 5647 FERRIER MONTREAL QUEBEC (514)738-2191 COS

ø

BLANK PAGE PAGE EN BLANC

START VI/JOB 5722/CXP3SCR2/CXP3OOO /21.55.29 H 21 JUL 85/ DJDE v. = AOO2, JDL=17FA, COPIES = 1 , END ;

¥

τ

0000000			000 000	00000000	0000000	00000000	
00 0000	00 0000	00 0000	0000	00 0000	0000	00 0000	
00 00 00	00 00 00	00 00 00	00 00 00	00 00 00	00 00 00	00 00 00	
00 00 00	00. 00 00	00 00 00	00 00 00	00 00 00	00 00 00	00 00 00	
00 00 00	00 00 00	00 00 00	00 00 00	00 00 00	00 00 00	00 00 00	
00 00 00	00 00 00	<b>00 00 00</b>	00 00 00	00 00 00	00 00 00	00 00 00	
00 00 00	00 00 A 00	00 00	00 00 00	00 00 00	00 00 00	00 00 00	
0000 00	0000 00	0000 00	0000 0000	0000 00	0000 00	0000 00	
000 00	000 00	000 00	000 00	000 00	000 00	000 00	
0000000000	0000000000	0000000000	0000000000	000000000	000000000	000000000	
00000000	00000000	00000000 00000000		00000000	00000000	0000000	
00000000 0000000000 00 00 00 00 00 00	00000000 0000000000 00 00 00 00 00 00	00000000 0000000000 00 0000 00 00 00	00000000 0000000000 00 00 00 00 00 00	00000000 0000000000 00 00 00 00 00 00	00000000 0000000000 00 0000 00 00 00	00000000 0000000000 00 00 00 00 00 00	
0000000000 00 0000 00 00 00 00 00 00	0000000000 00 0000 00 00 00 00 00 00	0000000000 00 0000 00 00 00 00 00 00	0000000000 00 0000 00 00 00	0000000000 00 0000 00 00 00 00 00 00	0000000000 00 0000 00 00 00 00 00 00	0000000000 00 0000 00 00 00 00 00 00	
0000000000 00 0000 00 00 00 00 00 00 00 00	0000000000 00 0000 00 00 00 00 00 00	0000000000 00 0000 00 00 00 00 00 00	0000000000 00 0000 00 00 00 00 00 00	0000000000 00 0000 00 00 00 00 00 00	0000000000 00 0000 00 00 00 00 00 00	0000000000 00 0000 00 00 00 00 00 00	
0000000000 00 0000 00 00 00 00 00 00 00 00	0000000000 00 0000 00 00 00 00 00 00 00 00	0000000000 00 0000 00 00 00 00 00 00 00 00	0000000000 00 0000 00 00 00 00 00 00 00 00	0000000000 00 0000 00 00 00 00 00 00 00 00	0000000000 00 0000 00 00 00 00 00 00 00 00	0000000000 00 00 00 00 00 00 00 00 00 00 00	
00000000000 00 0000 00 00 00 00 00 00 00 00	0000000000 00 0000 00 00 00 00 00 00 00 00	0000000000 00 00 00 00 00 00 00 00 00 00 00	0000000000 00 0000 00 00 00 00 00 00 00 00	0000000000 00 00 00 00 00 00 00 00 00 00 00	0000000000 00 0000 00 00 00 00 00 00 00 00	0000000000 00 00 00 00 00 00 00 00 00 00 00	
00000000000 00 00 00 00 00 00 00 00 00 00 00	0000000000 00 0000 00 00 00 00 00 00 00 00	0000000000 00 00 00 00 00 00 00 00 00 00 00	00000000000 00 00 00 00 00 00 00 00 00 00 00	00000000000 00 00 00 00 00 00 00 00 00 00 00	0000000000 00 0000 00 00 00 00 00 00 00 00	0000000000 00 00 00 00 00 00 00 00 00 00 00	
00000000000 00 0000 00 00 00 00 00 00 00 00	0000000000 00 0000 00 00 00 00 00 00 00 00	0000000000 00 00 00 00 00 00 00 00 00 00 00	00000000000 00 00 00 00 00 00 00 00 00 00 00 00 00 00 00 00 00 00	00000000000 00 00 00 00 00 00 00 00 00 00 00	0000000000 00 00 00 00 00 00 00 00 00 00 00 00 00 00 00 00 00 00	0000000000 00	
00000000000 00 00 00 00 00 00 00 00 00 00 00	0000000000 00 0000 00 00 00 00 00 00 00 00	0000000000 00 00 00 00 00 00 00 00 00 00 00	00000000000 00 00 00 00 00 00 00 00 00 00 00	00000000000 00 00 00 00 00 00 00 00 00 00 00	0000000000 00 0000 00 00 00 00 00 00 00 00	0000000000 00 00 00 00 00 00 00 00 00 00 00	
00000000000 00 00 00 00 00 00 00 00 00 00 00 00 00 00 00 0000 00 00000000	0000000000 00 00 00 00 00 00 00 00 00 00 00 00 00 00 00 0000 00	0000000000 00 00 00 00 00 00 00 00 00 00 00 00 00 00 00 0000 00 00000000	0000000000 00 00 00 00 00 00 00 00 00 00 00 00 00 00 00 0000 00 00000000	0000000000 00 00 00 00 00 00 00 00 00 00 00	0000000000 00 00 00 00 00 00 00 00 00 00 00 00 00 00 00 00 00 00	0000000000 00	
00000000000 00 00 00 00 00 00 00 00 00 00 00 00 00 00 00 0000 00 00000000	0000000000 00 00 00 00 00 00 00 00 00 00 00 00 00 00 00 0000 00	0000000000 00 00 00 00 00 00 00 00 00 00 00 00 00 00 00 0000 00 00000000	0000000000 00 00 00 00 00 00 00 00 00 00 00 00 00 00 00 0000 00 00000000	0000000000 00 00 00 00 00 00 00 00 00 00 00	0000000000 00 00 00 00 00 00 00 00 00 00 00 00 00 00 00 00 00 00	0000000000 00000000	

\$	0000000000		XX XX		PPPPPPPPPPPPPPPPPPPPPPPPPPPPPPPPPPPPPP		3333333333		\$\$\$\$\$\$\$\$\$\$\$ \$\$\$\$\$\$\$\$\$\$\$\$\$		222222222		RRRRRRRRRRRRRRRRRRRRRRRRRRRRRRRRRRRRRRR		2222222222
	CC	CC	xx	××	PP	PP	33	33	SS	SS	CC	cc	RR	RR	22 22
	CC		XX	XX	PP	PP		33	SS		CC		RR	RR	22
,	CC		XX	XX	PP	PP		33	SSS		CC		RR	RR	22
	CC		XXXX		PPPPPPPPPPP		3333		SSSSSSSS		CC		RRRRRRRRRRRR		22
	CC		XXXX PPPPPPPPPP		PPPPPP	3333		SSSSSSSS		cc		RRRRRRRRRR		22	
	CC		XX	XX	PP			33		SSS	CC		RR	RR ~	22
	CC		XX	XX	PP			33		SS	CC		RR	RR	22
	CC	CC	XX	XX	PP		33	33	SS	) SS	CC	CC	RR	RR	22
	CCCCCCCCC	CCC	XX	. XX	PP		333333	333333	SSSSS	SSSSSSS	CCCC	CCCCCCC	RR	RR	22222222222
	ccccccc	cc	XX	XX	PP		33333	33333	SSSS	SSSSSS	CCC	cccccc	RR	RR	22222222222

\*\*\*\*\*A START JOB 5722 CXP3SCR2 \$FORM=C516,COPY= 1 ROOM 21 55 29 H 21 JUL 85 PRINTR13 SYS SYS1 JOB 5722 START A\*\*\*\*

COS INFORMATION 5647 FERRIER MONTREAL QUEBEC (514)738-2191 COS COS INFORMATION 5647 FERRIER MONTREAL QUEBEC (514)738-2191 COS COS INFORMATION 5647 FERRIER MONTREAL QUEBEC (514)738-2191 COS COS INFORMATION 5647 FERRIER

DATE: 21 JUL 85 AT 23:56:02

DEPARTMENT 17\*

JOB ID: 4601 REPORT NO. 5

FILE ID: SIMPLEX.HOLES

INPUT PROCESSING TIME: 00:00:04

OUTPUT PROCESSING TIME: 00:00:02

REPORT COMPLETION CODE O

PAGES TO BIN 1 4

PAGES TO TRAY

PAPER PATH HOLES: \ C

LINES PRINTED: 109

TAPE MOUNTS

BLOCKS READ

BLOCKS SKIPPED. 0

RECORDS READ. 4

DUDE RECORDS READ: 1

MAXIMUM COPY COUNT. 1

OVERPRINTS C

COLLATE YES

SF/MF MULTI

SIMPLEX/DUPLEX SIMPLEX

JDE, JDL USED: A002, 17FA

ACCTINFO JDB 5722/CXP3CR2/CXP3000 /21 55.29 H 21 JUL 85/

INITIAL FONT LIST. 1624BL

1624EL

(DJDE MODIFIED)

INITIAL FORM LIST -NONE

INITIAL CME LIST '-NONE

COS INFORMATION 5647 FERRIER MONTREAL QUEBEC (514)738-2191 COS COS INFORMATION 5647 FERRIER MONTREAL QUEBEC (514)738-2191 COS COS INFORMATION 5647 FERRIER MONTREAL QUEBEC (514)738-2191 COS COS INFORMATION 5647 FERRIER MONTREAL QUEBEC (514)738-2191 COS

START. JT/JOB 5722/CXP3SCR2/CXP3000 /21.55.29 H 21 JUL 85/ DJDE G \_ [=('>>>> 3-HOLES LEADING ??' ) , ; DJDE JDE = C516, COPIES = 1 , JDL = 17FC, END ;

> BLANK PAGE Page en Blanc

17.26.17 JOB 5722 \$HASP373 CXP3SCR2 STARTED - INIT 6 - CLASS Y - SYS SYS1 17.28.29 JOB 5722 \$HASP395 CXP3SCR2 ENDED

----- JES2 JOB STATISTICS -----

19 JUL 85 JOB EXECUTION DATE

14 CARDS READ

9,905 SYSOUT PRINT RECORDS

0 SYSOUT PUNCH RECORDS

2.21 MINUTES ELAPSED TIME

/ID ABS CXP3,000,999,999,999 COPIES=001 MVS \*\*EXCESSIVE TIME ESTIMATED..ASSUMING 180 SERVICE UNITS /PARM COPIES=003,FILE='Al9JUL85.17.25.01',DELETE=T,DEVICE=2,FORMS='C516' /SYS TIME=MAX,NOSKIP,NOPRINT

COS INFORMATION 5647 FERRIER MONTREAL QUEBEC (514)738-2191 COS COS INFORMATION 5647 FERRIER MONTREAL QUEBEC (514)738-2191 COS COS INFORMATION 5647 FERRIER MONTREAL QUEBEC (514)738-2191 COS COS INFORMATION 5647 FERRIER MONTREAL QUEBEC (514)738-2191 COS

DATE 21 JUL 85 AT 23.56 07

DEPARTMENT: 17\*

JOB ID. 4601 REPORT NO 6

FILE ID SIMPLEX HOLES

INPUT PROCESSING TIME . 00.00:05

OUTPUT PROCESSING TIME: 00 00:02

REPORT - COMPLETION CODE: 50

PAGES TO BIN

PAGES TO TRAY

PAPER PATH HOLES 0

LINES PRINTED 88

TAPE MOUNTS.

BLOCKS READ:

BLOCKS SKIPPED - 0

RECORDS READ 3

DUDE RECORDS READ 2

MAXIMUM COPY COUNT.

OVERPRINTS .

COLLATE YES

SF/MF: MULTI

SIMPLEX/DUPLEX SIMPLEX

JDE . JDL USED ;

C516,17FC

ACCTINFO

JOB -5722/CXP3SCR2/CXP3000 /2.1.55 29 H 21 JUL 85/

INITIAL FONT LIST

OMT 105 .

OMT 1OB

(DUDE MODIFIED)

INITIAL FORM LIST

-NONE

INITIAL CME LIST:

-NONE

COS INFORMATION 5647 FERRIER MONTREAL QUEBEC (514)738-2191 COS COS INFORMATION 5647 FERRIER MONTREAL QUEBEC (514)738-2191 COS COS INFORMATION 5647 FERRIER MONTREAL QUEBEC (514)738-2191 COS COS INFORMATION 5647 FERRIER MONTREAL QUEBEC (514)738-2191 COS

BLANK PAGE PAGE EN BLANC

3SCR2/CXP3GOO /21.55.29 H 21 JUL 85/

START